TECHNICAL REPORT CERC-89-14

US Army Corps of Engineers

AD-A215 208

DIRECTIONAL SPECTRAL WAVE TRANSFORMATION IN THE NEARSHORE REGION

Report 1
DIRECTIONAL SPECTRAL PERFORMANCE CHARACTERISTICS

by

Michael J. Briggs, Peter J. Grace, Robert E. Jensen

Coastal Engineering Research Center

DEPARTMENT OF THE ARMY
Waterways Experiment Station, Corps of Engineers
3909 Halls Ferry Road, Vicksburg, Mississippi 39180-6199

DTIC
ELECTE
S
DEC 0 6 1989
D
E

November 1989
Final Report

Approved For Public Release; Distribution Unlimited

89 12 04 124

REPORT DOCUMENTATION PAGE	Form Approved OMB No. 0704-0188

1a. REPORT SECURITY CLASSIFICATION Unclassified	1b. RESTRICTIVE MARKINGS

2a. SECURITY CLASSIFICATION AUTHORITY	3. DISTRIBUTION/AVAILABILITY OF REPORT Approved for public release; distribution unlimited.
2b. DECLASSIFICATION/DOWNGRADING SCHEDULE	

4. PERFORMING ORGANIZATION REPORT NUMBER(S) Technical Report CERC-89-14	5. MONITORING ORGANIZATION REPORT NUMBER(S)

6a. NAME OF PERFORMING ORGANIZATION USAEWES, Coastal Engineering Research Center	6b. OFFICE SYMBOL (If applicable)	7a. NAME OF MONITORING ORGANIZATION

6c. ADDRESS (City, State, and ZIP Code) 3909 Halls Ferry Road Vicksburg, MS 39180-6199	7b. ADDRESS (City, State, and ZIP Code)

8a. NAME OF FUNDING/SPONSORING ORGANIZATION US Army Corps of Engineers	8b. OFFICE SYMBOL (If applicable)	9. PROCUREMENT INSTRUMENT IDENTIFICATION NUMBER

8c. ADDRESS (City, State, and ZIP Code) Washington, DC 20314-1000	10. SOURCE OF FUNDING NUMBERS			
	PROGRAM ELEMENT NO.	PROJECT NO.	TASK NO.	WORK UNIT ACCESSION NO. 31762

11. TITLE (Include Security Classification)
Directional Spectral Wave Transformation in the Nearshore Region; Report 1, Directional Spectral Performance Characteristics

12. PERSONAL AUTHOR(S)
Briggs, Michael J.; Grace, Peter J.; Jensen, Robert E.

13a. TYPE OF REPORT Final report	13b. TIME COVERED FROM _____ TO _____	14. DATE OF REPORT (Year, Month, Day) November 1989	15. PAGE COUNT 180

16. SUPPLEMENTARY NOTATION
Available from National Technical Information Service, 5285 Port Royal Road, Springfield, VA 22161.

17. COSATI CODES			18. SUBJECT TERMS (Continue on reverse if necessary and identify by block number)
FIELD	GROUP	SUB-GROUP	Directional wave spectra Physical models
			Jetty stability Wave calibration
			Nearshore wave modeling Wave transformation

19. ABSTRACT (Continue on reverse if necessary and identify by block number)
The effects of frequency and directional spreading on wave transformation in the nearshore region were investigated using a three-dimensional physical model of Yaquina Bay, Oregon. The 1:45 model consists of an entrance channel protected by two rubble-mound jetties with a sloping bottom and submerged reef offshore of the entrance. Unidirectional and directional wave spectra, representative of the six most severe hindcasted storms in the past 20 years, were numerically transformed to a shallow-water depth of -58 ft mllw. A range of spectral parameters, including frequency and directional spreading, were modeled. Incident and transformed wave elevations were measured using capacitance wave gages located offshore and near the jetty head, respectively. Descriptions of the simulation and generation, directional spectral analysis, and control signal correction algorithm are given. Comparisons of predicted and measured peak periods, wave heights, wave direction, frequency spectra, and directional spreading are presented and discussed.

(Continued)

20. DISTRIBUTION/AVAILABILITY OF ABSTRACT ☒ UNCLASSIFIED/UNLIMITED ☐ SAME AS RPT. ☐ DTIC USERS	21. ABSTRACT SECURITY CLASSIFICATION Unclassified
22a. NAME OF RESPONSIBLE INDIVIDUAL	22b. TELEPHONE (Include Area Code) 22c. OFFICE SYMBOL

DD Form 1473, JUN 86   Previous editions are obsolete.   SECURITY CLASSIFICATION OF THIS PAGE

19. ABSTRACT (Continued).

This study is divided into three phases. Phase 1, reported herein, is a calibration of the performance characteristics of the six unidirectional and six directional cases. A total of 36 cases was required to measure and correct the control signals for the two water depths.

Accession For	
NTIS GRA&I	☒
DTIC TAB	☐
Unannounced	☐
Justification	

By	
Distribution/	
Availability Codes	

Dist	Avail and/or Special
A-1	

PREFACE

This report is a product of the Laboratory Simulation of Spectral and
Directional Spectral Waves Work Unit 31762, Coastal Flooding and Storm
Protection Program, Civil Works Research and Development, at the US Army
Engineer Waterways Experiment Station's (WES's) Coastal Engineering Research
Center (CERC). Testing was conducted from July 1987 to January 1988, and data
reduction and report preparation were completed in February 1988.

This report was prepared by Mr. Michael J. Briggs, Research Hydraulic
Engineer, under direct supervision of Mr. Douglas G. Outlaw, Chief, Wave
Processes Branch (CW-P), CERC, and under general supervision of Mr. C. Eugene
Chatham, Chief, Wave Dynamics Division (CW), Mr. Charles C. Calhoun, Assistant
Chief, CERC, and Dr. James R. Houston, Chief, CERC. Mr. Peter J. Grace, Wave
Research Branch (CW-R), and Dr. Robert E. Jensen, Coastal Oceanography Branch,
Research Division (CR-O), coauthored portions of this report and furnished
valuable technical assistance. Messrs. John H. Lockhart, Jr., James E. Crews,
Charles W. Hummer, and John G. Housley, US Army Corps of Engineers, were
Technical Monitors for the Coastal Flooding and Storm Protection Program.
Dr. C. Linwood Vincent was Program Manager for Coastal Programs.

Numerous individuals contributed to successful completion of this
project. Two of the most important were Mrs. Debbie L. Green, Computer
Assistant, CW-P, and Mr. David A. Daily, Electronic Technician, Instrumenta-
tion Services Division. Mrs. Green assisted in every phase of the project,
including simulating frequency spectra, generating control signals, calibrat-
ing wave gages, collecting and reducing data, and preparing the report.
Mr. Daily maintained the directional spectral wave generator, wave gages, and
associated electronics, obtained the wave gage calibrations, and collected
data. Mr. William D. Corson, CR-O, selected and compiled pertinent WIS
hindcast storm data. Mr. Willie G. Dubose, CW-R, coordinated CERC's efforts
with those of the WES shops for model construction and participated in the
unidirectional tests. Dr. Leon E. Borgman, University of Wyoming, developed
the original directional wave simulation and analysis software and provided
many hours of fruitful discussions. Finally, Mrs. Lee Ann Germany, CW-P
Secretary, assisted in preparation of the final report, and Mrs. Shirley A. J.
Hanshaw of the WES Information Management Division edited this report.

1

Commander and Director of WES was COL Larry B. Fulton, EN. Technical Director was Dr. Robert W. Whalin.

CONTENTS

CONVERSION FACTORS, NON-SI TO SI (METRIC)
UNITS OF MEASUREMENT

Non-SI units of measurement used in this report can be converted to SI (metric) units as follows:

Multiply	By	To Obtain
degrees (angle)	0.01745329	radians
feet	0.3048	metres
horsepower (550 foot-pounds (force) per second)	745.6999	watts
inches	2.54	centimetres
knots (international)	0.5144444	metres per second
miles (US nautical)	1.852	kilometres
miles (US statute)	1.609437	kilometres
pounds (mass)	0.4535924	kilograms
square feet	0.09290304	square metres
square miles	2.589998	square kilometres

DIRECTIONAL SPECTRAL PERFORMANCE CHARACTERISTICS

PART I: INTRODUCTION

1. Irregular waves are routinely used in physical model tests of port facilities and breakwaters. Real ocean waves are short-crested, however, and have directional spreading which spreads energy over many directions. Sand et al. (1983) measured diffracted wave energy in the lee of an entrance breakwater for unidirectional and directional spectral waves. They found larger waves for the directional cases. The directional spectral wave genera- tor (DSWG) of the US Army Engineer Waterways Experiment Station's Coastal Engineering Research Center (CERC) provides a means to simulate real ocean environments in a laboratory physical model by incorporating this directional spreading. Thus, it appears that the inclusion of directional spreading can have a significant effect in the design of port facilities and breakwaters.

2. This report describes a three-dimensional (3-D), physical model study of a harbor entrance breakwater in Yaquina Bay, Oregon, using unidirec- tional and directional spectral waves. The model consists of an entrance channel protected by two rubble-mound jetties with a sloping bottom offshore of the entrance. The site is characterized by complex bathymetry, an offshore reef, and numerous rock outcrops. Unidirectional and directional spectra, representative of the most severe hindcasted storms in the past 20 years, were selected for study. A range of spectral parameters, including frequency and directional spreading, was modeled. Surface wave elevations were measured offshore and near the jetty head for two water depths: a low water level of -58 ft* mean lower low water (mllw) (+0 ft) and a high water level of -68 ft mllw (+10 ft) representative of a +8-ft tidal height and a 2-ft storm setup. Thus, effects of spectral parameters, including frequency and directional spreading on wave transformation in the nearshore region, are presented and compared. The study is divided into three phases, each contained in a separate report.

---

* A table of factors for converting non-SI units of measurement to SI (metric) units is presented on page 4.

3. The first phase, contained in this report, documents the initial calibration phase for verifying directional performance characteristics of the hindcasted storms. A series of six storms was selected from the Wave Information Studies (WIS) data base. They were multimodal in frequency and direction with locally generated wind-sea and distant swell components. These spectra were used as input to the numerical spectral wave model SHALWV (Hughes and Jensen 1986) that includes all source/sink functions and finite depth mechanisms such as refraction, shoaling, wave bottom interactions, and depth-related breaking. This numerical model transformed the deepwater spectra to a shallow-water depth of 58 ft, corresponding to the location of the wave generator in the model. The numerical model results were then used for physical model control signal generation. Peak wave periods were 12.5, 14.3, and 16.7 sec. Significant (zero-moment) wave heights ranged from 14.4 to 22.3 ft. For the unidirectional spectral cases, the overall mean wave direction was selected as the direction of the swell component. Six equivalent directional spectral cases were computed with peak periods of 14.3 and 16.7 sec and wave heights ranging from 15.4 to 23.0 ft. A description of the WIS hindcast model and the shallow-water transformation algorithm is contained in Part II.

4. The spectra were simulated as the product of a frequency spectrum and a directional spreading function. The frequency spectrum was discretely input at 20 selected frequencies of the numerically simulated spectra. For the directional spreading function, an empirically derived, wrapped normal spreading function was used for the unidirectional cases and discretely input at 16 equally spaced angles for the directional spectral cases. Control signals for each of the 61 paddles of the DSWG were created. Stroke time series were simulated in the frequency domain using a double summation, deterministic amplitude, random phase model (DSA method). In Part II, a description of this generation process for directional spectral waves in laboratory basins is presented.

5. Part III describes the theory of spectral analyses of the measured data. Included are frequency domain spectral, response amplitude operator (RAO), and directional spectral analyses. Standard fast fourier transform (FFT) techniques, including zero-meaning, windowing, and band averaging, are used for the spectral analysis. Because of leakage around and under the DSWG, electronic and mechanical losses, and basin response characteristics, the

original measured spectra did not usually reproduce the target spectrum. In addition, a water depth of 50 ft instead of 58 ft was inadvertently used when simulating the control signals. Thus, an RAO transfer function was calculated for each control signal to compensate for observed variations in peak period, wave height, and spectral shape. This RAO is the ratio of measured to predicted spectra at each frequency. After a run was completed, the RAO was calculated. It was then used to correct the control signal prior to making another run. The process can be iterative with several corrections required before a faithful reproduction of the desired spectral shape is obtained. Finally, a method based on the fourier series expansion of the directional spectrum was used for directional spectral analysis.

6. The purpose of the first phase was to verify the accuracy of the wave spectra created for a depth of 58 ft. Thus, the first phase consisted of three series of tests for each of the six unidirectional and six directional cases. The first series of 12 tests was measured at a depth of 50 ft and, as expected, the measured parameters turned out to be too small. The control signals were then corrected using the RAO for the particular storm and run again at the 58-ft level in series 2. Finally, the third series of 12 tests was run with the same corrected control signals from series 2 at the high water depth of 68 ft.

7. The second phase (Report 2) quantifies wave transformation between the six unidirectional and directional spectral cases in the nearshore region at the two water levels of 0.0 and +10.0 ft mllw. Three gages were used: one as an offshore reference or input gage and two others near the jetty head. Frequency response and coherence functions between the input and the two jetty gages are calculated to illustrate wave transformation on the shape of the frequency spectra. Effects of wave transformation on other spectral parameters are also presented and compared.

8. In the last phase (Report 3), the results from a parameter study on the effects of frequency and directional spreading are given. Frequency and directional spreading were varied within a prescribed range using the same peak period, wave height, and mean wave direction of the original directional spectra in phase 1. Low and high values of frequency and directional spreading were γ - 1.0 and 7.0 and σ - 10 and 30 deg, respectively. Thus, 24 cases were simulated for phase 3. The control signals were first calibrated as in phase 1 using a seven-gage array. During the calibration

7

process, three to four runs of each of the 24 cases were run in an iterative process to accurately reproduce the desired target spectra and ascertain the effectiveness of repeated iterations. The final step, analogous to phase 2, quantified wave transformation in the nearshore region for the 24 cases using the three-gage setup. This phase of testing involved over 120 runs of the 24 cases.

9. In Part IV, descriptions are given of the test setup, including the Yaquina Bay physical model, the directional wave basin and generator, and the wave elevation measurement system. Test cases are described, and test case generation and analysis parameters are given. The directional wave basin was lined with wave absorber frames to minimize reflections. Capacitance wave gages with remote-controlled stepper motors were used. They were arranged in a 2-3-1-7 linear array incorporated in a cross pattern centrally located 20 ft in front of the DSWG about its center line. The unit lag spacing was designed to optimize resolution within the lower and upper cutoff frequencies while minimizing spatial aliasing.

10. Test results and analyses are presented in Part V. Time domain analysis results include time series traces of wave elevation for each test case. Frequency domain results include comparisons of predicted and measured peak wave periods, zero-moment wave height, peak wave direction, frequency spectra, and directional spreading function. Also, RAO transfer functions as a function of frequency for each test case are presented.

11. Finally, Part VI contains a summary of results and recommendations for future research and improvements. The recommendations of the International Association of Hydraulic Research (IAHR) (1986) List of Sea State Parameters are followed wherever possible throughout this report and in the computer software implemented for wave generation and analysis.

8

PART II: SIMULATION AND GENERATION THEORY

Wave Information Studies Deepwater Storm Hindcast

12. WIS is a long-term wind wave hindcast program funded by the US Army Corps of Engineers (USACE) to provide a 20-year wave climatology along all United States coastlines. At the onset of the project, USACE recognized that long-term gaging operations covering extensive coastal locations are extremely expensive and too time consuming to quantify climatological changes in the wave environment. Hence, a hindcast study was initiated employing historical weather information as input to state-of-the-art numerical wind and wave models. It is recognized that the synthesized wave climates are not perfect, but from all comparisons to measured data sets, the hindcast results are found to be relatively consistent.

13. The WIS study is divided into three primary parts: Phase I, Phase II, and Phase III (e.g., Corson et al. 1987). The reasoning for the division is based on a certain scaling constraint. The Phase I portion of WIS relies on the construction of large-scale synoptic events that are on the order of 100's of nautical miles, with temporal changes greater than 6 hr. This includes creation of the wind fields which feed energy back into the wave field. Phase II is based on much smaller scale features, incorporating the Phase I wave information and secondary energy sources defined from the specification of mesoscale events superimposed on the synoptic scale features. The atmospheric response scales for this phase are on the order of 10's of nautical miles, and temporal changes are on the order of 3 to 6 hr. The Phase III portion of WIS defines the wave climate in the nearshore region. The method of solution includes transformation of Phase II wave estimates to shallow water where the mechanisms of refraction, shoaling, and nonlinear transfers of energy describe the changes in the wave climate. Only the Phase I and II portions of WIS were used in this study.

WIS modeling procedure

14. The procedure employed in the calculation of the deepwater (Phase I) wave climate is threefold. Digital pressure field information is obtained from Meteorology International, Inc., through the Fleet Numerical Weather Center. These data sets are used to compute (Corson et al. 1980) surface pressure fields for use in a Planetary Boundary Layer Wind Model

(Resio et al. 1982) to generate wind fields. The modeled region includes the
entire North Pacific Ocean (Figure 1). Ship observation wind data are then

MERCATOR PROJECTION OF PACIFIC OCEAN
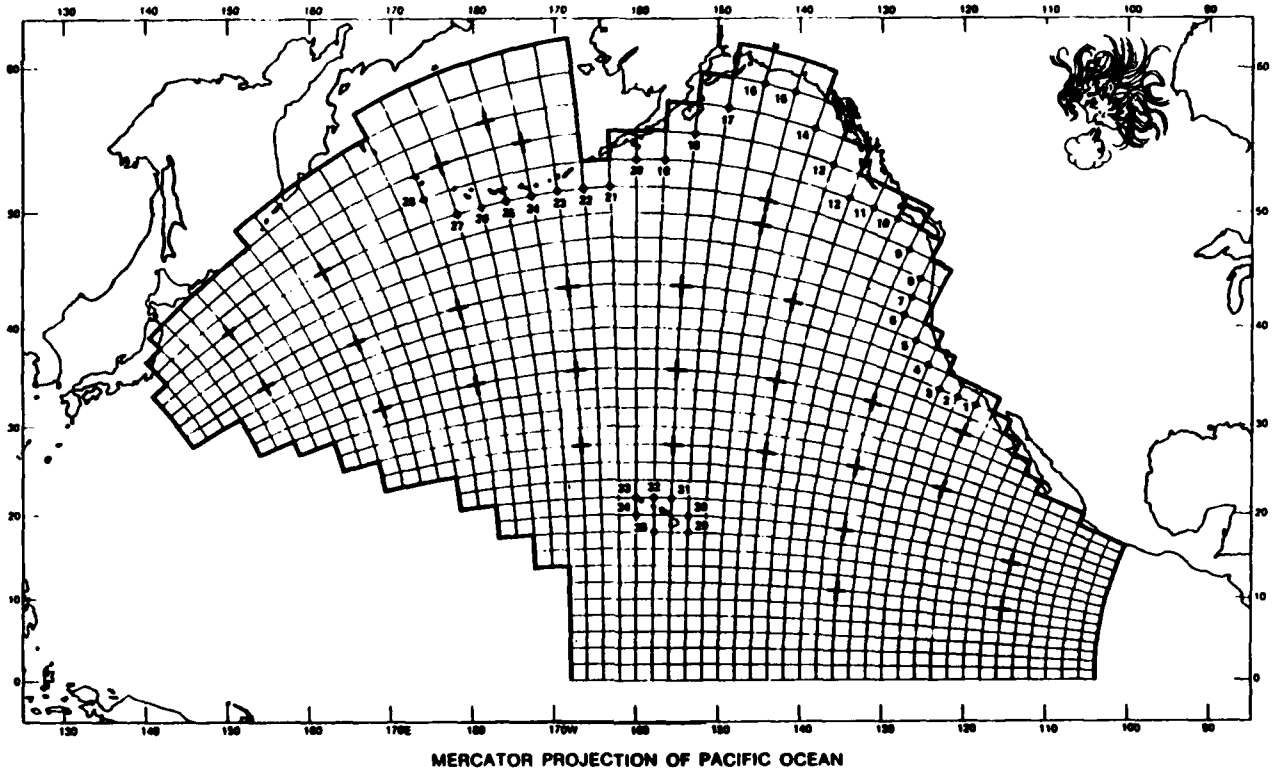
Figure 1. WIS Phase I model grid

blended into the simulated wind fields which are verified by existing data
sources. Finally, the wave modeling continues with the WIS discrete spectral
wave model (Resio 1982).

15. The wind field information is used as the governing input to the
discrete spectral wave model. In the area defined by the storm system, local
wind-seas are created. Energy from the wind field is directly transferred to
the water surface where it promotes wave growth. Nonlinear wave-wave interac-
tions (Hasselmann 1962) transfer packets of energy from frequency band to
frequency band, reestablishing a stable energy level. As the storm propagates
toward the east, the local wind-sea will, by the wave model's definition,
transform into swell conditions no longer capable of receiving additional
energy from the winds. Hence, a two-population wave system is simulated.

16. The Phase II portion of the study is analogous to Phase I, with an
additional source of wave input defined at its outermost boundary from the
Phase I hindcast effort. Also, the grid size is reduced from approximately
120 to 30 nautical miles (Figure 2). All wave and spectral estimates employed

10
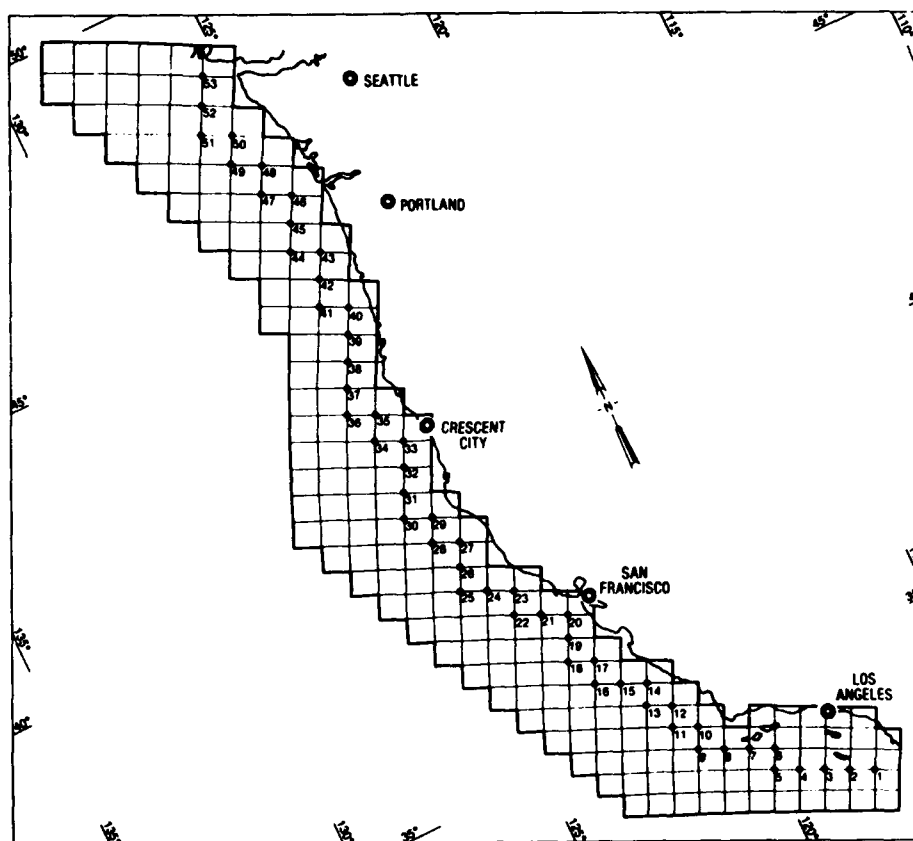
Figure 2. WIS Phase II model grid

in this study were derived from Phase II sta 42, located west of Yaquina Bay
(44.82° N 125.01° W).

Deepwater storm conditions

17. Twenty years of hindcast information is generated at 3-hr inter-
vals, or 58,440 estimates of wind-wave and swell conditions. This time series
is then massaged into more usable products, summarized in the WIS data reports
for Phase I (Corson et al. 1986) and Phase II (Corson et al. 1987). Table 1
is an example from these data reports showing extreme wave heights in metres
for each storm condition tabulated on a monthly basis for Phase II sta 42.
The top five storms were selected as the most representative extreme condi-
tions. Also included were preliminary wave estimates from a WIS hindcast of
the 22-31 January 1983 storm sequence. Maximum conditions in the six storm
events were not always selected, however, to allow some variation of peak
periods. Table 2 lists zero-moment wave height H_{mo} ,* peak period T_p ,
principal wave direction, and wind speed and direction for the six deepwater

---

* For convenience, symbols and abbreviations are listed in the Notation
  (Appendix G).

11

Table 1

Extreme Wave Heights* for 20 Years

Deepwater WIS Phase II, Sta 42

						Months						
Year	Jan	Feb	Mar	Apr	May	Jun	Jul	Aug	Sep	Oct	Nov	Dec
1956	8.8	6.4	7.0	5.5	4.1	3.3	3.7	2.6	2.8	4.9	4.5	7.8
1957	5.6	7.3	6.0	4.4	3.9	2.8	2.9	2.3	4.2	5.2	6.4	7.6
1958	8.4	7.2	5.6	7.1	4.0	2.5	3.6	2.9	3.6	6.0	6.9	7.8
1959	8.5	6.9	5.1	5.2	4.4	3.0	3.6	2.9	3.6	6.0	6.9	7.8
1960	8.5	8.3	5.7	4.7	3.7	3.1	2.9	3.2	2.8	6.9	8.0	7.4
1961	8.9	6.9	6.4	5.2	3.8	3.3	2.4	2.7	3.9	5.5	6.8	7.2
1962	6.3	6.1	5.5	4.1	3.0	3.6	2.8	3.3	5.7	7.4	8.0	9.4
1963	6.3	7.3	7.1	3.9	4.0	4.2	3.0	2.4	3.5	9.6	6.5	8.8
1964	9.7	6.0	6.7	5.2	5.3	3.3	3.2	2.9	3.5	4.3	6.8	7.9
1965	7.9	5.9	3.9	4.5	4.3	4.1	2.9	2.5	3.2	6.7	7.6	8.3
1966	9.0	5.6	5.3	4.2	3.5	3.0	2.6	2.6	3.7	4.8	5.9	9.2
1967	8.4	5.0	5.7	4.7	2.8	2.9	2.5	2.2	4.0	5.4	6.5	9.1
1968	8.6	7.1	5.0	4.0	3.3	2.7	2.7	2.5	3.8	5.0	6.5	9.0
1969	6.5	8.1	5.4	6.1	4.0	2.7	2.9	2.3	4.0	5.1	8.1	10.6
1970	8.5	6.5	6.3	5.2	3.3	3.1	2.8	3.3	3.1	6.4	6.8	9.7
1971	9.4	7.0	8.8	4.8	5.2	2.8	3.1	4.8	3.3	5.1	7.9	7.2
1972	10.3	7.5	5.9	6.3	3.4	3.6	3.9	2.8	4.1	4.7	6.5	9.4
1973	8.3	6.6	6.1	4.8	4.5	4.3	3.4	3.2	4.2	5.4	8.1	9.8
1974	10.9	6.9	8.0	6.1	4.4	4.3	3.6	2.9	3.2	5.0	7.8	7.4
1975	6.4	6.2	6.4	4.5	3.6	3.3	2.4	2.5	1.9	5.5	7.4	8.5

* In metres.

Table 2

Maximum Deepwater Wave Conditions for Yaquina Bay

Date	Time	H_{mo} m	T_p sec	Wave Direction deg	Wind Speed knots	Wind Direction deg
69/12/11	21:00	9.74	14	216	39	188
70/12/30	15:00	9.23	13	246	34	218
72/01/20	09:00	6.85	11	232	29	218
73/12/13	00:00	9.03	14	227	28	193
74/01/15	18:00	10.78	17	213	34	208
83/01/26	18:00	8.80	17	--	30	227

wave conditions obtained from Phase I. Directions are measured counterclock-
wise from east and are the directions from which the wind and waves come.

Numerical Transformation to Shallow Water

18. For each wave estimate tabulated by WIS, two-dimensional (2-D)
spectra are also provided. The spectra are defined for 20 frequency bands
(from 0.03 through 0.22 at 0.01-Hz intervals) and 16 direction bands (at
22.5-deg intervals). It was found that these estimates were representative of
deepwater conditions and not indicative of conditions existing at the wave
generator located in a water depth of 58 ft (1.29-ft model). The required
estimates for this depth were provided employing SHALWV, a time-dependent,
arbitrary water depth pseudo-discrete spectral wave model (Hughes and Jensen
1986).

19. The computer program SHALWV, similar in structure to the WIS
deepwater discrete wave model (Resio 1982), solves the energy balance equation
using finite difference techniques. Information is stored in a discrete
matrix of frequency and direction bands for each computational point, but the
sources and sinks in the energy balance equation associated with energy input,
transfer, and dissipation are represented in a parameterized fashion. Wave
energy in each discrete frequency-direction band is propagated independently
using a first-order upstream scheme. This is a stepwise solution that
estimates for each discrete band the wave ray along which the energy contained
in that band must propagate to arrive at the grid point of interest by the end
of the time-step. An estimate of this energy is obtained by an interpolation
method that first projects the wave ray farther back in time until a grid
boundary is crossed. Finally, this estimated energy is propagated along the
wave ray as refraction and shoaling effects are estimated, reaching the grid
point at the end of the time-step. After the propagation sequence, energy is
added to or removed from each discrete energy band by the source terms. At
the end of the time-step, the directional spectrum at each grid point is the
sum of the independently propagated spectral elements and the changes in
energy caused by the selected source/sink mechanisms.

20. Although the input wave spectrum derived from the WIS data base and
SHALWV are both time-dependent, the physical model could not vary input condi-
tions to simulate a storm sequence. Hence, SHALWV was run in a steady state

13

mode. The required input spectral conditions (Table 2) were duplicated for
approximately 10 hr (prototype) to ensure that all input energy from the
boundary had sufficient time to reach the shallow-water locations. Also, a
representative wind condition was employed, derived from vector averaging each
3-hr wind occurring during the elapsed simulation period.

SHALWV modeling procedure

21. All SHALWV simulations were performed on a 5-nautical mile grid,
covering approximately 300 square miles (Figure 3). The width of the grid was
defined so that the WIS Phase II, sta 42, location and the output location
(for future physical modeling studies) would fall on a grid intersection. The
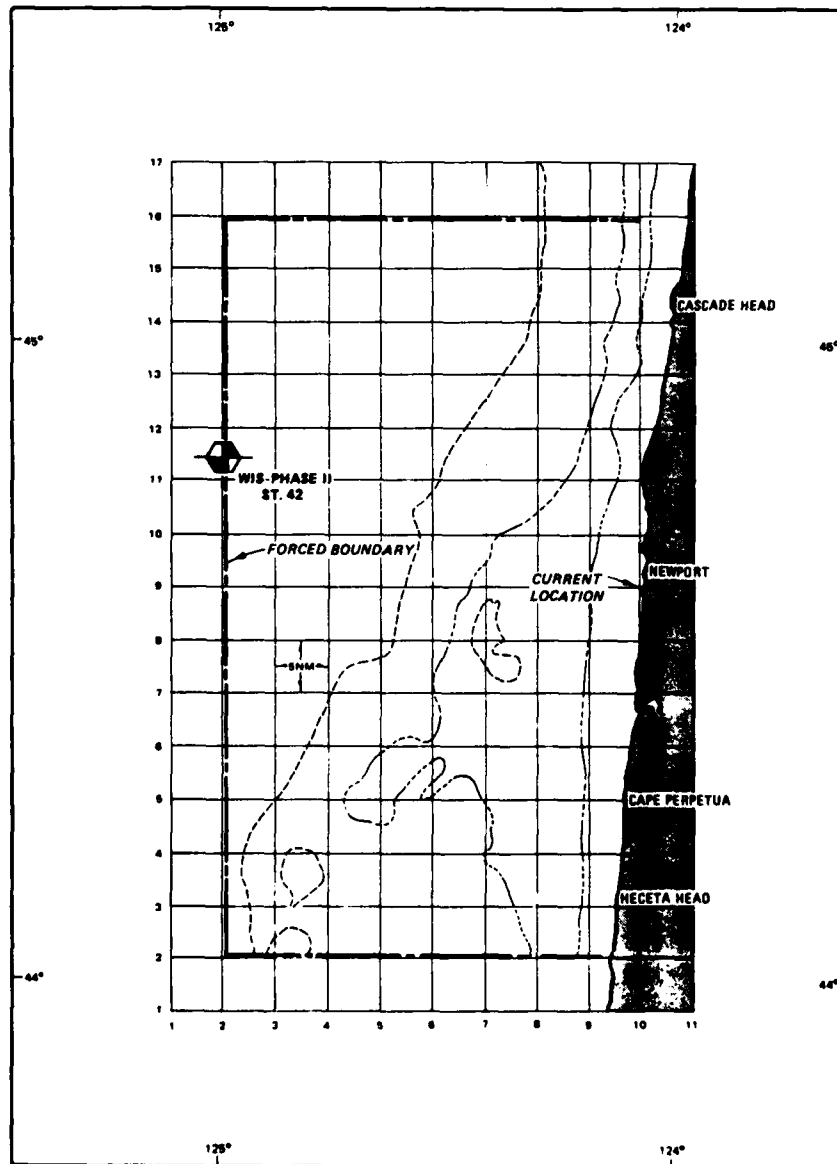

Figure 3. SHALWV model grid

14

north/south extent of the grid was selected so that bottom topographic features to the southwest of Yaquina Bay were adequately resolved. All water depth estimates, defined at each grid intersection, were based on an averaging procedure accounting for the variation surrounding each point. In general, if a shallow-water depth existed near the grid point, water depths were strongly weighted with respect to the depth of the shallowest point in the region.

22. An accurate representation of wave climate in a study area is strongly influenced by its input conditions. This is true for both physical and numerical model studies. As the boundary information becomes more representative of actual conditions, the results become more refined. For example, one could describe input waves (assuming an irregular wave environment) in the form of H_{mo}, T_p, and (for the 2-D case) $\bar{\theta}$. One could also estimate the same input via empirical Joint North Sea Wave Project (JONSWAP) (Hasselmann et al. 1973) spectral parameters defined by T_p, H_{mo}, and $\bar{\theta}$ as before and, in addition, a Phillips' equilibrium constant α, a spectral peakedness or peak enhancement parameter γ, and two spectral width parameters σ_a and σ_b. A more complex and better description would be in terms of a one-dimensional (1-D) frequency spectrum and an associated $\bar{\theta}$ of the spectrum. Finally, one could define the directional distribution in addition to the frequency distribution defining a 2-D spectrum, independent of external assumptions governing each distribution. As the number of dependent variables increases, the number of assumptions associated with a distribution decreases (Table 3). Thus, if high resolution 2-D spectra exist, one should use them.

23. Three methods based on the input boundary conditions in Table 3 were used to transform each of the deepwater storm conditions to shallow water. The amount of energy was kept constant in each. Test methods 1 and 2 were described by the actual WIS Phase II 1-D frequency spectra $\bar{\theta}$ and an assumed Cosine[4] directional distribution about $\bar{\theta}$. Test method 1 (swell only) was simulated without additional wind sources and was a baseline for comparisons of the net effect of local wind-wave generation. Method 2 incorporated wind-sea and swell components. Finally, method 3 used the full hindcast frequency and spreading estimates from the WIS Phase II data base.

Shallow-water storm conditions

24. Table 4 lists the prototype shallow-water spectral parameters for the six storm cases. Test methods 1, 2, and 3 results are labeled "swell only," "wind-sea and swell," and "directional cases," respectively.
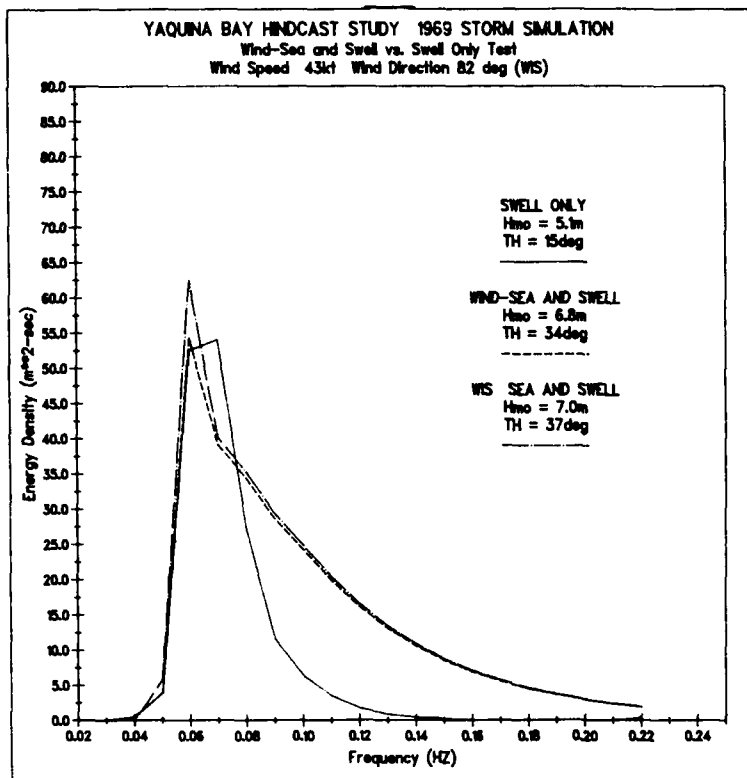
15

Table 3
Resolution of Input Spectral Conditions

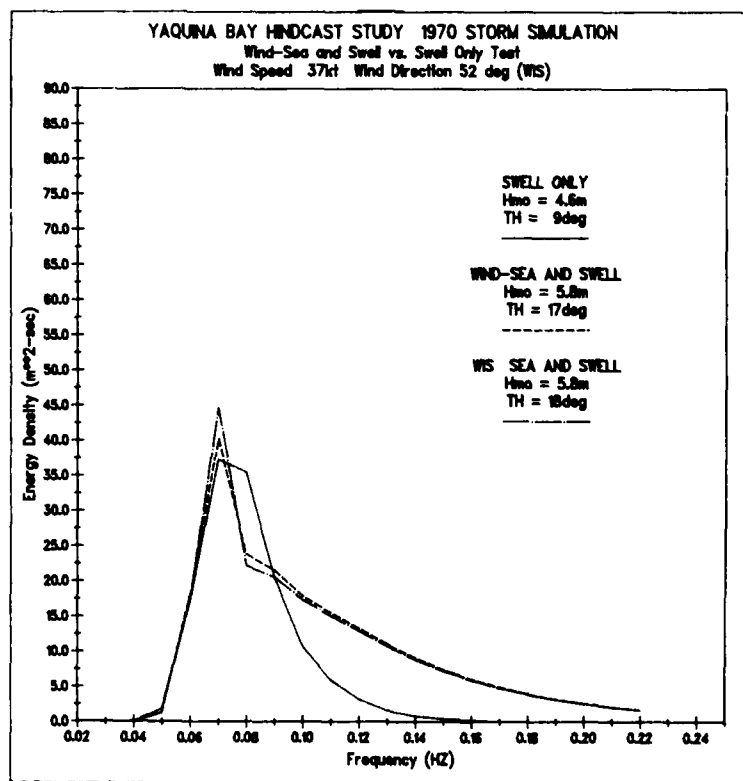| Input Type	Parameters	Assumptions
Wave parameters	$(T_p, H_{mo}, \bar{\theta})$	Frequency distribution Directional distribution
Spectral parameters	$(T_p, \alpha, \gamma,$ $\sigma_a, \sigma_b, \bar{\theta})$	Directional distribution
1-D spectrum	$E(f), \bar{\theta}$	Directional distribution
2-D spectrum	$E(f,\theta)$	None

Table 4
Shallow Water Prototype Wave Parameters

Storm Year	Method 1 Swell Only T_p sec	H_{mo} ft (m)	$\bar{\theta}$ deg	Method 2 Wind-Sea & Swell T_p sec	H_{mo} ft (m)	$\bar{\theta}$ deg	Method 3 Directional Cases T_p sec	H_{mo} ft (m)	$\bar{\theta}$ deg
1969	14.3	16.7(5.1)	15	16.7	22.3(6.8)	34	16.7	23.0(7.0)	37
1970	14.3	15.1(4.6)	9	14.3	19.0(5.8)	17	14.3	19.0(5.8)	18
1972	12.5	12.8(3.9)	19	12.5	14.4(4.4)	20	14.3	15.4(4.7)	13
1973	14.3	15.4(4.7)	15	14.3	16.7(5.1)	17	14.3	17.1(5.2)	7
1974	16.7	15.7(4.8)	21	16.7	19.0(5.8)	17	16.7	20.3(6.2)	30
1983	16.7	16.7(5.1)	14	16.7	18.7(5.7)	16	16.7	20.3(6.2)	16

Figures 4a to 4f show the frequency spectra for each of the six storms. The x-axis ranges from 0.02 to 0.24 Hz. The y-axis is scaled from 0 to 90 m^2/Hz. As expected, the inclusion of wind effects drastically changes the energy level in method 2 relative to the "swell only" method 1. Estimating the $\bar{\theta}$ and the directional distribution by a Cosine[4] enhances the energy level within three frequency bands centered on T_p. Also, the spectrum is forced to a new equilibrium state when the wind speeds are sufficiently high. The one exception is for the 1972 storm (Figure 4c), where the difference between method 1 and method 2 spectral shapes is unchanged at the peak but shows signs of generating a secondary peak at 0.16 Hz.

16

YAQUINA BAY HINDCAST STUDY 1969 STORM SIMULATION
Wind-Sea and Swell vs. Swell Only Test
Wind Speed 43kt Wind Direction 82 deg (WIS)

SWELL ONLY
Hmo = 5.1m
TH = 15deg

WIND-SEA AND SWELL
Hmo = 6.8m
TH = 34deg

WIS SEA AND SWELL
Hmo = 7.0m
TH = 37deg

a. 1969 Storm

YAQUINA BAY HINDCAST STUDY 1970 STORM SIMULATION
Wind-Sea and Swell vs. Swell Only Test
Wind Speed 37kt Wind Direction 52 deg (WIS)

SWELL ONLY
Hmo = 4.6m
TH = 9deg

WIND-SEA AND SWELL
Hmo = 5.8m
TH = 17deg

WIS SEA AND SWELL
Hmo = 5.8m
TH = 18deg

b. 1970 Storm

Figure 4.   Shallow-water prototype frequency spectra (Sheet 1 of 3)
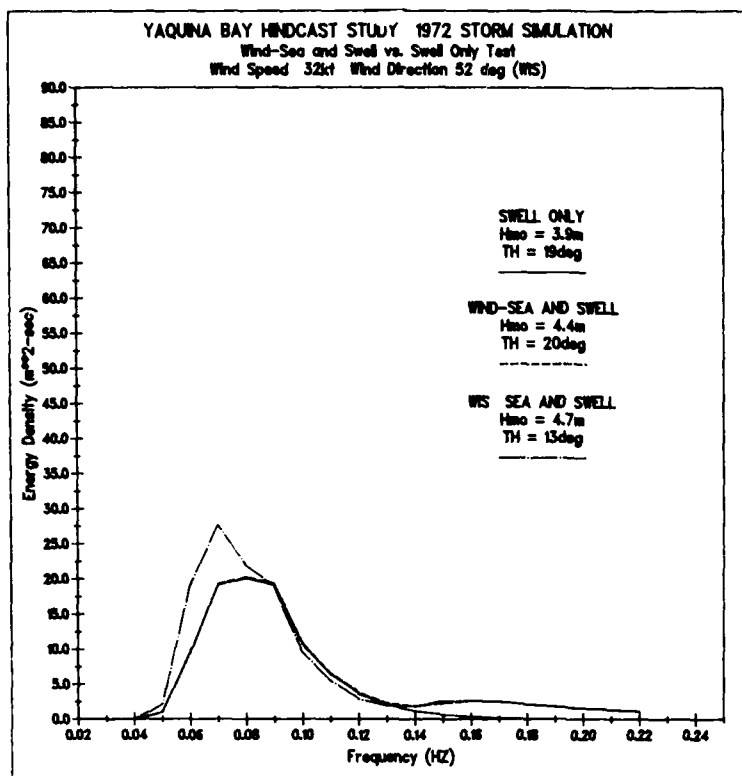
c. 1972 Storm
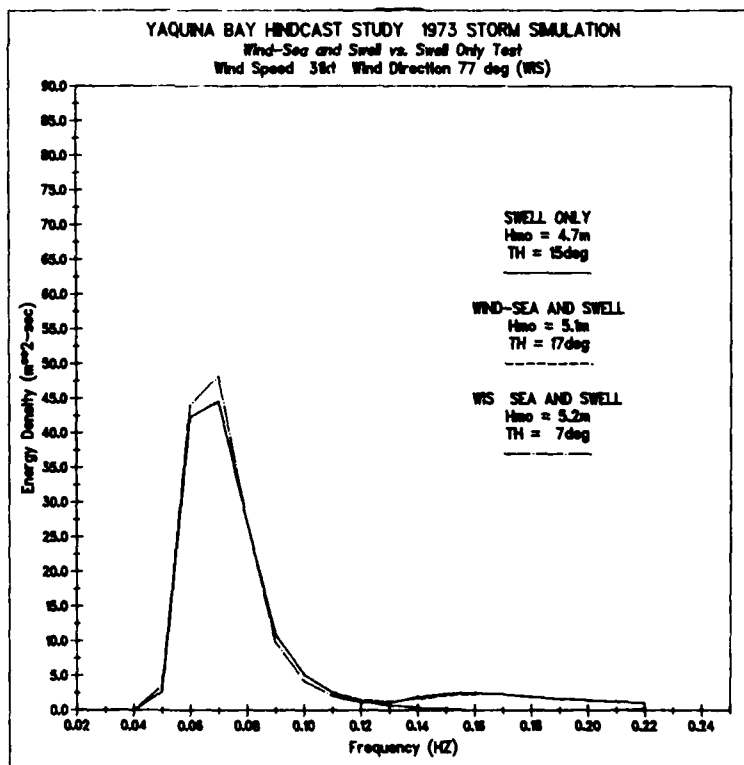
d. 1973 Storm

Figure 4. (Sheet 2 of 3)

YAQUINA BAY HINDCAST STUDY 1974 STORM SIMULATION
Wind-Sea and Swell vs. Swell Only Test
Wind Speed 38kt Wind Direction 62 deg (WIS)

SWELL ONLY
Hmo = 4.8m
TH = 21deg

WIND-SEA AND SWELL
Hmo = 5.8m
TH = 17deg
- - - - - - - -

WIS SEA AND SWELL
Hmo = 6.2m
TH = 30deg

e. 1974 Storm

YAQUINA BAY HINDCAST STUDY 1983 STORM SIMULATION
Wind-Sea and Swell vs. Swell Only Test
Wind Speed 33kt Wind Direction 43 deg (WIS)

SWELL ONLY
Hmo = 5.1m
TH = 14deg

WIND-SEA AND SWELL
Hmo = 5.7m
TH = 18deg
- - - - - - - -

WIS SEA and SWELL
Hmo = 6.2m
TH = 18deg

f. 1983 Storm

Figure 4. (Sheet 3 of 3)

25. Figures 5a to 5f illustrate the directional distribution for the six storms. The x-axis is from 0 to 360 deg, with increments of 22.5 deg. The y-axis ranges from 0.0 to 4.0 m^2/rad. All are single peaked except for the 1969 storm which indicates a secondary peak at 67.5 deg. In general, the actual directional distribution (i.e. test method 3) deintensifies the peak of the distribution and promotes a wider distribution. The differences in directional distributions between the three methods of numerical wave trans- formation vary according to the storm. The differences are slight in the 1973, 1974, and 1983 storms. In the 1969, 1970, and 1972 storms these differences are appreciable.

26. These results are only indicative of these specific tests and cannot be generalized to other input conditions. Based on this evaluation, the method 2 results were used to model the unidirectional series cases and the method 3 results for the directional series cases. Appendix A contains complete listings of the frequency spectrum and directional spectrum for the six unidirectional and six directional spectral cases.

Directional Wave Spectrum Parameterization

27. A directional or unidirectional wave spectrum $S(f,\theta)$ is usually parameterized as the product of two parts: a 1-D frequency spectrum $S(f)$ and a directional spreading function $D(f,\theta)$ as

$$S(f,\theta) = S(f) \ D(f,\theta) \tag{1}$$

where

  f - frequency

  θ - wave direction

The frequency spectrum and spreading function are subject to the following constraints:

$$S(f) = \int_0^{2\pi} S(f,\theta) \ d\theta \tag{2}$$

$$\int_0^{2\pi} D(f,\theta) \ d\theta = 1$$

20

YAQUINA BAY HINDCAST STUDY 1969 STORM SIMULATION
Wind-Sea and Swell vs. Swell Only Test
Wind Speed 43kt Wind Direction 82 deg (WIS)

SWELL ONLY
Hmo = 5.1m
TH = 15deg

WIND-SEA AND SWELL
Hmo = 6.8m
TH = 34deg

WIS SEA AND SWELL
Hmo = 7.0
th = 37deg

a. 1969 Storm

b. 1970 Storm

YAQUINA BAY HINDCAST STUDY 1970 STORM SIMULATION
Wind-Sea and Swell vs. Swell Only Test
Wind Speed 37kt Wind Direction 52 deg (WIS)

SWELL ONLY
Hmo = 4.8m
TH = 9deg

WIND-SEA AND SWELL
Hmo = 5.8m
TH = 17deg

WIS SEA AND SWELL
Hmo = 5.8m
TH = 18deg

Figure 5.   Shallow-water prototype directional spectra (Sheet 1 of 3)

21

c. 1972 Storm
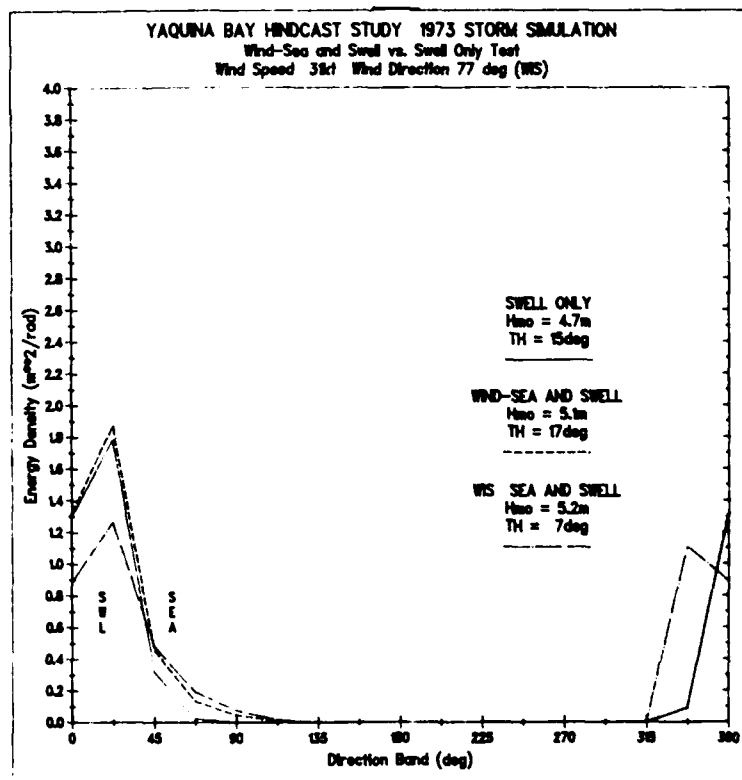
d. 1973 Storm

Figure 5.   (Sheet 2 of 3)

22

YAQUINA BAY HINDCAST STUDY 1974 STORM SIMULATION
Wind-Sea and Swell vs. Swell Only Test
Wind Speed 38kt Wind Direction 62 deg (WS)

SWELL ONLY
Hmo = 4.8m
TH = 21deg

WIND-SEA AND SWELL
Hmo = 5.9m
TH = 32deg
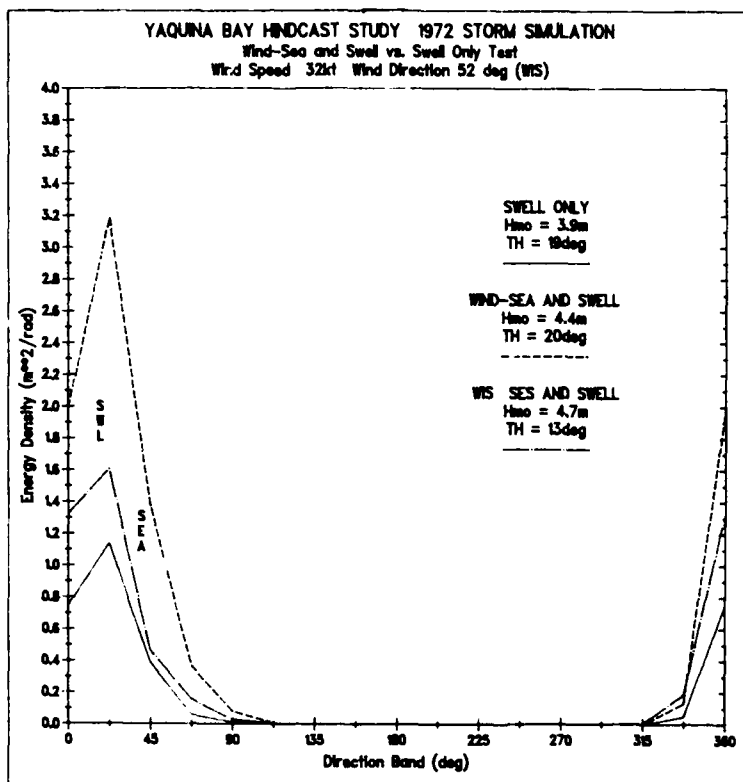
WS SEA AND SWELL
Hmo = 6.2m
TH = 30deg

e.   1974 Storm

f.   1983 Storm

YAQUINA BAY HINDCAST STUDY 1983 STORM SIMULATION
Wind-Sea and Swell vs. Swell Only Test
Wind Speed 33kt Wind Direction 43 deg (WS)

SWELL ONLY
Hmo = 5.1m
TH = 14deg

WIND-SEA AND SWELL
Hmo = 5.7m
TH = 18deg

WS SEA AND SWELL
Hmo = 6.2m
TH = 18deg

Figure 5.   (Sheet 3 of 3)

23

Detailed discussions of the frequency spectrum and spreading functions are in the paragraphs below.

Frequency spectrum

28. The desired or target frequency spectrum may be input in one of two ways. It can be calculated according to the formula for an empirical TMA or Ochi-Hubble or input discretely from a numerical or field observation. Any number of frequencies can be used, and the spectrum can be multimodal (i.e. with multiple peaks).

29. The depth-limited TMA spectral form is a function of five parameters: f_p , α , γ , σ , and water depth h . The first four parameters are those associated with the JONSWAP spectrum. The peak enhancement factor controls the peakedness of the spectrum and typically varies from 1 to 3.3 for sea conditions to 7 and higher for swell waves. Both α and γ influence the energy contained in the wave spectrum. Typical values for the left σ_a and right σ_b spectral width parameters are 0.07 and 0.09, respectively. Like the JONSWAP spectrum, a wide range of single peaked spectra may be simulated by varying these five parameters.

Directional spreading function

30. The directional spreading function may be either an empirical wrapped normal (Borgman 1984) or input discretely at even increments within 360 deg. Values of the spreading function between 181 and 359 deg are usually set to zero to prevent the simulation of incoming or reflected waves. The wrapped normal spreading function was used in this study. It is a function of the principal direction θ_m and the spreading standard deviation σ_m . Both are linear functions of frequency f , consisting of a constant and slope component. The fourier series representation for the wrapped normal spreading function is

$$D(f,\theta) = \frac{1}{2\pi} + \frac{1}{\pi} \sum_{\ell=1}^{L} \exp\left[\frac{-(\ell\sigma_m)^2}{2}\right] \cos \ell(\theta - \theta_m) \tag{3}$$

where

$$\sigma_m = \sigma_0 + \sigma_1(f - f_p)$$
$$\theta_m = \theta_0 + \theta_1(f - f_p)$$

The number of harmonic terms L is arbitrarily selected to adequately represent the fourier series of the directional spreading function. It can be of the order of 5, or as large as $6.0/\sigma_m$. For the unidirectional cases, both θ_1 and σ_1 were set to zero and σ_0 to 1.

31. The wrapped normal spreading function falls off rapidly for a unidirectional spectrum for differences in angle, $\theta - \theta_m$, greater than 0 deg. Table 5 illustrates this effect. Thus, care must be exercised in selecting the number of directional increments for simulating a unidirectional spreading function. A minimum of 36 increments (i.e. 10-deg intervals) will ensure that the angular difference never exceeds 5 deg.

<div align="center">

Table 5

Falloff of Wrapped Normal

Spreading Function

</div>

$\theta - \theta_m$ deg	$D(f,\theta)$ 1/rad
0	22.86
1	13.86
2	3.09
3	0.25
4	0.01
5	E-04
6	E-06
7	0.00

Wave Elevation Realizations

32. The psuedo-integral model for the unidirectional spectral surface elevation time series η at paddle location (x,y) and time t is

$$\eta(x,y,t) = 2 \int_0^\infty \int_0^{2\pi} A(f) \exp(-i\Phi) \exp(i\phi) \qquad (4)$$

where

$A(f)$ = amplitude function described below

Φ = independent random phase, uniformly distributed on $(0,2\pi)$

ϕ = kx cos θ + ky sin θ - 2πft

<div align="center">

25

</div>

k — wave number

θ — direction toward which waves travel, clockwise from x-axis

$i - \sqrt{-1}$

33. The model described by Equation 4 is a double summation model (Borgman 1969) since both frequency and direction are independent variables. Although this method is the preferred model to represent a directional sea, it is phase locked or phase dependent since different directions are summed at the same frequency. This phase locking gives a fluctuating RMS (i.e. variance of the variance) which tends to go to zero, however, as the number of fourier components becomes large (Pinkster 1984). Thus, a long time series should be used. An alternate model to the double summation model is the single summation model. This model is sometimes preferred because less computer time and space are required and possible phase locking is not a concern. In this model, a single direction is randomly selected for each frequency component. A procedure for selecting this single direction (Sand and Mynett 1987) is to assign a cumulative directional distribution for each frequency and select a value using a uniform random distribution U(0,1) .

Frequency domain simulation

34. Realizations of the desired time series described in Equation 4 for the specified directional wave spectrum are simulated in the frequency domain using one of two methods and then fourier transformed to the time domain. The first method is a DSA model, and the second method is a nondeterministic (Rayleigh) amplitude, random phase (NSA) model (Hudspeth et al. 1983, Elgar et al. 1984, Tucker et al. 1984, Isaacson 1985). Both methods are known also by other names, including the Random Phase Method for the DSA method and the Random Coefficient Method for the NSA method (Sand and Mynett 1987).

35. In the DSA method, the fourier coefficients are calculated from the target spectrum with the deterministic amplitude A constrained to be

$$A(f) = \sqrt{(2\ S(f,\theta)\ df\ d\theta)} \tag{5}$$

They are then coupled with random phases and inverse fourier transformed using a "235" FFT to give the surface elevation time series. The length of the time series N is the product of the integers 2, 3, and 5 raised to integer powers, as follows:

$$N = 2^K\ 3^L\ 5^M \tag{6}$$

26

In this method, the simulated spectrum always matches the target spectrum.

36. In the NSA method, Equation 4 is rewritten in an equivalent complex fourier series form. The complex amplitude A is defined by

$$A(f) = U(f) - i\, V(f) \qquad (7)$$

where

$U(f)$ = real amplitude component

$V(f)$ = imaginary amplitude component

Both components are independent Rayleigh random variables with zero means and variance $S(f,\theta)\, df\, d\theta$. These U and V components are obtained by first generating Gaussian distributed, zero mean, unit variance random variables which are then multiplied by the desired standard deviation, i.e., $\sqrt{(S(f,\theta)\, df\, d\theta)}$. The inverse method of generating new random variables from a normal distribution is used to obtain the U and V components. If the normal or Gaussian probability function is defined by

$$P(x) = u = \frac{1}{2\pi} \int_{-\infty}^{x} \exp\left(\frac{-t^2}{2}\right) dt \qquad (8)$$

then a new random variable x given by

$$x = P^{-1}(u) \qquad (9)$$

can be generated using the approximation from Abramowitz and Stegun (1970)

$$x = t - \frac{c_0 + c_1 t + c_2 t^2}{1 + d_1 t + d_2 t^2 + d_3 t^3} \qquad (10)$$

where

$$t = \sqrt{\left[\ln\left(\frac{1}{u^2}\right)\right]}$$

$c_0 = 2.515517$ $\qquad\qquad$ $d_1 = 1.432788$

$c_1 = 0.802853$ $\qquad\qquad$ $d_2 = 0.189269$

$c_2 = 0.010328$ $\qquad\qquad$ $d_3 = 0.001308$

Again, an inverse FFT gives the simulated wave elevation time series. The NSA method differs from the DSA method in that the simulated spectral estimates do not exactly match the target spectrum, but vary statistically about the true or desired spectral values. The variance of the variance is said to be more realistic than with the DSA method.

37. If there are many frequency and directional components in the wave train (i.e. of the order of 1,000 components), there is little difference between the DSA and NSA options for the complex wave amplitude. Both are asymptotically equivalent by the Central Limit theorem and behave very nearly as a Gaussian process in that case (Rice 1944, 1945; Elgar et al. 1985). However, with some increase in computer time, the addition of the Rayleigh variable in the complex amplitude produces an exact Gaussian process. This addition is particularly useful for wave trains which are very narrow banded in both frequency and direction.

38. In summary, the least random simulations involve the single summation model and the DSA method. The double summation model and NSA methods produce greater variance of the variance of the synthesized record. The procedures used in this study are predominantly the double summation model and the DSA method of frequency domain simulation.

Transfer Functions

39. Once the wave elevation time series have been simulated for each of the 61 DSWG paddles, they are converted to corresponding stroke time series using a height-to-stroke transfer function. The 3-D form F_3 , which includes directional effects (Sand 1979), was originally derived by Biesel (1954) and is valid for all nondimensional water depths kh , where h is still-water depth, and has the following form:

$$F_3(f) = \frac{2 \cosh (2kh - 1)}{\cos \theta \ [\sinh (2kh) + 2kh]} \tag{11}$$

Figure 6 illustrates how F_3 varies for frequencies between 0.05 to 2 Hz for the range of $\bar{\theta}$ of -2 and -21 deg used in this study. The wave breaking
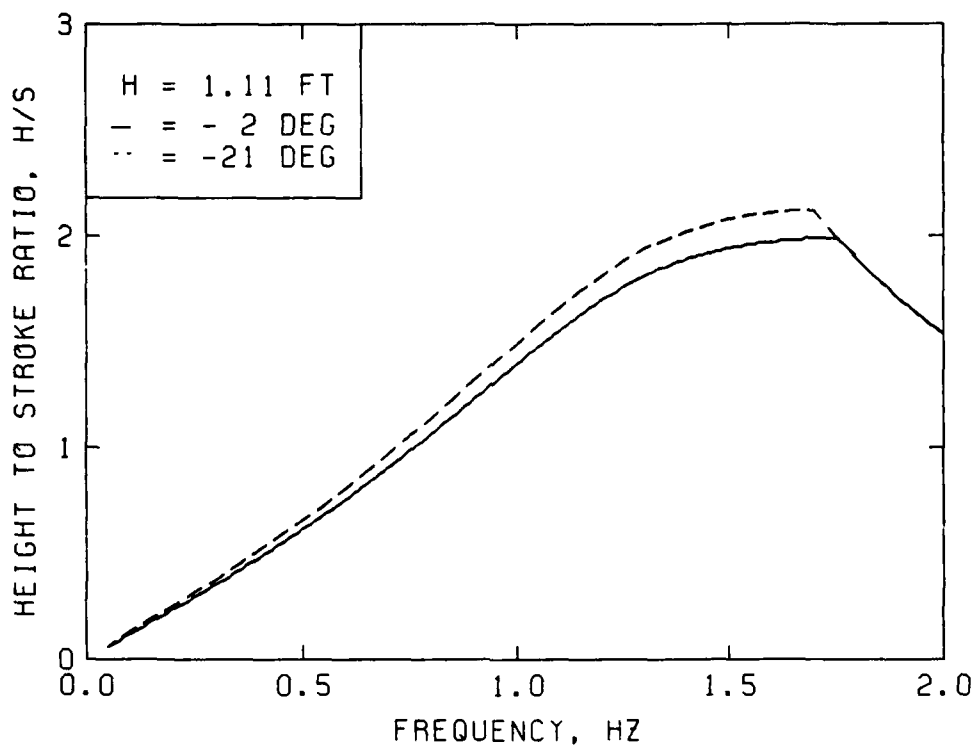
Figure 6. Height-to-stroke transfer function

limit at the higher frequencies is also shown. The highest wave which can be
generated at the wave maker is

$$H_b = 0.1 \ L \ \tanh kh \qquad\qquad (12)$$

where L is wavelength.*

40. Finally, the stroke time-history is converted to a voltage time-
history using the conversion factor for the wave maker. For the maximum
stroke of 12 in., the DSWG has a peak-to-peak voltage of 20 V in 4,096 digital
units. Thus, the conversion factor is 341.33 A/D units/in. or a resolution of
0.00293 in. per A/D unit.

---

* Personal communication, 1986, John Ahrens, Wave Research Branch, Wave
  Dynamics Division, Coastal Engineering Research Center, Vicksburg, MS.

PART III: SPECTRAL ANALYSIS THEORY

41.   Theoretical descriptions of the time series, directional spectra, and RAO transfer function analyses are presented in this part. In all analyses, it is assumed that the wave elevation time series is a discrete, real-valued time sequence with equal time intervals $t = n\Delta t$. The relationship between the total length of the time series T_r and the total number of points N is $T_r = N\Delta t$. The value of N , although even, does not have to be a power of 2. The basic frequency increment is defined by $\Delta f = 1.0/T_r$.

Time Series Analysis

42.   The time series analysis package performs both time and frequency domain analyses of measured surface elevation data. Currently, the package allows 12 different processes to be run on the data. Time domain processes include time series strip charts of the raw data, zero upcrossing or downcrossing, crest and trough height, and autocorrelation and cross correlation. Frequency domain processes include autospectra or cross spectra, frequency response between channels, coherence, and Goda reflection. Only two of the processes were used in this study: surface elevation time series strip charts and single channel spectral analysis. It is beyond the scope of this report to give a detailed description of the theoretical development of each process in the time series analysis.

43.   The strip chart option plots the raw time series data for one or more of the available gages. The time series have not been detrended. The plots are cross-scaled to facilitate readability.

44.   Spectral density estimates are calculated for individual gages after preprocessing to detrend and window the time series. Detrend options include removing the mean or a linear or second order trend. Window options include 10 or 50 percent cosine bell or cubic polynomial. The data are fourier transformed, band averaged between lower and upper cutoff frequencies, and plotted. Measured spectral estimates for each gage are saved for later use in calculating RAO estimates. Three different methods are used to calculate the peak frequency and corresponding period. The single line method gives the frequency having the largest energy content. The Delft method gives the mean frequency of all frequencies having energy content greater than or

equal to 80 percent of the maximum. The CERC method gives the center frequency of the band of 11 consecutive frequencies having the largest total energy density. Zeroth, first, and second moments are estimated. Goda's (1970) peakedness parameter Q_p is also calculated. Finally, the average period from the zeroth and second moments is estimated.

Directional Spectral Analysis

45. Four different methods for estimating $S(f,\theta)$ from an array of N surface wave gages are available. These are (a) an eigenfunction procedure, (b) a method based on the fourier series expansion of the directional spectrum, (c) the Maximum Likelihood Method (MLM), and (d) the Maximum Entropy Method (MEM). Because of its simplicity, only the fourier method is used here.

Spectral formulation

46. The fourier series method is based on the relation (Borgman 1979) that the autospectra $S_{ii}(f)$ and cross spectra $S_{ij}(f)$ between all pairs of wave elevation time series can be expressed as a linear combination of the directional components of $S(f,\theta)$ at that frequency. If the wave elevation time series η is defined as in Equation 4, then a system of equations for the spectral matrix of autospectrum and cross spectra in terms of $S(f,\theta)$ is

$$S_{ii}(f) = \int_0^{2\pi} S(f,\theta) \, d\theta \tag{13}$$

$$S_{ij}(f) = \int_0^{2\pi} S(f,\theta) \exp(iB_{ij}) \, d\theta \tag{14}$$

where

$B_{ij} = k \, X_{ij} \cos\theta + k \, Y_{ij} \sin\theta$

$X_{ij} = x_i - x_j$

$Y_{ij} = y_i - y_j$

x = x-axis gage coordinates at location i or j

y = y-axis gage coordinates at location i or j

The cross spectrum is composed of real cospectra C_{ij} and imaginary quadrature Q_{ij} components.

Parameterization of directional spectra

47. The first step toward solving the set of equations above is to parameterize $S(f,\theta)$ as the product of a frequency spectrum and a directional spreading function (Equation 1). The autospectral density $S_{ii}(f)$ for each of N gages is estimated, and then a combined best estimate $S(f)$ is obtained using a harmonic mean.

$$\overline{S}(f) = \left[\prod_{i=1}^{N} S_{ii}(f) \right]^{1/N} \tag{15}$$

The directional spreading function is initially approximated by a truncated fourier series expansion of L harmonics. Usually, a value of $L = 5$ is sufficient, although a larger number may be used. Also, the value of L used may be substantially different from the value used to create the spreading function, thus affecting the measured shape. (See Directional spreading function, paragraphs 30-31.)

$$D(f,\theta) = \frac{1}{2\pi} + \sum_{\ell=1}^{L} a_M(f) \cos (\ell\theta) + b_M(f) \sin (\ell\theta) \tag{16}$$

where

$a_M(f)$ = real fourier coefficient of the spreading function

$b_M(f)$ = imaginary fourier coefficient of the spreading function

Spectral estimation of measured data

48. The next step is to calculate measured autospectral and cross-spectral density estimates for each gage and each gage pair, respectively. A 10 percent cosine bell window is applied in the time domain, and the cross-spectral matrix is calculated using the "235" FFT.

49. A Gaussian smoothing function is then used to smooth the estimates. This procedure is like "band averaging" since raw spectral estimates are smoothed in the frequency domain. However, it tends to give a smoother transition since it is more of a weighted moving average in that overlapping

32

is used. The Gaussian smoothed line spectra $\bar{S}_m$ for each frequency $m\Delta f$ is defined as

$$\bar{S}_m = \frac{\displaystyle\sum_{j=-J}^{J} w_j \, S_{m-j}}{\displaystyle\sum_{j=-J}^{J} w_j} \qquad (17)$$

where w_j is a weighting function defined below, and S_{m-j} is the raw autospectral or cross-spectral estimate at frequency $(m-j)\,\Delta f$. The weights are defined over an integer number of spectral lines J equivalent to 3σ standard deviations of a Gaussian curve.

$$w_j = \exp\left[-\frac{(j\Delta t)^2}{2\sigma}\right] \qquad (18)$$

Since the area under a Gaussian curve equals $\sqrt{(2\pi)}\sigma$, an equivalent rectangle having the same area has a height of 1.0 (at x = 0) and a bandwidth b defined by

$$\sigma = \frac{b}{\sqrt{(2\pi)}} \qquad (19)$$

50. For Gaussian smoothing the number of bands averaged in each smoothed spectral estimate is considerably greater than a comparable frequency domain band averaging procedure. In band averaging, the resolution bandwidth b is the product of the number of bands averaged and the basic frequency increment Δf of the line spectra. In Gaussian smoothing the number of bands M in the smoothed average is given by

$$M = \frac{6\sigma}{\Delta f} \qquad (20)$$

33

Solution procedure

51. The S_{ii} for each gage are inserted into the left-hand side of Equation 13. They are also substituted into Equation 15 to calculate S. The $\overline{S}_{ij}$ are calculated for each pair of gages and substituted into the left-hand side of Equation 14. The estimate for $\overline{S}$ and the parameterized directional spreading function $D(f,\theta)$ is substituted into the right-hand side of Equation 14 for $S(f,\theta)$. Thus, for N gages, a set of N^2 simultaneous linear equations (i.e. N autospectral equations of the form of Equation 13 and $N(N - 1)/2$ pairs of cross-spectral equations of the form of Equation 14) can be solved for the fourier coefficients of the spreading function. However, since some of these equations may be theoretically zero, the number of available equations is usually less than N^2. The matrix form of this set of equations is

$$\{SPECTRA\} = [TRANSFER] * \{DIR\} \tag{21}$$

The vector $\{SPECTRA\}$ consists of the measured S_{ij} estimates. The vector $\{DIR\}$ is composed of the fourier coefficients for $D(f,i)$ at frequency f and is to be estimated. The matrix $[TRANSFER]$ is therefore

$$[TRANSFER] = \int_0^{2\pi} \begin{bmatrix} \cos \\ \\ \sin \end{bmatrix} (B_{ij}) \begin{bmatrix} \cos \\ \\ \sin \end{bmatrix} (\ell\theta)\, d\theta \tag{22}$$

52. For an array of surface gages, Equation 22 could be expressed in the form of Bessel functions of order 1 (Borgman 1969, Borgman and Panicker 1970). Since the number of available equations (i.e. N^2) is greater than the number of unknown fourier coefficients (i.e., 10 coefficients for five harmonics), a least squares fourier transform method for numerical integration is used. The first step is inversion of the $[TRANSFER]$ matrix to solve for the a_M and b_M spreading coefficients contained in the vector $\{DIR\}$. The technique for doing this is based on the vector linear regression model, as follows:

$$\{Y\} = [X] * \{B\} + \{\epsilon\} \tag{23}$$

34

where

> (Y) - n-component vector of dependent variables
>
> [X] - n × k matrix of independent variables
>
> (B) - k-component vector of regression coefficients
>
> (ε) - n-component vector of prediction errors

The least square solution for (B) is given by the solution to the "normal equations"

$$([X]' * [X]) * (B) - [X]' * (Y) \tag{24}$$

where the prime denotes the matrix transpose. Principal components regression is used to invert Equation 21 based on the development of the Moore-Penrose generalized inverse from the eigenvector analysis of (X' * X) (Searle 1982).

53. The advantage of the fourier method is its simplicity. The disadvantage is the arbitrary truncation of the fourier series at L (-5) harmonics where this number of coefficients (i.e. 2L + 1) is considerably less than the number of equations available. Stepwise regression tends to minimize this truncation effect. Jennrich (1977) specifies this least squares procedure which sequentially selects the "best" first harmonic coefficients. Next, "best" second harmonic coefficients are added and another least squares iteration is performed with all coefficients. This procedure continues with "best" higher order harmonic coefficients being added one at a time until little improvement is realized after a least squares iteration.

54. The use of eigenvalue analysis helps to overcome the disastrous effects of an almost singular (X' * X) matrix in Equation 24. It provides a number of eigenvalues which are significantly nonzero as an upper limit on the number of coefficients which can be estimated with the stepwise regression technique.

55. The $D(f,\theta)$ given in Equation 16 results in a distorted estimate of the true spreading function due to the truncation. This estimate is improved by fitting a parameterized wrapped normal formula (Equation 3) to the spreading function (Borgman 1979). Assuming that the lower order fourier coefficients are the least distorted by the truncation, they are used in the parameterized model to obtain estimates of the higher order coefficients. A new set of fourier coefficients (both lower and higher order) is calculated using an iterative procedure until convergence is reached.

Principal direction and directional spread

56. If the wrapped normal spreading function is defined as in Equation 3, the full-circle fourier coefficients a_M and b_M are

$$\begin{bmatrix} a_M(f) \\ b_M(f) \end{bmatrix} = \frac{1}{\pi} \int_0^{2\pi} D(f,\theta) \begin{bmatrix} \cos \\ \sin \end{bmatrix} (\ell\theta) \, d\theta \tag{25}$$

The corresponding coefficients for the first harmonic a_1 and b_1 are then

$$\begin{bmatrix} a_1(f) \\ b_1(f) \end{bmatrix} = \frac{1}{\pi} \begin{bmatrix} \cos \\ \sin \end{bmatrix} \theta_m \exp\left(\frac{-\sigma_m^2}{2}\right) \tag{26}$$

Therefore, the principal direction θ_m at frequency f is

$$\theta_m(f) = \arctan\left(\frac{b_1(f)}{a_1(f)}\right) \tag{27}$$

The mean of all θ_m over all frequencies for all selected gages equals $\bar{\theta}$.

57. Taking the magnitude of Equation 26 and rearranging gives the directional spread or standard deviation σ_m at frequency f

$$\sigma_m(f) = \sqrt{\left(-2\ell n \left\{\pi \sqrt{\left[a_1^2(f) + b_1^2(f)\right]}\right\}\right)} \tag{28}$$

58. At each frequency $(N - 1)$ independent estimates of each fourier coefficient are obtained. Various methods, including a weighted average or least squares, could be used to select a "best" choice. A simple average is used. A similar set of equations could be obtained for θ_m and σ_m if the second or higher order harmonic coefficients were used.

RAO Functions

59. The height-to-stroke transfer function discussed in Part II is based on theoretical, ideal hydromechanical aspects of wave generation. Because of leakage around and under a "wetback" wave maker, electronic and

36

mechanical losses of the DSWG, and basin response characteristics, the desired wave spectrum is usually not faithfully reproduced. Although the differences in spectral shape, peak period, and wave height may be slight, it is necessary to correct the control signal for accurate reproduction in future runs. Thus, an RAO transfer function is calculated.

60. The raw measured S_{ii} for each gage and predicted S_p spectral estimates are first Gaussian smoothed (see paragraph 50) to a desired bandwidth which must be equal to or greater than Δf. The RAO is then calculated in the frequency domain at each smoothed frequency as

$$RAO_i(f) = \sqrt{\frac{S_{ii}(f)}{S_p(f)}} \qquad i = 1,2,3,\ldots N \qquad (29)$$

An average of all points within each band or the midpoint in each band may be selected for each band. In addition to RAO's for individual gages, an average of all or a selected number of gages may be calculated. The RAO is set equal to 1.0 for those frequencies outside lower and upper cutoff frequencies (IAHR 1987) because of low signal-to-noise ratios. Also, RAO's greater than 10.0 or less than 0.1 are set to these respective upper and lower limits.

61. The stroke control signals s_c for each of the 61 paddles which produced the measured spectra are fourier transformed to the frequency domain for correction. The real and imaginary fourier coefficients U and V are divided at each frequency $m\Delta f$ by the appropriate value of the smoothed and averaged RAO. The RAO for an individual gage or an average of selected gages can be used. The fourier transform relationship is

$$U(m) - i\ V(m) = \Delta t \sum_{n=0}^{N-1} s_c(n\Delta t)\ \exp\left(\frac{-i2\pi mn}{N}\right) \qquad (30)$$

The corrected fourier coefficients are then inverse fourier transformed to the time domain to give the new control signal

$$s_c(n\Delta t) = \Delta f \sum_{m=0}^{N-1} [U(m) - iV(m)] \exp\left(\frac{i2\pi mn}{N}\right) \tag{31}$$

The square root in Equation 29 is necessary because spectral estimates are squared quantities of the fourier coefficients

$$S_{ii}(m) = \frac{1}{T_r}\left[U^2(m) + V^2(m)\right] \qquad i = 1,2,3,\ldots N \tag{32}$$

62. The maximum crest and minimum trough digital values are 2,048 and -2,047, respectively. The digital control signals for the DSWG are low-pass filtered and converted to analog form at run time. If the slope on a crest or trough is too steep near these maximum values, the paddles tend to overshoot, and protective displacement sensors shutdown the system to prevent damage. These system limits pose a problem for spectra with long peak periods and high wave heights. If the maximum crest and minimum trough values are reduced, a buffer zone is created to compensate for this overshoot without shutting the system down. Too small a value will not help the overshoot phenomenon. Too large a value will cause an excessive number of crests and troughs to be reduced, causing more overshoot and excessive low-frequency energy content. A value of ±50 digital units, or 2.5% of the total stroke (i.e. 50/2,048), was used in this study. The new maximum and minimum values were 1,948 and -1,947 units, respectively. The effect of this compensation on the resulting spectra and transfer functions is expected to be minimal.

PART IV: TEST SETUP

Yaquina Bay Physical Model

63. Yaquina Bay is an estuary located on the Oregon coast approximately 110 miles south of the mouth of the Columbia River (Figure 7). Two rubble-mound jetties protect the 40-ft-deep, 400-ft-wide entrance channel which passes through a narrow opening in an offshore reef. This basaltic reef lies 3,500 ft seaward of river mile 0.0 and extends northward for approximately 17 miles from a point 2,500 ft south of the channel. The parallel jetties were constructed on an azimuth of S62°W and offer excellent protection against waves from the west and northwest.
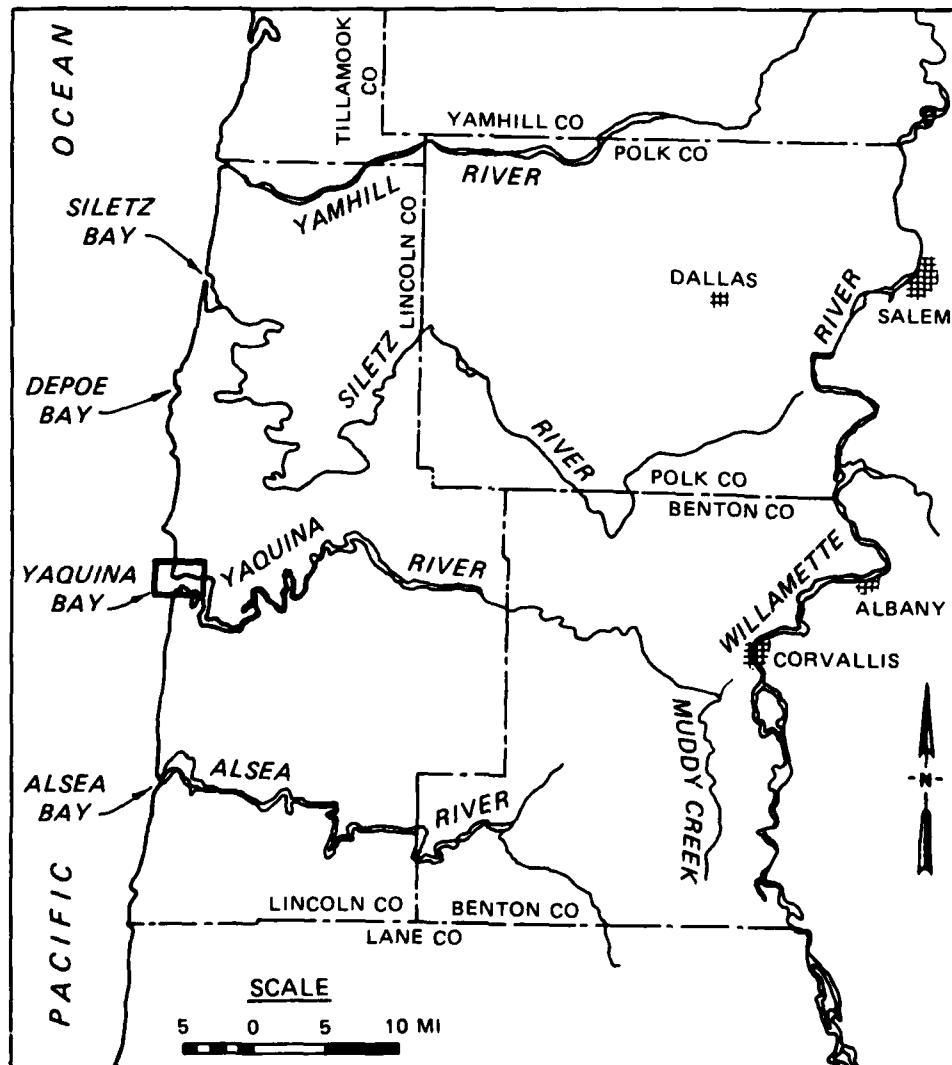
Figure 7. Yaquina Bay, Oregon, location map

39

64. A 3-D physical model was constructed at an undistorted scale of 1:45, model to prototype, based on several factors, including (a) DSWG size and capabilities, (b) required nearshore bathymetry, (c) available stone sizes, and (d) preclusion of scale effects. Thus, it was not possible to model the entire entrance channel, nearshore bathymetry, and inner harbor. Since the main focus of the study was on the jetty head area, only 32 ft of the north jetty and 21 ft of the south jetty were modeled. The nearshore bathymetric features and offshore reef were duplicated to the extent that further wave transformation prior to interacting with the channel entrance was properly modeled. Thus, the DSWG was located at a depth corresponding to 58 ft mllw prototype (1.29-ft model). Figure 8 is a schematic of the wave basin illustrating the complex bathymetry modeled in this study. The north jetty was meticulously constructed to ensure accurate as-built conditions.
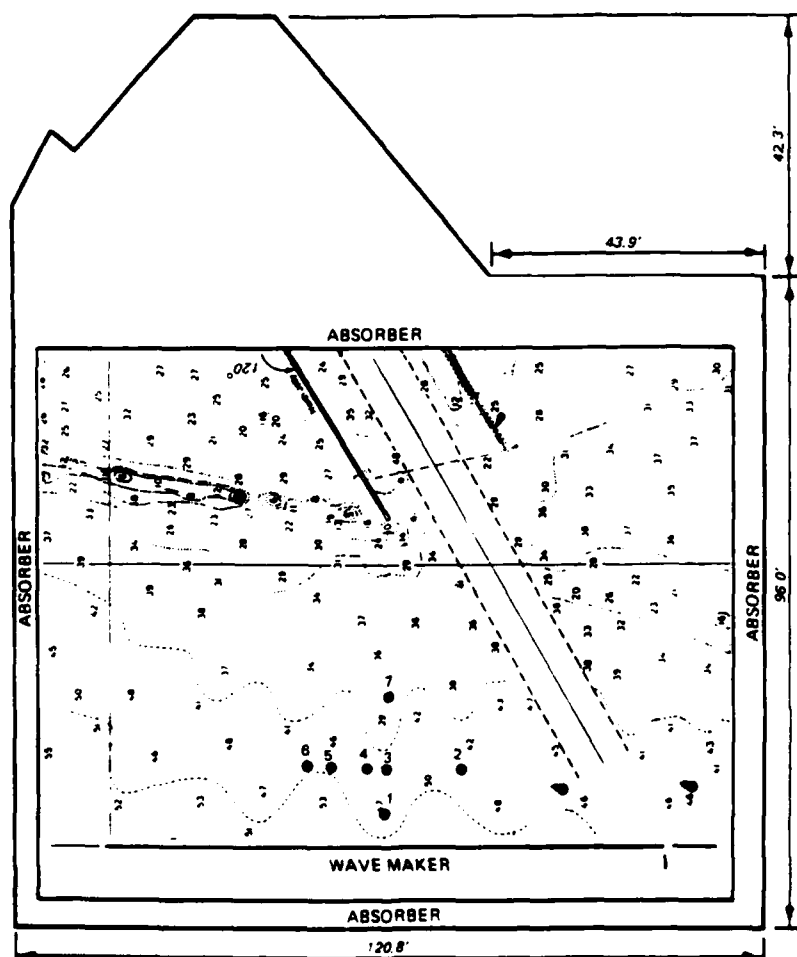

Figure 8. Schematic of DSWG basin, model
contours, and gage locations

The interested reader is referred to a report by Grace and Dubose (1988) for a detailed description.

Wave Basin and Generator

Wave basin

65. The study was conducted in CERC's 96-ft-long by 121-ft-wide directional spectral wave basin. The basin has a unique beach/wave absorption system. The perimeter was lined with wave absorber frames consisting of 2-in. layers of rubberized horsehair installed between two layers of expanded sheet metal. Flume tests by Briggs and Barnes* (unpublished) for a range of wave periods and heights demonstrated the effectiveness of the frame design. The average measured reflection coefficient of 12 percent is equivalent to a comparable gravel beach with a slope of 6 to 11 deg which could be installed in the basin. Additional wave absorption was provided behind the beach segments by two rows (4 ft) of horsehair extending through the water column.

Directional spectral wave generator

66. The directional spectral wave generator (DSWG) is an electronically controlled, electromechanical system. It is 90 ft long and consists of 60 paddles in four modules of 15 paddles each. Each paddle is 1.5 ft wide and 2.5 ft high. The paddles are independently driven in translational motion at each of the 61 joints by 0.75-hp electric motors. In each joint is a flexible-plate seal to provide continuity and minimize the introduction of spurious waves (Outlaw and Briggs 1986).

Wave Elevation Measurement System

Gage arrangement

67. Seven capacitance wave gages were used to measure surface wave elevations in the basin. They were mounted in aluminum frames to minimize interference due to support legs and arranged in a directional array. Embedded in this array was a five-gage linear array patterned after the larger linear array design of Oltman-Shay at CERC's Field Research Facility (Crowson et al. 1988). The linear array provides superior resolution capability for wave components at or near the same frequency and slightly different

---

* M. J. Briggs and L. Barnes, 1987, "Passive Wave Absorber Design for Laboratory Basins" (Unpublished).

directions. This capability results if the waves are directional or have been refracted.

68. A well-designed linear array must have a total length equal to the largest wavelength (i.e. lowest frequency) at the largest angle expected. It also must be short enough to avoid aliasing the higher frequency, smaller wavelength components. Spatial aliasing occurs when half the wavelength of the highest frequency wave does not exceed the distance between sensors. When this happens, it is impossible to discern the smaller wave from the longer wave. Thus, there is a classic tradeoff in that we want the longest array to optimize resolution of the low-frequency components and the shortest spacing to minimize aliasing of the high-frequency waves. The secret to this tradeoff is to select a minimum distance between two sensors which minimizes aliasing at the high-frequency cutoff desired while simultaneously providing an overall length which optimizes resolution at the low-frequency cutoff. By clever arrangement of a limited number of gages, both objectives can be achieved. Rather than the gages being spaced a uniform distance apart, they are spaced at multiples of a unit lag length based on the criteria above. Thus, all wavelengths between the smallest and longest are covered by combinations of various gages. For the 2-3-1-7 array (i.e. gages spaced 2 lag lengths, 3 lag lengths, etc.), wave periods with half wavelengths equal to 1, 2, 3, 4, 5, 6, 7, 8, 11, and 13 lags are discernible.

69. The procedure consists of calculating the depth-limited wavelength for the low- and high-frequency cutoffs desired. The y-axis wave number component k_y is calculated as

$$k_y = k \sin \theta \tag{33}$$

where a maximum wave direction to the linear array of $\theta = 21$ deg was assumed. The orientation of the x- and y-axes is shown in Figure 8, and the wave direction is measured clockwise from the x-axis. The corresponding y-axis wavelength component L_y is then

$$L_y = \frac{2\pi}{k_y} \tag{34}$$

Finally, the array length capable of resolving this wavelength is equal to one-third to one-half of L_y . Based on this procedure, a lag spacing of

42

24 in. (2.0 ft) was selected for this study.

70. The two remaining gages (#1 and #7) were positioned in front of and behind the linear array for redundancy and possible reflection analysis. Gage #7 was not available for use during all of the tests. Table 6 summarizes the x- and y-axis coordinates of each of the seven gages in the directional array. Figure 8 illustrates the gage locations for the seven gages relative to the DSWG and the model contours.

Table 6

Directional Array Coordinates

Gage No.	X-axis, ft	Y-axis, ft
1	5	45
2	10	31
3	10	45
4	10	47
5	10	53
6	10	57
7	20	45

Gage and depth calibration

71. The measurement rods on the gages had an overall length of 12 in. They were calibrated over an 8-in. range each day prior to conducting tests. A Jordan controller stepper motor was used to automatically raise and lower the rod through a series of 11 steps to obtain calibration coefficients using a least squares linear or quadratic fit. This averaging technique, using 21 voltage samples per gage, minimizes the effects of slack in the gear drives and hysteresis in the sensors. Table 7 lists the quadratic fit, maximum deviation calibration coefficients (in units of feet times 10^{-5}) for each gage for each day of testing. The water depth was maintained within ±0.001 ft of the desired level by an automatic water level float and solenoid control valve.

Data Acquisition and Control System

72. An automated data acquisition and control system (ADACS) is used to create wave generator control signals for each of the 60 wave paddles, monitor wave paddle displacement feedback, and collect and analyze time series experimental data from the wave basin. The ADACS is controlled by a DEC VAX 11/750 central processing unit with capability for digital control signal

43

Table 7

Spectral Stability Tests, Quadratic Fit Calibration Coefficients for Capacitance Wave Gages, Yaquina Bay Jetty Stability Study in DSWG Basin*

No.	Date & Time	Gage No.							Min	Max	Avg.
		RD01	RD02	RD03	RD04	RD05	RD06	RD07			
1	Jul 17, 1987	124	100	286	171	363	333	328	100	363	231
2	Jul 22, 1987	086	111	202	260	370	329	360	086	370	228
3	Oct 16, 1987	220	**	238	215	330	277	266	215	330	272
4	Oct 20, 1987	130	306	190	231	080	099	**	080	306	193
5	Dec 01, 1987	158	259	224	171	167	281	234	158	281	219
6	Dec 02, 1987	258	346	141	187	073	099	216	073	346	209
7	Feb 16, 1988	158	399	323	110	452	236	380	110	452	281
		1,134	1,521	1,604	1,345	1,835	1,654	1,784	822	2,448	1,633
	Average:	162	253	229	192	262	236	255	117	349	233

* Maximum deviation values (x 10^{-5} ft).
** Calibration coefficients misplaced.

44

output through an IEEE 488 interface and 120 channels of analog to digital input (Briggs and Hampton 1987). The DSWG control signal is updated at a rate of 20 Hz.

Test Case Description

73. The numerically transformed shallow-water storms described in Part II (Table 4) were converted for use in the DSWG using the 1:45 scale. Table 8 summarizes the model parameters for the six unidirectional and six

Table 8

Target Model Wave Parameters*

Storm ID	Period sec	Height in.	$\overline{\theta}$ deg	γ	Approximate σ_m deg	α
			Unidirectional Series			
1969	2.49	5.95	-15	1.6	1	0.01290
1970	2.13	5.07	-9	1.9	1	0.01300
1972**	1.86	3.85	-19	31.0	1	0.00001
1973†	2.13	4.46	-15	27.0	1	0.00100
1974	2.49	5.16	-21	2.2	1	0.00950
1983	2.49	4.99	-14	2.7	1	0.00834
			Directional Series			
1969	2.49	6.12	-10	1.6	30	0.01290
1970	2.13	5.07	-2	1.9	20	0.01300
1972**	2.13	4.11	-11	31.0	20	0.00001
1973†	2.13	4.55	-4	27.0	20	0.00100
1974	2.49	5.42	-21	2.2	10	0.00950
1983	2.49	5.42	-9	2.7	10	0.00834

* All cases used $\sigma_a = 0.07$ and $\sigma_b = 0.09$ except 1972 and 1973 cases.
** 1972, $\sigma_a = 0.99$ and $\sigma_b = 0.35$.
† 1973, $\sigma_a = 0.99$ and $\sigma_b = 0.25$.

directional cases. These 12 cases consisted of three different periods with unique H_{mo} and $\overline{\theta}$ values for each case. The value of $\overline{\theta}$ used in the unidirectional cases was selected based on the swell direction from the hindcasted cases. The values of γ and α listed in the table are approximate, based on a TMA spectral shape (Vincent 1984). The value of σ_m was visually determined from plots of the target directional spectra.

74. These cases were inadvertently generated for a water depth of

45

1.11 ft (i.e. 50-ft prototype). The required water depth at the DSWG was actually 1.29 ft (i.e. 58-ft prototype). Thus, the control signals were run initially at a depth of 1.11 ft (series U1 and D1), corrected using the RAO transfer function, and rerun at the correct depth of 1.29 ft (series U2 and D2). The corrected control signals were then run at the deeper storm depth of 1.51 ft (series U3 and D3). Table 9 summarizes the 18 unidirectional and 18 directional test cases run in this calibration phase. The first series was generated without the model contours in place (i.e. flat bottom). A gain factor of 0.95 was required for the 1969 and 1983 storms in the D2 and D3 series because of DSWG stroke and velocity limitations for the long periods.

Test Case Parameters

Simulation and generation phase

75. The DSA method of frequency domain simulation was used for all cases. Discrete values of the scaled frequency spectrum were used for both unidirectional and directional spectral cases. For the unidirectional cases, a wrapped normal spreading function was calculated with a directional increment of 5 deg (i.e. 72 increments). Discrete values from the WIS shallow-water spectra at 22.5 deg (i.e. 16 increments) were input for the directional spectral cases.

76. The D/A rate for the DSWG is 20 Hz (i.e. time increment of 0.05 sec), so 61 time series of 12,000 points, or 600-sec record length, were generated. This record length corresponds to an even frequency increment of 0.00167 Hz or 1,171 frequencies between the lower and upper cutoff frequencies of 0.05 to 2.0 Hz.

Data collection and analysis phases

77. **Data collection.** After a waiting time of 25 sec (35 sec for U2 series only) to allow slower traveling high-frequency components to travel beyond the farthest gage, wave elevation data were sampled at 10 Hz (i.e. time increment of 0.1 sec). A minimum of 200 waves at the peak period was collected as recommended by Goda (1985). Table 10 lists the record lengths, number of points collected in a record, and the frequency increment for each of the three peak wave periods.

78. **Frequency spectral analysis.** The complete data records were zero-meaned, tapered by a 10 percent cosine bell window, and band averaged

Table 9
Summary of Test Cases

Test Code	Test ID	Storm Year	Depth ft	No. Gages	Contours	Gain
			Unidirectional Series			
69U1	YS69022	1969	1.11	7	No	1.00
70U1	YS70022	1970	1.11	7	No	1.00
72U1	YS72021	1972	1.11	7	No	1.00
73U1	YS73021	1973	1.11	7	No	1.00
74U1	YS74022	1974	1.11	7	No	1.00
83U1	YS83022	1983	1.11	7	No	1.00
69U2	YS6903S	1969	1.29	7	Yes	1.00
70U2	YS7003S	1970	1.29	7	Yes	1.00
72U2	YS7203S	1972	1.29	7	Yes	1.00
73U2	YS7303S	1973	1.29	7	Yes	1.00
74U2	YS7403S	1974	1.29	7	Yes	1.00
83U2	YS8303S	1983	1.29	7	Yes	1.00
69U3	YS69032	1969	1.51	7	Yes	1.00
70U3	YS70031	1970	1.51	6	Yes	1.00
72U3	YS72031	1972	1.51	6	Yes	1.00
73U3	YS73031	1973	1.51	7	Yes	1.00
74U3	YS74031	1974	1.51	7	Yes	1.00
83U3	YS83031	1983	1.51	6	Yes	1.00
			Directional Series			
69D1	YD6903	1969	1.11	7	No	1.00
70D1	YD7003	1970	1.11	7	No	1.00
72D1	YD7203	1972	1.11	7	No	1.00
73D1	YD7303	1973	1.11	7	No	1.00
74D1	YD7403	1974	1.11	7	No	1.00
83D1	YD8303	1983	1.11	7	No	1.00
69D2	YD69036	1969	1.29	7	Yes	0.95
70D2	YD70036	1970	1.29	7	Yes	1.00
72D2	YD72036	1972	1.29	7	Yes	1.00
73D2	YD73036	1973	1.29	7	Yes	1.00
74D2	YD74036	1974	1.29	7	Yes	1.00
83D2	YD83036	1983	1.29	7	Yes	0.95
69D3	YD69037	1969	1.51	7	Yes	0.95
70D3	YD70037	1970	1.51	6	Yes	1.00
72D3	YD72037	1972	1.51	6	Yes	1.00
73D3	YD73037	1973	1.51	7	Yes	1.00
74D3	YD74037	1974	1.51	7	Yes	1.00
83D3	YD83037	1983	1.51	6	Yes	0.95

within the lower and upper cutoff frequencies of 0.2013 and 1.476 Hz, respectively. Table 10 lists the frequency dependent frequency spectral analysis parameters. A different number of spectral bands was averaged to achieve the same resolution bandwidth of 0.0671 Hz in each case.

79. _Directional spectral analysis._ The data were again zero-meaned, tapered by a 10 percent cosine bell window, and smoothed with a Gaussian smoothing function with an effective width of 0.0671 Hz between the same lower and upper cutoff frequencies. Because of the limitations of the "235" FFT, not all of the data for the 1.86- and 2.49-sec peak period cases were analyzed. Table 10 also lists the relevant parameters for the directional spectral analysis. The directional spreading increment used was 22.5 deg (i.e., 16 increments). This is the same increment generated by the WIS hindcast model. The predicted values were calculated without tapering the control signals.

Table 10

Collection and Analysis Parameters

Description	Peak Period, sec		
	$T_p = 1.86$	$T_p = 2.13$	$T_p = 2.49$
Data Collection			
Record length, sec	373	432	507
No. points in record	3,730	4,320	5,070
Frequency increment, Hz	0.0027	0.0023	0.0020
Frequency Spectral Analysis			
Record length, sec	373	432	507
No. points in record	3,730	4,320	5,070
Frequency increment, Hz	0.0027	0.0023	0.0020
Smoothed bandwidth, Hz	0.0670	0.0671	0.0671
No. frequency components analyzed	476	552	647
No. frequency components smoothed	25	29	34
Degrees of freedom	50	58	68
Directional Spectral Analysis			
Record length, sec	364.5	432	500
No. points in record	3,645	4,320	5,000
Frequency increment, Hz	0.0027	0.0023	0.0020
Smoothed bandwidth, Hz	0.0671	0.0671	0.0671
No. frequency components analyzed	466	553	640
No. frequency components smoothed	59	69	80

PART V: TEST RESULTS AND ANALYSIS

80.   In this part, test results are presented and discussed for surface
elevation time series, frequency spectra, directional spreading functions,
response amplitude operator, peak wave periods, and zero-moment wave heights.
The 1974 storm is representative of the six storms and is used throughout as
an example. For the unidirectional series, cases 74U1, 74U2, and 74U3 are
used. Similarly, cases 74D1, 74D2, and 74D3 are used for the directional
series. Results from both series for the other five storms are contained in
Appendices B-F.

Surface Elevation Time Series Plots

81.   The measured wave elevation time series for the three unidirec-
tional cases are shown in Figure 9. The directional cases are shown in
Figure 10. Plots for the other 17 unidirectional and 17 directional cases are
included in Appendix B. Only gages 1, 3, and 4 are shown because they are
least affected by the bathymetry. The x-axis length is 500 sec for all cases,
and the y-axis scales have increments of 0.60 ft.

82.   The effect of the RAO correction can be seen by comparing the size
of the trace between U1 and U2 series (Figures 9a and 9b) and D1 and D2 series
(Figures 10a and 10b) cases. The effect of the deeper water depth of 1.51 ft
can be seen by comparing the second and third series plots (i.e., Figures 9b
and 9c for the unidirectional and 10b and 10c for the directional series).

Frequency Spectra

83.   Figure 11 illustrates the measured versus predicted frequency
spectra for the three unidirectional cases: U1, U2, and U3. The correspond-
ing graphs for the directional series D1, D2, and D3 are shown in Figure 12.
Plots of the other cases are included in Appendix C. The x-axis is from 0 to
2.0 Hz. The y-axis ranges from 0 to 0.08 ft^2/Hz. The dashed line is the
predicted spectrum for a depth of 1.29 ft, and the solid line gives the
measured average spectrum for gages 1, 3, and 4.

84.   Although the target spectral shape of all series 1 unidirectional
and directional cases was measured, the spectral amplitude was smaller than
the desired target value. The series 2 plots show the effectiveness of one
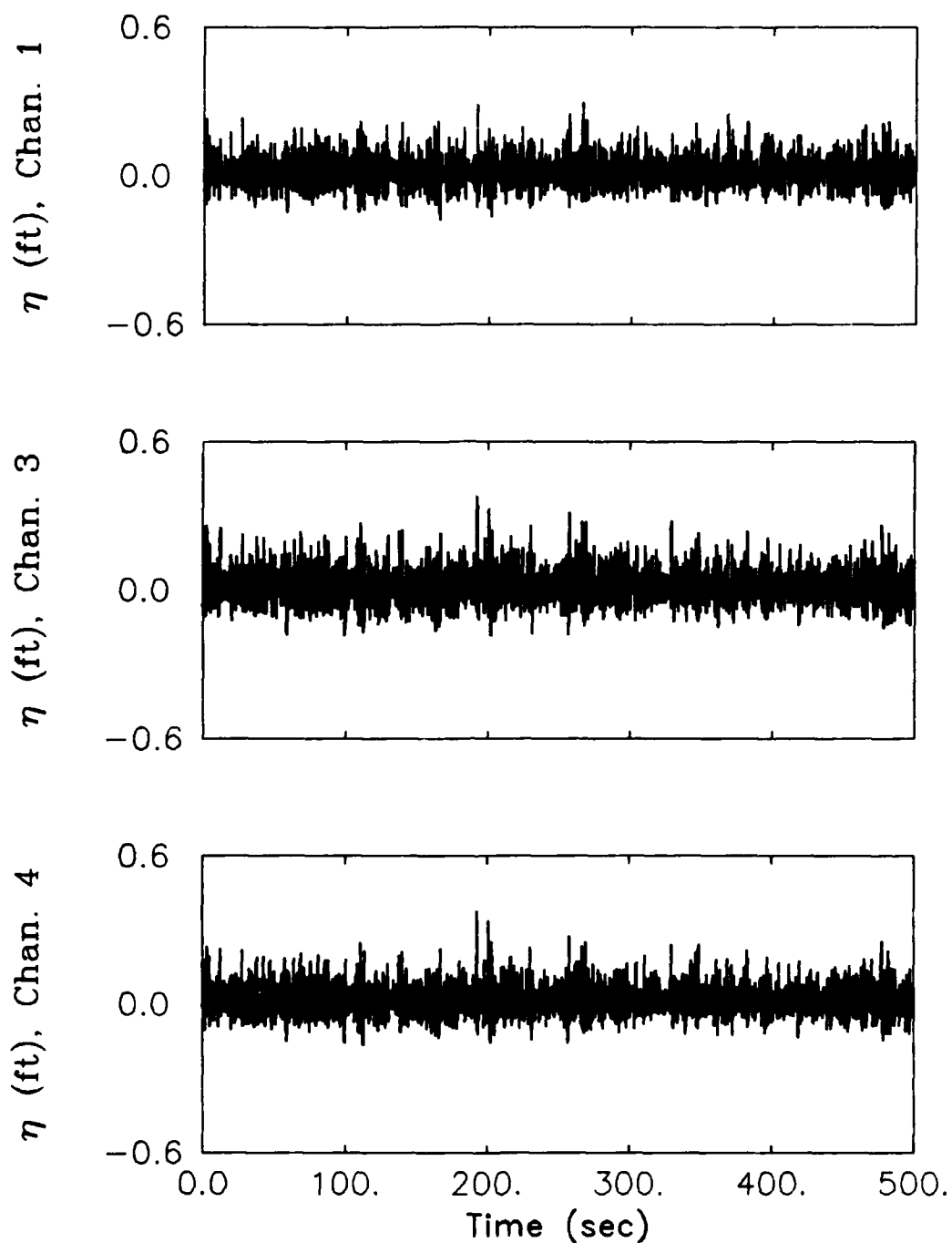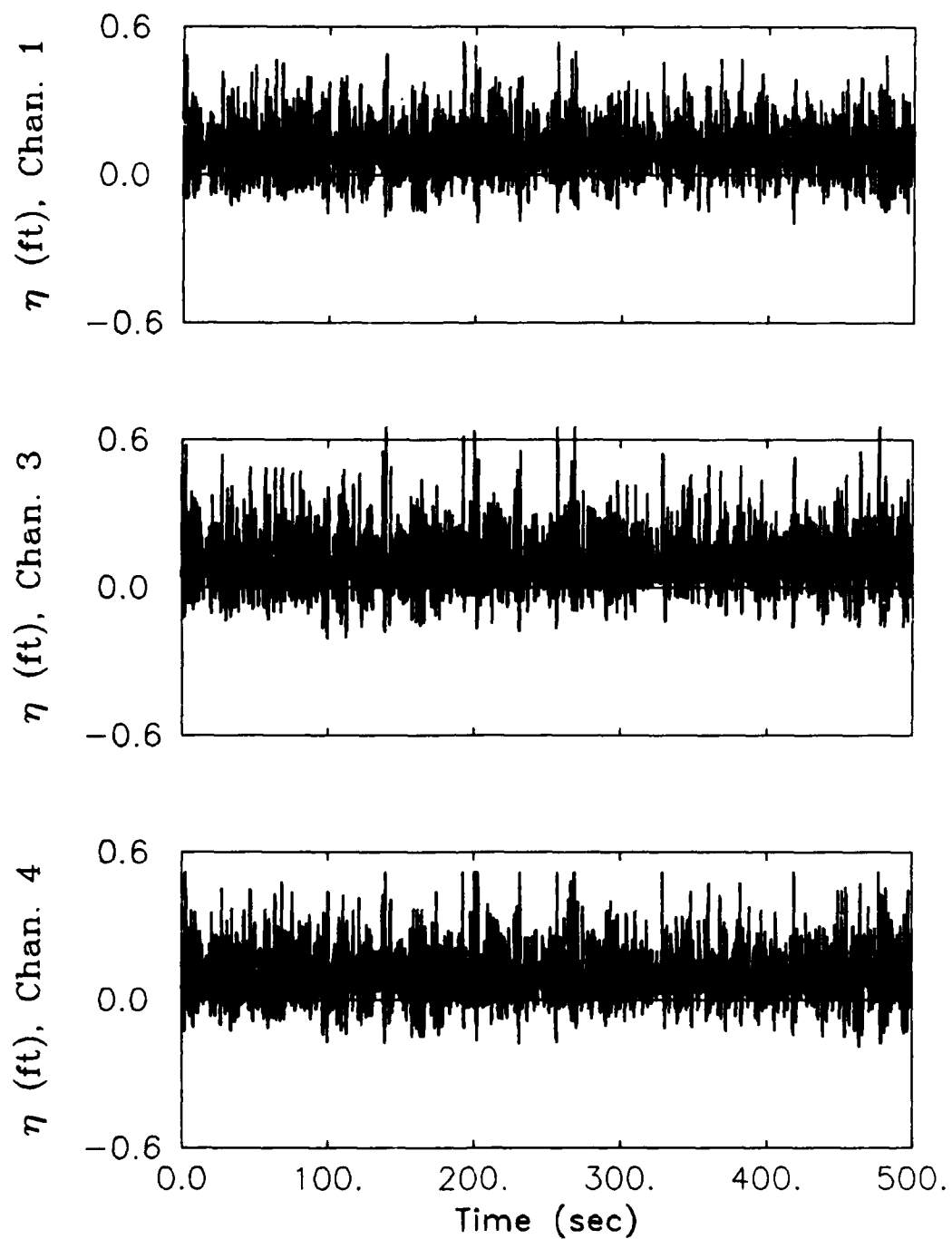
**Measured Wave Elevation Time Series
CASE 74U1 -- Fp=.4, Hm0=5.16, H=1.11**

a.   Case 74U1

Figure 9.   Measured wave elevation time series
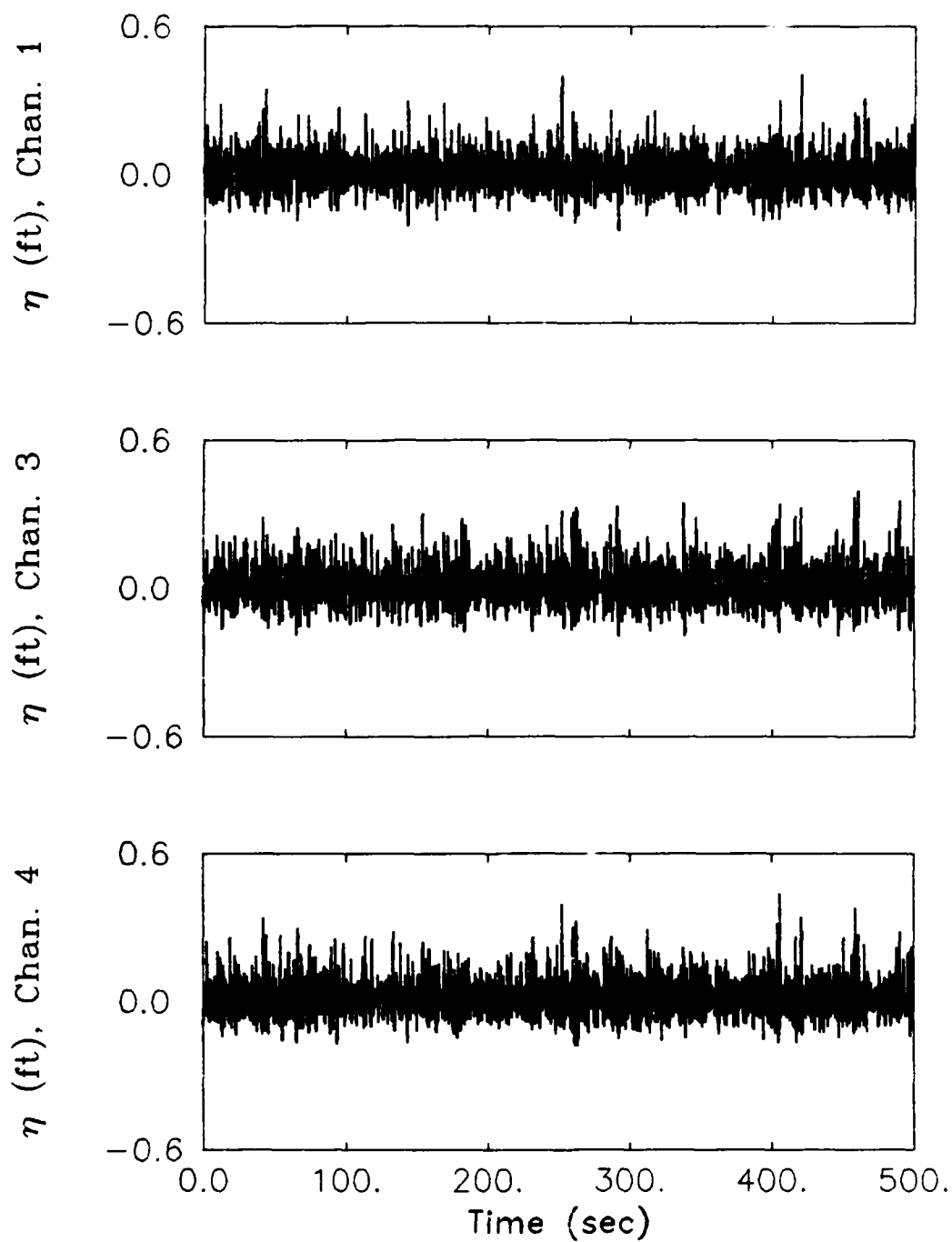for unidirectional series (Sheet 1 of 3)
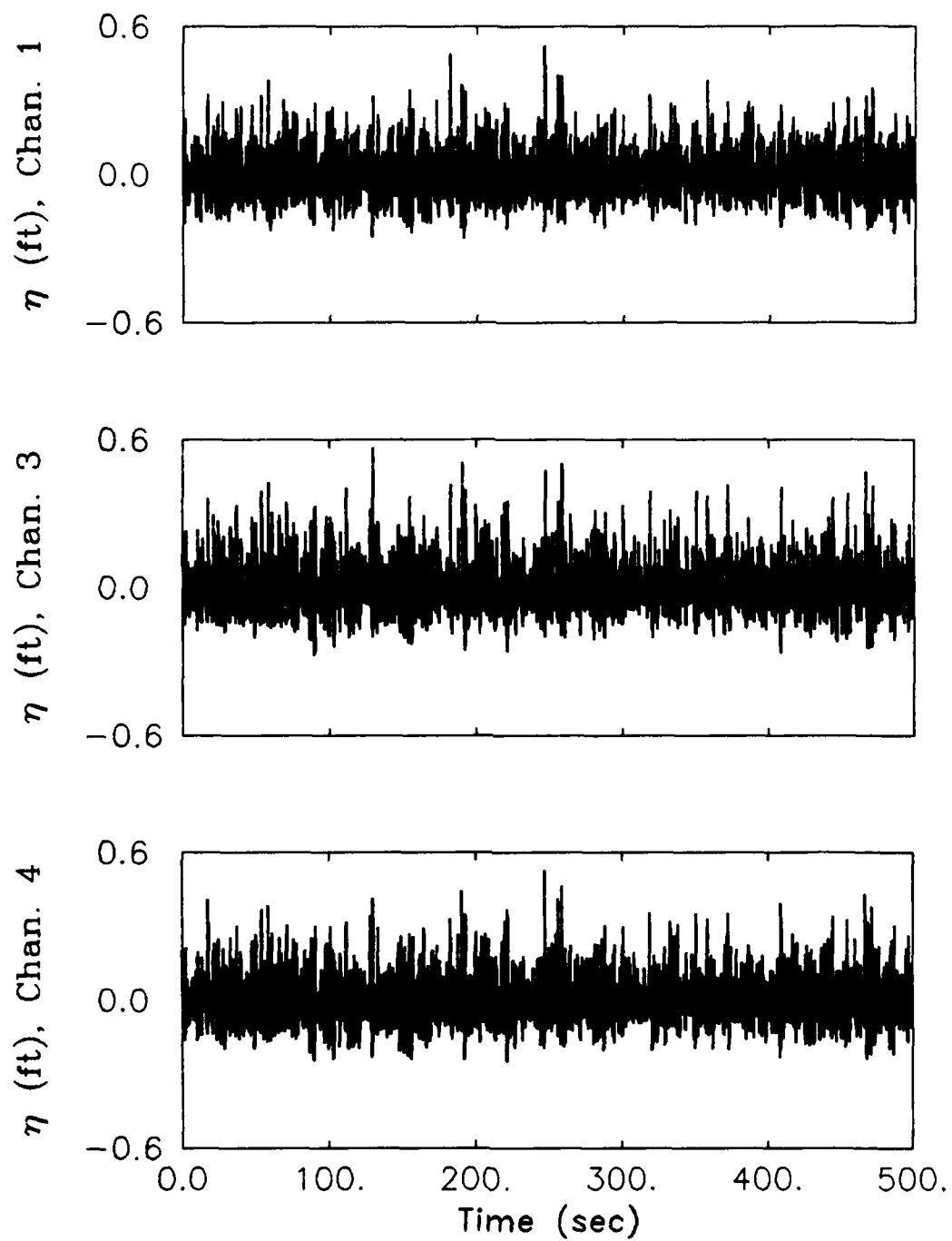
Measured Wave Elevation Time Series
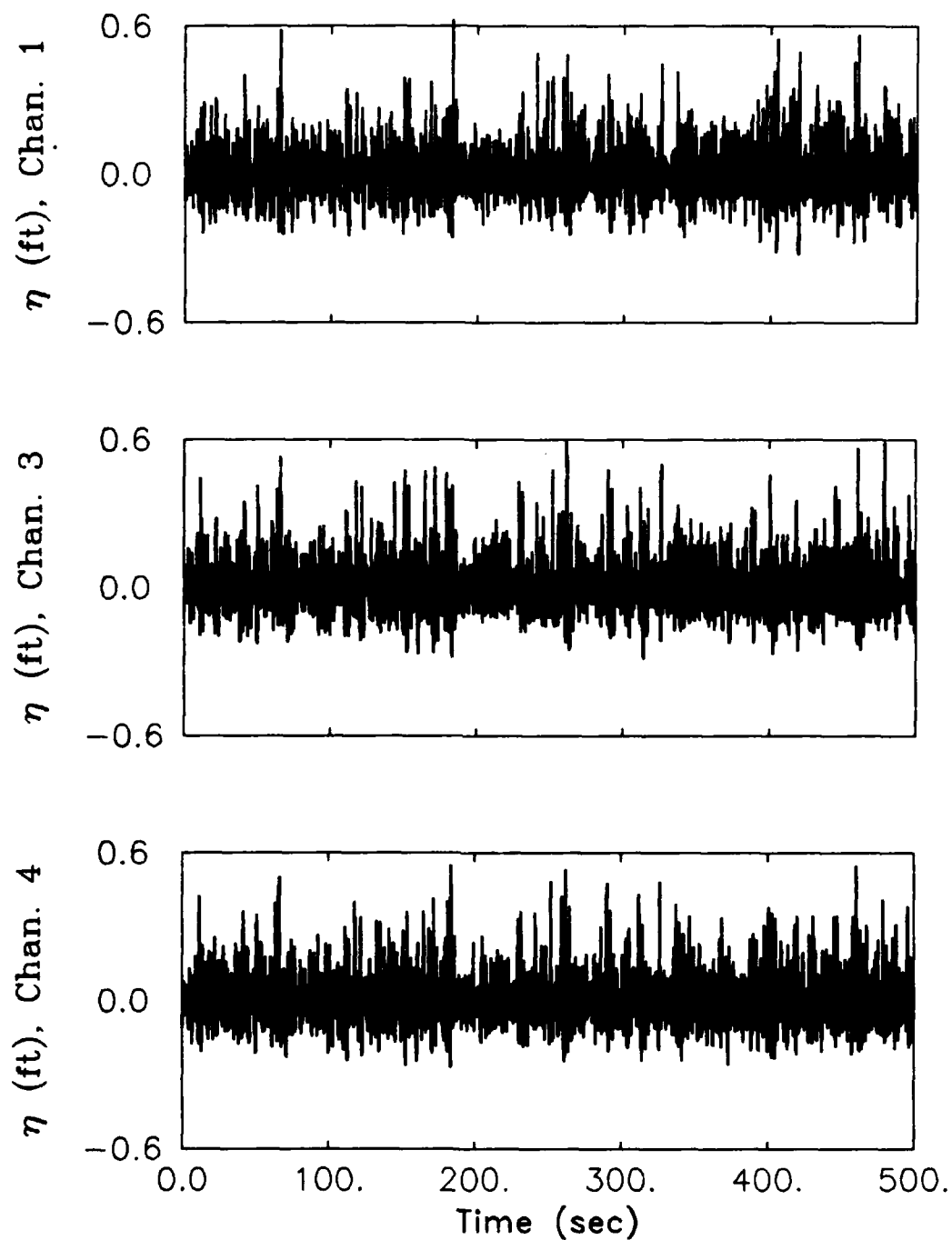CASE 74U2 -- Fp=.4, Hm0=5.16, H=1.29

b.   Case 74U2

Figure 9.   (Sheet 2 of 3)

Measured Wave Elevation Time Series
CASE 74U3 -- Fp=.4, Hm0=5.16, H=1.51

c. Case 74U3

Figure 9. (Sheet 3 of 3)

Measured Wave Elevation Time Series
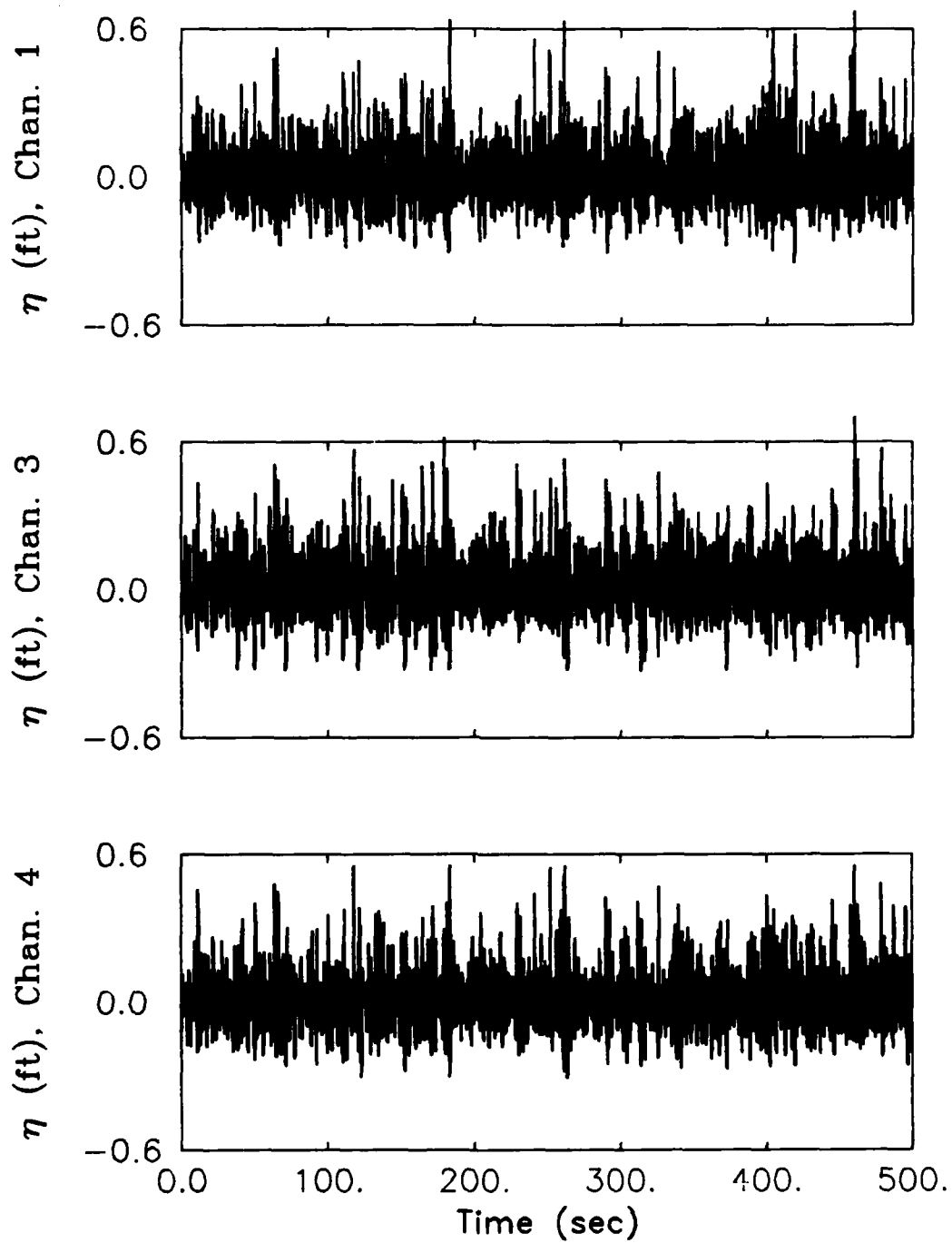CASE 74D1 -- Fp=.4, Hm0=5.42, H=1.11

a. Case 74D1

Figure 10. Measured wave elevation time series
for directional series (Sheet 1 of 3)

Measured Wave Elevation Time Series
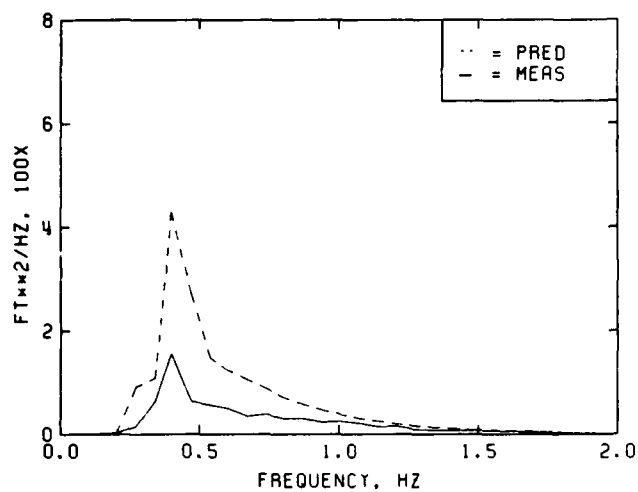**CASE 74D2 -- Fp=.4, Hm0=5.42, H=1.29**

b.   Case 74D2

Figure 10.   (Sheet 2 of 3)

Measured Wave Elevation Time Series
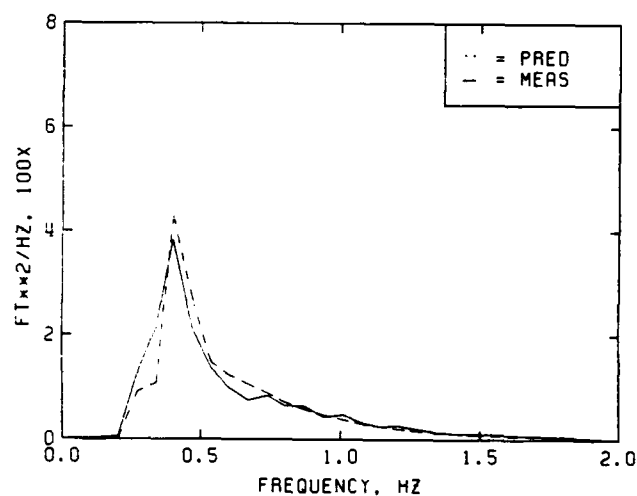**CASE 74D3 -- Fp=.4, Hm0=5.42, H=1.51**
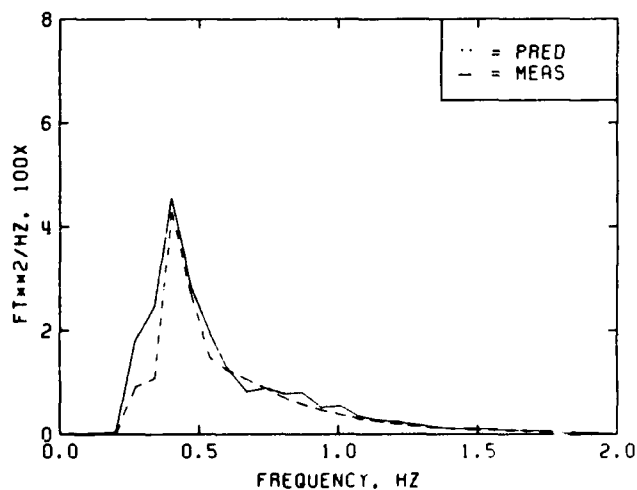
c.   Case 74D3

Figure 10.   (Sheet 3 of 3)

55

a. Case 74U1

MEASURED VS PREDICTED FREQUENCY SPECTRA
CASE 74U1 -- FP=0.40, HMO=5.16, H=1.11

b. Case 74U2
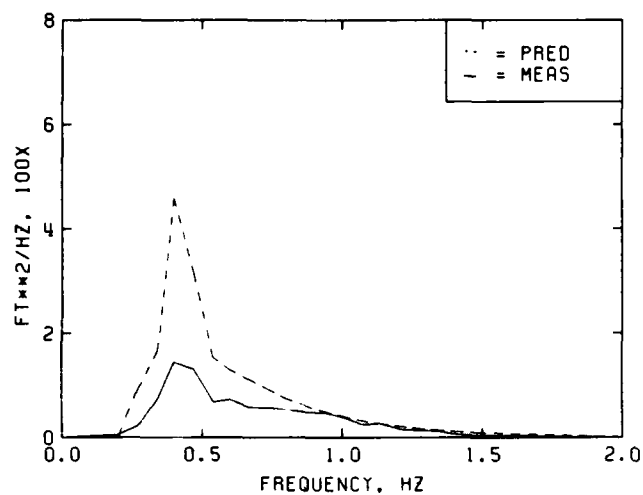
MEASURED VS PREDICTED FREQUENCY SPECTRA
CASE 74U2 -- FP=0.40, HMO=5.16, H=1.29

c. Case 74U3

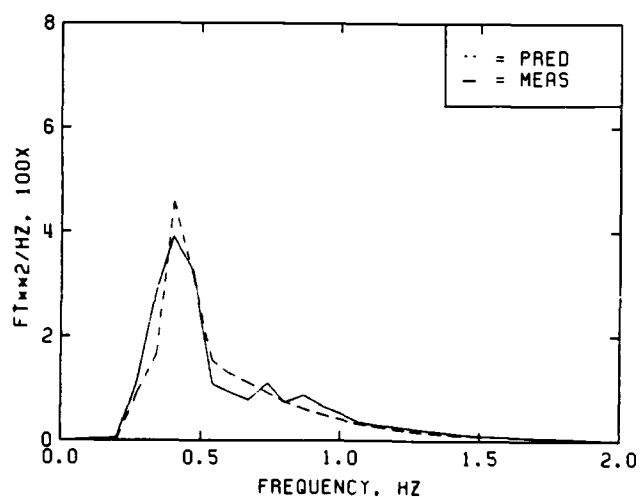MEASURED VS PREDICTED FREQUENCY SPECTRA
CASE 74U3 -- FP=0.40, HMO=5.16, H=1.51

Figure 11.   Measured versus predicted frequency
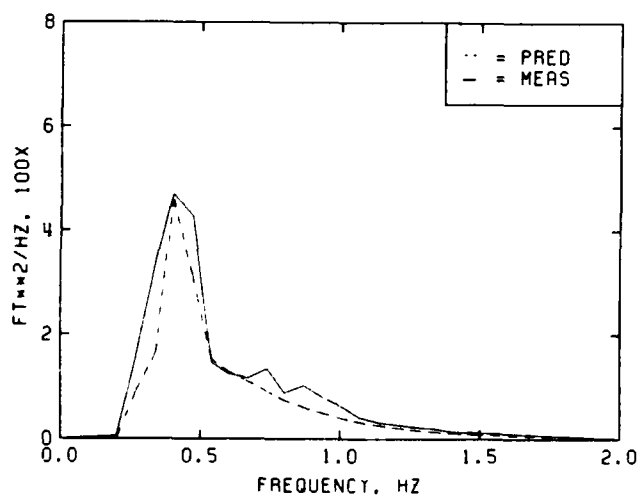spectra for unidirectional series

a. Case 74D1

MEASURED VS PREDICTED FREQUENCY SPECTRA
CASE 74D1 -- FP=0.40, HMO=5.42, H=1.11

b. Case 74D2

MEASURED VS PREDICTED FREQUENCY SPECTRA
CASE 74D2 -- FP=0.40, HMO=5.42, H=1.29

c. Case 74D3

MEASURED VS PREDICTED FREQUENCY SPECTRA
CASE 74D3 -- FP=0.40, HMO=5.42, H=1.51

Figure 12. Measured versus predicted frequency
spectra for directional series

iteration of the RAO compensation. Agreement between the desired and measured spectra is very good in the 1974 storm for both unidirectional and directional cases. The 1973 and 1983 unidirectional cases and the 1972 and 1973 directional cases were slightly larger than desired, however. The 1969 directional case was slightly smaller in the high-frequency region because large angles of spreading caused energy to be unmeasurable by the gage array. The series 3 plots show an increase in the measured spectra due to the increase in water depth to 1.51 ft.

Directional Spreading Functions

85. The measured directional spreading function estimates for the unidirectional series U1, U2, and U3 are shown in Figure 13. Figure 14 shows the measured versus predicted spreading functions for the three directional cases D1, D2, and D3. All spreading values are at the peak frequency for a directional increment of 22.5 deg to correspond to the directional series input. Measured values are the average of gages 1, 3, and 4 and the predicted values are for all 61 paddles. The x-axis ranges from -180 to 180 deg, while the y-axis scale is 0.0 to 3.0 rad^{-1}. Spreading functions for the other cases are included in Appendix D.

86. Predicted values are not shown on the unidirectional plots because the directional increment of 22.5 deg was not fine enough to show the true shape of the predicted spread. (See paragraph 31, Part II.) The idealized value would be a Dirac delta function or spike at the particular direction corresponding to the $\bar{\theta}$. The truncation of the fourier series tends to produce negative side lobes as an artifact of the fourier transform method. Thus, negative spreading function estimates can sometimes be produced at wave directions on either side of $\bar{\theta}$. These negative values have been suppressed and set to zero on these plots. Use of higher resolution methods such as the MLM or MEM methods would probably eliminate this effect. Future studies are planned to investigate these two methods.

87. Agreement between the measured and predicted spreading functions was excellent for the unidirectional and directional 1974 storm cases. The spreading appeared to intensify for the unidirectional case after the RAO correction was applied. For the directional D2 case, the agreement also improved. Not much change was evident for the series 3 cases. The same

58
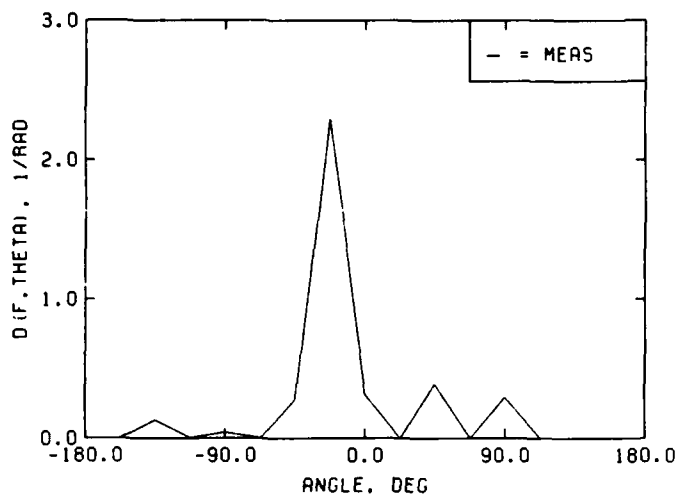
a.   Case 74U1

MEASURED DIRECTIONAL SPREADING
CASE 74U1 -- FP=0.40, HMO=5.42, D=-21, H=1.11

b.   Case 74U2
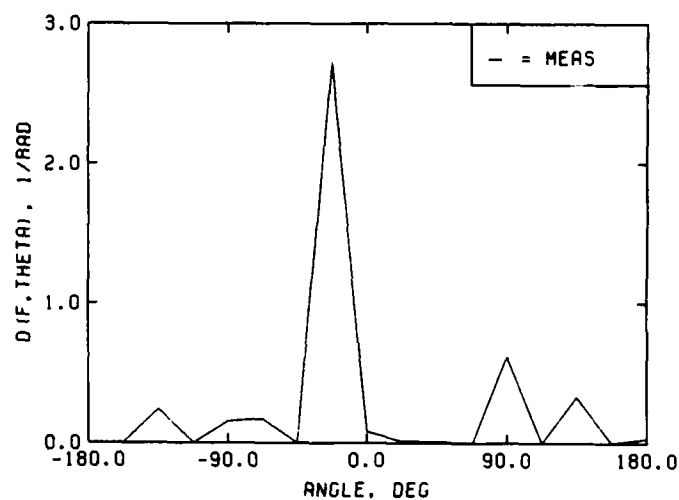
MEASURED DIRECTIONAL SPREADING
CASE 74U2 -- FP=0.40, HMO=5.42, D=-21, H=1.29

c.   Case 74U3

MEASURED DIRECTIONAL SPREADING
CASE 74U3 -- FP=0.40, HMO=5.42, D=-21, H=1.51

Figure 13.   Measured directional spreading for
unidirectional series

59
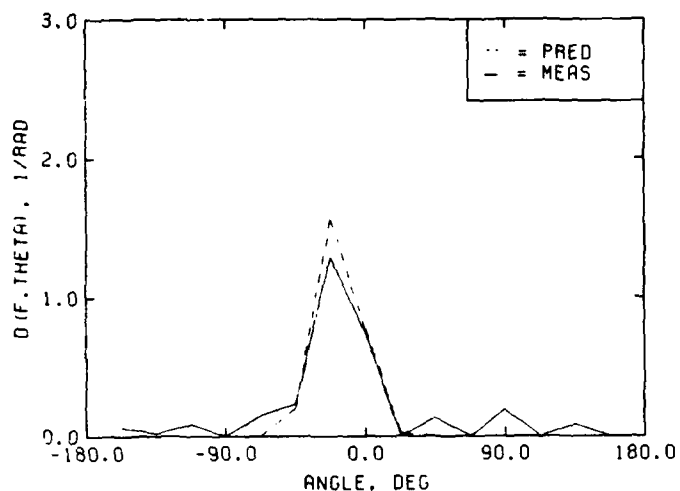
a.   Case 74D1

MEASURED VS PREDICTED DIRECTIONAL SPREADING
CASE 74D1 -- FP=0.40, HMO=5.42, D=-36, H=1.11

b.   Case 74D2
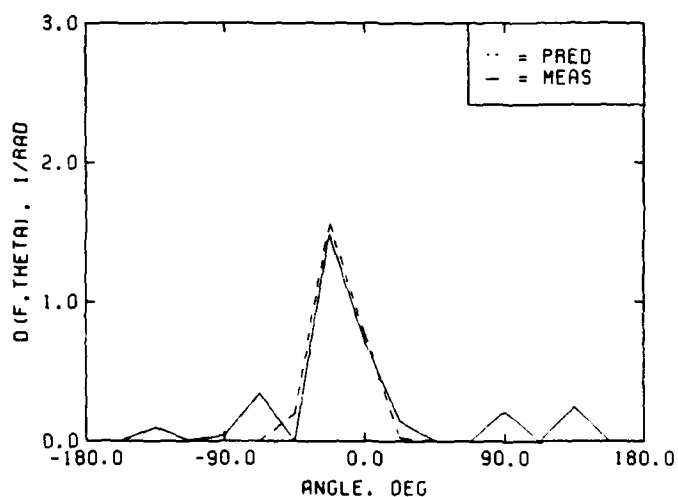
MEASURED VS PREDICTED DIRECTIONAL SPREADING
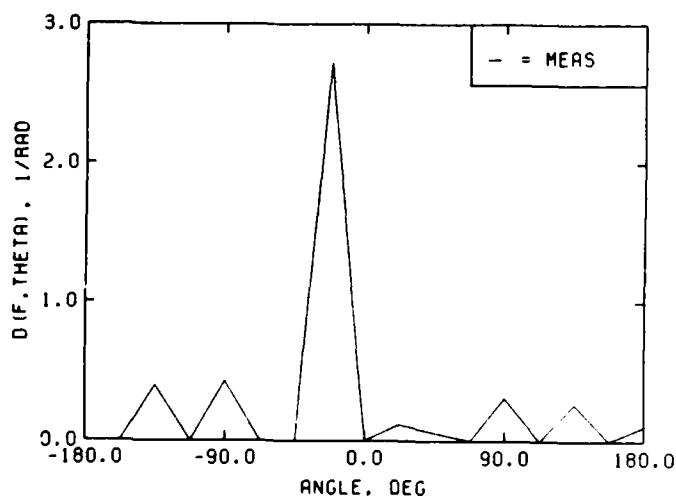CASE 74D2 -- FP=0.40, HMO=5.42, D=-21, H=1.29

c.   Case 74D3

MEASURED VS PREDICTED DIRECTIONAL SPREADING
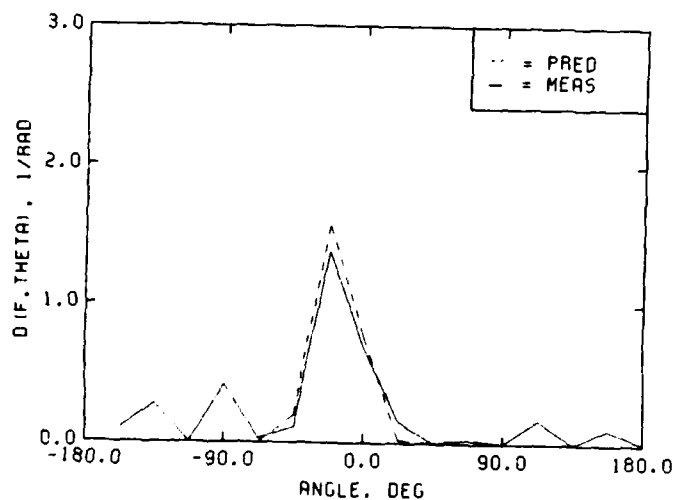CASE 74D3 -- FP=0.40, HMO=5.42, D=-21, H=1.51

Figure 14.   Measured versus predicted spreading
for directional series

60

comments generally are true for the other five storms in both unidirectional and directional series 2 and 3. Exceptions were the 1970 and 1983 unidirectional storms in series 3. A noticeable smearing of the directional spreading was evident. In the directional series, the 1973 storm was slightly underpredicted for all three series. Agreement between measured and predicted $\bar{\theta}$ is generally excellent for all cases.

RAO Functions

88. Figure 15 presents semi-log plot of the RAO transfer function for the 1974 unidirectional and directional cases. The RAO's for the other cases are included in Appendix E. The RAO's for each gage and the average for gages 1, 3, and 4 are shown. The RAO estimates were Gaussian smoothed to 0.0671 Hz, and all estimates within contiguous 0.0671-Hz bands were averaged. Values less than 1.0 indicate that the spectrum must be increased at a particular frequency. Likewise, values greater than 1.0 indicate the opposite trend. As discussed previously, the RAO was used to adjust the control signal to compensate for DSWG and basin characteristics. The effect of one iteration on the measured spectral characteristics was excellent.

Peak Wave Periods

89. The peak wave period was calculated using the CERC method (see Part III). Appendix F contains tabular listings and plots of measured periods for each gage for each of the three unidirectional and directional test series. The tabular listings also contain averages of (a) gages 1, 3, and 4 and (b) all seven gages. The average values for gages 1, 3, and 4 from these appendix tables are listed in Table 11 for each storm for the three test series. These values are normalized by the target period for each storm and reported in Table 11. Averages of these normalized values for the six storms are also given.

90. Figure 16 illustrates the influence of depth on the normalized peak periods for the unidirectional and directional series, respectively. The average values are also shown. Normalized period is plotted against water depth. For the unidirectional series, the periods tended to decrease due to the RAO correction and the increase in depth from 1.11 to 1.29 ft. The one exception is the 1972 storm, which increased. The increase in depth from

61
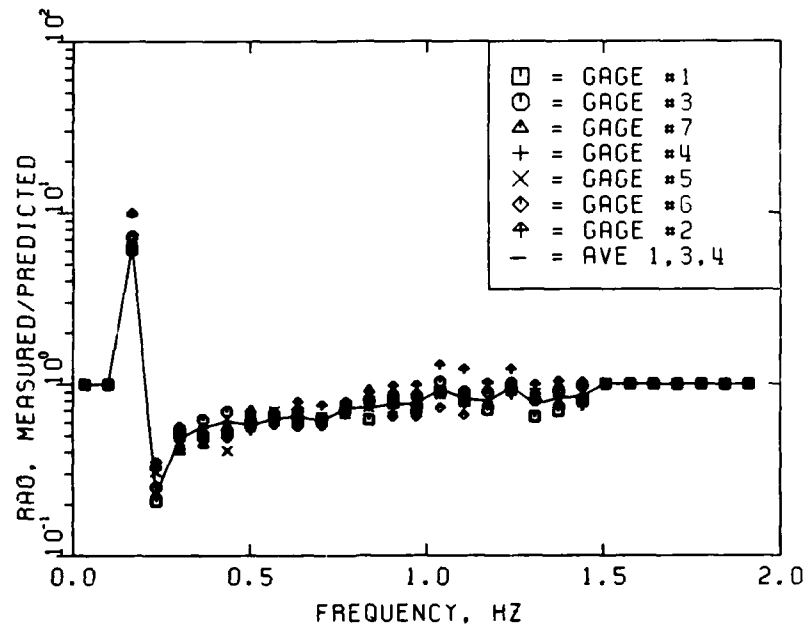
RAO FROM MEASURED FREQUENCY SPECTRA
74U1 -- TP=2.49, HMO=5.16, D=-21, H=1.11

a.   Case 74U1
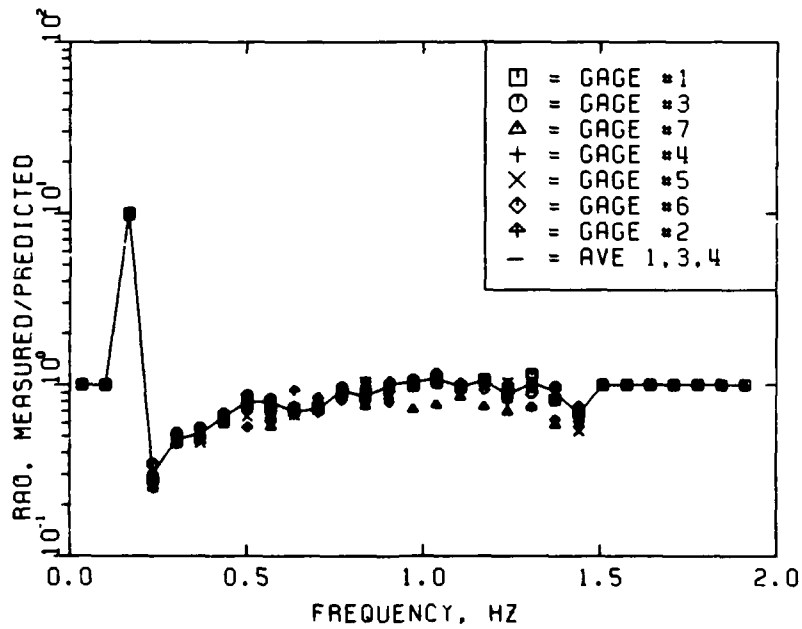
RAO FROM MEASURED FREQUENCY SPECTRA
74D1 -- TP=2.49, HMO=5.42, D=-36, H=1.11

b.   Case 74D1

Figure 15.   RAO from measured frequency spectra

Table 11

Measured and Normalized Wave Peak Periods Versus Water Depth

| Storm Year	Target Period sec	Depth = 1.11 ft Avg 1,3 & 4 sec	Normal*	Depth = 1.29 ft Avg 1,3 & 4 sec	Normal	Depth = 1.51 ft Avg 1,3 & 4 sec	Normal
			Unidirectional Series				
1969	2.49	2.51	1.01	2.46	0.99	2.47	0.99
1970	2.13	2.24	1.05	2.22	1.04	2.20	1.03
1972	1.86	1.74	0.94	2.22	1.19	2.04	1.10
1973	2.13	2.30	1.08	2.28	1.07	2.26	1.06
1974	2.49	2.51	1.01	2.49	1.00	2.53	1.02
1983	2.49	2.53	1.02	2.51	1.01	2.53	1.02
Avg			1.02		1.05		1.05
			Directional Series				
1969	2.49	2.48	1.00	2.49	1.00	2.49	1.00
1970	2.13	1.90	0.89	2.01	0.94	2.10	0.99
1972	2.13	2.35	1.10	2.52	1.18	2.53	1.19
1973	2.13	2.49	1.17	2.52	1.18	2.51	1.18
1974	2.49	2.29	0.92	2.56	1.03	2.57	1.03
1983	2.49	2.47	0.99	2.47	0.99	2.47	0.99
Avg			1.01		1.05		1.06

* Normal = Avg 1,3, and 4/Target.

1.29 to 1.51 ft caused the periods to decrease except for the 1974 and 1983 storms. For the directional series, the periods tended to increase between both depths, except for the 1969 and 1983 storms which remained unchanged.

91. Figure 17 shows the influence of directional spreading and depth on peak period transformation for the two depths of 1.29 and 1.51 ft. Normalized directional peak period is plotted against normalized unidirectional peak period for five of the storms. The 1972 storm is not plotted because it lies off the edge of the plot. The left-most, or lower, symbol represents the lower water depth. A 45-deg line is shown to indicate equivalence between unidirectional and directional periods. A value above the line implies that the directional period is larger than the corresponding unidirectional period for the same depth. Conversely, a value below the line indicates the opposite relationship. A horizontal line between points on the graph for a storm indicates a constant directional period which is unaffected by changes in water depth. Likewise, a vertical line between points indicates a constant
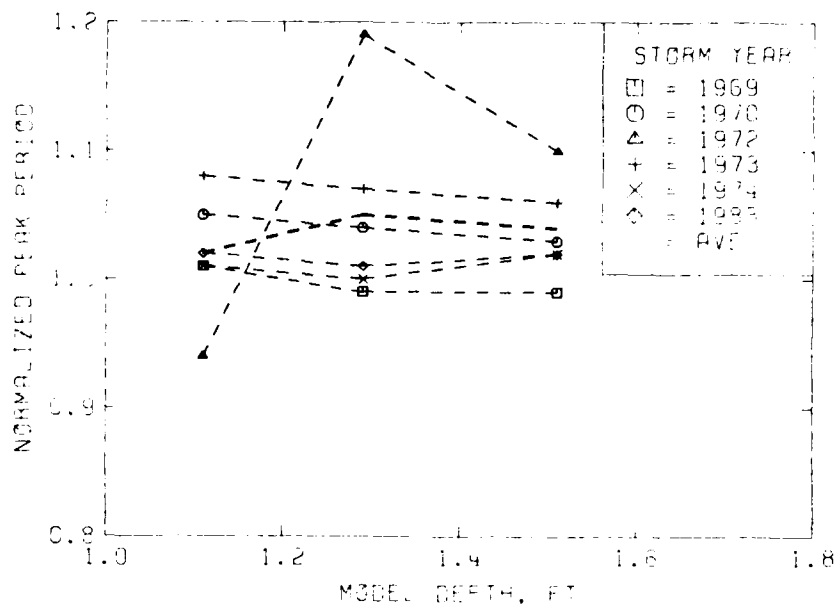
a. Unidirectional series
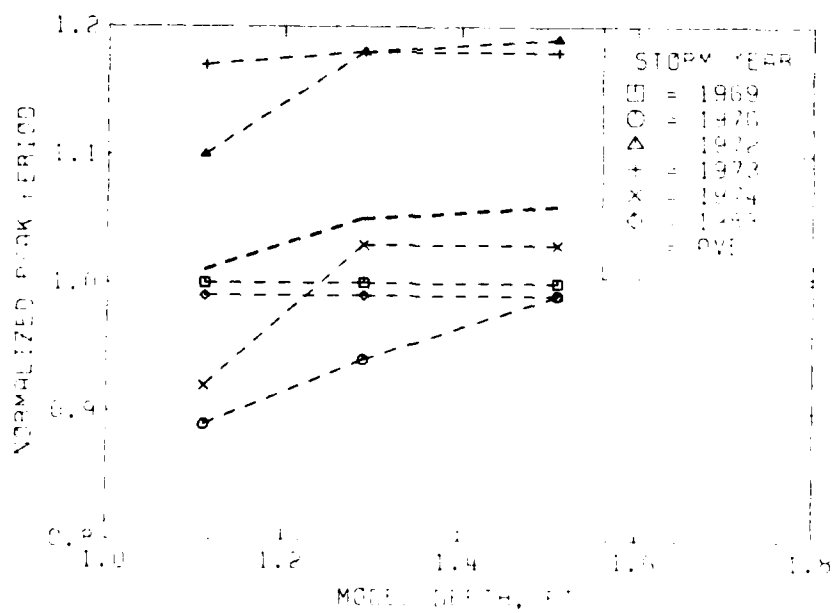
b. Directional species

Figure 16. Influence of depth on normalized
peak period

64
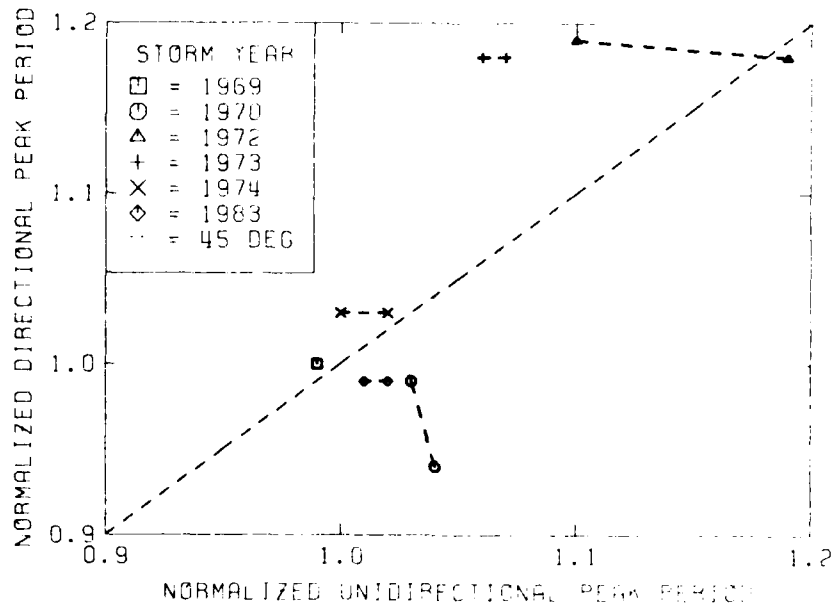
Figure 17. Influence of directional spreading
and depth on peak period transformation

unidirectional period. The 1983 storm is interesting because the directional
period decreased, while the unidirectional period increased with the increase
in depth.

92. In general, after correction the periods matched their target
values within an average of 5 percent for all storms. For the unidirectional
series, the low normalized period was 0.99 for the 1969 storm, and the high
was 1.19 for the 1972 storm. For the directional series, the low was 0.94 for
the 1970 storm, and the high was 1.18 for the 1972 and 1973 storms. The
periods appeared to be more invariant for the directional series than the
unidirectional for an increase in depth from 1.29 to 1.51 ft.

Zero-Moment Wave Heights

93. Appendix G also contains tabular listings and plots of measured
zero-moment wave heights for each gage for each of the three unidirectional
and directional test series. The tabular listings also contain averages of
(a) gages 1, 3, and 4 and (b) all seven gages. The average value for gages 1,
3, and 4 from these appendix tables is listed in Table 12 for each storm for

65

Table 12

Measured and Normalized Wave Heights Versus Water Depth

Storm Year	Target Height in.	Depth - 1.11 ft Avg 1,3 & 4 in.	Normal*	Depth - 1.29 ft Avg 1,3 & 4 in.	Normal	Depth - 1.51 ft Avg 1,3 & 4 in.	Normal	Ratio 1.51/1.29
				Unidirectional Series				
1969	5.95	4.01	0.67	5.79	0.97	6.43	1.08	1.11
1970	5.07	3.83	0.76	4.98	0.98	5.66	1.12	1.14
1972	3.85	2.40	0.62	3.86	1.00	4.34	1.13	1.13
1973	4.46	2.78	0.62	4.91	1.10	5.53	1.24	1.13
1974	5.16	3.17	0.61	5.10	0.99	5.58	1.08	1.09
1983	4.99	3.20	0.64	5.40	1.08	6.07	1.22	1.13
Avg			0.65		1.02		1.15	1.12
				Directional Series				
1969	6.12	4.10	0.67	5.37	0.88	5.91	0.97	1.10
1970	5.07	3.79	0.75	4.99	0.98	5.61	1.11	1.13
1972	4.11	2.70	0.66	4.44	1.08	5.16	1.26	1.17
1973	4.55	2.71	0.60	5.35	1.18	5.99	1.32	1.12
1974	5.42	3.74	0.69	5.48	1.01	6.14	1.13	1.12
1983	5.42	3.52	0.65	6.06	1.12	6.75	1.25	1.12
Avg			0.67		1.04		1.17	1.13

* Normal - Avg 1,3, and 4/Target.

the three test series. These values are normalized by the target wave height for each storm and reported in Table 12. Averages of these normalized values for the six storms are also given.

94. Figure 18 illustrates the influence of depth on the normalized wave heights for the unidirectional and directional series, respectively. The average value is also shown. Normalized height is plotted against water depth. For the unidirectional series, heights increased sharply due to the RAO correction and the increase in depth from 1.11 to 1.29 ft. The 1970 storm increased but less rapidly. The increase in depth from 1.29 to 1.51 ft caused the heights to increase at a rate to be expected because of the increase in water depth. For the directional series, heights increased between both depths in a similar fashion to those in the unidirectional series. The 1969 and 1970 storms, however, increased at a slower rate between 1.11 and 1.29 ft than the others.

a. Unidirectional series
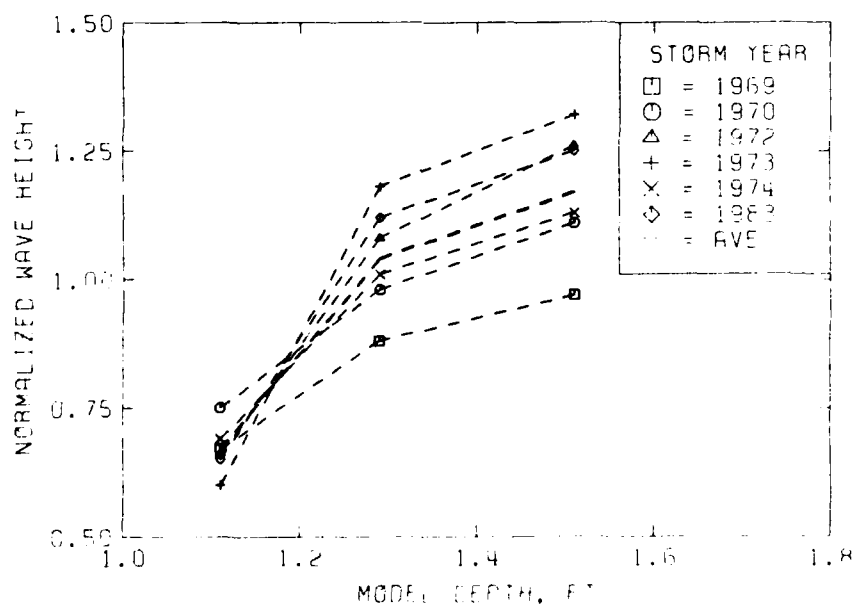
b. Directional series

Figure 18.   Influence of depth on
normalized wave height

67

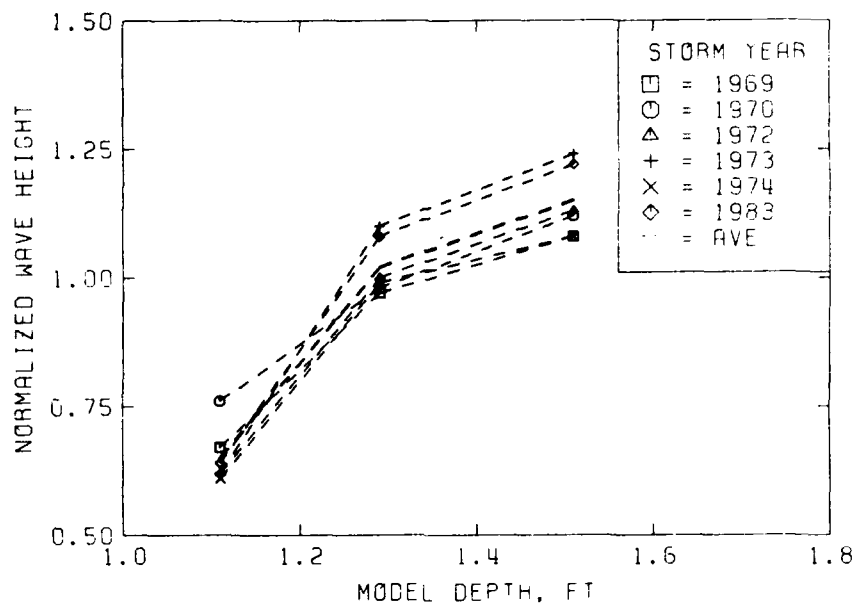95. Figure 19 shows the influence of directional spreading and depth on wave height transformation for the two depths of 1.29 and 1.51 ft. Normalized directional wave height is plotted against normalized unidirectional wave height for all of the storms. The left-most symbol represents the lower water depth. A 45-deg line is shown to indicate equivalence between unidirectional and directional heights. A value above the line implies that the directional height is larger than the corresponding unidirectional height for the same depth. Conversely, a value below the line indicates the opposite relationship. A line parallel to the 45-deg line indicates that there was no change in the relationship due to the increase in depth. The 1969 storm exhibited this behavior. A decrease in the line connecting two depths indicates an increase in the unidirectional height relative to the directional height in going to the deeper water depth. The 1970 storm was an example. Finally, an increase in the line shows an increase in directional height due to an increase in depth (1972 and 1974 storms). The directional wave heights were larger than the equivalent unidirectional heights in all cases except for the 1969 and 1970 storms.

96. In general, after correction the heights matched their target values within an average of 4 percent for all six storms. For the
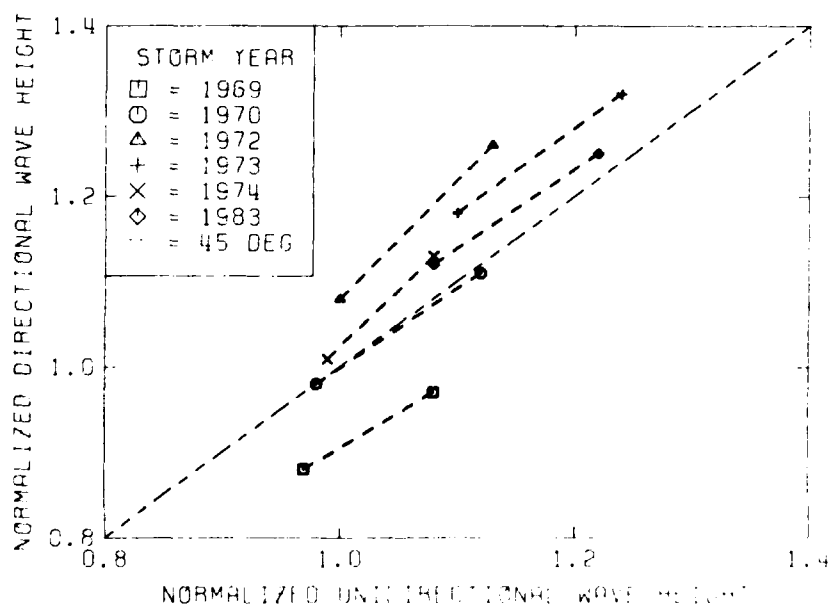
Figure 19. Influence of directional spreading and depth on wave height transformation

68

unidirectional series, the low normalized height was 0.97 for the 1969 storm, and the high was 1.10 for the 1973 storm. For the directional series, the low was 0.88 for the 1969 storm, and the high was 1.18 for the 1973 storm. Heights increased for all cases with the increase in water depth from 1.29 to 1.51 ft.

97. Table 12 also lists the ratio of the normalized height at 1.51 ft divided by the value at 1.29 ft. The average increase for both unidirectional and directional cases was 12 to 13 percent. The 1972 and 1974 directional cases tended to increase more than their corresponding unidirectional cases. Other directional cases increased slightly less than the unidirectional cases.

PART VI: SUMMARY AND RECOMMENDATIONS

98.   The DSWG provides a means to simulate real ocean environments in a laboratory physical model by incorporating directional spreading. Inclusion of this spreading has been found by previous researchers in the coastal hydraulic community to have a significant effect on the design of coastal structures, including port facilities, harbors, and breakwaters.

99.   Effects of frequency and directional spreading on wave transformation in the nearshore region were investigated using a 3-D physical model of Yaquina Bay, Oregon. The 1:45 (all units reported here are prototype values) scale model consisted of an entrance channel protected by two rubble-mound jetties with a sloping bottom and submerged reef offshore of the entrance. Unidirectional and directional spectra, representative of the most severe hindcasted storms in the past 20 years, were numerically transformed to a shallow-water depth of 58 ft. These storms had peak periods of 12.5, 14.3, and 16.7 sec and zero-moment wave heights ranging from 14.4 to 23.0 ft. Surface elevation measurements were made at two water depths: 0.0 and +10.0 mllw.

100.   This study is divided into three phases. Phase 1, reported herein, is a calibration of the performance characteristics of the six unidirectional and directional spectral cases chosen for study. A total of 36 cases was required to measure and correct the control signals for the two water depths. Phases 2 and 3 will be reported in separate volumes at a later date. In phase 2, 24 runs were made to quantify wave transformation of the 12 calibrated unidirectional and directional conditions from phase 1 at two locations near the north jetty head. The third phase is a parameter study on the effects of frequency and directional spreading on wave transformation near the jetty head. The same peak period and wave height values from the phase 1 directional cases were used to create 24 new directional wave spectra with a range of frequency and directional spreading parameters. These cases were calibrated, iteratively corrected several times, and measured in the same nearshore region near the jetty head.

101.   The purpose of the first phase was to verify the accuracy of the wave spectra created for a depth of 58 ft. Thus, this phase consisted of three series of tests for each of the six unidirectional and six directional cases. The control signals for these 12 cases had inadvertently been created

70

for a water depth of 50 ft instead of 58 ft. Thus, the first series of 12 tests was measured at this shallow depth and, as expected, the measured parameters were smaller than desired. The control signals were then corrected and run again for each unidirectional and directional case at the correct depth of 58 ft as series 2. Finally, the third series of 12 tests was run with the same corrected control signals from series 2 at the deeper depth of 68 ft (i.e. +10 ft mllw).

102. The spectra were simulated as the product of a frequency spectrum and a directional spreading function. The frequency spectrum was discretely input at 20 frequencies between 0.02 and 0.22 Hz using the shallow-water results from the numerical transformation. For the directional spreading function, an empirically derived wrapped normal spreading function was used for the unidirectional cases, and it was discretely input at 16 intervals of 22.5 deg for the directional cases. A stroke time series for each paddle was simulated in the frequency domain using a DSA random phase model. A total of 67.08 min or 12,000 points between cutoff limits of 0.01 and 0.30 Hz were generated for each case. A height-to-stroke transfer function was then used to convert the signals to the appropriate strokes. Finally, they were converted to analog voltage signals.

103. One assumes that the use of hindcasted storms more accurately models extremal conditions for a particular site than an assumed empirical frequency spectral shape (i.e., Pierson-Moskowitz, JONSWAP, TMA, etc.) and spreading function (i.e. Cosine[4], wrapped normal, etc.). If the discrete directional spectrum is available, it is better to use it if a directional spectrum is required. For the unidirectional conditions of this location, the wind-sea and swell procedure (method 2) worked better relative to the swell only procedure for shallow-water transformation. The WIS sea and swell procedure (method 3) was more appropriate for the directional cases.

104. In phase 1, measurements were made at seven locations within the basin by capacitance wave gages. The gages were arranged in a 2-3-1-7 linear array embedded in a directional array in the shape of a cross. It was centrally located 20 ft in front of the DSWG along its center line. A unit lag spacing of 2.00 ft was selected to optimize resolution while minimizing spatial aliasing.

105. A minimum of 200 waves at the peak period was collected with a sampling frequency of 10 Hz. Spectral, directional spectral, and RAO analyses

were performed for each case. Although all seven gages were used in these analyses, an average of only three is reported. These three gages, numbers 1, 3, and 4, were close together and least affected by the contours of the model. The one exception was that all seven gages were used for the spreading function analysis.

106. Standard fast fourier transform techniques, including zero-meaning, windowing with a 10 percent cosine bell, and band averaging between lower and upper cutoff frequencies of 0.02 and 0.22 Hz, respectively, were used for the frequency spectral analysis. The same resolution bandwidth of 0.01 Hz was used for all cases by averaging different numbers of adjacent bands.

107. Directional spectral analysis was based on the fourier series expansion of the directional spreading function. The measured surface data for each gage was zero-meaned, windowed, fourier transformed with a "235" FFT, and Gaussian smoothed with the same bandwidth and cutoff limits as before to obtain the cross-spectral matrix of autospectra and cross spectra. This matrix is substituted into the parameterized spreading function to obtain a set of N^2 simultaneous, linear equations. A least squares fourier transform method for numerical integration is used to invert a matrix of independent variables to solve for the fourier coefficients of the spreading function. The technique for doing this is a linear, stepwise regression model.

108. Because of leakage around and under the DSWG, electronic and mechanical losses, and basin response characteristics, the measured spectra do not usually reproduce the target spectra. The height-to-stroke transfer function only compensates for an ideal wave maker. In addition, a water depth of 50 ft instead of 58 ft was inadvertently used to create the control signals. Thus, an RAO transfer function was calculated for each spectral control signal to compensate for observed variations in peak period, wave height, or spectral shape. The RAO is the ratio of measured to predicted spectral density for each gage at each frequency. After the initial run of each case in series 1, the RAO was computed and used to correct the control signal for future runs in series 2 and 3. Phase 3 of this study will report on the relative effectiveness of multiple iterations with the RAO.

109. In general, the shape of the measured unidirectional and directional frequency spectra agreed very well with the predicted values after the RAO corrections. The 1973 and 1983 unidirectional cases and the 1972 and

1973 directional cases were slightly larger than desired, however. This is not critical because measured values are normalized by the actual incident conditions rather than the desired conditions. The 1969 directional case was slightly smaller in the high-frequency region because large angles of spreading caused energy to be unmeasurable by the gage array.

110. Agreement between the measured and predicted spreading functions and θ was generally excellent for all cases. The spreading appeared to intensify for the unidirectional cases after the RAO correction was applied. For the directional cases, the agreement also improved. A significant transformation of the directional distribution of energy occurred in the 1970 and 1983 unidirectional cases in the water depth of 68 ft. This increase in depth produced a noticeable smearing of directional energy. In the directional series, the 1973 storm was slightly underpredicted for both water depths.

111. At the time of these experiments, the WIS and SHALW programs only generated a directional grid of 16 increments at 22.5 deg. Finer grid spacing of 5 to 10 deg would be more useful for future physical model comparisons, especially for unidirectional waves.

112. Measured peak wave periods were normalized by their target values. In general, after RAO correction they matched their target values within an average of 5 percent for all storms. They tended to decrease for the unidirectional cases due to increase in depth. For the directional cases, the opposite trend occurred. For most cases, the normalized directional periods were larger than their corresponding unidirectional counterparts. For the unidirectional series, the low normalized period was 0.99 for the 1969 storm, and the high was 1.19 for the 1972 storm. For the directional series, the low was 0.94 for the 1970 storm, and the high was 1.18 for the 1972 and 1973 storms. The 1972 storm was difficult to achieve for both unidirectional and directional cases. The periods appeared to be more invariant for the directional series than the unidirectional series for an increase in depth from 58 to 68 ft.

113. Measured zero-moment wave heights were also normalized by their target values. An increase in depth caused all cases to increase in height, a result to be expected according to linear wave theory. Generally, the unidirectional cases had larger heights than the directional cases. The one exception was the 1970 storm. In general, after the RAO correction the

heights matched their target values within an average of 4 percent for all six storms. For the unidirectional series, the low normalized height was 0.97 for the 1969 storm, and the high was 1.10 for the 1973 storm. For the directional series, the low was 0.88 for the 1969 storm, and the high was 1.18 for the 1973 storm. The 1973 storm could have been reduced using an overall gain factor lower than 1.00 during runtime.

114. To quantify the effect of an increase in water depth on a projected storm height, the ratio of measured height at 58 ft was divided by the measured value at 68 ft. The average increase for both unidirectional and directional cases was 12 to 13 percent. The 1972 and 1974 directional cases tended to increase more than their unidirectional counterparts. The other directional cases increased slightly less than the unidirectional cases. Thus, the increase or decrease in wave height for a particular storm at a particular location is dependent on all of its parameters, not just the amount of directional spreading.

REFERENCES

Abramowitz, M., and Stegun, I. A. 1970. Handbook of Mathematical Functions with Formulas, Graphs, and Mathematical Tables, Dover Publications, New York.

Biesel, F. 1954. "Wave Machines," Proceedings of the 1st Conference on Ships and Waves, Hoboken, NJ, pp 288-304.

Borgman, L. E. 1969. "Directional Spectra Models for Design Use," Offshore Technology Conference, University of California at Berkeley, Berkeley, CA.

_____. 1979. "Directional Wave Spectra from Wave Sensors," Ocean Wave Climate, M. Earle and A. Malahoff, eds., Plenum Press, New York, pp 269-300.

_____. 1984 (Nov). "Directional Spectrum Estimation for the Sxy Gauges," Report to US Army Engineer Waterways Experiment Station, L. E. Borgman, Inc., pp 1-104.

Borgman, L. E., and Panicker N. N. 1970. "Design Study for a Suggested Wave Gage Array off Point Mugu, California," Technical Report Hel 1-14, Hydraulic Engineering Laboratory, University of California at Berkeley, Berkeley, CA.

Briggs, M. J., and Hampton, M. L. 1987. "Directional Spectral Wave Generator Basin Response to Monochromatic Waves," Technical Report CERC-87-6, US Army Engineer Waterways Experiment Station, Vicksburg, MS, pp 1-88.

Corson, W. D., Resio, D. T., and Vincent, C. L. 1980. "Wave Information Study of U. S. Coastlines; Surface Pressure Field Reconstruction for Wave Hindcasting Purposes," Technical Report HL-80-11, Report 1, US Army Engineer Waterways Experiment Station, Vicksburg, MS.

Corson, W. D., Abel, C. E., Brooks, R. M., Farrar, P. D., Groves, B. J., Jensen, R. E., Payne, J. B., Ragsdale, D. S., and Tracy, B. A. 1986. "Pacific Coast Hindcast Deepwater Wave Information," WIS Report 14, US Army Engineer Waterways Experiment Station, Vicksburg, MS.

Corson, W. D., Abel, C. E., Brooks, R. M., Farrar, P. D., Groves, B. J., Payne, J. B., McAneny, D. S., and Tracy, B. A. 1987. "Pacific Coast Hindcast Phase II Wave Information," WIS Report 16, US Army Engineer Waterways Experiment Station, Vicksburg, MS.

Crowson, R. A., Birkemeier, William A., Klein, Harriet M., and Miller, Herman C. 1988 (Sep). "SUPERDUCK Nearshore Processes Experiment; Summary of Studies, CERC Field Research Facility," Technical Report CERC-88-12, US Army Engineer Waterways Experiment Station, Vicksburg, MS.

Elgar, S., Guza, R. T., and Seymour, R. J. 1984. "Groups of Waves in Shallow Water," Journal of Geophysical Research, Vol 89, No. C3, pp 3623-3634.

_____. 1985. "Wave Group Statistics from Numerical Simulations of a Random Sea," Applied Ocean Research, Vol 7, No. 2, pp 93-96.

Goda, Yoshimi. 1970. "Numerical Experiments on Wave Statistics with Spectral Simulation," Report of the Port and Harbour Research Institute, Vol 9, No. 3, pp 3-57.

_____. 1985. Random Seas and Design of Maritime Structures, University of Tokyo Press, Japan, pp 1-323.

Grace, P. J., and Dubose, W. G. 1988. "Jetty Rehabilitation Stability Study, Yaquina Bay, Oregon," Technical Report CERC-88-14, US Army Engineer Waterways Experiment Station, Vicksburg, MS, pp 1-48.

Hasselmann, K. 1962. "On the Non-linear Energy Transfer in a Gravity-Wave Spectrum - General Theory," Journal of Fluid Mechanics, Vol 12, Part 1, pp 481-500.

Hasselmann, K., Barnett, T. P., Bouws, E., Carlson, H., Cartwright, D. E., Enke, K., Ewing, J. A., Gienapp, H., Hasselmann, D. E., Cruseman, T., Meerburg, A., Muller, P., Olbers, D. J., Richter, K., Sell, W., and Walden, H. 1973. "Measurements of Wind-Wave Growth and Swell Decay During the Joint North Sea Wave Project JONSWAP," Deutsch Hydrogr. Zeit., Vol 8 (Suppl A8), No. 12.

Hudspeth, R. T., Nath, J. H., and Sollitt, C. K. 1983. "Digital to Analog Wavemaker Simulations," Symposium on Wavemaker Design, University of Delaware, Newark, DE.

Hughes, S. A., and Jensen, R. E. 1986. "A User's Guide to SHALWV, Numerical Model for Simulation of Shallow-Water Wave Growth, Propagation, and Decay," Instruction Report CERC-86-2, US Army Engineer Waterways Experiment Station, Vicksburg, MS.

International Association of Hydraulic Research Working Group on Wave Generation and Analysis. 1986 (Jan). "List of Sea State Parameters," Supplement to Bulletin No. 52, pp 1-24.

Isaacson, M. 1985. "Laboratory Measurement and Generation of Directional Surface Waves," International Association of Hydraulic Research 21st Congress, Melbourne, Australia.

Jennrich, R. I. 1977. "Stepwise Regression," Statistical Methods for Computers, K. Enslein, A. Ralston, and H. Wilf, eds., Wiley InterScience, pp 58-75.

Outlaw, D. G., and Briggs, M. J. 1986 (Aug). "Directional Irregular Wave Generator for Shallow Water Basins," 21st American Towing Tank Conference, Washington, DC, pp 1-6.

Pinkster, J. A. 1984. "Numerical Modelling of Directional Seas," Proceedings of the Symposium on Description and Modelling of Directional Seas, Technical University of Denmark, Copenhagen.

Resio, D. T. 1982. "The Estimation of Wind-Wave Generation in a Discrete Spectral Model," WIS Report 5, US Army Engineer Waterways Experiment Station, Vicksburg, MS.

Resio, D. T., Vincent, C. L., and Corson, W. D. 1982. "Objective Specification of Atlantic Ocean Wind Fields from Historical Data," WIS Report 4, US Army Engineer Waterways Experiment Station, Vicksburg, MS.

Rice, S. O. 1944. "Mathematical Analysis of Random Noise," Reprinted in Selected Papers on Noise and Stochastic Processes, Dover Publications, New York.

_____. 1945. "Mathematical Analysis of Random Noise," Bell System Technical Journal, Vol 24.

Sand, S. E. 1979. "Three-Dimensional Structure of Ocean Waves," Series Paper No. 24, Institute of Hydrodynamics and Hydraulic Engineering, Technical University of Denmark, Copenhagen.

Sand, S. E., and Mynett, A. E. 1987 (Sep). "Directional Wave Generation and Analysis," IAHR Seminar on Wave Analysis and Generation in Laboratory Basins, XXII Congress, Lausanne, Switzerland, pp 209-235.

Sand, S. E., Kirkegaard, J., Larsen, J., and Rodenhuis, G. S. 1983 (Mar). "Numerical and Physical Modeling of Directional Diffraction of Waves," Coastal and Port Engineering in Developing Countries, Colombo, Sri Lanka.

Searle, S. R. 1982. Matrix Algebra Useful in Statistics, John Wiley and Sons, New York, pp 1-438.

Tucker, M. J., Challenor, P. G., and Carter, D. J. T. 1984. "Numerical Simulation of a Random Sea: A Common Error and Its Effect Upon Wave Group Statistics," Applied Ocean Research, Vol 6, No. 2, pp 118-122.

Vincent, C. L. 1984. "Equilibrium Range Coefficient of Wind Wave Spectra in Water of Finite Depth," 19th International Conference on Coastal Engineering, Houston, TX.

APPENDIX A: LISTING OF SHALLOW-WATER WAVE SPECTRA

YS6901. TP 16.7 SEC, HM0 = 6.8 M. DIR = 15 DEG
YAQUINA BAY JETTY STABILITY STUDY
DISCRETE VALUES OF PROTOTYPE SHALLOW WATER FREQUENCY & DIRECTIONAL SPECTRA
RESULTS FROM JENSEN'S SHOALING & REFRACTION NUMERICAL MODEL
FORMAT: 10 LINES HEADER PRIOR TO FREQUENCY SPECTRUM
METRIC UNITS

FREQUENCY SPECTRUM
ACROSS: 20 VALUES FOR FREQUENCIES BETWEEN 0.03 TO 0.22 HZ @ 0.01 HZ INCREMENT

```
 0.   0.51  3.95 54.32 39.14 34.30 28.62 24.25 19.91 16.14
13.02 10.54  8.50  6.86  5.53  4.45  3.59  2.89  2.33  1.88
```

===

DIRECTIONAL SPECTRUM
DOWN: 20 FREQUENCIES BETWEEN 0.03 TO 0.22 HZ @ 0.01 HZ INCREMENTS
ACROSS: 16 DIRECTIONS BETWEEN 0 TO 360 DEG @ 22.5 DEG INCREMENTS
FORMAT: 10 LINES HEADER PRIOR TO DIRECTIONAL SPECTRUM

IDN = 1   I = 10   J = 9   ISTA = 1

CENTRAL ANGLE BANDS FOR TWO-DIMENSIONAL SPECTRA

0.	22.	45.	67.	90.	112.	135.	157.	180.	202.	225.	247.	270.	292.	315.	337.
0.00	0.00	0.00	0.00	0.00	0.00	0.00	0.00	0.00	0.00	0.00	0.00	0.00	0.00	0.00	0.00
0.71	0.48	0.14	0.00	0.00	0.00	0.00	0.00	0.00	0.00	0.00	0.00	0.00	0.00	0.00	0.11
4.85	4.70	4.18	0.00	0.00	0.00	0.00	0.00	0.00	0.00	0.00	0.00	0.00	0.00	0.00	0.39
56.14	73.51	6.60	1.33	2.12	0.15	0.03	0.00	0.00	0.00	0.00	0.00	0.00	0.00	0.00	4.50
7.79	49.17	10.78	6.05	7.50	0.29	0.04	0.00	0.00	0.00	0.00	0.00	0.00	0.00	0.00	2.49
24.46	36.69	11.00	17.36	17.60	0.42	0.04	0.00	0.00	0.00	0.00	0.00	0.00	0.00	0.00	1.54
10.09	15.76	9.48	18.25	18.37	0.55	0.04	0.00	0.00	0.00	0.00	0.00	0.00	0.00	0.00	0.61
5.65	9.04	7.33	16.36	16.94	0.67	0.04	0.00	0.00	0.00	0.00	0.00	0.00	0.00	0.00	0.35
3.55	5.58	5.25	14.25	14.30	0.72	0.04	0.00	0.00	0.00	0.00	0.00	0.00	0.00	0.00	0.23
2.53	3.88	5.60	11.82	10.19	0.61	0.03	0.00	0.00	0.00	0.00	0.00	0.00	0.00	0.00	0.13
0.97	3.89	6.04	9.22	6.35	0.44	0.03	0.00	0.00	0.00	0.00	0.00	0.00	0.00	0.00	0.04
0.86	3.82	5.74	6.70	4.47	0.27	0.02	0.00	0.00	0.00	0.00	0.00	0.00	0.00	0.00	0.07
1.04	3.37	5.51	5.17	3.15	0.19	0.02	0.00	0.00	0.00	0.00	0.00	0.00	0.00	0.00	0.07
0.65	2.72	4.90	4.38	2.45	0.16	0.02	0.00	0.00	0.00	0.00	0.00	0.00	0.00	0.00	0.04
0.31	1.84	3.86	3.63	1.95	0.15	0.02	0.00	0.00	0.00	0.00	0.00	0.00	0.00	0.00	0.03
0.31	1.40	2.67	3.08	1.79	0.13	0.01	0.00	0.00	0.00	0.00	0.00	0.00	0.00	0.00	0.03
0.28	1.14	2.06	2.47	1.46	0.11	0.01	0.00	0.00	0.00	0.00	0.00	0.00	0.00	0.00	0.03
0.24	0.97	1.65	1.99	1.15	0.09	0.01	0.00	0.00	0.00	0.00	0.00	0.00	0.00	0.00	0.02
0.20	0.82	1.50	1.67	0.72	0.07	0.01	0.00	0.00	0.00	0.00	0.00	0.00	0.00	0.00	0.02
0.17	0.63	1.50	1.67	0.72	0.07	0.01	0.00	0.00	0.00	0.00	0.00	0.00	0.00	0.00	0.01

YS7001, TP = 14.3 SEC, HM0 = 5.8 M, DIR = 9 DEG
YAQUINA BAY JETTY STABILITY STUDY
DISCRETE VALUES OF PROTOTYPE SHALLOW WATER FREQUENCY & DIRECTIONAL SPECTRA
RESULTS FROM JENSEN'S SHOALING & REFRACTION NUMERICAL MODEL
FORMAT: 10 LINES HEADER PRIOR TO FREQUENCY SPECTRUM
METRIC UNITS

FREQUENCY SPECTRUM
ACROSS: 20 VALUES FOR FREQUENCIES BETWEEN 0.03 TO 0.22 HZ @ 0.01 HZ INCREMENT

0.   0.   1.38 18.09 40.24 23.80 21.46 17.81 15.48 13.28
10.99 9.02 7.37 6.02   4.89   3.96   3.20   2.58   2.09   1.69

===

DIRECTIONAL SPECTRUM
DOWN: 20 FREQUENCIES BETWEEN 0.03 TO 0.22 HZ @ 0.01 HZ INCREMENTS
ACROSS: 16 DIRECTIONS BETWEEN 0 TO 360 DEG @ 22.5 DEG INCREMENTS
FORMAT: 10 LINES HEADER PRIOR TO DIRECTIONAL SPECTRUM

IDN =   1   I = 10   J = 9   ISTA = 1

CENTRAL ANGLE BANDS FOR TWO-DIMENSIONAL SPECTRA

0.	22.	45.	67.	90.	112.	135.	157.	180.	202.	225.	247.	270.	292.	315.	337.
0.00	0.00	0.00	0.00	0.00	0.00	0.00	0.00	0.00	0.00	0.00	0.00	0.00	0.00	0.00	0.00
0.00	0.00	0.00	0.00	0.00	0.00	0.00	0.00	0.00	0.00	0.00	0.00	0.00	0.00	0.00	0.00
1.86	1.19	0.01	0.00	0.00	0.00	0.00	0.00	0.00	0.00	0.00	0.00	0.00	0.00	0.00	0.47
21.18	19.73	0.48	0.00	0.00	0.00	0.00	0.00	0.00	0.00	0.00	0.00	0.00	0.00	0.00	4.67
48.14	42.01	1.53	0.33	0.31	0.00	0.00	0.00	0.00	0.00	0.00	0.00	0.00	0.00	0.04	10.78
27.11	24.69	2.06	0.91	0.82	0.01	0.00	0.00	0.00	0.00	0.00	0.00	0.00	0.00	0.14	6.04
22.13	21.32	3.86	2.45	2.08	0.02	0.00	0.00	0.00	0.00	0.00	0.00	0.00	0.00	0.18	5.47
15.48	15.48	5.41	4.40	3.73	0.03	0.00	0.00	0.00	0.00	0.00	0.00	0.00	0.00	0.20	4.23
10.71	10.92	6.26	6.10	4.94	0.05	0.00	0.00	0.00	0.00	0.00	0.00	0.00	0.00	0.18	3.16
6.97	7.38	6.18	6.48	4.91	0.07	0.00	0.00	0.00	0.00	0.00	0.00	0.00	0.00	0.14	2.15
4.61	5.77	4.68	5.53	3.67	0.08	0.00	0.00	0.00	0.00	0.00	0.00	0.00	0.00	0.05	1.31
2.87	5.41	4.78	4.02	2.44	0.06	0.00	0.00	0.00	0.00	0.00	0.00	0.00	0.00	0.03	1.61
2.13	4.91	4.79	2.87	1.50	0.04	0.00	0.00	0.00	0.00	0.00	0.00	0.00	0.00	0.02	0.40
1.53	4.31	4.81	2.28	0.99	0.03	0.00	0.00	0.00	0.00	0.00	0.00	0.00	0.00	0.03	0.26
0.97	3.33	4.69	1.82	0.51	0.02	0.00	0.00	0.00	0.00	0.00	0.00	0.00	0.00	0.02	0.16
0.86	2.55	3.95	1.50	0.40	0.01	0.00	0.00	0.00	0.00	0.00	0.00	0.00	0.00	0.03	0.17
0.66	2.09	3.22	1.30	0.29	0.01	0.00	0.00	0.00	0.00	0.00	0.00	0.00	0.00	0.02	0.12
0.62	1.56	2.54	1.05	0.21	0.01	0.00	0.00	0.00	0.00	0.00	0.00	0.00	0.00	0.03	0.13
0.49	1.26	2.09	0.83	0.00	0.01	0.00	0.00	0.00	0.00	0.00	0.00	0.00	0.00	0.02	0.10
0.44	1.06	1.66	0.00	0.00	0.01	0.00	0.00	0.00	0.00	0.00	0.00	0.00	0.00	0.01	0.09

YS72Ø1, TP = 12.5 SEC, HMØ = 4.4 M, DIR = 19 DEG
YAQUINA BAY JETTY STABILITY STUDY
DISCRETE VALUES OF PROTOTYPE SHALLOW WATER FREQUENCY & DIRECTIONAL SPECTRA
RESULTS FROM JENSEN'S SHOALING & REFRACTION NUMERICAL MODEL
FORMAT: 1Ø LINES HEADER PRIOR TO FREQUENCY SPECTRUM
METRIC UNITS

FREQUENCY SPECTRUM
ACROSS: 2Ø VALUES FOR FREQUENCIES BETWEEN Ø.Ø3 TO Ø.22 HZ @ Ø.Ø1 HZ INCREMENT

Ø. Ø. 1.Ø8 9.44 19.3Ø 2Ø.23 19.22 1Ø.83 6.52 3.78
2.22 1.81 2.32 2.61 2.5Ø 2.Ø8 1.77 1.53 1.33 1.15

==

DIRECTIONAL SPECTRUM
DOWN: 2Ø FREQUENCIES BETWEEN Ø.Ø3 TO Ø.22 HZ @ Ø.Ø1 HZ INCREMENTS
ACROSS: 16 DIRECTIONS BETWEEN Ø TO 36Ø DEG @ 22.5 DEG INCREMENTS
FORMAT: 1Ø LINES HEADER PRIOR TO DIRECTIONAL SPECTRUM

IDN = 1   I = 1Ø   J = 9   ISTA = 1

CENTRAL ANGLE BANDS FOR TWO-DIMENSIONAL SPECTRA

Ø.	22.	45.	67.	90.	112.	135.	157.	180.	202.	225.	247.	270.	292.	315.	337.
Ø.ØØ	Ø.ØØ	Ø.ØØ	Ø.ØØ	Ø.ØØ	Ø.ØØ	Ø.ØØ	Ø.ØØ	Ø.ØØ	Ø.ØØ	Ø.ØØ	Ø.ØØ	Ø.ØØ	Ø.ØØ	Ø.ØØ	Ø.ØØ
Ø.ØØ	Ø.ØØ	Ø.ØØ	Ø.ØØ	Ø.ØØ	Ø.ØØ	Ø.ØØ	Ø.ØØ	Ø.ØØ	Ø.ØØ	Ø.ØØ	Ø.ØØ	Ø.ØØ	Ø.ØØ	Ø.ØØ	Ø.ØØ
1.5Ø	1.Ø9	Ø.22	Ø.ØØ	Ø.ØØ	Ø.ØØ	Ø.ØØ	Ø.ØØ	Ø.ØØ	Ø.ØØ	Ø.ØØ	Ø.ØØ	Ø.ØØ	Ø.ØØ	Ø.ØØ	Ø.16
11.81	11.Ø7	2.95	Ø.74	Ø.92	Ø.ØØ	Ø.ØØ	Ø.ØØ	Ø.ØØ	Ø.ØØ	Ø.ØØ	Ø.ØØ	Ø.ØØ	Ø.ØØ	Ø.ØØ	Ø.93
17.93	27.Ø2	6.19	Ø.62	Ø.ØØ	Ø.ØØ	Ø.ØØ	Ø.ØØ	Ø.ØØ	Ø.ØØ	Ø.ØØ	Ø.ØØ	Ø.ØØ	Ø.ØØ	Ø.ØØ	1.25
16.31	26.35	9.96	1.1Ø	Ø.ØØ	Ø.ØØ	Ø.ØØ	Ø.ØØ	Ø.ØØ	Ø.ØØ	Ø.ØØ	Ø.ØØ	Ø.ØØ	Ø.ØØ	Ø.ØØ	1.Ø1
14.1Ø	24.Ø6	7.83	1.14	Ø.ØØ	Ø.ØØ	Ø.ØØ	Ø.ØØ	Ø.ØØ	Ø.ØØ	Ø.ØØ	Ø.ØØ	Ø.ØØ	Ø.ØØ	Ø.ØØ	Ø.83
6.71	12.Ø2	5.48	1.ØØ	Ø.ØØ	Ø.ØØ	Ø.ØØ	Ø.ØØ	Ø.ØØ	Ø.ØØ	Ø.ØØ	Ø.ØØ	Ø.ØØ	Ø.ØØ	Ø.ØØ	Ø.39
3.44	6.38	3.31	Ø.95	Ø.Ø5	Ø.ØØ	Ø.ØØ	Ø.ØØ	Ø.ØØ	Ø.ØØ	Ø.ØØ	Ø.ØØ	Ø.ØØ	Ø.ØØ	Ø.ØØ	Ø.21
1.75	3.32	2.Ø1	1.27	Ø.28	Ø.ØØ	Ø.ØØ	Ø.ØØ	Ø.ØØ	Ø.ØØ	Ø.ØØ	Ø.ØØ	Ø.ØØ	Ø.ØØ	Ø.ØØ	Ø.11
Ø.98	1.87	1.47	1.36	Ø.31	Ø.Ø2	Ø.ØØ	Ø.ØØ	Ø.ØØ	Ø.ØØ	Ø.ØØ	Ø.ØØ	Ø.ØØ	Ø.ØØ	Ø.ØØ	Ø.Ø7
Ø.67	1.42	1.88	1.41	Ø.33	Ø.Ø2	Ø.ØØ	Ø.ØØ	Ø.ØØ	Ø.ØØ	Ø.ØØ	Ø.ØØ	Ø.ØØ	Ø.ØØ	Ø.ØØ	Ø.Ø5
Ø.69	1.73	2.18	1.23	Ø.29	Ø.Ø1	Ø.ØØ	Ø.ØØ	Ø.ØØ	Ø.ØØ	Ø.ØØ	Ø.ØØ	Ø.ØØ	Ø.ØØ	Ø.ØØ	Ø.Ø5
Ø.7Ø	2.Ø4	2.31	1.Ø3	Ø.25	Ø.Ø1	Ø.ØØ	Ø.ØØ	Ø.ØØ	Ø.ØØ	Ø.ØØ	Ø.ØØ	Ø.ØØ	Ø.ØØ	Ø.ØØ	Ø.Ø4
Ø.47	1.8Ø	2.Ø4	Ø.92	Ø.22	Ø.Ø1	Ø.ØØ	Ø.ØØ	Ø.ØØ	Ø.ØØ	Ø.ØØ	Ø.ØØ	Ø.ØØ	Ø.ØØ	Ø.ØØ	Ø.Ø2
Ø.31	1.39	1.85	Ø.82	Ø.2Ø	Ø.Ø1	Ø.ØØ	Ø.ØØ	Ø.ØØ	Ø.ØØ	Ø.ØØ	Ø.ØØ	Ø.ØØ	Ø.ØØ	Ø.ØØ	Ø.Ø2
Ø.23	1.12	1.64	Ø.73	Ø.21	Ø.Ø1	Ø.ØØ	Ø.ØØ	Ø.ØØ	Ø.ØØ	Ø.ØØ	Ø.ØØ	Ø.ØØ	Ø.ØØ	Ø.ØØ	Ø.Ø1
Ø.17	Ø.9Ø	1.4Ø				Ø.ØØ	Ø.ØØ	Ø.ØØ	Ø.ØØ	Ø.ØØ	Ø.ØØ	Ø.ØØ	Ø.ØØ	Ø.ØØ	Ø.Ø1
Ø.17	Ø.77	1.14				Ø.ØØ	Ø.ØØ	Ø.ØØ	Ø.ØØ	Ø.ØØ	Ø.ØØ	Ø.ØØ	Ø.ØØ	Ø.ØØ	Ø.Ø1
	Ø.65														Ø.Ø1

YS73Ø1, TP = 14.3 SEC, HMØ = 5.1 M, DIR = 15 DEG
YAQUINA BAY JETTY STABILITY STUDY
DISCRETE VALUES OF PROTOTYPE SHALLOW WATER FREQUENCY & DIRECTIONAL SPECTRA
RESULTS FROM JENSEN'S SHOALING & REFRACTION NUMERICAL MODEL
FORMAT: 1Ø LINES HEADER PRIOR TO FREQUENCY SPECTRUM
METRIC UNITS

FREQUENCY SPECTRUM
ACROSS: 2Ø VALUES FOR FREQUENCIES BETWEEN Ø.Ø3 TO Ø.22 HZ @ Ø.Ø1 HZ INCREMENT

Ø. Ø. 2.69 42.32 44.68 27.29 1Ø.99 5.17 2.58 1.45
1.24 1.71 2.19 2.42 2.33 1.95 1.67 1.45 1.26 1.Ø6

===

DIRECTIONAL SPECTRUM
DOWN: 2Ø FREQUENCIES BETWEEN Ø.Ø3 TO Ø.22 HZ @ Ø.Ø1 HZ INCREMENTS
ACROSS: 16 DIRECTIONS BETWEEN Ø TO 36Ø DEG @ 22.5 DEG INCREMENTS
FORMAT: 1Ø LINES HEADER PRIOR TO DIRECTIONAL SPECTRUM

IDN = 1   I = 1Ø   J = 9   ISTA = 1

CENTRAL ANGLE BANDS FOR TWO-DIMENSIONAL SPECTRA

Ø.	22.	45.	67.	90.	112.	135.	157.	180.	2Ø2.	225.	247.	270.	292.	315.	337.
Ø.ØØ	Ø.ØØ	Ø.ØØ	Ø.ØØ	Ø.ØØ	Ø.ØØ	Ø.ØØ	Ø.ØØ	Ø.ØØ	Ø.ØØ	Ø.ØØ	Ø.ØØ	Ø.ØØ	Ø.ØØ	Ø.ØØ	Ø.ØØ
3.35	3.16	3.15	Ø.ØØ	Ø.ØØ	Ø.ØØ	Ø.ØØ	Ø.ØØ	Ø.ØØ	Ø.ØØ	Ø.ØØ	Ø.ØØ	Ø.ØØ	Ø.ØØ	Ø.ØØ	Ø.27
44.2Ø	56.89	7.47	Ø.ØØ	Ø.ØØ	Ø.ØØ	Ø.ØØ	Ø.ØØ	Ø.ØØ	Ø.ØØ	Ø.ØØ	Ø.ØØ	Ø.ØØ	Ø.ØØ	Ø.ØØ	3.52
43.58	59.81	7.66	Ø.ØØ	Ø.ØØ	Ø.ØØ	Ø.ØØ	Ø.ØØ	Ø.ØØ	Ø.ØØ	Ø.ØØ	Ø.ØØ	Ø.ØØ	Ø.ØØ	Ø.ØØ	2.9Ø
24.7Ø	35.62	5.4Ø	Ø.ØØ	Ø.ØØ	Ø.ØØ	Ø.ØØ	Ø.ØØ	Ø.ØØ	Ø.ØØ	Ø.ØØ	Ø.ØØ	Ø.ØØ	Ø.ØØ	Ø.ØØ	1.5Ø
8.73	13.35	3.83	Ø.32	Ø.ØØ	Ø.ØØ	Ø.ØØ	Ø.ØØ	Ø.ØØ	Ø.ØØ	Ø.ØØ	Ø.ØØ	Ø.ØØ	Ø.ØØ	Ø.ØØ	Ø.19
3.34	5.49	2.18	Ø.47	Ø.ØØ	Ø.ØØ	Ø.ØØ	Ø.ØØ	Ø.ØØ	Ø.ØØ	Ø.ØØ	Ø.ØØ	Ø.ØØ	Ø.ØØ	Ø.ØØ	Ø.Ø8
1.43	2.41	1.24	Ø.46	Ø.ØØ	Ø.ØØ	Ø.ØØ	Ø.ØØ	Ø.ØØ	Ø.ØØ	Ø.ØØ	Ø.ØØ	Ø.ØØ	Ø.ØØ	Ø.ØØ	Ø.Ø5
Ø.73	1.22	Ø.99	Ø.53	Ø.ØØ	Ø.ØØ	Ø.ØØ	Ø.ØØ	Ø.ØØ	Ø.ØØ	Ø.ØØ	Ø.ØØ	Ø.ØØ	Ø.ØØ	Ø.ØØ	Ø.Ø4
Ø.62	Ø.99	1.38	1.Ø5	Ø.28	Ø.Ø4	Ø.ØØ	Ø.ØØ	Ø.ØØ	Ø.ØØ	Ø.ØØ	Ø.ØØ	Ø.ØØ	Ø.ØØ	Ø.ØØ	Ø.Ø2
Ø.45	1.13	1.83	1.45	Ø.54	Ø.Ø7	Ø.ØØ	Ø.ØØ	Ø.ØØ	Ø.ØØ	Ø.ØØ	Ø.ØØ	Ø.ØØ	Ø.ØØ	Ø.ØØ	Ø.Ø2
Ø.36	1.32	2.Ø1	1.63	Ø.64	Ø.1Ø	Ø.Ø1	Ø.ØØ	Ø.ØØ	Ø.ØØ	Ø.ØØ	Ø.ØØ	Ø.ØØ	Ø.ØØ	Ø.ØØ	Ø.Ø2
Ø.28	.43	2.Ø3	1.58	Ø.64	Ø.12	Ø.Ø1	Ø.ØØ	Ø.ØØ	Ø.ØØ	Ø.ØØ	Ø.ØØ	Ø.ØØ	Ø.ØØ	Ø.ØØ	Ø.Ø2
Ø.18	.23	1.71	1.38	Ø.58	Ø.1Ø	Ø.Ø1	Ø.ØØ	Ø.ØØ	Ø.ØØ	Ø.ØØ	Ø.ØØ	Ø.ØØ	Ø.ØØ	Ø.ØØ	Ø.Ø1
Ø.15	1.98	1.47	1.21	Ø.53	Ø.1Ø	Ø.Ø1	Ø.ØØ	Ø.ØØ	Ø.ØØ	Ø.ØØ	Ø.ØØ	Ø.ØØ	Ø.ØØ	Ø.ØØ	Ø.Ø1
Ø.Ø9	Ø.77	1.31	1.11	Ø.51	Ø.Ø9	Ø.Ø1	Ø.ØØ	Ø.ØØ	Ø.ØØ	Ø.ØØ	Ø.ØØ	Ø.ØØ	Ø.ØØ	Ø.ØØ	Ø.Ø1
Ø.Ø9	Ø.56	Ø.98	1.ØØ	Ø.52	Ø.1Ø	Ø.Ø1	Ø.ØØ	Ø.ØØ	Ø.ØØ	Ø.ØØ	Ø.ØØ	Ø.ØØ	Ø.ØØ	Ø.ØØ	Ø.Ø1
Ø.11	Ø.5Ø	Ø.84	Ø.88	Ø.43	Ø.Ø8	Ø.Ø1	Ø.ØØ	Ø.ØØ	Ø.ØØ	Ø.ØØ	Ø.ØØ	Ø.ØØ	Ø.ØØ	Ø.ØØ	Ø.Ø1

VS7401, TP = 16.7 SEC, HM0 = 5.9 M, DIR = 21 DEG
YAQUINA BAY JETTY STABILITY STUDY
DISCRETE VALUES OF PROTOTYPE SHALLOW WATER FREQUENCY & DIRECTIONAL SPECTRA
RESULTS FROM JENSEN'S SHOALING & REFRACTION NUMERICAL MODEL
FORMAT: 10 LINES HEADER PRIOR TO FREQUENCY SPECTRUM
METRIC UNITS

FREQUENCY SPECTRUM
ACROSS: 20 VALUES FOR FREQUENCIES BETWEEN 0.03 TO 0.22 HZ @ 0.01 HZ INCREMENT

0.   11.44 13.62 54.12 34.10 18.56 15.63 13.39 11.07 9.00
7.28   5.88 4.75 3.84 3.10 2.50 2.01 1.62 1.31 1.06

===

DIRECTIONAL SPECTRUM
DOWN: 20 FREQUENCIES BETWEEN 0.03 TO 0.22 HZ @ 0.01 HZ INCREMENTS
ACROSS: 16 DIRECTIONS BETWEEN 0 TO 360 DEG @ 22.5 DEG INCREMENTS
FORMAT: 10 LINES HEADER PRIOR TO DIRECTIONAL SPECTRUM

IDN = 1   I = 10   J = 9   ISTA = 1

CENTRAL ANGLE BANDS FOR TWO-DIMENSIONAL SPECTRA

0.	22.	45.	67.	90.	112.	135.	157.	180.	202.	225.	247.	270.	292.	315.	337.
0.00	0.00	0.00	0.00	0.00	0.00	0.00	0.00	0.00	0.00	0.00	0.00	0.00	0.00	0.00	0.00
0.00	0.00	0.00	0.00	0.00	0.00	0.00	0.00	0.00	0.00	0.00	0.00	0.00	0.00	0.00	0.00
13.88	19.49	2.02	1.31	25.79	0.00	0.00	0.00	0.00	0.00	0.00	0.00	0.00	0.00	0.00	0.53
41.82	84.05	0.87	0.00	0.00	0.00	0.00	0.00	0.00	0.00	0.00	0.00	0.00	0.00	0.00	1.30
21.20	51.65	10.63	0.00	0.00	0.00	0.00	0.00	0.00	0.00	0.00	0.00	0.00	0.00	0.00	0.52
7.53	21.85	13.47	2.53	3.04	0.06	0.00	0.00	0.00	0.00	0.00	0.00	0.00	0.00	0.00	0.14
4.71	14.62	12.13	3.77	3.73	0.07	0.00	0.00	0.00	0.00	0.00	0.00	0.00	0.00	0.00	0.06
2.65	9.53	12.83	5.30	4.23	0.09	0.00	0.00	0.00	0.00	0.00	0.00	0.00	0.00	0.00	0.02
1.31	5.67	12.26	6.52	3.92	0.11	0.00	0.00	0.00	0.00	0.00	0.00	0.00	0.00	0.00	0.01
0.69	3.41	10.64	7.39	3.23	0.11	0.00	0.00	0.00	0.00	0.00	0.00	0.00	0.00	0.00	0.01
0.57	2.65	8.10	7.39	2.54	0.10	0.00	0.00	0.00	0.00	0.00	0.00	0.00	0.00	0.00	0.01
0.53	2.61	5.28	5.93	1.66	0.07	0.00	0.00	0.00	0.00	0.00	0.00	0.00	0.00	0.00	0.00
0.41	2.21	4.18	3.94	2.06	0.04	0.00	0.00	0.00	0.00	0.00	0.00	0.00	0.00	0.00	0.00
0.20	1.84	3.44	2.85	1.51	0.03	0.00	0.00	0.00	0.00	0.00	0.00	0.00	0.00	0.00	0.00
0.12	1.40	3.36	2.25	1.09	0.02	0.00	0.00	0.00	0.00	0.00	0.00	0.00	0.00	0.00	0.00
0.10	1.06	2.55	1.86	0.78	0.02	0.00	0.00	0.00	0.00	0.00	0.00	0.00	0.00	0.00	0.00
0.09	0.83	2.05	1.60	0.54	0.01	0.00	0.00	0.00	0.00	0.00	0.00	0.00	0.00	0.00	0.00
0.08	0.69	1.65	1.29	0.40	0.01	0.00	0.00	0.00	0.00	0.00	0.00	0.00	0.00	0.00	0.00
0.07	0.57	1.33	1.03	0.31	0.01	0.00	0.00	0.00	0.00	0.00	0.00	0.00	0.00	0.00	0.00
0.06	0.47	1.10	0.82	0.23	0.01	0.00	0.00	0.00	0.00	0.00	0.00	0.00	0.00	0.00	0.00

YS8301, TP - 16.7 SEC, HM0 = 5.7 M, DIR = 14 DEG
YAQUINA BAY JETTY STABILITY STUDY
DISCRETE VALUES OF PROTOTYPE SHALLOW WATER FREQUENCY & DIRECTIONAL SPECTRA
RESULTS FROM JENSEN'S SHOALING & REFRACTION NUMERICAL MODEL
FORMAT: 10 LINES HEADER PRIOR TO FREQUENCY SPECTRUM
METRIC UNITS

FREQUENCY SPECTRUM
ACROSS: 20 VALUES FOR FREQUENCIES BETWEEN 0.03 TO 0.22 HZ @ 0.01 HZ INCREMENT

```
0.   0.   12.25 58.64 44.74 23.67 10.28 8.86 7.84 6.74
5.66 4.69 3.85 3.15 2.57 2.08 1.69 1.36 1.10 .89
```

===

DIRECTIONAL SPECTRUM
DOWN: 20 FREQUENCIES BETWEEN 0.03 TO 0.22 HZ @ 0.01 HZ INCREMENTS
ACROSS: 16 DIRECTIONS BETWEEN 0 TO 360 DEG @ 22.5 DEG INCREMENTS
FORMAT: 10 LINES HEADER PRIOR TO DIRECTIONAL SPECTRUM

IDN =   1   I = 10   J = 9   ISTA = 1

CENTRAL ANGLE BANDS FOR TWO-DIMENSIONAL SPECTRA

0.	22.	45.	67.	90.	112.	135.	157.	180.	202.	225.	247.	270.	292.	315.	337.
0.00	0.00	0.00	0.00	0.00	0.00	0.00	0.00	0.00	0.00	0.00	0.00	0.00	0.00	0.00	0.00
0.00	0.00	0.00	0.00	0.00	0.00	0.00	0.00	0.00	0.00	0.00	0.00	0.00	0.00	0.00	0.00
14.04	15.51	0.36	0.00	0.00	0.00	0.00	0.00	0.00	0.00	0.00	0.00	0.00	0.00	0.00	1.28
62.47	77.66	4.33	0.00	0.00	0.00	0.00	0.00	0.00	0.00	0.00	0.00	0.00	0.00	0.00	4.87
46.10	59.39	5.32	0.00	0.00	0.00	0.00	0.00	0.00	0.00	0.00	0.00	0.00	0.00	0.00	3.11
21.20	32.05	5.71	0.07	0.02	0.00	0.00	0.00	0.00	0.00	0.00	0.00	0.00	0.00	0.00	1.31
8.25	13.13	4.21	0.51	0.03	0.00	0.00	0.00	0.00	0.00	0.00	0.00	0.00	0.00	0.00	0.48
5.56	10.26	5.87	1.14	0.04	0.00	0.00	0.00	0.00	0.00	0.00	0.00	0.00	0.00	0.00	0.34
3.89	8.01	6.63	1.63	0.05	0.00	0.00	0.00	0.00	0.00	0.00	0.00	0.00	0.00	0.00	0.26
2.49	5.73	7.08	1.75	0.05	0.01	0.00	0.00	0.00	0.00	0.00	0.00	0.00	0.00	0.00	0.19
1.55	3.88	7.04	1.67	0.04	0.01	0.00	0.00	0.00	0.00	0.00	0.00	0.00	0.00	0.00	0.13
1.58	3.70	4.79	1.53	0.21	0.01	0.00	0.00	0.00	0.00	0.00	0.00	0.00	0.00	0.00	0.15
1.38	3.37	3.18	1.31	0.27	0.04	0.00	0.00	0.00	0.00	0.00	0.00	0.00	0.00	0.00	0.13
1.11	2.85	2.38	1.16	0.22	0.21	0.00	0.00	0.00	0.00	0.00	0.00	0.00	0.00	0.00	0.10
0.77	2.19	2.13	0.97	0.19	0.27	0.00	0.00	0.00	0.00	0.00	0.00	0.00	0.00	0.00	0.06
0.54	1.66	1.89	0.81	0.21	0.22	0.00	0.00	0.00	0.00	0.00	0.00	0.00	0.00	0.00	0.04
0.42	1.32	1.50	0.69	0.19	0.19	0.00	0.00	0.00	0.00	0.00	0.00	0.00	0.00	0.00	0.03
0.33	1.02	1.20	0.57	0.16	0.21	0.00	0.00	0.00	0.00	0.00	0.00	0.00	0.00	0.00	0.03
0.27	0.81	0.98	0.48	0.15	0.19	0.00	0.00	0.00	0.00	0.00	0.00	0.00	0.00	0.00	0.02
0.21	0.64	0.78	0.48	0.15	0.16	0.00	0.00	0.00	0.00	0.00	0.00	0.00	0.00	0.00	0.02

FREQUENCY SPECTRUM
ACROSS: 20 VALUES FOR FREQUENCIES BETWEEN 0.03 TO 0.22 HZ @ 0.01 HZ INCREMENT

0.00 0.00 5.80 62.55 40.19 35.22 29.38 24.90 20.45 16.57
13.37 10.82 8.73 7.04 5.68 4.57 3.68 2.96 2.39 1.93

===

DIRECTIONAL SPECTRUM
DOWN: 20 FREQUENCIES BETWEEN 0.03 TO 0.22 HZ @ 0.01 HZ INCREMENTS
ACROSS: 16 DIRECTIONS BETWEEN 0 TO 360 DEG @ 22.5 DEG INCREMENTS
FORMAT: 10 LINES HEADER PRIOR TO DIRECTIONAL SPECTRUM

IDN = 1969   I = 10   J = 9   ISTA = 1

CENTRAL ANGLE BANDS FOR TWO-DIMENSIONAL SPECTRA

0.	22.	45.	67.	90.	112.	135.	157.	180.	202.	225.	247.	270.	292.	315.	337.
0.00	0.00	0.00	0.00	0.00	0.00	0.00	0.00	0.00	0.00	0.00	0.00	0.00	0.00	0.00	0.00
0.00	0.00	0.06	0.00	0.00	0.00	0.00	0.00	0.00	0.00	0.00	0.00	0.00	0.00	0.00	1.41
9.19	4.11	2.77	0.00	0.00	0.00	0.00	0.00	0.00	0.00	0.00	0.00	0.00	0.00	0.00	7.16
75.48	73.88	4.73	1.02	1.59	0.13	0.02	0.00	0.00	0.00	0.00	0.00	0.00	0.00	0.00	6.45
42.94	45.47	16.50	9.08	11.30	0.35	0.04	0.00	0.00	0.00	0.00	0.00	0.00	0.00	0.00	4.48
17.04	30.90	15.84	22.00	22.29	0.46	0.04	0.00	0.00	0.00	0.00	0.00	0.00	0.00	0.00	1.72
4.10	8.38	14.02	22.32	21.86	0.63	0.04	0.00	0.00	0.00	0.00	0.00	0.00	0.00	0.00	0.85
1.13	2.56	10.79	20.26	18.41	0.76	0.04	0.00	0.00	0.00	0.00	0.00	0.00	0.00	0.01	0.25
0.44	1.18	7.28	18.71	14.05	0.76	0.04	0.00	0.00	0.00	0.00	0.00	0.00	0.00	0.00	0.04
0.16	1.15	6.33	15.78	9.36	0.60	0.03	0.00	0.00	0.00	0.00	0.00	0.00	0.00	0.00	0.03
0.12	1.81	5.99	12.95	5.92	0.45	0.03	0.00	0.00	0.00	0.00	0.00	0.00	0.00	0.00	0.08
0.13	1.40	4.53	9.18	6.13	0.26	0.02	0.00	0.00	0.00	0.00	0.00	0.00	0.00	0.00	0.04
0.02	0.84	3.67	7.08	5.24	0.18	0.02	0.00	0.00	0.00	0.00	0.00	0.00	0.00	0.00	0.02
0.01	0.52	2.70	5.76	4.30	0.15	0.02	0.00	0.00	0.00	0.00	0.00	0.00	0.00	0.00	0.01
0.02	0.32	1.95	4.70	3.75	0.14	0.01	0.00	0.00	0.00	0.00	0.00	0.00	0.00	0.00	0.00
0.00	0.24	1.57	3.80	3.25	0.12	0.01	0.00	0.00	0.00	0.00	0.00	0.00	0.00	0.00	0.00
0.00	0.20	1.23	2.97	2.69	0.10	0.01	0.00	0.00	0.00	0.00	0.00	0.00	0.00	0.00	0.00
0.00	0.17	0.89	2.39	2.20	0.09	0.01	0.00	0.00	0.00	0.00	0.00	0.00	0.00	0.00	0.00
0.00	0.13		2.11	1.71	0.07	0.01	0.00	0.00	0.00	0.00	0.00	0.00	0.00	0.00	0.00
0.00							0.00	0.00	0.00	0.00	0.00	0.00	0.00	0.00	0.00

A9

YD7003, TP = 14.3 SEC, HM0 = 5.8 M, DIR = 2 DEG
YAQUINA BAY JETTY STABILITY STUDY
DISCRETE VALUES OF PROTOTYPE SHALLOW WATER FREQUENCY & DIRECTIONAL SPECTRA
RESULTS FROM JENSEN'S SHOALING & REFRACTION NUMERICAL MODEL, DISCRETE DIR SPEC
FORMAT: 10 LINES HEADER PRIOR TO FREQUENCY SPECTRUM
METRIC UNITS

FREQUENCY SPECTRUM
ACROSS: 20 VALUES FOR FREQUENCIES BETWEEN 0.03 TO 0.22 HZ @ 0.01 HZ INCREMENT

0.0 0.0 1.91 17.17 44.73 22.14 20.49 17.29 15.05 12.91
10.59 8.77 7.17 5.86 4.75 3.85 3.11 2.51 2.03 1.64

===

DIRECTIONAL SPECTRUM
DOWN: 20 FREQUENCIES BETWEEN 0.03 TO 0.22 HZ @ 0.01 HZ INCREMENTS
ACROSS: 16 DIRECTIONS BETWEEN 0 TO 360 DEG @ 22.5 DEG INCREMENTS
FORMAT: 10 LINES HEADER PRIOR TO DIRECTIONAL SPECTRUM

IDN = 1970   I = 10   J = 9   ISTA = 1

CENTRAL ANGLE BANDS FOR TWO-DIMENSIONAL SPECTRA

0.	22.	45.	67.	90.	112.	135.	157.	180.	202.	225.	247.	270.	292.	315.	337.
0.00	0.00	0.00	0.00	0.00	0.00	0.00	0.00	0.00	0.00	0.00	0.00	0.00	0.00	0.00	0.00
0.00	0.00	0.00	0.00	0.00	0.00	0.00	0.00	0.00	0.00	0.00	0.00	0.00	0.00	0.00	0.00
3.34	0.91	0.27	0.00	0.00	0.00	0.00	0.00	0.00	0.00	0.00	0.00	0.00	0.00	0.00	0.62
15.76	13.61	0.34	0.19	0.17	0.01	0.00	0.00	0.00	0.00	0.00	0.00	0.00	0.00	0.01	14.08
57.78	33.57	1.15	0.81	0.73	0.02	0.00	0.00	0.00	0.00	0.00	0.00	0.00	0.00	0.11	22.29
27.48	17.61	5.21	2.97	2.19	0.03	0.00	0.00	0.00	0.00	0.00	0.00	0.00	0.00	0.11	9.75
19.60	19.33	9.55	6.12	3.23	0.05	0.00	0.00	0.00	0.00	0.00	0.00	0.00	0.00	0.20	6.37
11.32	15.16	12.52	9.74	3.17	0.06	0.00	0.00	0.00	0.00	0.00	0.00	0.00	0.00	0.13	2.71
4.96	9.50	11.73	11.28	2.74	0.06	0.00	0.00	0.00	0.00	0.00	0.00	0.00	0.00	0.05	1.76
2.25	5.21	8.37	10.46	2.04	0.05	0.00	0.00	0.00	0.00	0.00	0.00	0.00	0.00	0.01	0.61
1.21	3.31	5.66	7.41	2.65	0.03	0.00	0.00	0.00	0.00	0.00	0.00	0.00	0.00	0.01	0.20
0.97	3.07	4.21	5.18	2.47	0.02	0.00	0.00	0.00	0.00	0.00	0.00	0.00	0.00	0.01	0.09
0.85	3.04	4.04	3.66	1.83	0.01	0.00	0.00	0.00	0.00	0.00	0.00	0.00	0.00	0.01	0.05
0.52	2.63	4.02	2.87	1.33	0.01	0.00	0.00	0.00	0.00	0.00	0.00	0.00	0.00	0.01	0.04
0.36	2.19	3.57	2.28	1.10	0.01	0.00	0.00	0.00	0.00	0.00	0.00	0.00	0.00	0.02	0.03
0.31	1.65	2.91	1.80	0.80	0.01	0.00	0.00	0.00	0.00	0.00	0.00	0.00	0.00	0.02	0.03
0.26	1.31	2.38	1.49	0.60	0.01	0.00	0.00	0.00	0.00	0.00	0.00	0.00	0.00	0.00	0.03
0.26	1.10	1.89	1.18	0.46	0.01	0.00	0.00	0.00	0.00	0.00	0.00	0.00	0.00	0.00	0.03
0.23	0.89	1.56	0.00	0.00	0.00	0.00	0.00	0.00	0.00	0.00	0.00	0.00	0.00	0.00	0.03
0.20	0.76	0.00	0.00	0.00	0.00	0.00	0.00	0.00	0.00	0.00	0.00	0.00	0.00	0.00	0.02

YD7203, TP = 14.3 SEC, HMØ = 4.7 M, DIR = 11
YAQUINA BAY JETTY STABILITY STUDY
DISCRETE VALUES OF PROTOTYPE SHALLOW WATER FREQUENCY & DIRECTIONAL SPECTRA
RESULTS FROM JENSEN'S SHOALING & REFRACTION NUMERICAL MODEL, DISCRETE DIR SPEC
FORMAT: 10 LINES HEADER PRIOR TO FREQUENCY SPECTRUM
METRIC UNITS

FREQUENCY SPECTRUM
ACROSS: 20 VALUES FOR FREQUENCIES BETWEEN 0.03 TO 0.22 HZ @ 0.01 HZ INCREMENT

```
0.0  0.0  2.19 19.05 27.20 21.86 18.98  9.52  5.43  2.90
1.87 1.80 2.63  2.60  2.49  2.09  1.76  1.53  1.33  1.14
```

===

DIRECTIONAL SPECTRUM
DOWN: 20 FREQUENCIES BETWEEN 0.03 TO 0.22 HZ @ 0.01 HZ INCREMENTS
ACROSS: 16 DIRECTIONS BETWEEN 0 TO 360 DEG @ 22.5 DEG INCREMENTS
FORMAT: 10 LINES HEADER PRIOR TO DIRECTIONAL SPECTRUM

IDN = 1972   I = 10   J = 10   ISTA = 9

CENTRAL ANGLE BANDS FOR TWO-DIMENSIONAL SPECTRA

0.	22.	45.	67.	90.	112.	135.	157.	180.	202.	225.	247.	270.	292.	315.	337.
0.00	0.00	0.00	0.00	0.00	0.00	0.00	0.00	0.00	0.00	0.00	0.00	0.00	0.00	0.00	0.00
0.00	0.00	0.00	0.00	0.00	0.00	0.00	0.00	0.00	0.00	0.00	0.00	0.00	0.00	0.00	0.00
3.86	1.00	0.14	0.00	0.00	0.00	0.00	0.00	0.00	0.00	0.00	0.00	0.00	0.00	0.00	0.72
33.09	11.05	0.70	0.00	0.00	0.00	0.00	0.00	0.00	0.00	0.00	0.00	0.00	0.00	0.00	4.23
44.49	20.41	4.58	0.08	0.10	0.00	0.00	0.00	0.00	0.00	0.00	0.00	0.00	0.00	0.05	4.95
24.08	22.63	8.16	0.00	0.00	0.00	0.00	0.00	0.00	0.00	0.00	0.00	0.00	0.00	0.19	2.54
14.76	22.68	7.08	0.60	0.00	0.00	0.00	0.00	0.00	0.00	0.00	0.00	0.00	0.00	0.17	1.05
5.42	9.93	4.56	1.03	0.01	0.00	0.00	0.00	0.00	0.00	0.00	0.00	0.00	0.00	0.12	0.52
2.62	4.99	2.74	1.24	0.01	0.00	0.00	0.00	0.00	0.00	0.00	0.00	0.00	0.00	0.07	0.24
0.97	2.10	1.79	1.22	0.01	0.00	0.00	0.00	0.00	0.00	0.00	0.00	0.00	0.00	0.05	0.13
0.46	1.12	1.52	1.34	0.11	0.01	0.00	0.00	0.00	0.00	0.00	0.00	0.00	0.00	0.01	0.06
0.42	1.12	2.22	1.71	0.38	0.03	0.00	0.00	0.00	0.00	0.00	0.00	0.00	0.00	0.01	0.05
0.58	1.72	2.23	1.61	0.38	0.02	0.00	0.00	0.00	0.00	0.00	0.00	0.00	0.00	0.01	0.03
0.51	1.84	2.31	1.58	0.36	0.02	0.00	0.00	0.00	0.00	0.00	0.00	0.00	0.00	0.01	0.03
0.34	1.68	2.05	1.39	0.33	0.02	0.00	0.00	0.00	0.00	0.00	0.00	0.00	0.00	0.00	0.02
0.26	1.25	1.84	1.15	0.26	0.01	0.00	0.00	0.00	0.00	0.00	0.00	0.00	0.00	0.00	0.02
0.19	1.02	1.63	1.00	0.22	0.01	0.00	0.00	0.00	0.00	0.00	0.00	0.00	0.00	0.00	0.02
0.18	0.83	1.40	0.87	0.21	0.01	0.00	0.00	0.00	0.00	0.00	0.00	0.00	0.00	0.00	0.01
0.15	0.72	1.14	0.79	0.21	0.01	0.00	0.00	0.00	0.00	0.00	0.00	0.00	0.00	0.00	0.01
0.15	0.60														

YD73C3, TP = 14.3 SEC, HMO = 5.2 M, DIR = 4 DEG
YAQUINA BAY JETTY STABILITY STUDY
DISCRETE VALUES OF PROTOTYPE SHALLOW WATER FREQUENCY AND DIRECTIONAL SPECTRA
RESULTS FROM JENSEN'S SHOALING & REFRACTION NUMERICAL MODEL, DISCRETE DIR SPEC
FORMAT: 10 LINES HEADER PRIOR TO FREQUENCY SPECTRUM
METRIC UNITS

FREQUENCY SPECTRUM
ACROSS: 20 VALUES FOR FREQUENCIES BETWEEN 0.03 TO 0.22 HZ @ 0.01 HZ INCREMENT

0.0 0.0 3.52 44.02 48.25 27.21 9.84 4.24 2.07 1.13
1.08 1.99 2.43 2.57 2.31 1.92 1.63 1.41 1.23 1.08

===

DIRECTIONAL SPECTRUM
DOWN: 20 FREQUENCIES BETWEEN 0.03 TO 0.22 HZ @ 0.01 HZ INCREMENTS
ACROSS: 16 DIRECTIONS BETWEEN 0 TO 360 DEG @ 22.5 DEG INCREMENTS
FORMAT: 10 LINES HEADER PRIOR TO DIRECTIONAL SPECTRUM

IDN = 1973   I = 10   J = 9   ISTA = 1

CENTRAL ANGLE BANDS FOR TWO-DIMENSIONAL SPECTRA

0.	22.	45.	67.	90.	112.	135.	157.	180.	202.	225.	247.	270.	292.	315.	337.
0.00	0.00	0.00	0.00	0.00	0.00	0.00	0.00	0.00	0.00	0.00	0.00	0.00	0.00	0.00	0.00
0.00	0.00	0.00	0.00	0.00	0.00	0.00	0.00	0.00	0.00	0.00	0.00	0.00	0.00	0.00	0.00
1.04	0.00	0.02	0.00	0.00	0.00	0.00	0.00	0.00	0.00	0.00	0.00	0.00	0.00	0.00	7.39
23.83	0.50	0.89	0.00	0.00	0.00	0.00	0.00	0.00	0.00	0.00	0.00	0.00	0.00	0.00	60.12
36.21	27.27	5.38	0.00	0.00	0.00	0.00	0.00	0.00	0.00	0.00	0.00	0.00	0.00	0.00	30.04
20.29	51.24	9.07	0.00	0.00	0.00	0.00	0.00	0.00	0.00	0.00	0.00	0.00	0.00	0.00	10.79
5.53	29.12	8.24	0.00	0.00	0.00	0.00	0.00	0.00	0.00	0.00	0.00	0.00	0.00	0.00	1.86
1.09	9.43	6.07	0.64	0.00	0.00	0.00	0.00	0.00	0.00	0.00	0.00	0.00	0.00	0.00	0.30
0.27	2.69	3.08	0.99	0.00	0.00	0.00	0.00	0.00	0.00	0.00	0.00	0.00	0.00	0.00	0.07
0.08	0.85	1.50	1.00	0.04	0.00	0.00	0.00	0.00	0.00	0.00	0.00	0.00	0.00	0.00	0.02
0.03	0.28	1.09	1.24	0.17	0.00	0.00	0.00	0.00	0.00	0.00	0.00	0.00	0.00	0.00	0.01
0.11	0.20	1.57	1.83	0.72	0.01	0.00	0.00	0.00	0.00	0.00	0.00	0.00	0.00	0.00	0.00
0.12	0.67	1.87	2.27	1.04	0.21	0.01	0.00	0.00	0.00	0.00	0.00	0.00	0.00	0.00	0.01
0.08	0.86	1.98	2.08	1.11	0.19	0.02	0.00	0.00	0.00	0.00	0.00	0.00	0.00	0.00	0.02
0.03	0.70	1.86	2.06	1.05	0.16	0.01	0.00	0.00	0.00	0.00	0.00	0.00	0.00	0.00	0.01
0.02	0.52	1.46	1.78	0.95	0.14	0.01	0.00	0.00	0.00	0.00	0.00	0.00	0.00	0.00	0.01
0.02	0.42	1.29	1.53	0.75	0.11	0.01	0.00	0.00	0.00	0.00	0.00	0.00	0.00	0.00	0.01
0.01	0.31	1.11	1.33	0.71	0.10	0.01	0.00	0.00	0.00	0.00	0.00	0.00	0.00	0.00	0.01
0.01	0.30	0.85	1.20	0.64	0.11	0.01	0.00	0.00	0.00	0.00	0.00	0.00	0.00	0.00	0.00
0.02	0.23	0.68	1.11	0.62	0.09	0.01	0.00	0.00	0.00	0.00	0.00	0.00	0.00	0.00	0.00

```
YD7403, TP = 16.7 SEC, HMØ = 6.2 M, DIR = 36 DEG
YAQUINA BAY JETTY STABILITY STUDY
DISCRETE VALUES OF PROTOTYPE SHALLOW WATER FREQUENCY & DIRECTIONAL SPECTRA
RESULTS FROM JENSEN'S SHOALING & REFRACTION NUMERICAL MODEL, DISCRETE DIR SPEC
FORMAT: 10 LINES HEADER PRIOR TO FREQUENCY SPECTRUM
METRIC UNITS

FREQUENCY SPECTRUM
ACROSS:  20 VALUES FOR FREQUENCIES BETWEEN 0.03 TO 0.22 HZ @ 0.01 HZ INCREMENT

0.00 11.66 20.84 57.87 39.77 19.29 16.25 13.91 11.50 9.36
7.57  6.12  4.94  3.99  3.22  2.60  2.09  1.68  1.36 1.10

=====================================================================

DIRECTIONAL SPECTRUM
DOWN:   20 FREQUENCIES BETWEEN 0.03 TO 0.22 HZ @ 0.01 HZ INCREMENTS
ACROSS: 16 DIRECTIONS BETWEEN 0 TO 360 DEG @ 22.5 DEG INCREMENTS
FORMAT: 10 LINES HEADER PRIOR TO DIRECTIONAL SPECTRUM

IDN = 1974    I = 10    J = 9    ISTA = 1
```

CENTRAL ANGLE BANDS FOR TWO-DIMENSIONAL SPECTRA

0.	22.	45.	67.	90.	112.	135.	157.	180.	202.	225.	247.	270.	292.	315.	337.
0.00	0.00	0.00	0.00	0.00	0.00	0.00	0.00	0.00	0.00	0.00	0.00	0.00	0.00	0.00	0.00
0.00	0.00	2.06	1.34	0.00	0.00	0.00	0.00	0.00	0.00	0.00	0.00	0.00	0.00	0.00	3.06
26.81	22.53	0.66	0.00	26.29	0.00	0.00	0.00	0.00	0.00	0.00	0.00	0.00	0.00	0.00	1.24
44.39	90.51	11.22	0.00	0.00	0.00	0.00	0.00	0.00	0.00	0.00	0.00	0.00	0.00	0.00	0.98
25.13	59.26	15.92	1.92	0.00	0.05	0.00	0.00	0.00	0.00	0.00	0.00	0.00	0.00	0.00	1.00
8.35	22.74	12.78	3.25	2.29	0.07	0.00	0.00	0.00	0.00	0.00	0.00	0.00	0.00	0.00	0.63
5.13	14.58	14.49	5.52	3.21	0.10	0.00	0.00	0.00	0.00	0.00	0.00	0.00	0.00	0.00	0.40
2.85	8.66	13.68	7.24	4.22	0.11	0.00	0.00	0.00	0.00	0.00	0.00	0.00	0.00	0.00	0.10
1.40	4.96	11.39	8.56	4.09	0.12	0.00	0.00	0.00	0.00	0.00	0.00	0.00	0.00	0.00	0.03
0.62	2.68	8.40	8.37	3.43	0.10	0.00	0.00	0.00	0.00	0.00	0.00	0.00	0.00	0.00	0.01
0.56	2.31	5.30	6.56	2.63	0.07	0.00	0.00	0.00	0.00	0.00	0.00	0.00	0.00	0.00	0.01
0.54	2.53	4.19	4.32	1.67	0.04	0.00	0.00	0.00	0.00	0.00	0.00	0.00	0.00	0.00	0.01
0.42	2.30	3.54	3.04	1.96	0.03	0.00	0.00	0.00	0.00	0.00	0.00	0.00	0.00	0.00	0.01
0.22	1.97	3.46	2.36	1.45	0.02	0.00	0.00	0.00	0.00	0.00	0.00	0.00	0.00	0.00	0.01
0.14	1.50	3.12	1.99	1.04	0.02	0.00	0.00	0.00	0.00	0.00	0.00	0.00	0.00	0.00	0.02
0.11	1.10	2.62	1.75	0.77	0.02	0.00	0.00	0.00	0.00	0.00	0.00	0.00	0.00	0.00	0.02
0.11	0.82	2.09	1.37	0.52	0.01	0.00	0.00	0.00	0.00	0.00	0.00	0.00	0.00	0.00	0.02
0.11	0.69	1.70	1.12	0.39	0.01	0.00	0.00	0.00	0.00	0.00	0.00	0.00	0.00	0.00	0.02
0.08	0.57	1.36	0.88	0.30	0.01	0.00	0.00	0.00	0.00	0.00	0.00	0.00	0.00	0.00	0.02
0.07	0.47	1.11	0.73	0.23	0.01	0.00	0.00	0.00	0.00	0.00	0.00	0.00	0.00	0.00	0.01

A13

YD8303. TP . 16.7 SEC. HMO = 6.2 M. DIR = 9 DEG
YAQUINA BAY JETTY STABILITY STUDY
DISCRETE VALUES OF PROTOTYPE SHALLOW WATER FREQUENCY & DIRECTIONAL SPECTRA
RESULTS FROM JENSEN'S SHOALING & REFRACTION NUMERICAL MODEL. DISCRETE DIR SPEC
FORMAT: 10 LINES HEADER PRIOR TO FREQUENCY SPECTRUM
METRIC UNITS

FREQUENCY SPECTRUM
ACROSS: 20 VALUES FOR FREQUENCIES BETWEEN 0.03 TO 0.22 HZ @ 0.01 HZ INCREMENT

```
0.0 0.0 17.16 86.43 57.31 19.42 9.89 8.53 7.54 6.49
5.44 4.51 3.71 3.03 2.47 2.00 1.62 1.31 1.06 0.86
```

==

DIRECTIONAL SPECTRUM
DOWN: 20 FREQUENCIES BETWEEN 0.03 TO 0.22 HZ @ 0.01 HZ INCREMENTS
ACROSS: 16 DIRECTIONS BETWEEN 0 TO 360 DEG @ 22.5 DEG INCREMENTS
FORMAT: 10 LINES HEADER PRIOR TO DIRECTIONAL SPECTRUM

IDN = 1983   I = 10   J = 9   ISTA = 1

CENTRAL ANGLE BANDS FOR TWO-DIMENSIONAL SPECTRA

0.	22.	45.	67.	90.	112.	135.	157.	180.	202.	225.	247.	270.	292.	315.	337.
0.00	0.00	0.00	0.00	0.00	0.00	0.00	0.00	0.00	0.00	0.00	0.00	0.00	0.00	0.00	0.00
0.00	0.00	0.00	0.00	0.00	0.00	0.00	0.00	0.00	0.00	0.00	0.00	0.00	0.00	0.00	2.25
21.18	20.06	0.22	0.00	0.00	0.00	0.00	0.00	0.00	0.00	0.00	0.00	0.00	0.00	0.00	8.50
110.74	100.50	0.37	0.00	0.00	0.00	0.00	0.00	0.00	0.00	0.00	0.00	0.00	0.00	0.00	2.94
66.41	75.07	1.52	0.00	0.00	0.00	0.00	0.00	0.00	0.00	0.00	0.00	0.00	0.00	0.00	0.37
13.99	26.31	8.78	0.10	0.03	0.00	0.00	0.00	0.00	0.00	0.00	0.00	0.00	0.00	0.00	0.06
3.61	9.95	11.42	1.33	0.05	0.01	0.00	0.00	0.00	0.00	0.00	0.00	0.00	0.00	0.00	0.02
1.36	5.50	13.45	2.87	0.06	0.01	0.00	0.00	0.00	0.00	0.00	0.00	0.00	0.00	0.00	0.01
0.66	3.27	12.34	3.73	0.07	0.01	0.00	0.00	0.00	0.00	0.00	0.00	0.00	0.00	0.00	0.02
0.37	1.89	10.45	3.40	0.51	0.04	0.00	0.00	0.00	0.00	0.00	0.00	0.00	0.00	0.00	0.02
0.51	2.18	7.66	3.11	0.75	0.05	0.00	0.00	0.00	0.00	0.00	0.00	0.00	0.00	0.00	0.01
0.53	2.01	5.10	2.62	0.73	0.02	0.00	0.00	0.00	0.00	0.00	0.00	0.00	0.00	0.00	0.01
0.41	1.60	3.58	2.31	0.57	0.01	0.00	0.00	0.00	0.00	0.00	0.00	0.00	0.00	0.00	0.01
0.29	1.24	2.75	1.93	0.45	0.01	0.00	0.00	0.00	0.00	0.00	0.00	0.00	0.00	0.00	0.01
0.22	0.92	2.30	1.58	0.43	0.01	0.00	0.00	0.00	0.00	0.00	0.00	0.00	0.00	0.00	0.01
0.20	0.72	1.94	1.27	0.38	0.00	0.00	0.00	0.00	0.00	0.00	0.00	0.00	0.00	0.00	0.01
0.14	0.59	1.55	0.98	0.29	0.00	0.00	0.00	0.00	0.00	0.00	0.00	0.00	0.00	0.00	0.01
0.12	0.49	1.22	0.80	0.32	0.00	0.00	0.00	0.00	0.00	0.00	0.00	0.00	0.00	0.00	0.01
0.12	0.42	0.99	0.60	0.00	0.00	0.00	0.00	0.00	0.00	0.00	0.00	0.00	0.00	0.00	0.01
		0.71													

A14

APPENDIX B: WAVE ELEVATION TIME SERIES
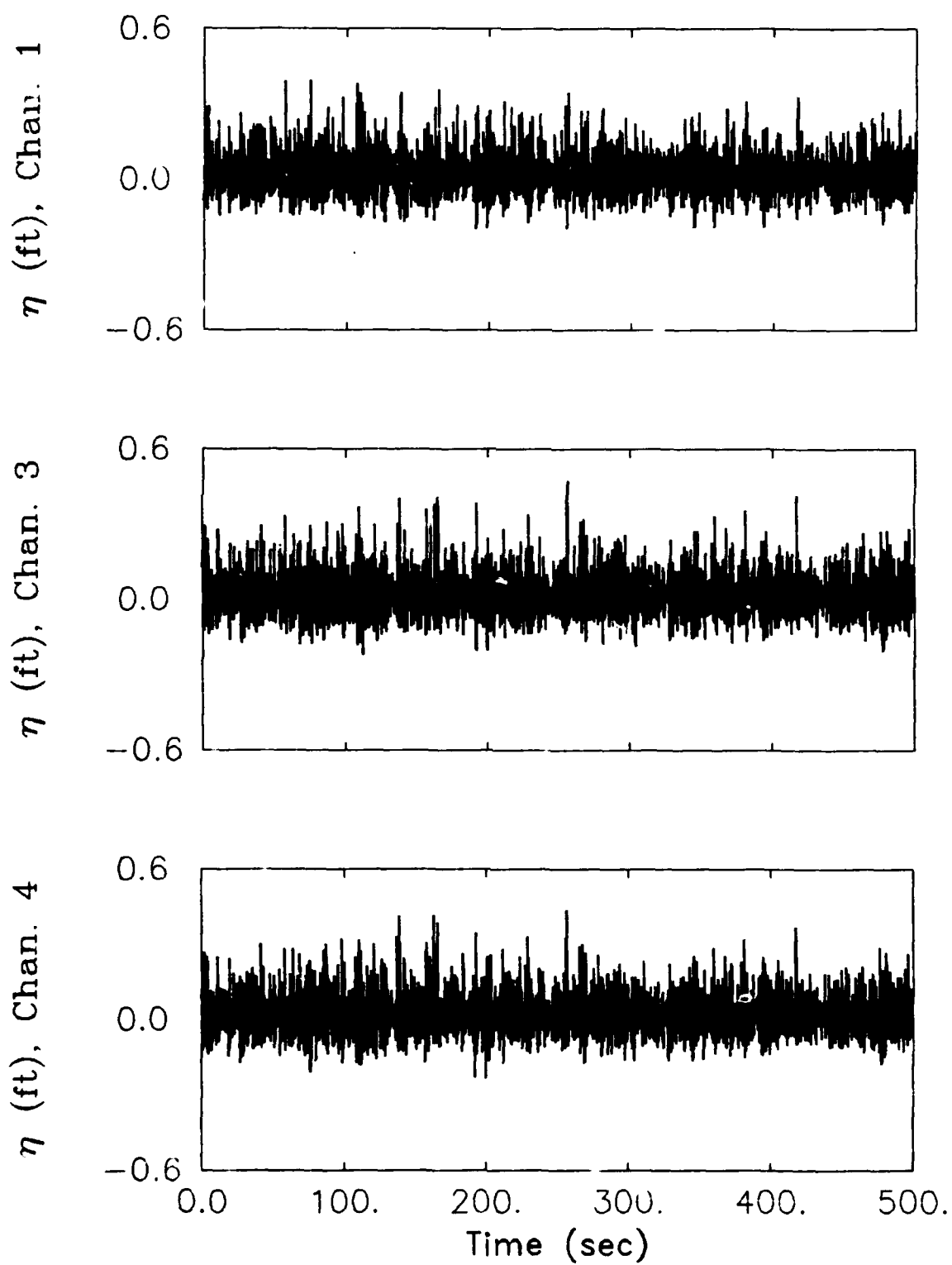
Measured Wave Elevation Time Series
CASE 69U1 —— Fp=.4, Hm0=5.95, H=1.11
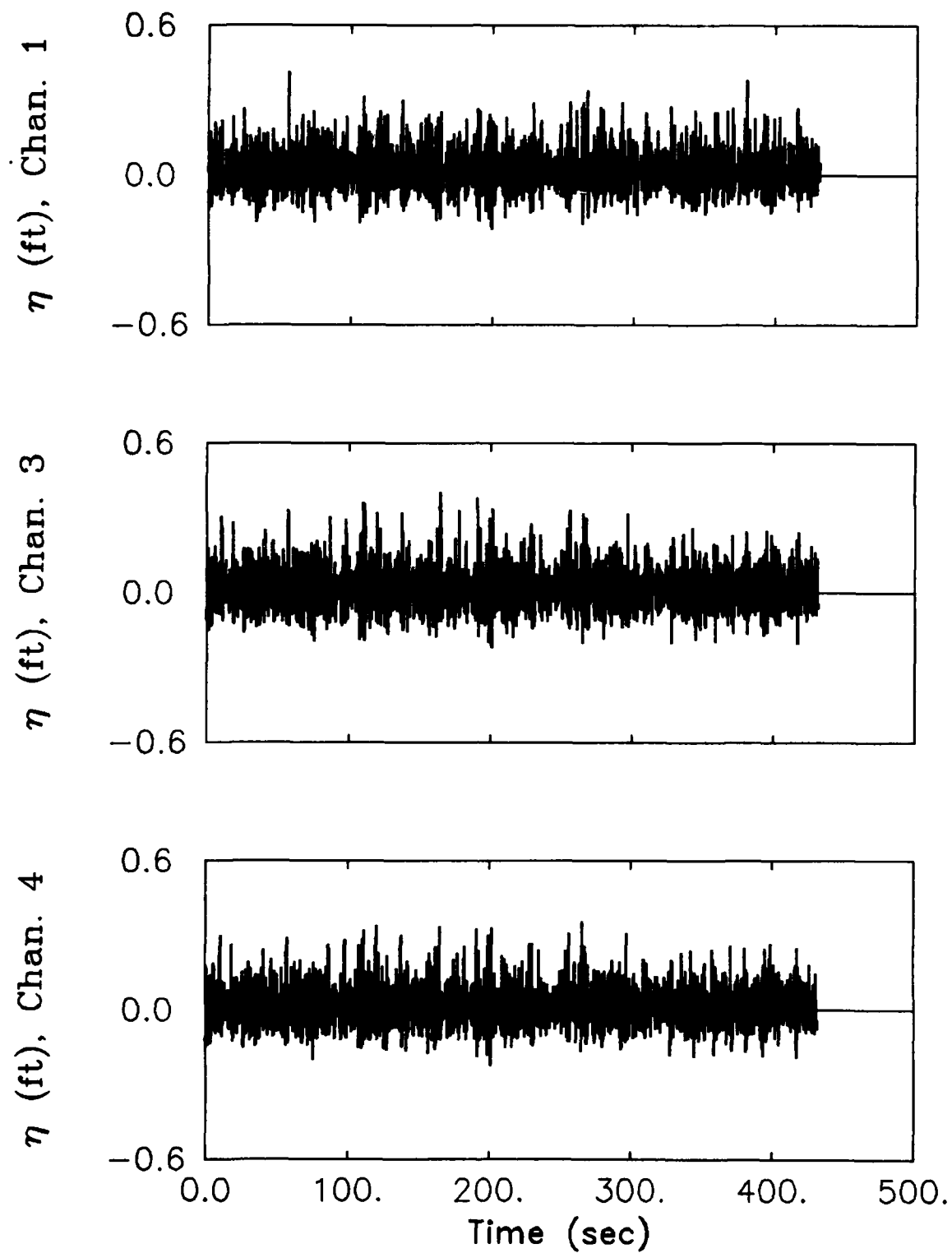
Measured Wave Elevation Time Series
CASE 70U1 —— Fp=.47, Hm0=5.07, H=1.11

B4
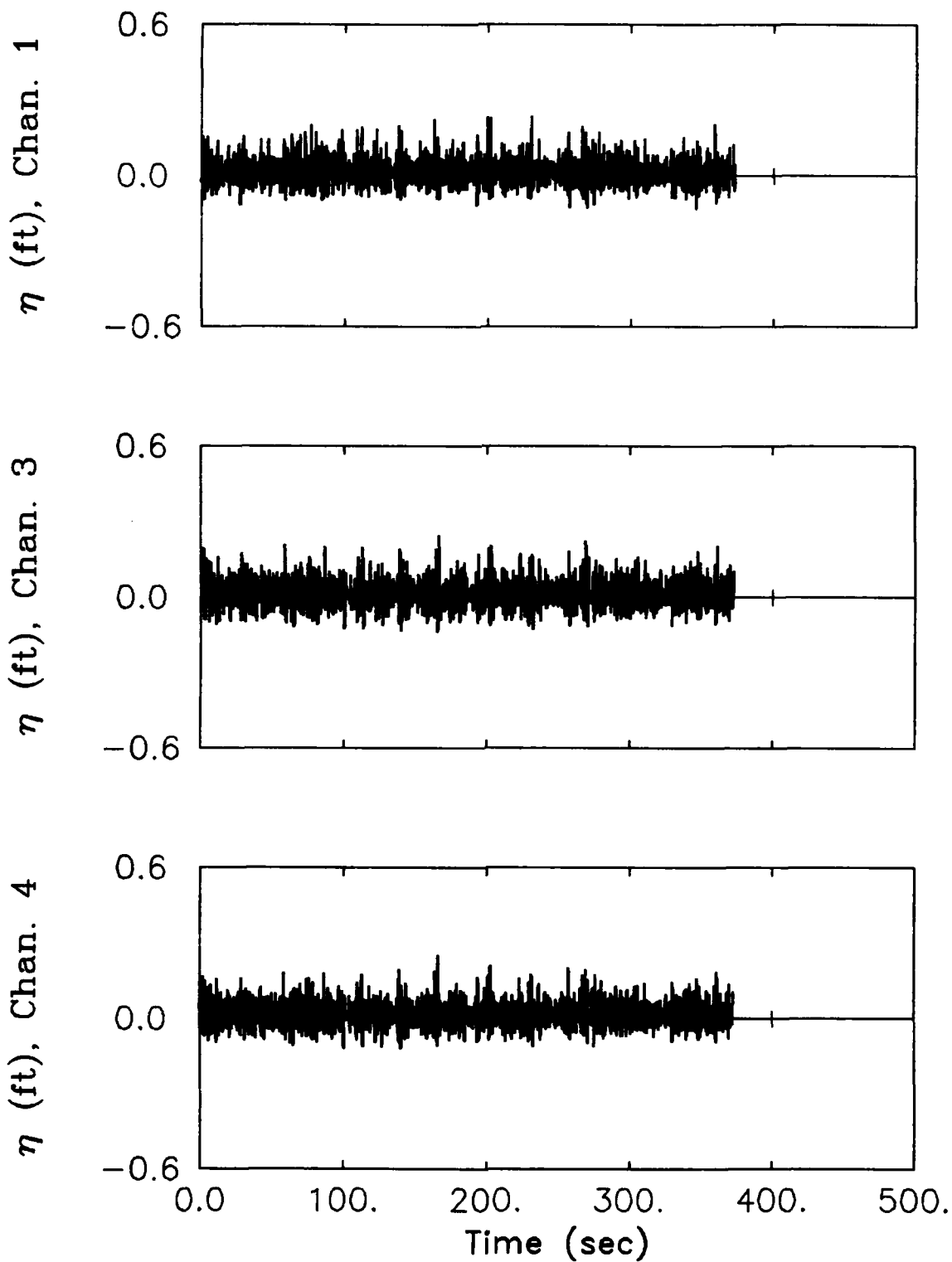
Measured Wave Elevation Time Series
CASE 72U1 -- Fp=.54, Hm0=3.85, H=1.11
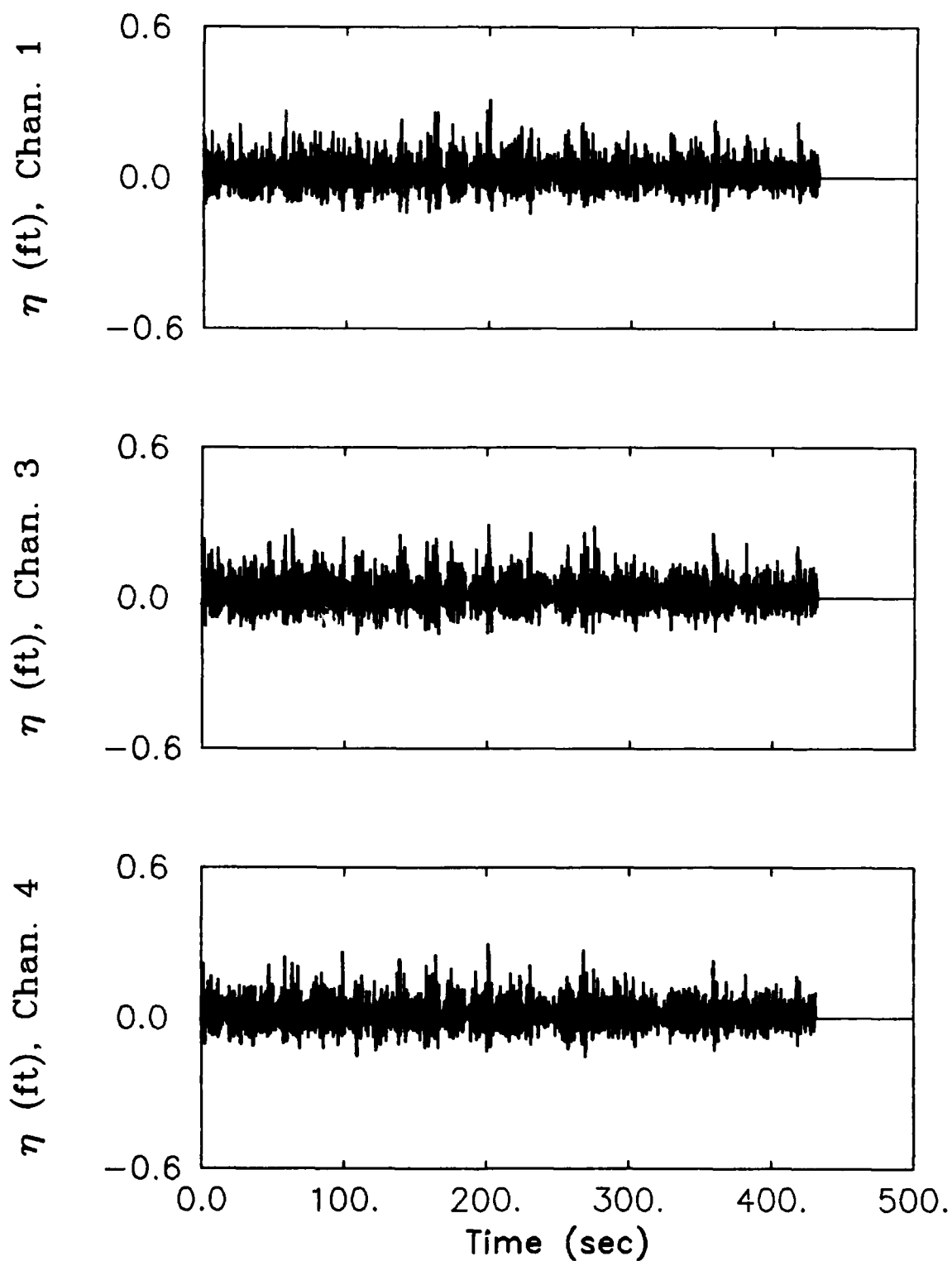
Measured Wave Elevation Time Series
CASE 73U1 -- Fp=.47, Hm0=4.46, H=1.11
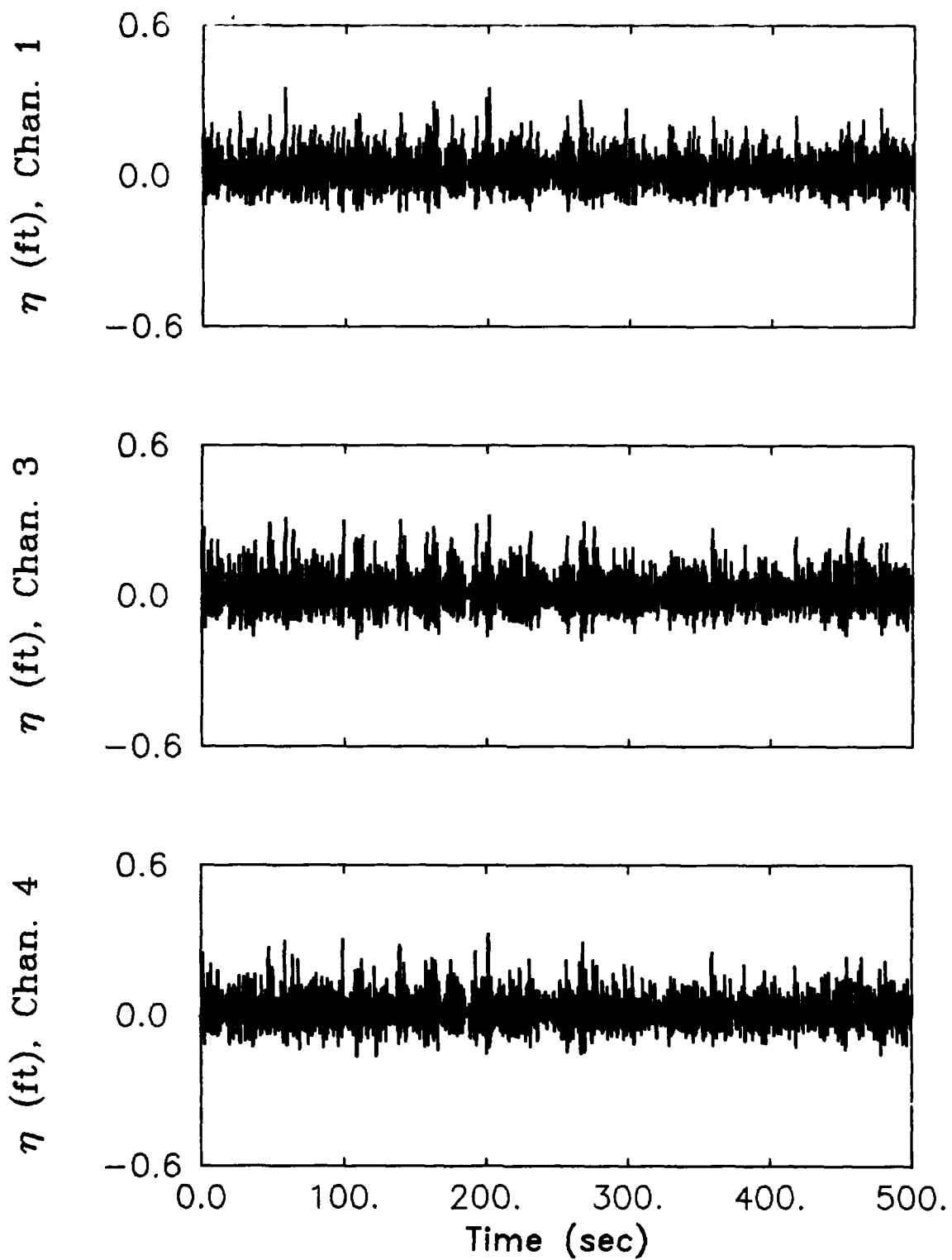
Measured Wave Elevation Time Series
CASE 83U1 —— Fp=.4, Hm0=4.99, H=1.11
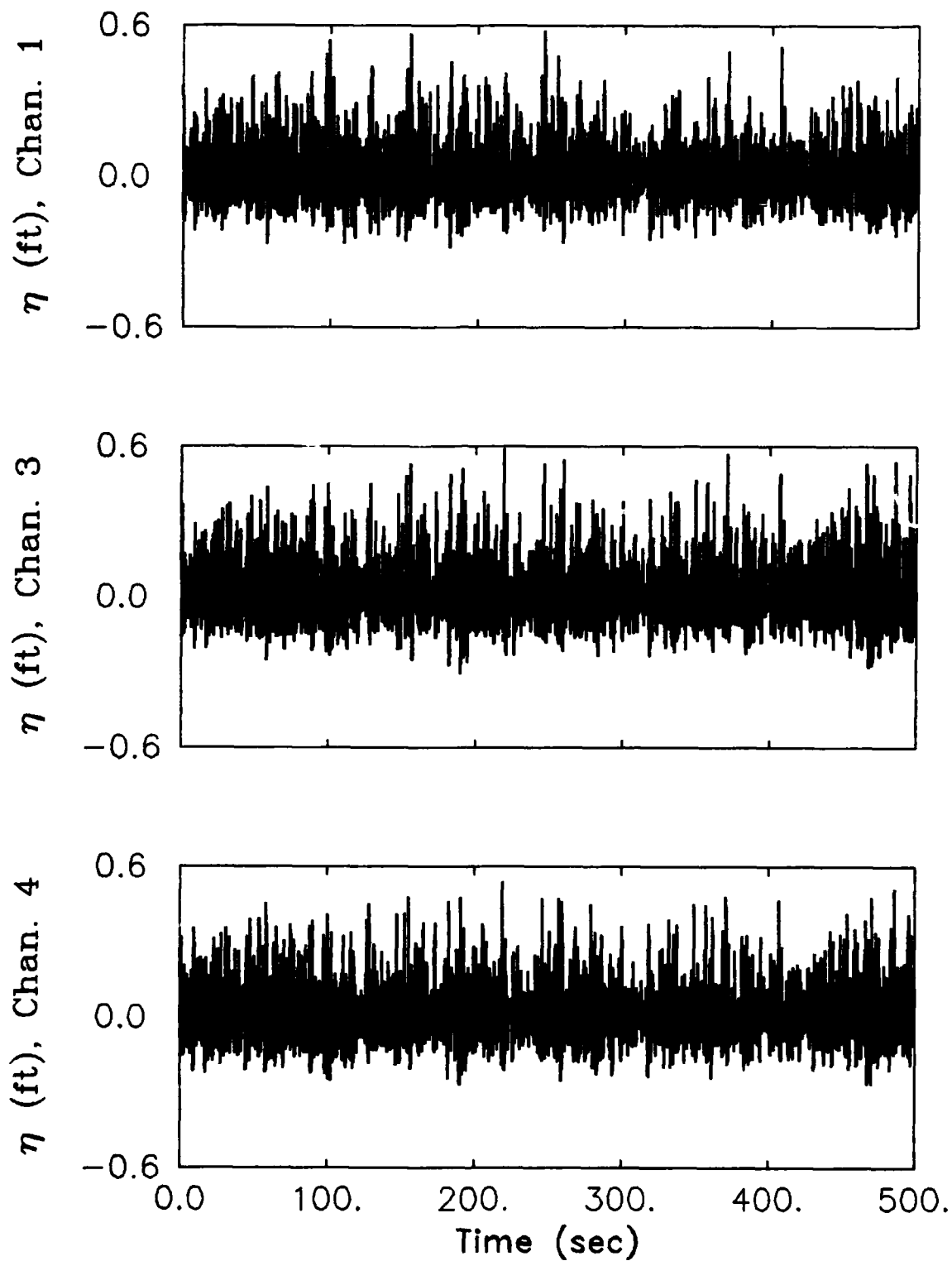
Measured Wave Elevation Time Series
CASE 69U2 -- Fp=.4, Hm0=5.95, H=1.29
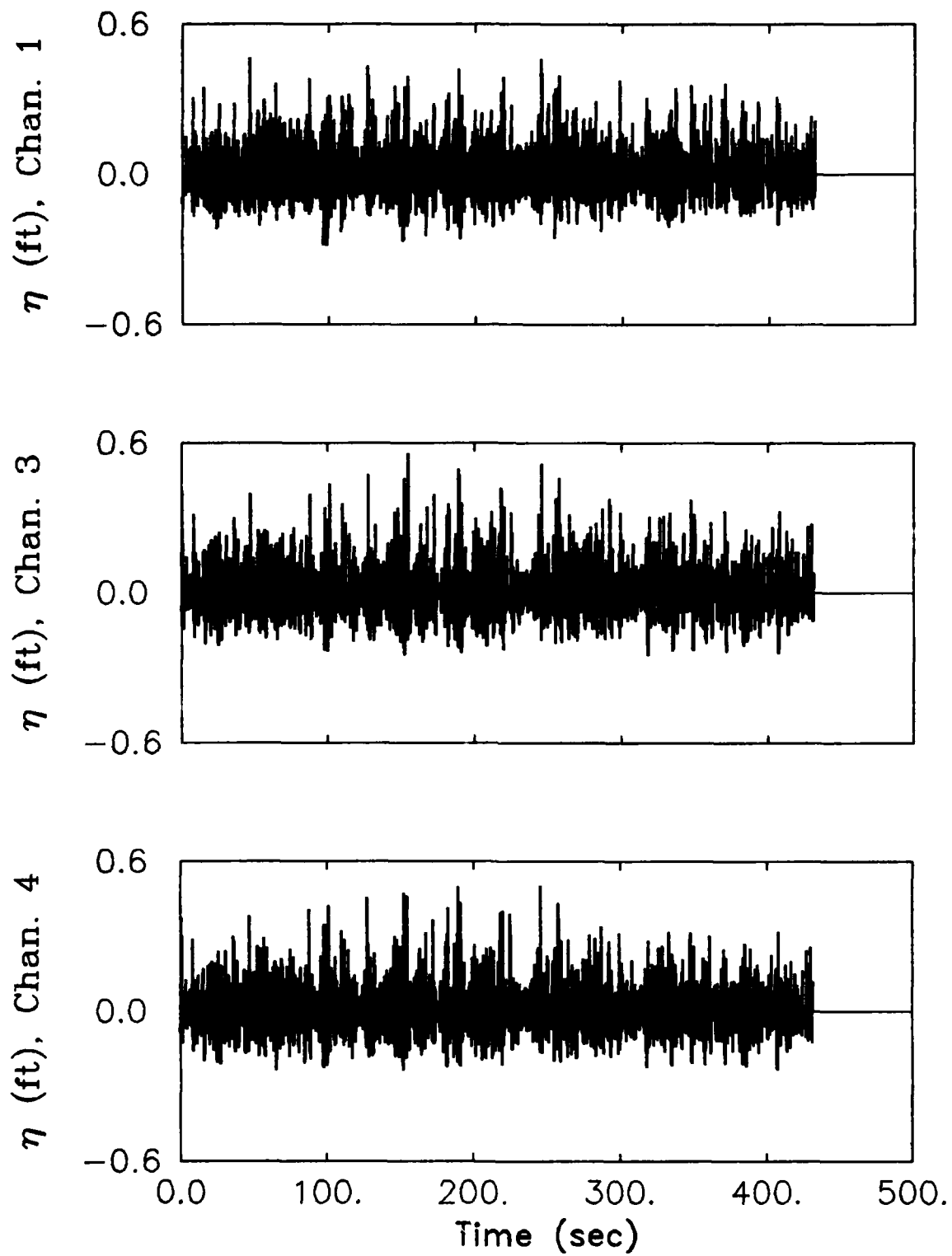
Measured Wave Elevation Time Series
CASE 70U2 -- Fp=.47, Hm0=5.07, H=1.29
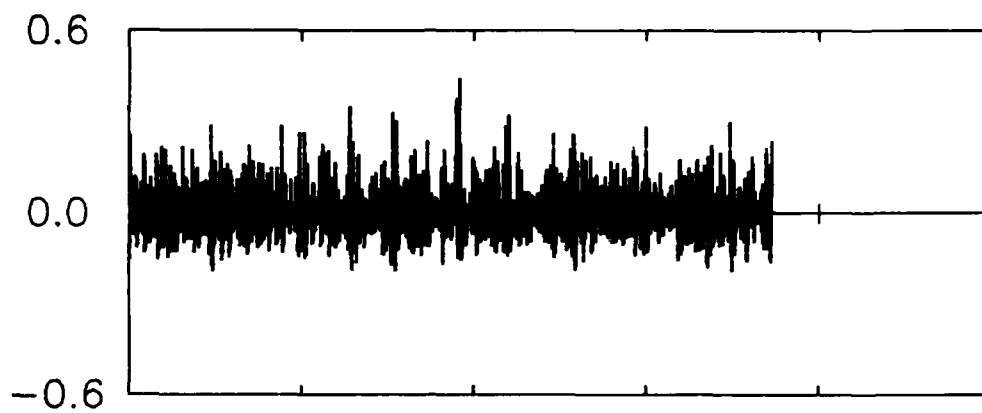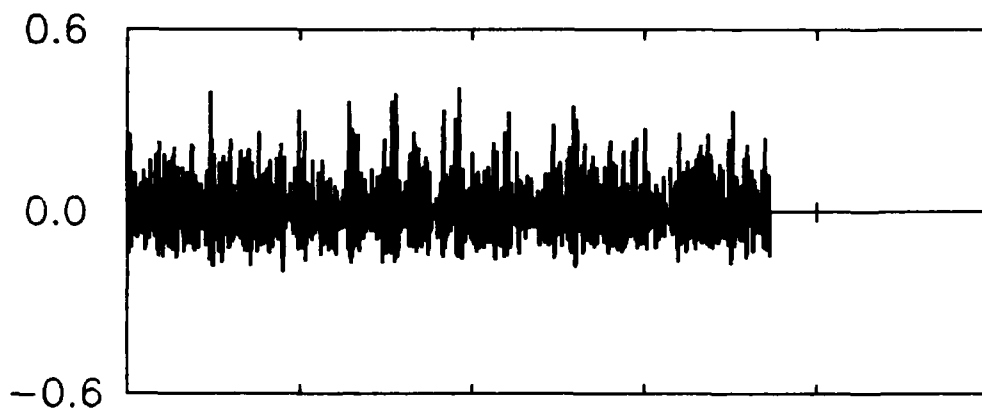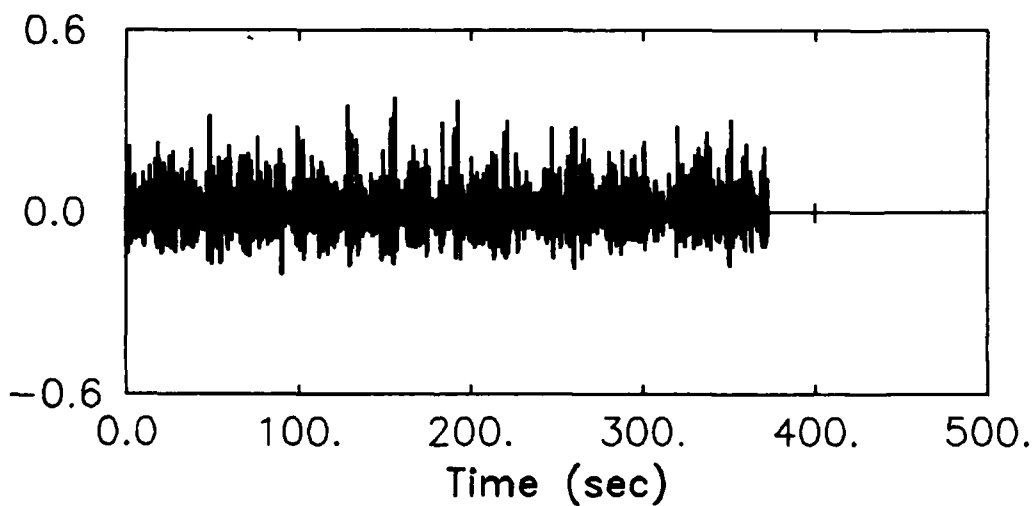
Measured Wave Elevation Time Series
CASE 72U2 –– Fp=.54, Hm0=3.85, H=1.29

B10
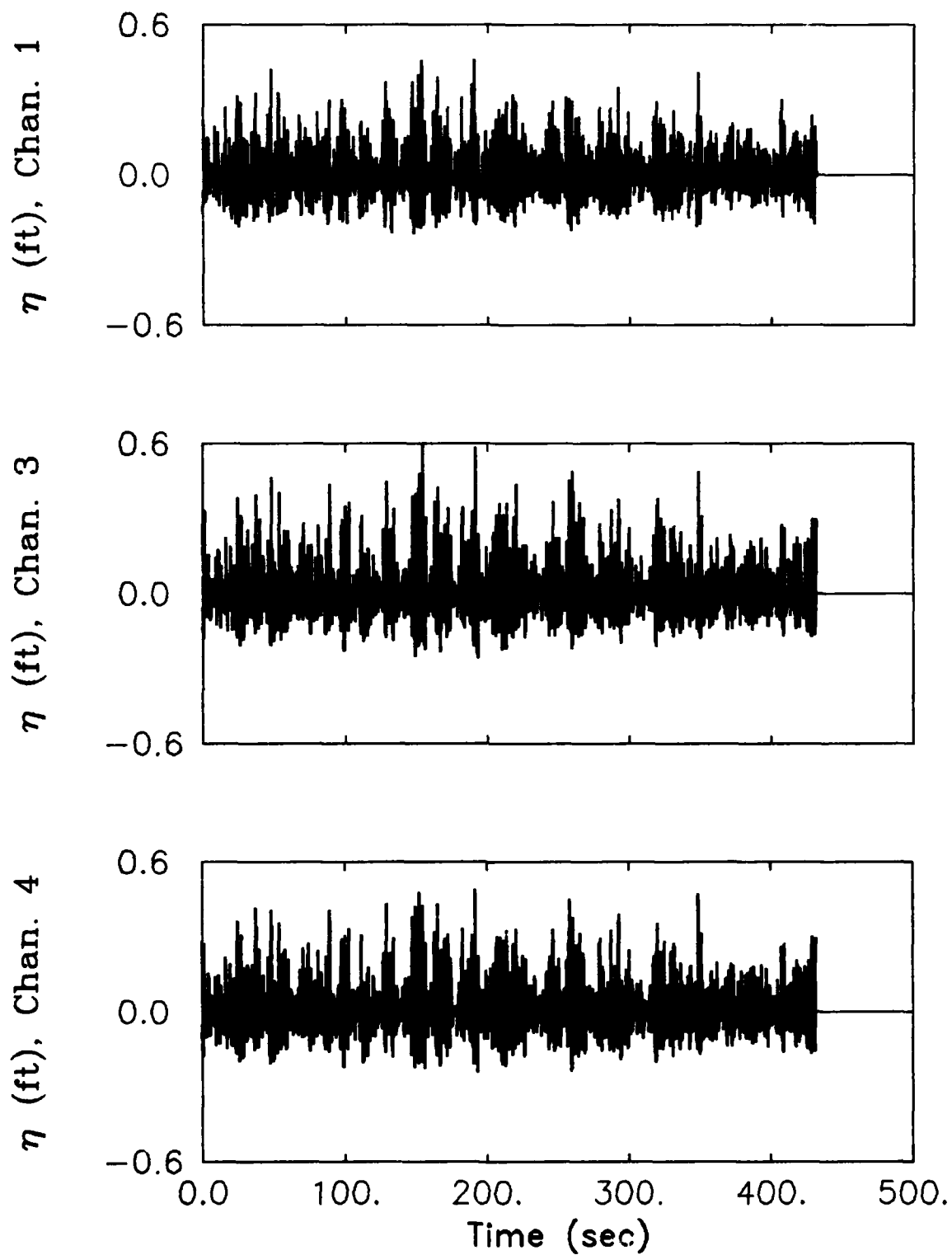
Measured Wave Elevation Time Series
CASE 73U2 –– Fp=.47, Hm0=4.46, H=1.29

B11
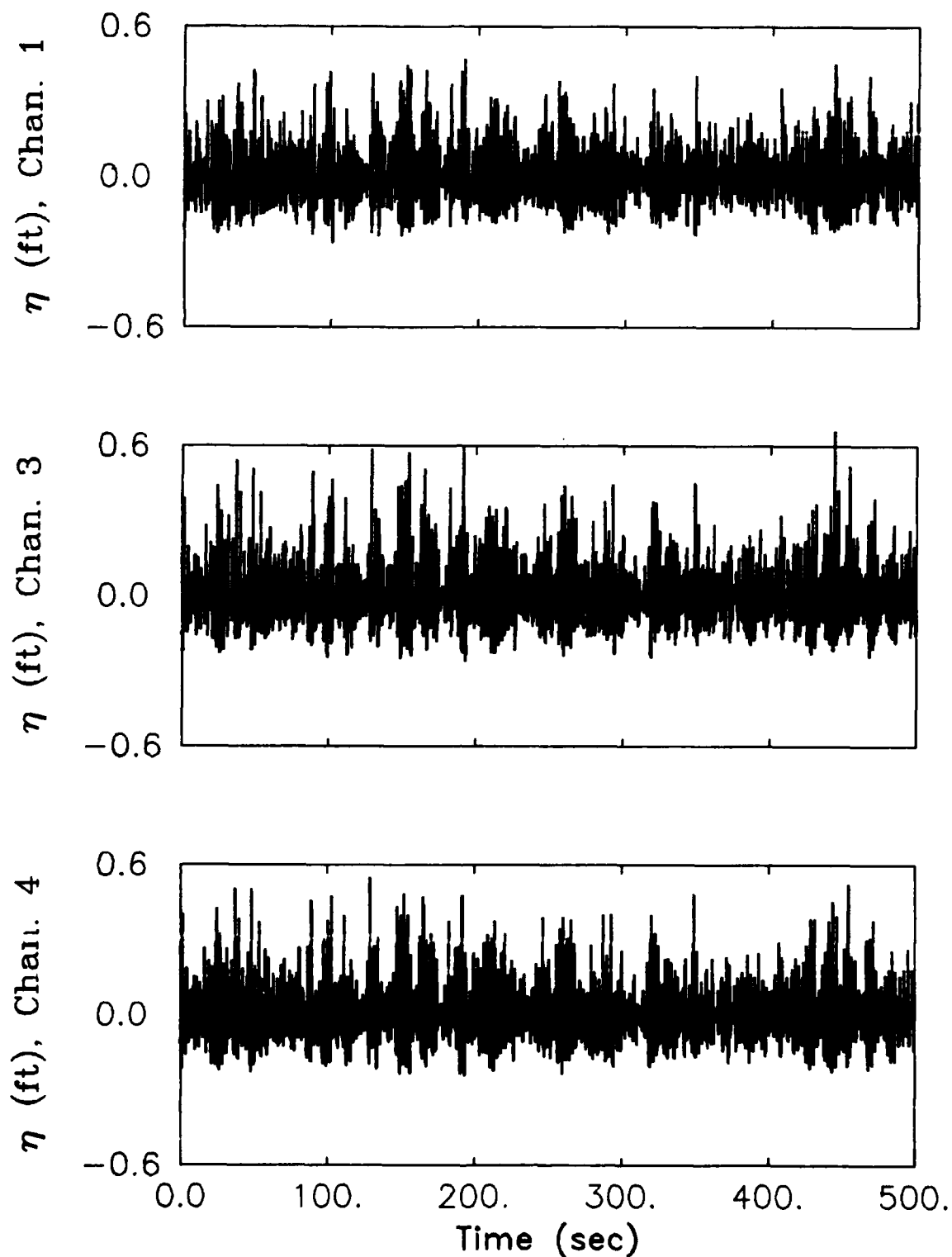
Measured Wave Elevation Time Series
CASE 83U2 -- Fp=.4, Hm0=4.99, H=1.29
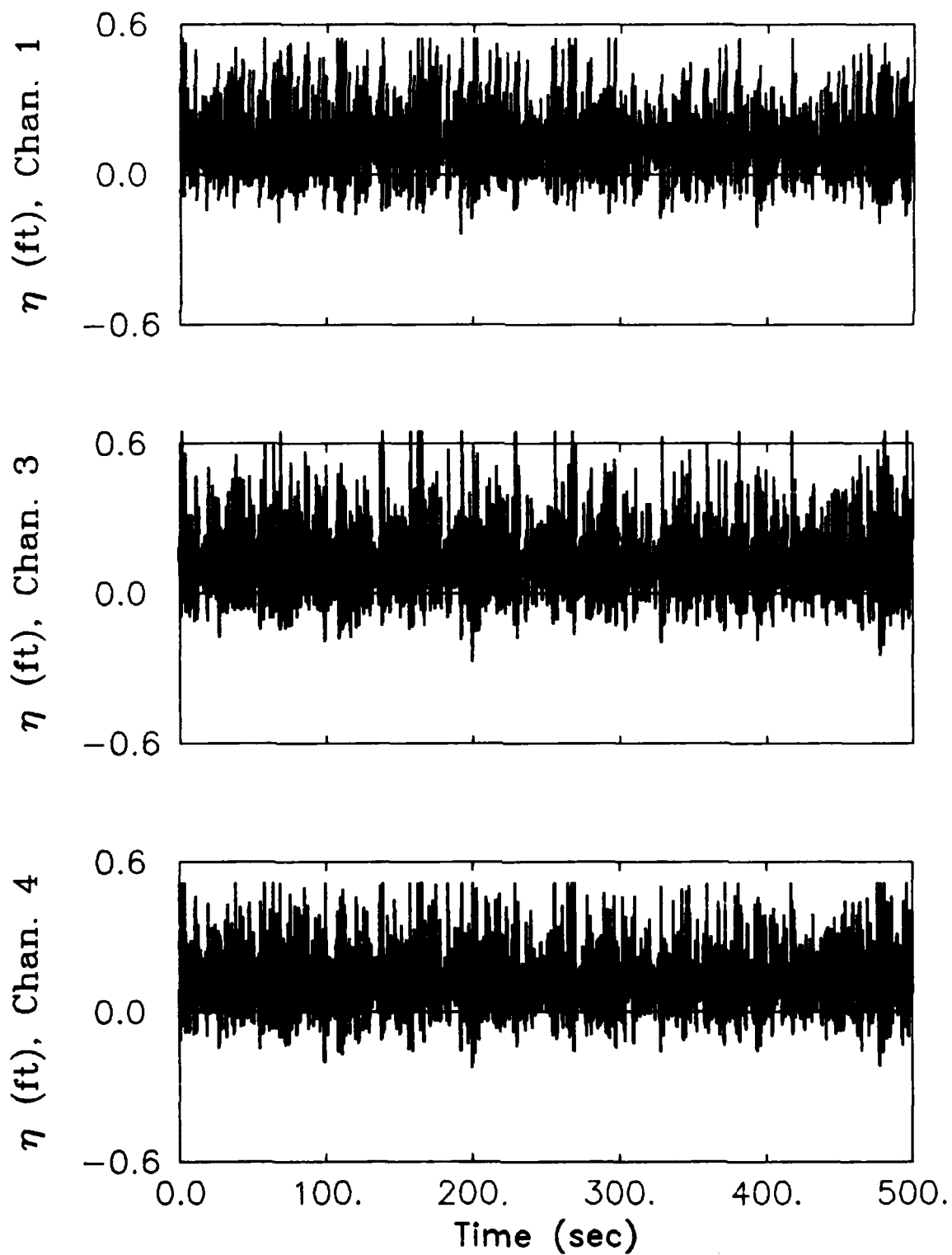
Measured Wave Elevation Time Series
CASE 69U3 -- Fp=.4, Hm0=5.95, H=1.51
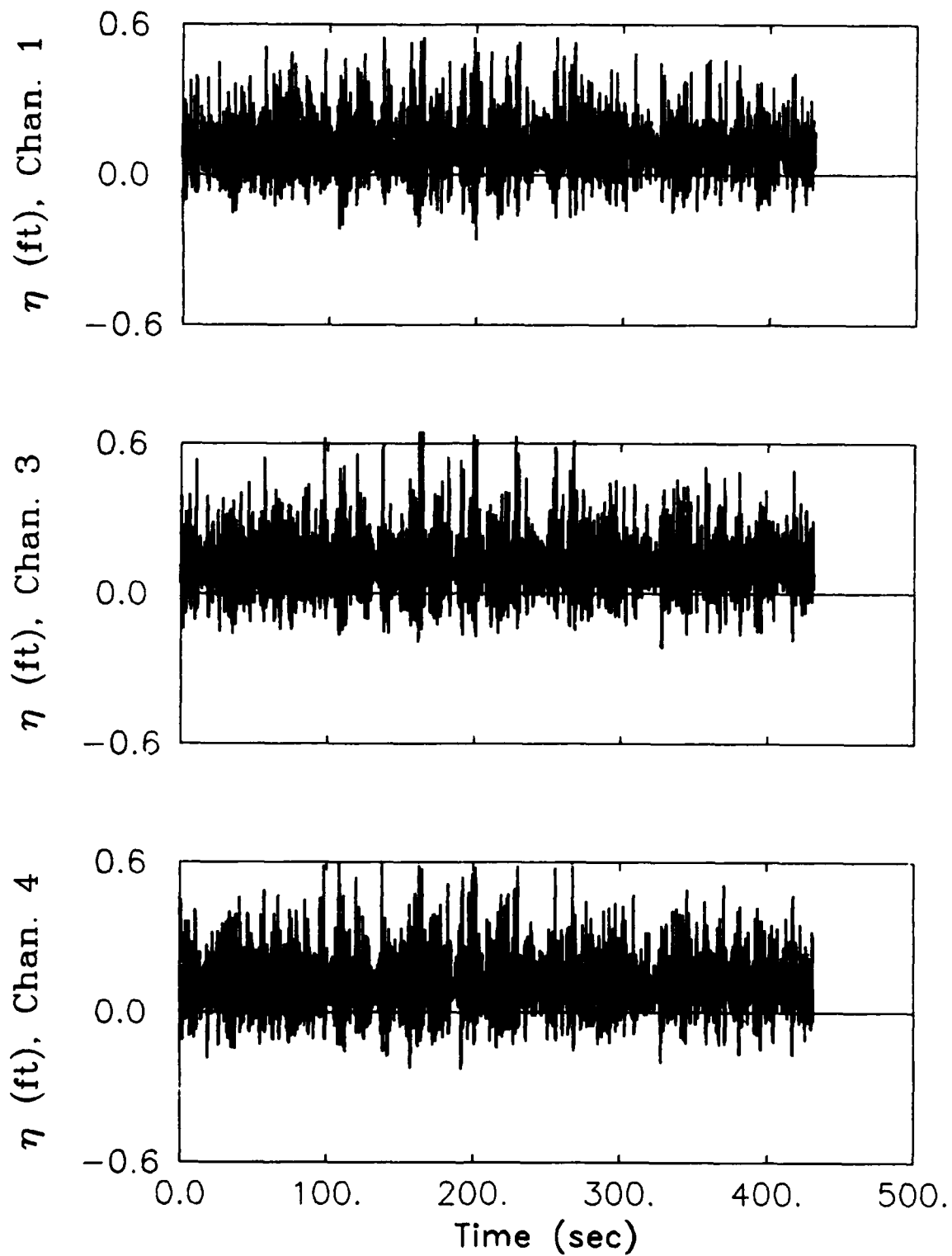
Measured Wave Elevation Time Series
CASE 70U3 -- Fp=.47, Hm0=5.07, H=1.51

B14
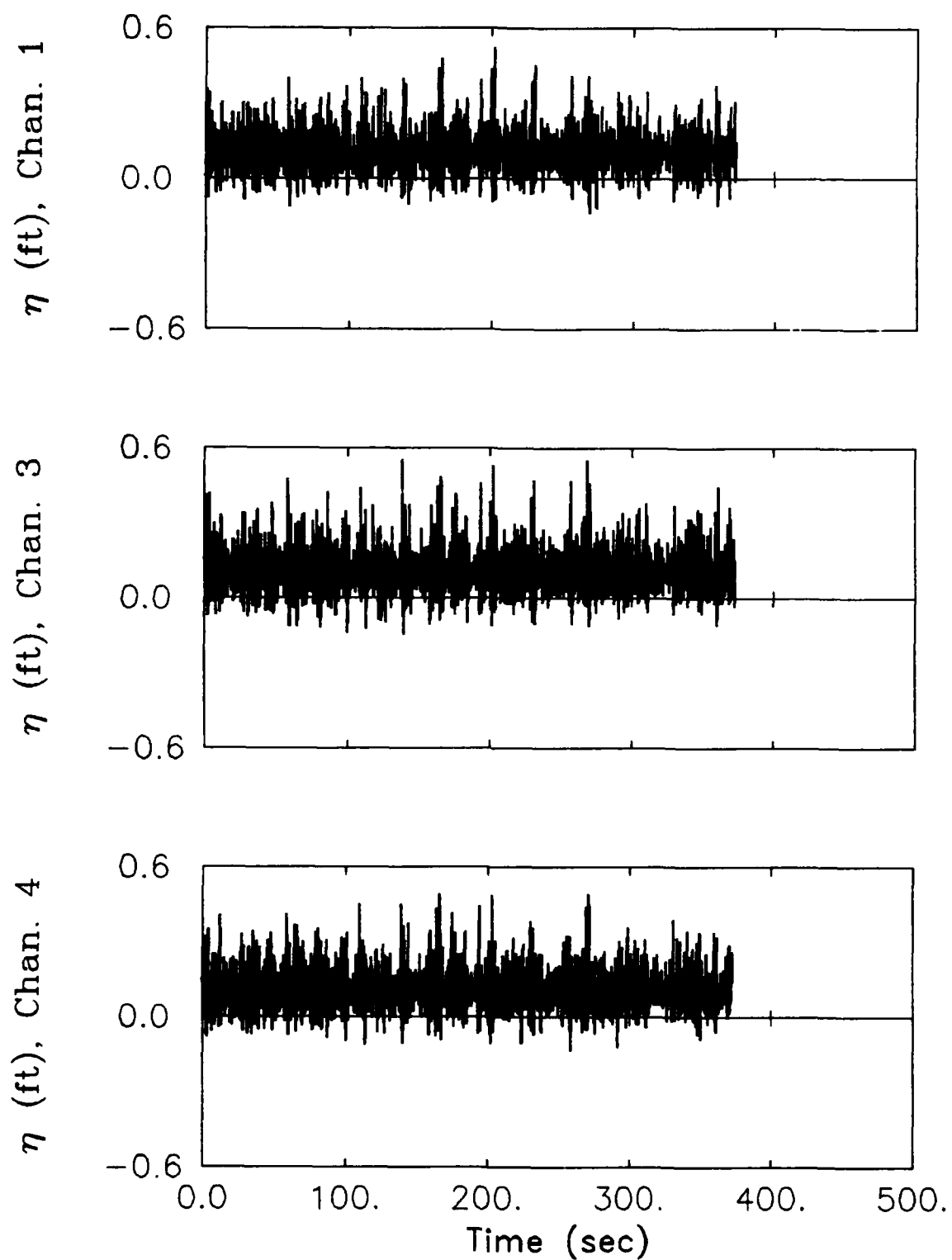
Measured Wave Elevation Time Series
CASE 72U3 —— Fp=.54, Hm0=3.85, H=1.51
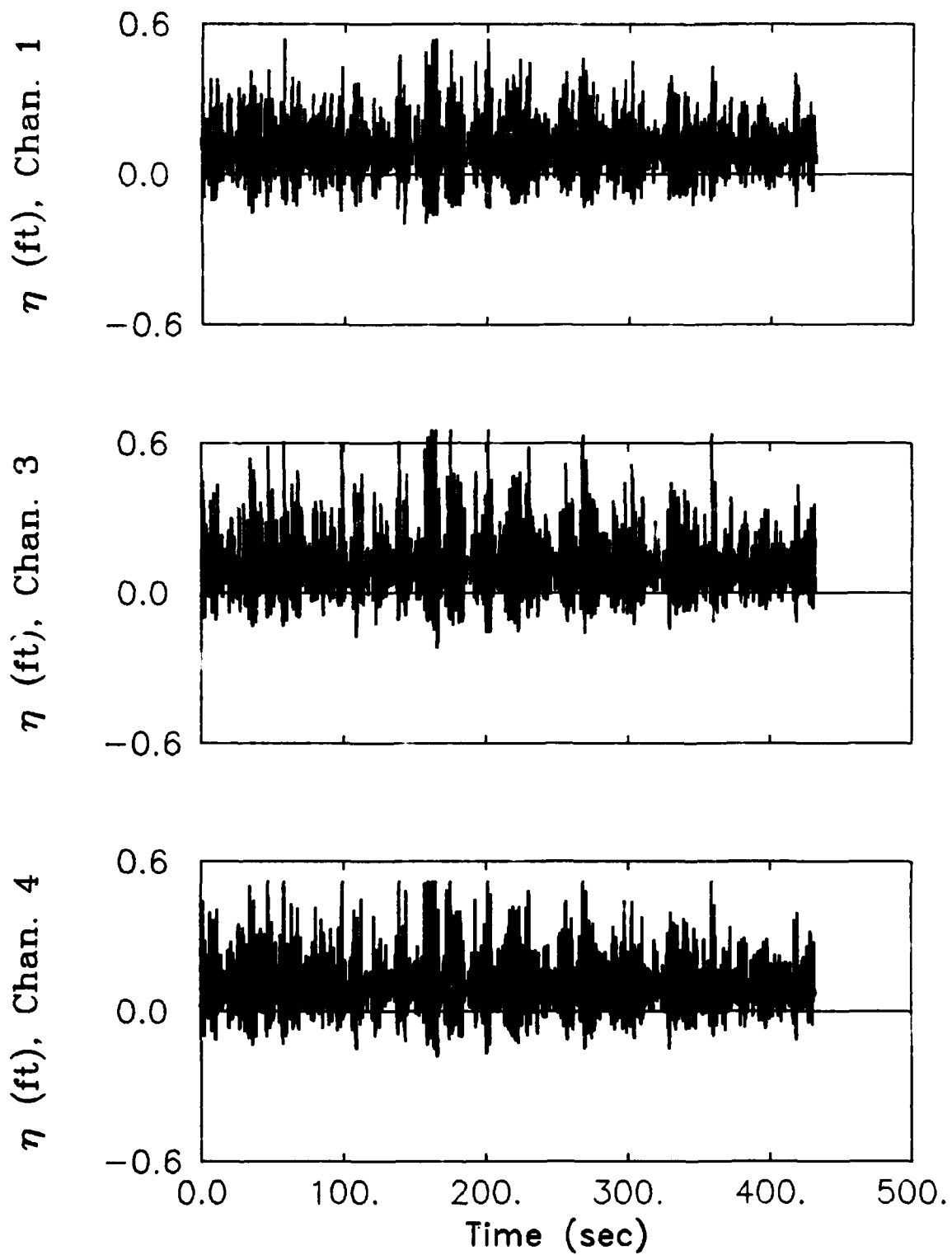
Measured Wave Elevation Time Series
CASE 73U3 -- Fp=.47, Hm0=4.46, H=1.51

B16
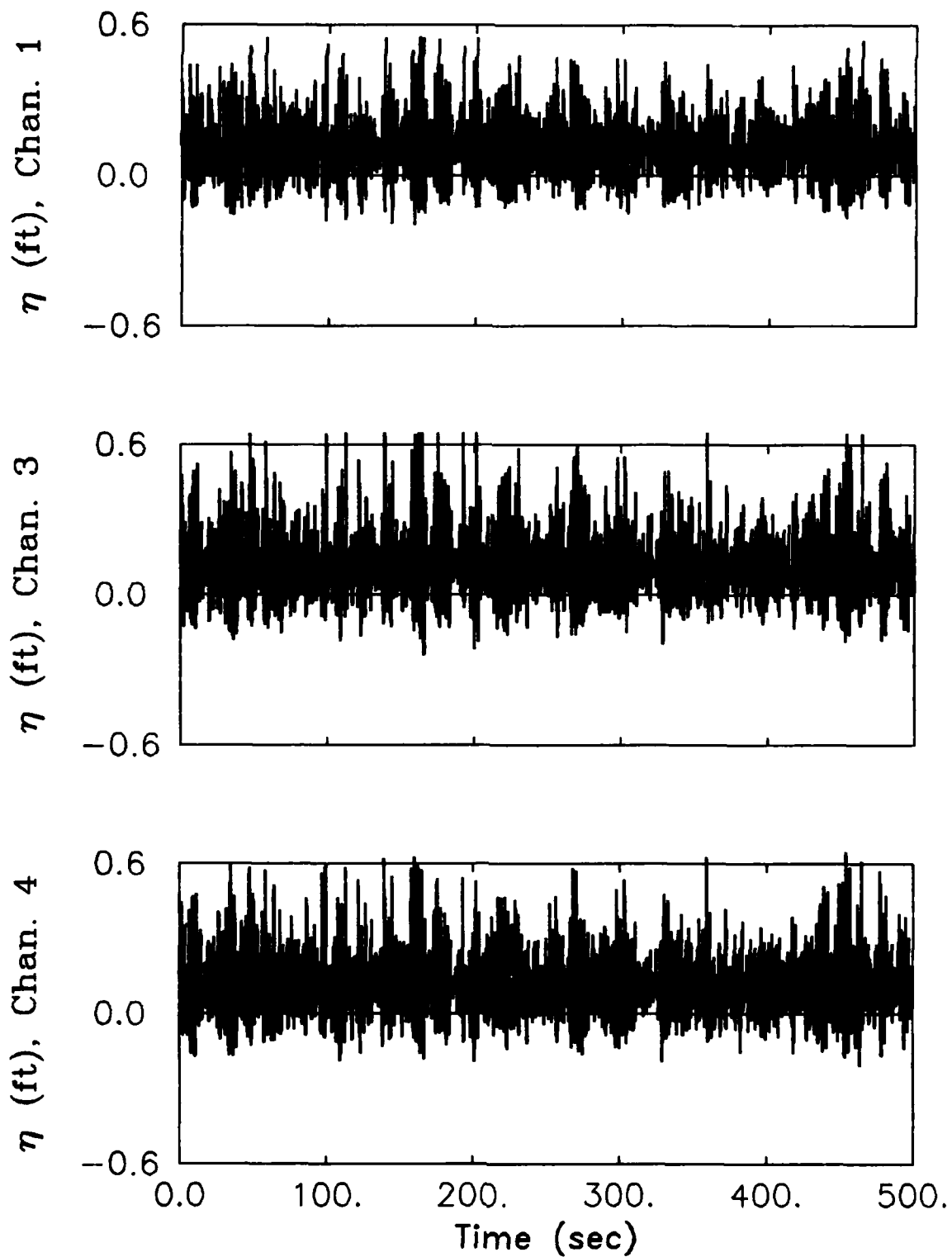
Measured Wave Elevation Time Series
CASE 83U3 —— Fp=.4, Hm0=4.99, H=1.51

B17
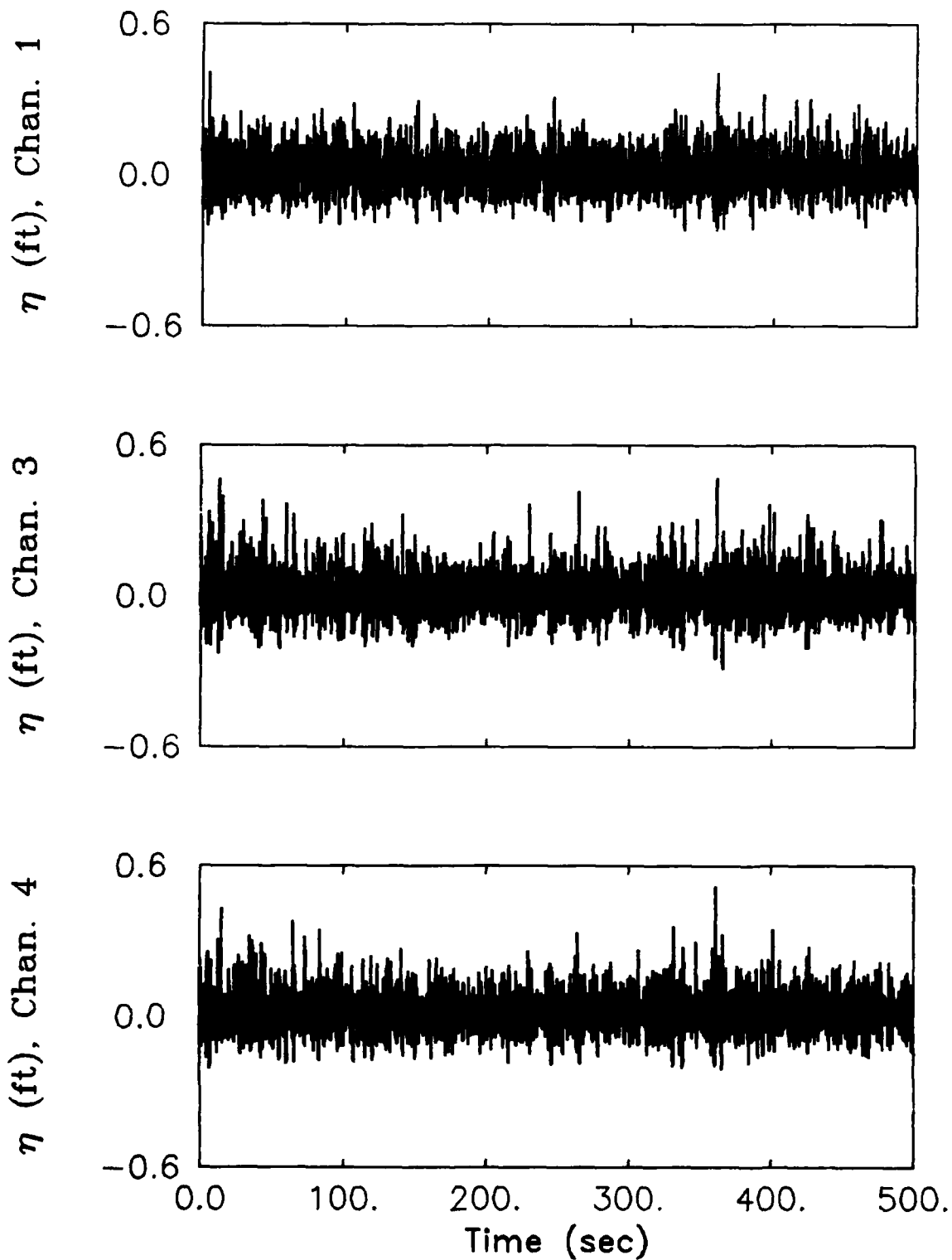
Measured Wave Elevation Time Series
CASE 69D1 -- Fp=.4, Hm0=6.12, H=1.11
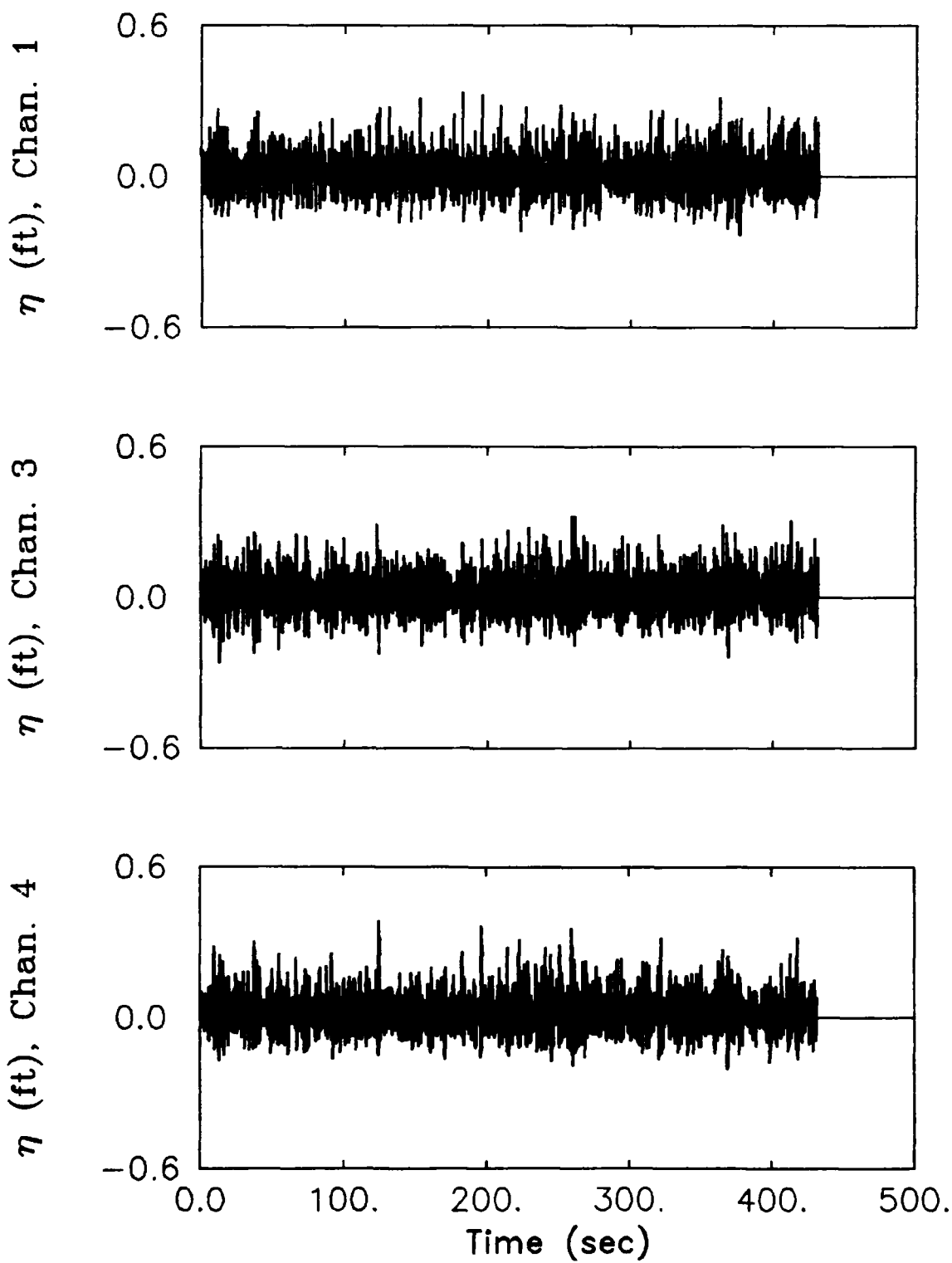
Measured Wave Elevation Time Series
CASE 70D1 -- Fp=.47, Hm0=5.07, H=1.11
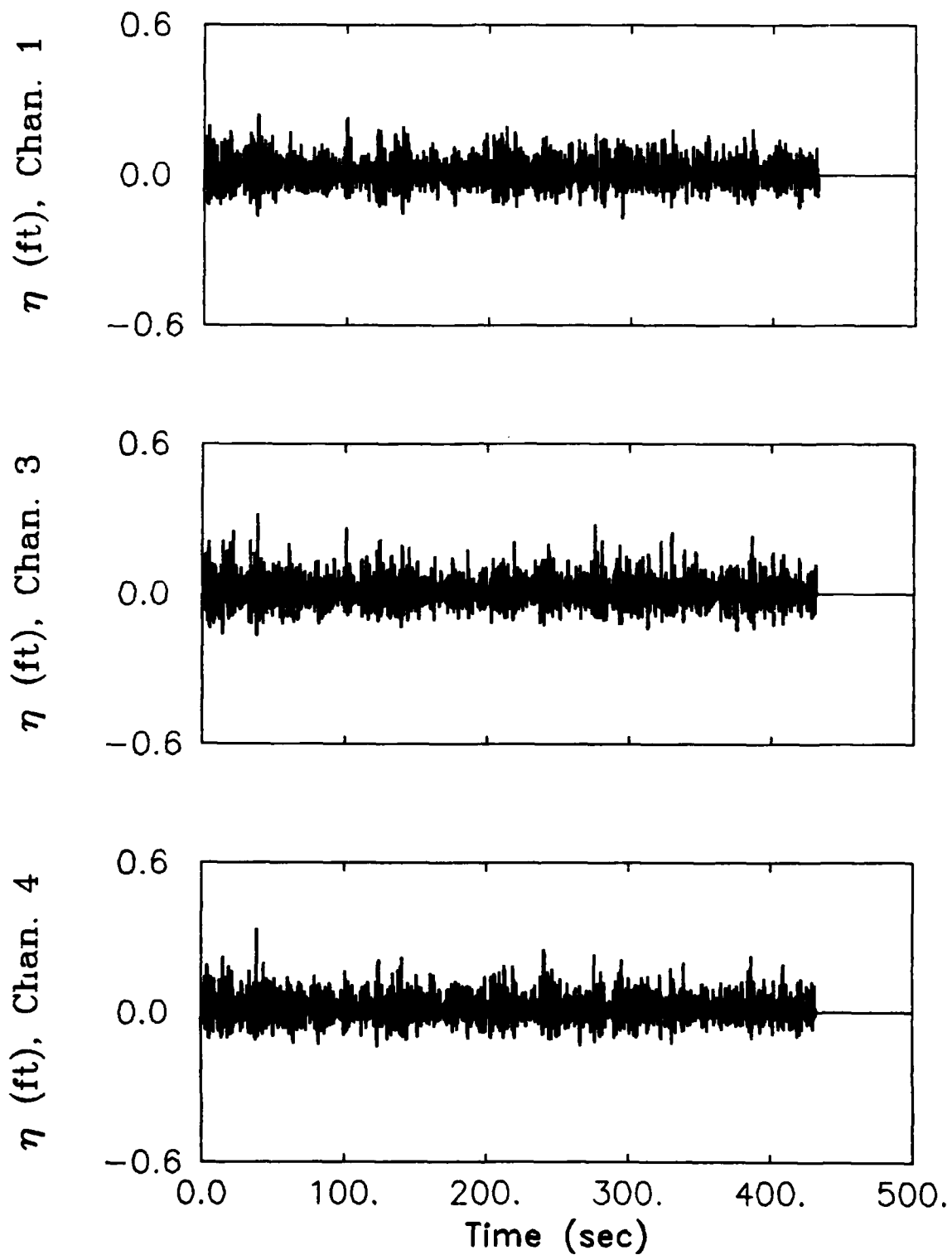
Measured Wave Elevation Time Series
CASE 72D1 -- Fp=.47, Hm0=4.11, H=1.11
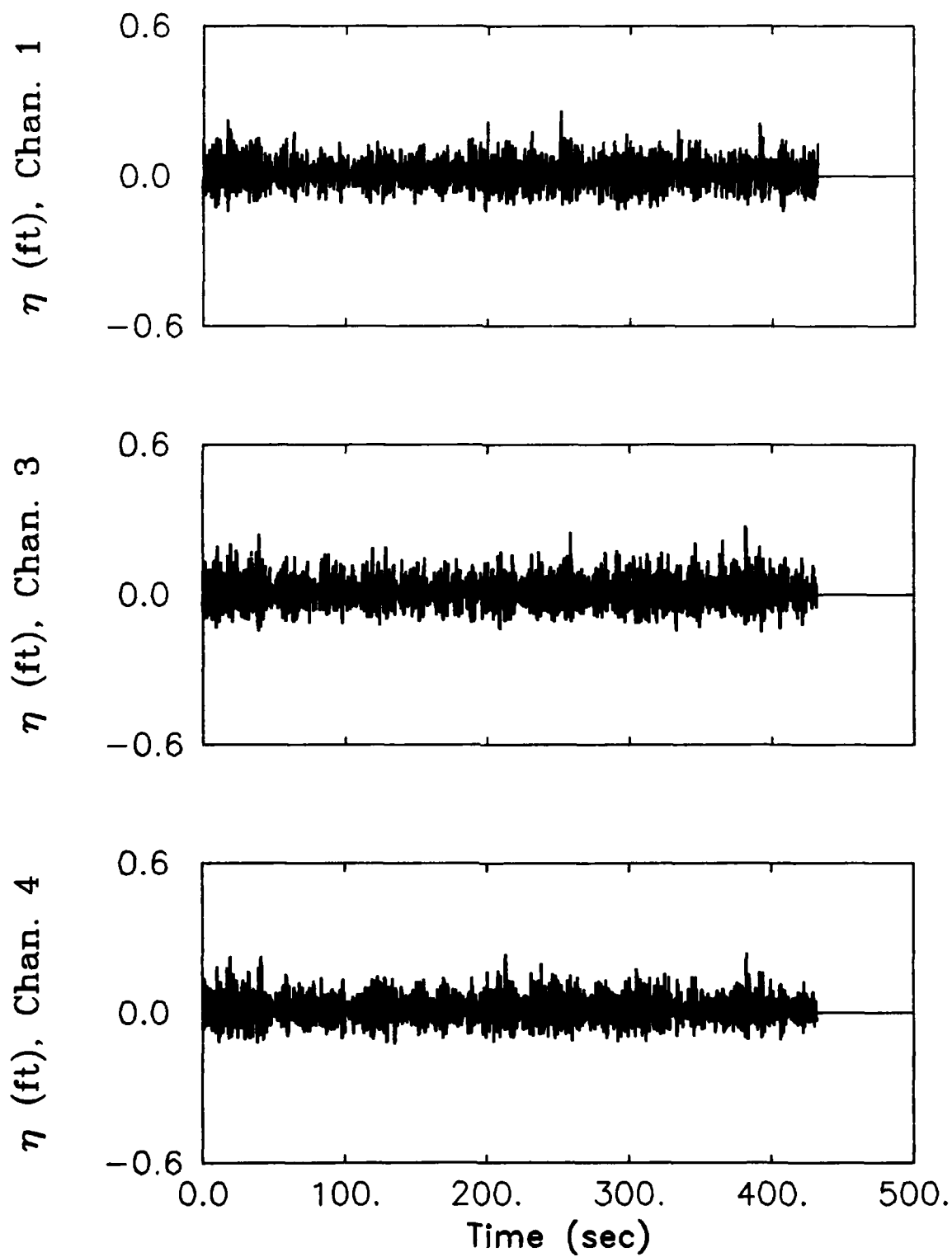
Measured Wave Elevation Time Series
CASE 73D1 -- Fp=.47, Hm0=4.55, H=1.11
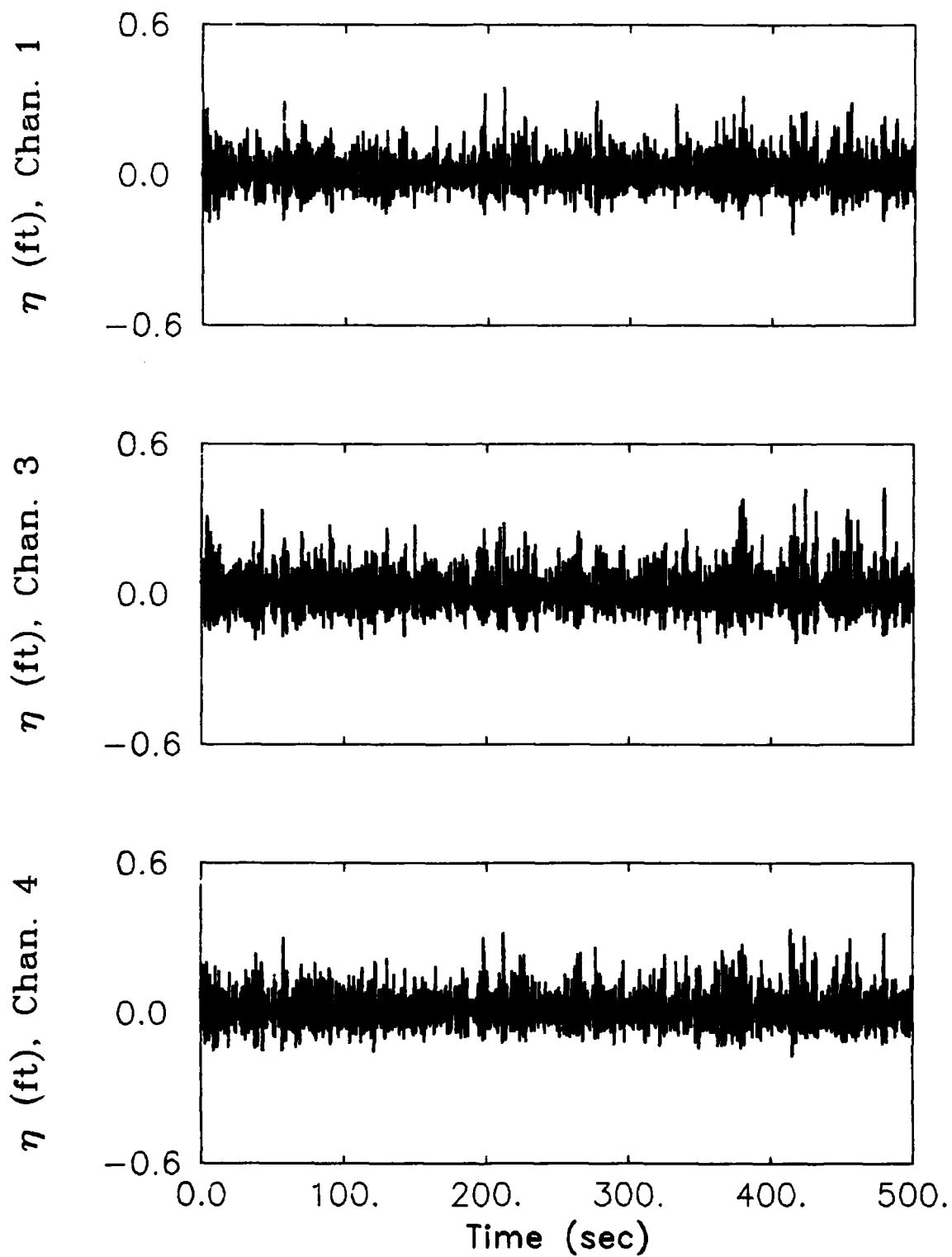
Measured Wave Elevation Time Series
CASE 83D1 -- Fp=.4, Hm0=5.42, H=1.11
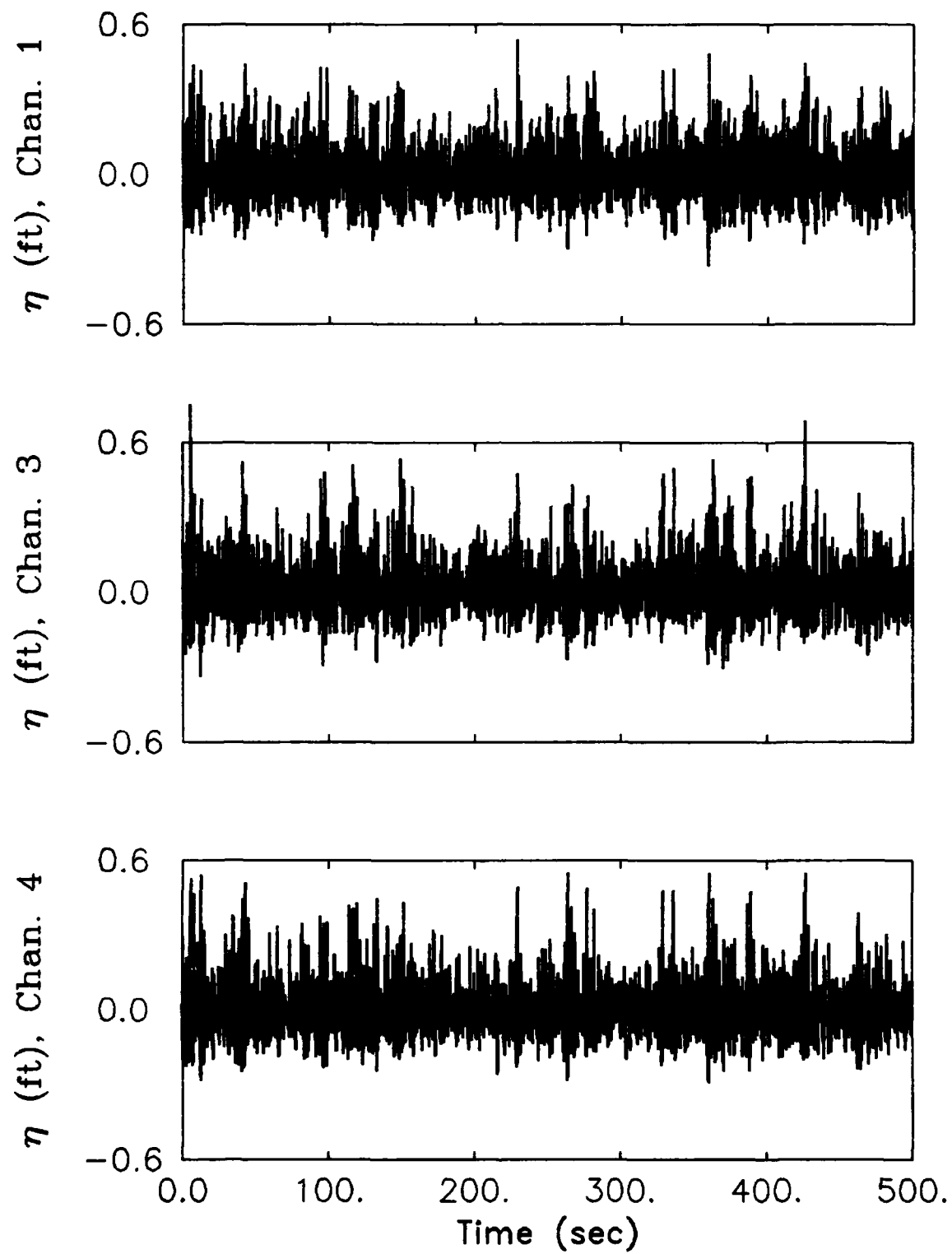
Measured Wave Elevation Time Series
CASE 69D2 -- Fp=.4, Hm0=6.12, H=1.29

B23
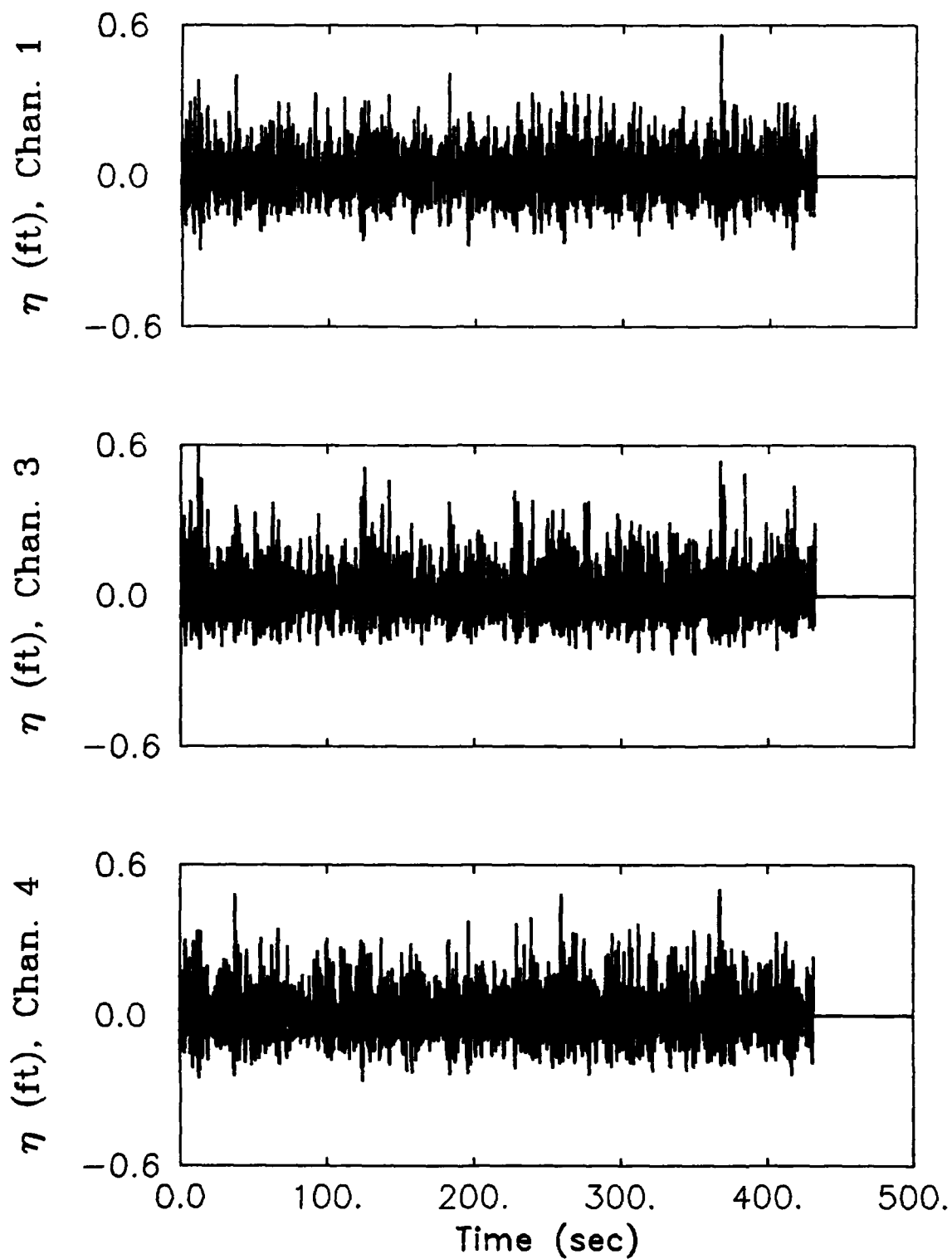
Measured Wave Elevation Time Series
CASE 70D2 -- Fp=.47, Hm0=5.07, H=1.29
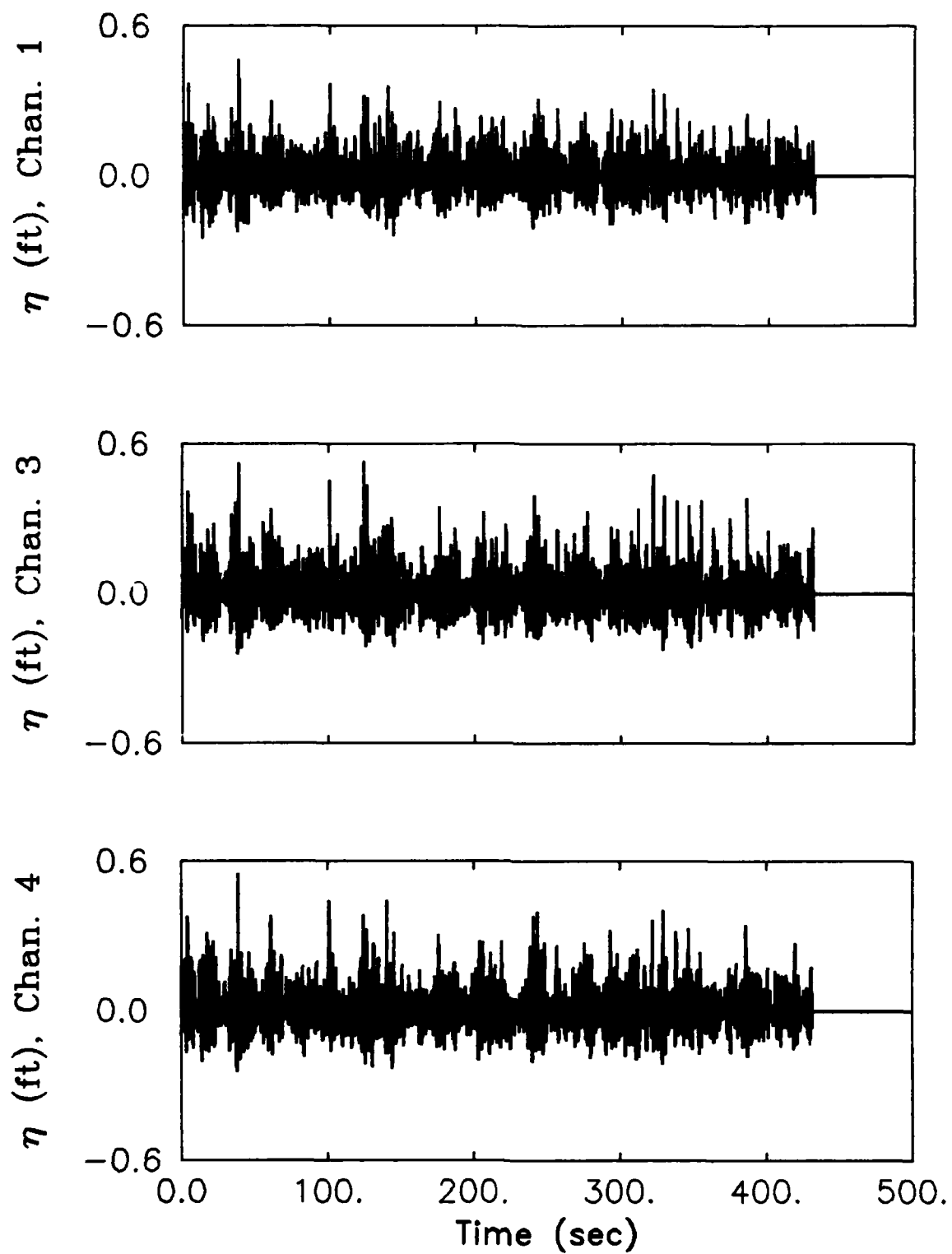
Measured Wave Elevation Time Series
CASE 72D2 -- Fp=.47, Hm0=4.11, H=1.29
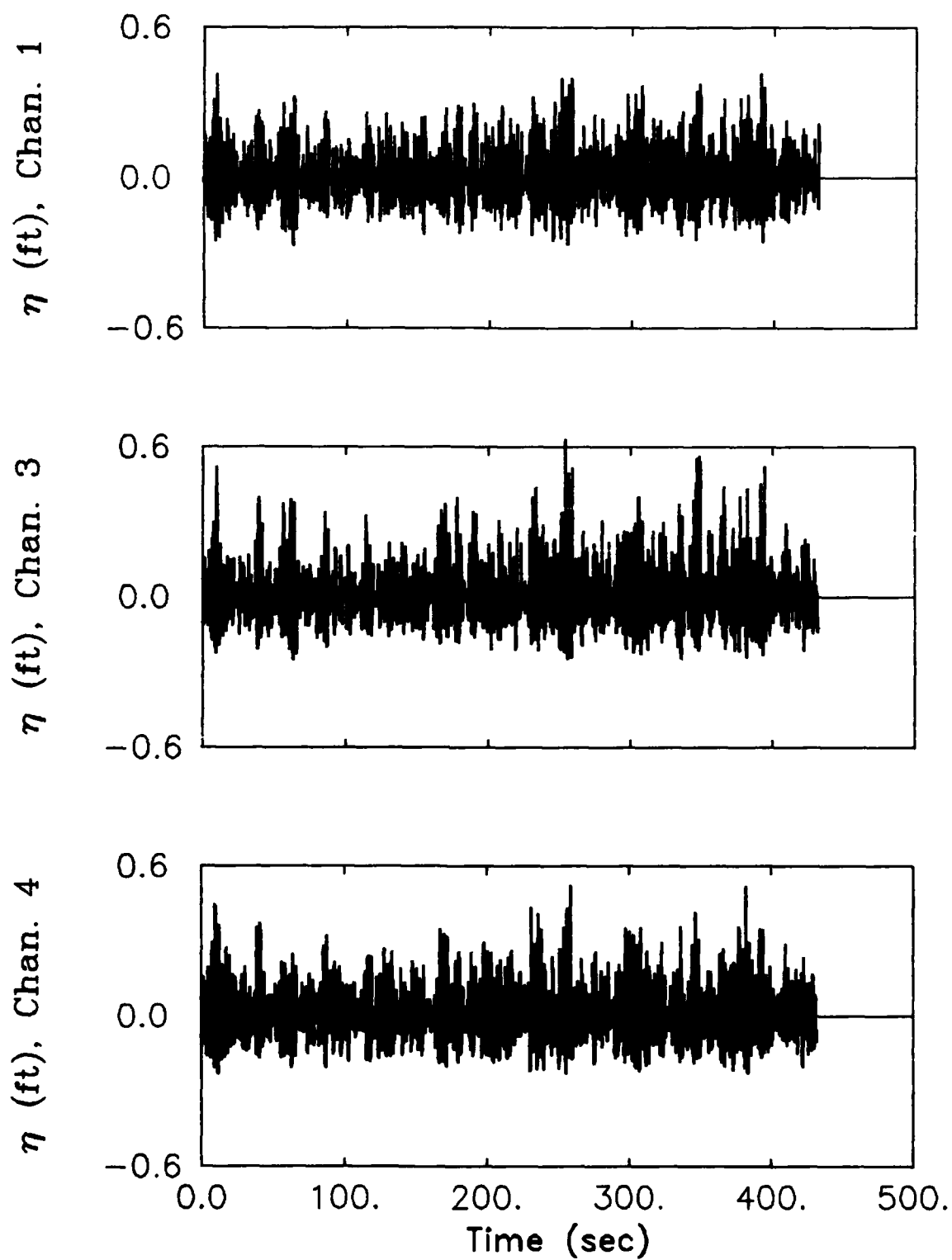
Measured Wave Elevation Time Series
CASE 73D2 -- Fp=.47, Hm0=4.55, H=1.29

B26
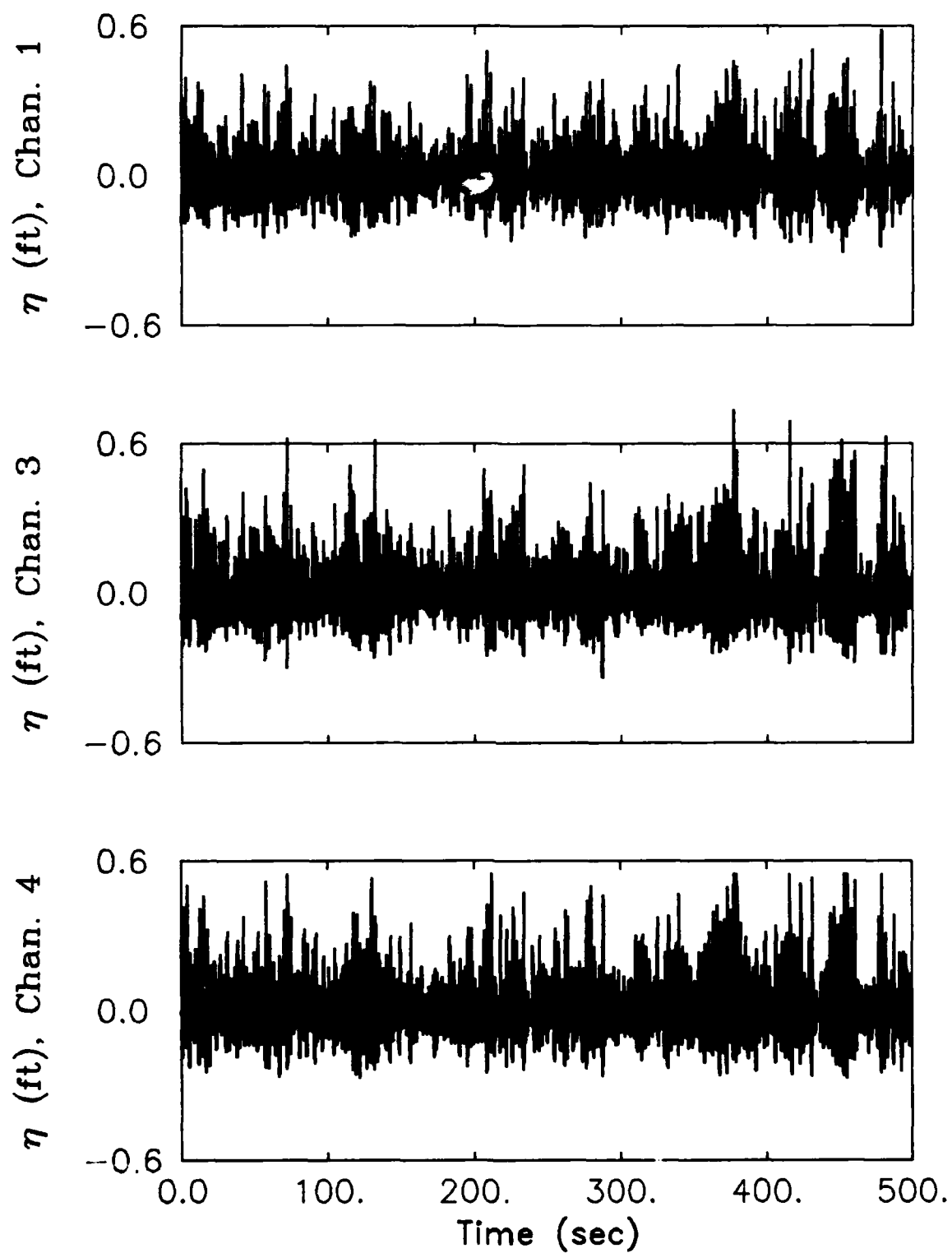
Measured Wave Elevation Time Series
CASE 83D2 -- Fp=.4, Hm0=5.42, H=1.29

B27
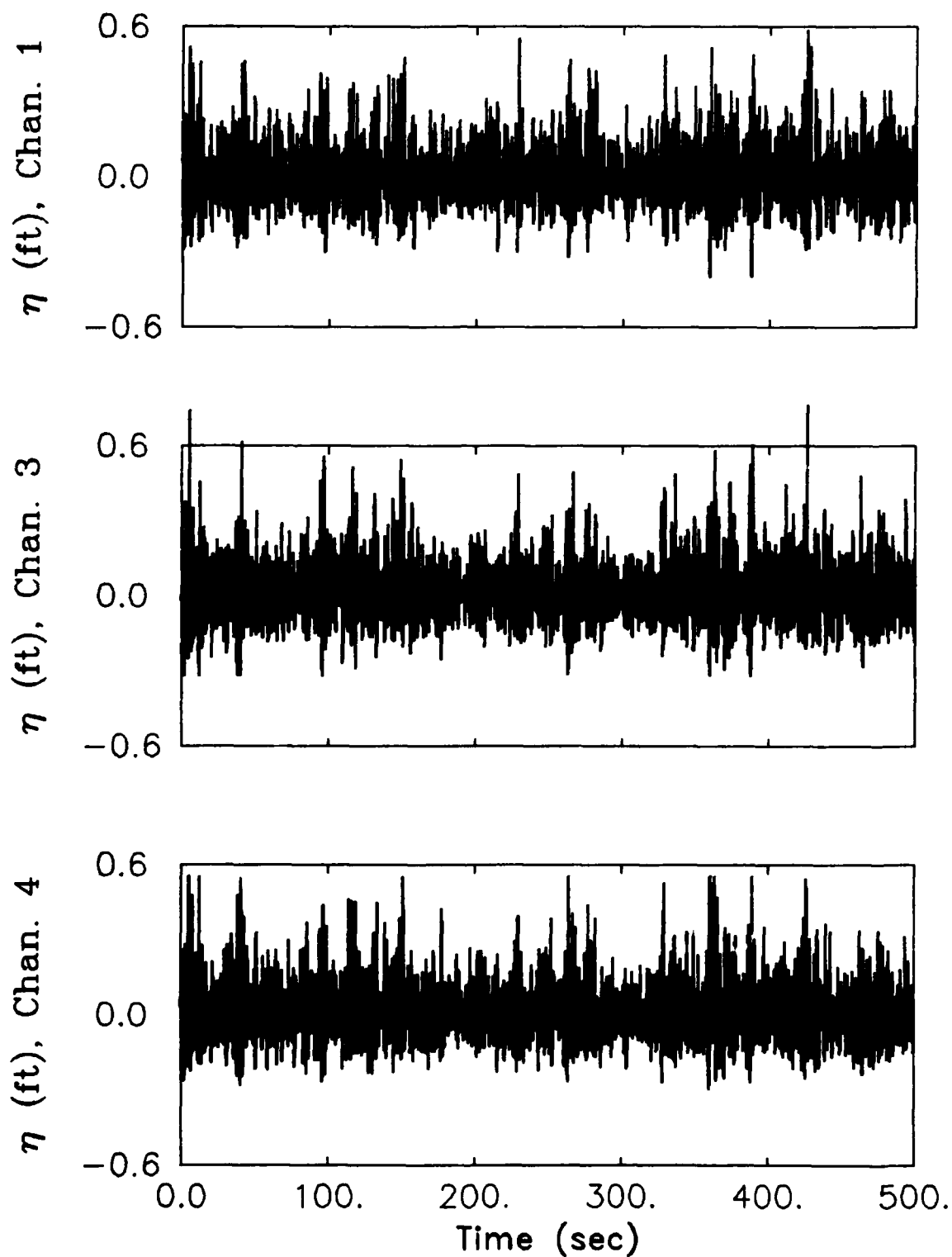
Measured Wave Elevation Time Series
CASE 69D3 —— Fp=.4, Hm0=6.12, H=1.51

B28
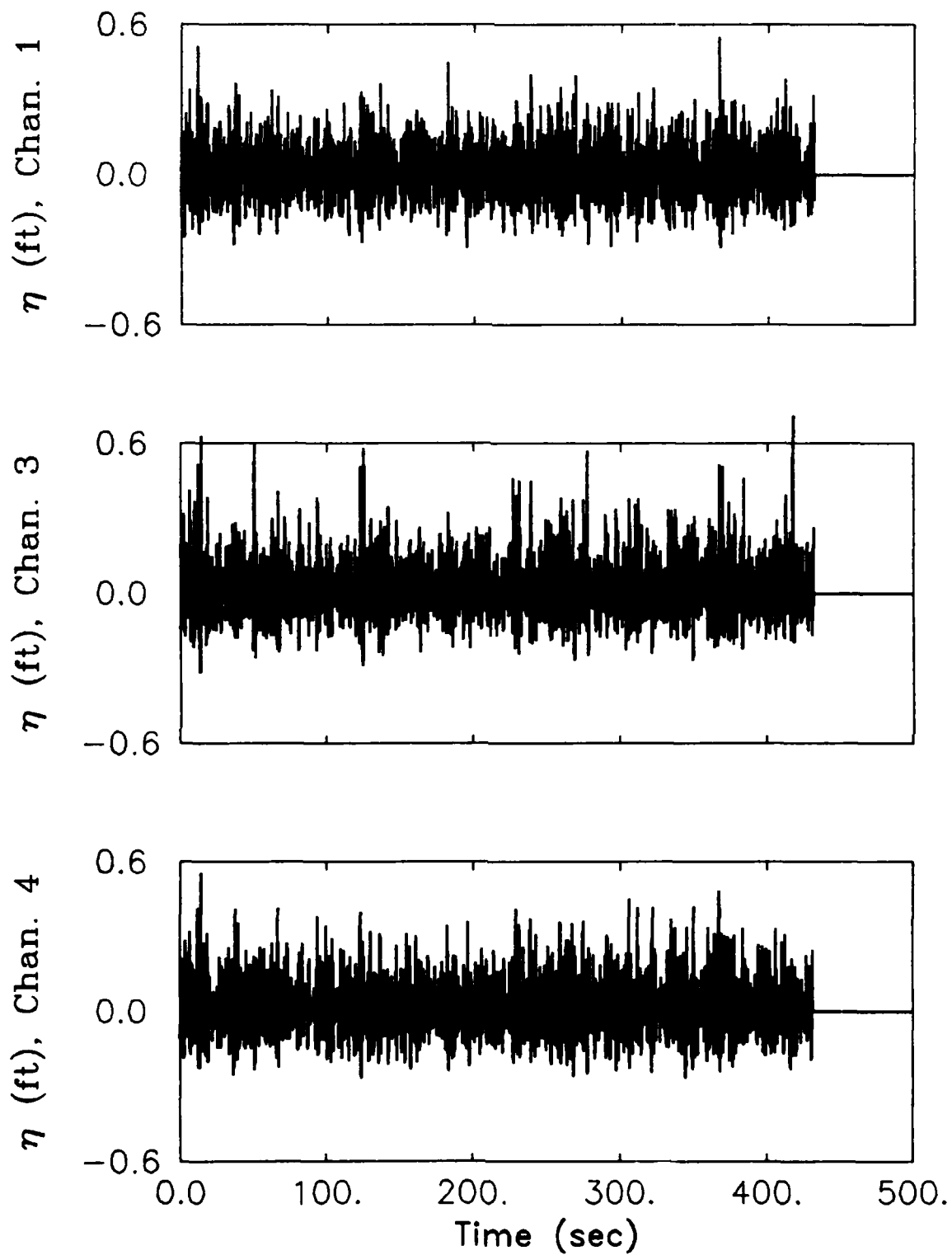
Measured Wave Elevation Time Series
CASE 70D3 -- Fp=.47, Hm0=5.07, H=1.51

B29
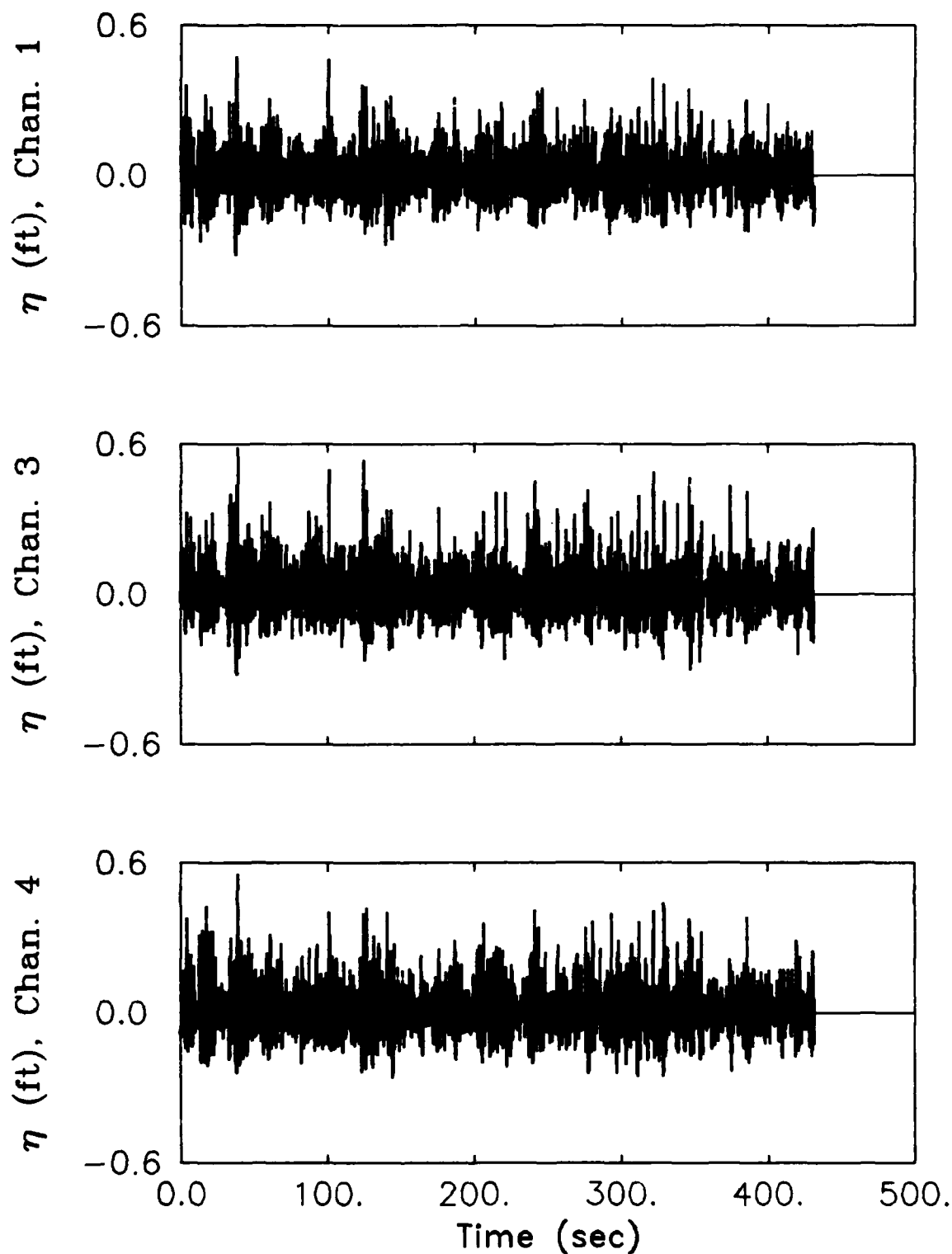
Measured Wave Elevation Time Series
CASE 72D3 -- Fp=.47, Hm0=4.11, H=1.51

B30
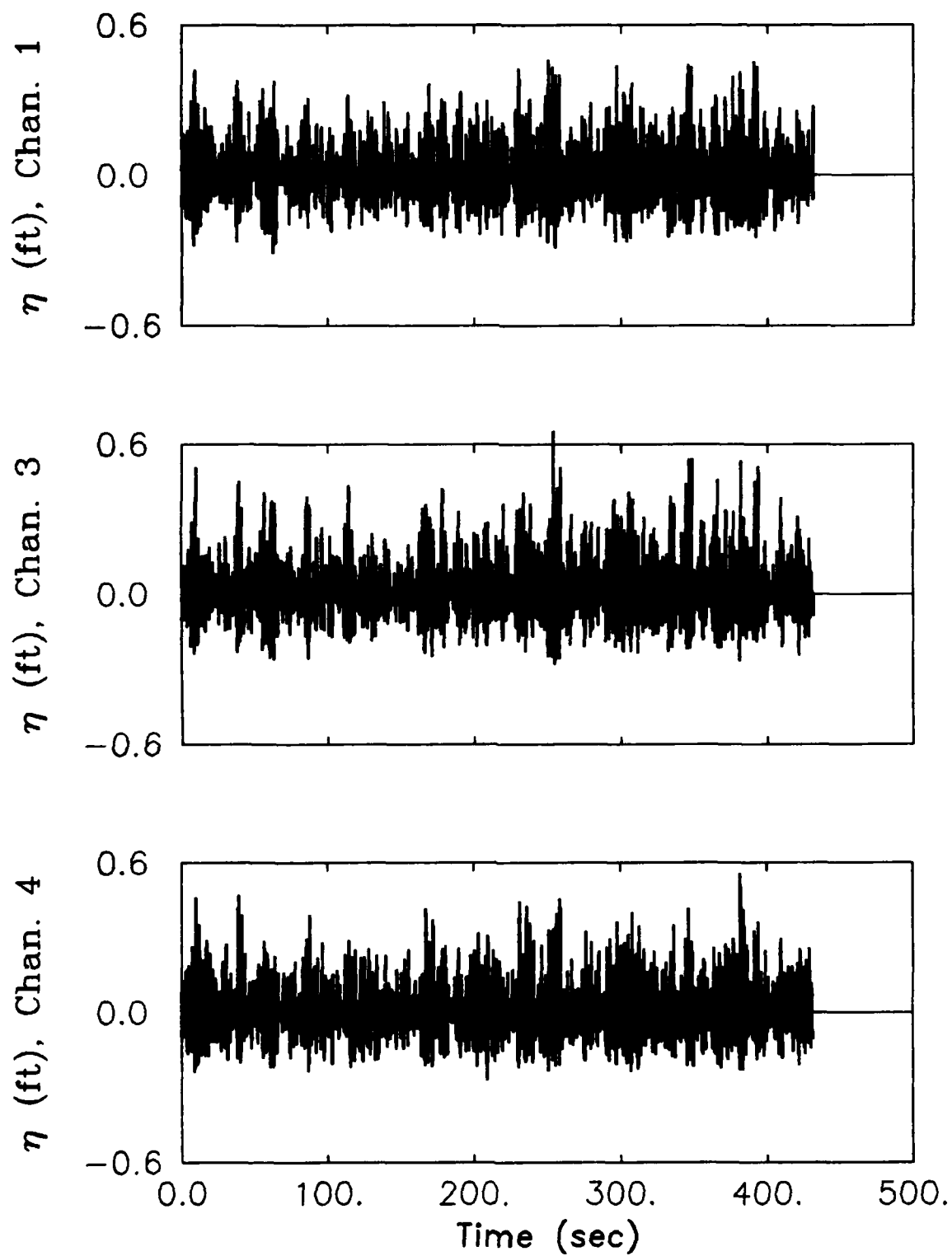
Measured Wave Elevation Time Series
CASE 73D3 -- Fp=.47, Hm0=4.55, H=1.51

B31
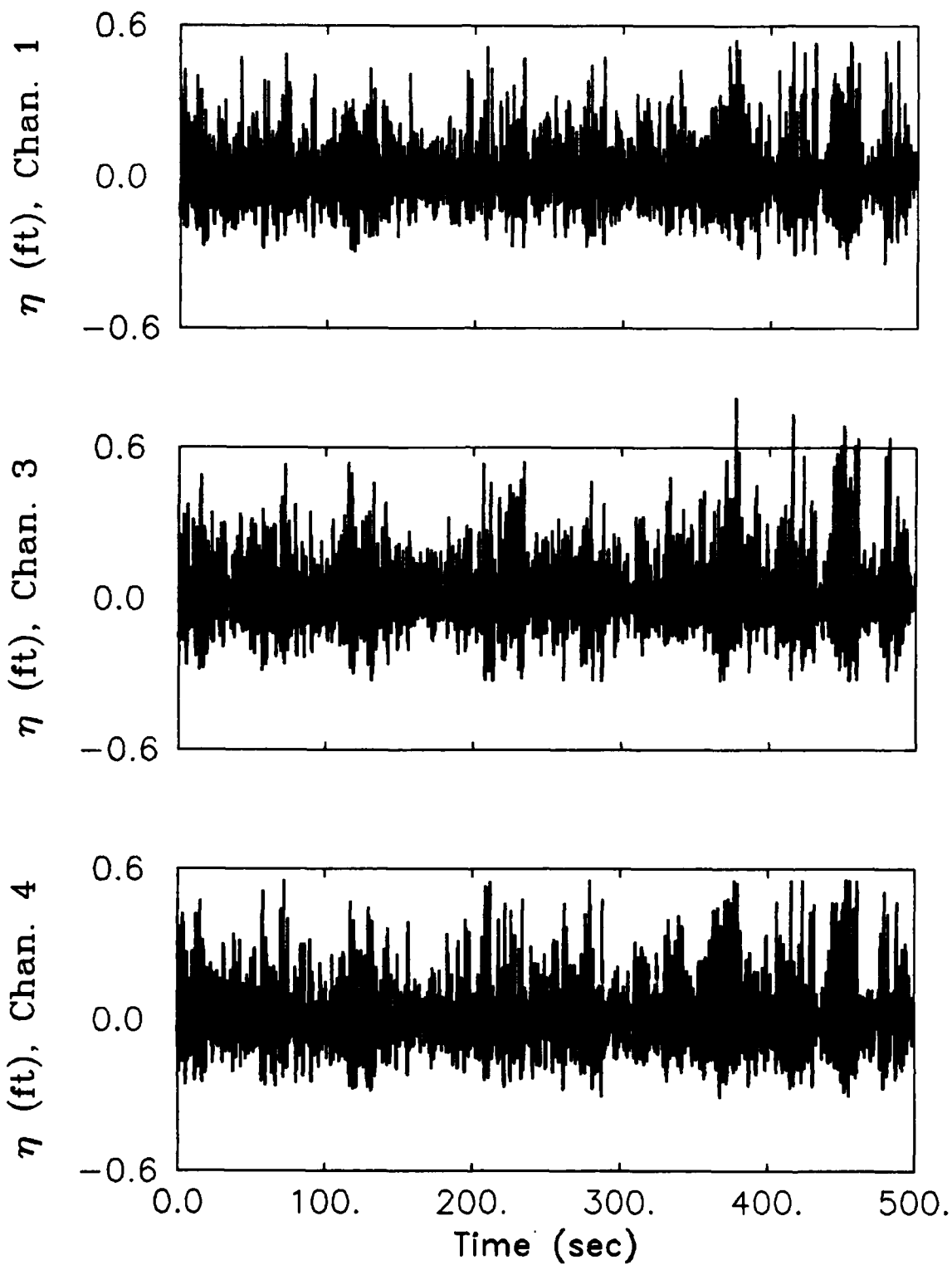
Measured Wave Elevation Time Series
CASE 83D3 —— Fp=.4, Hm0=5.42, H=1.51

B32

APPENDIX C: MEASURED FREQUENCY SPECTRA
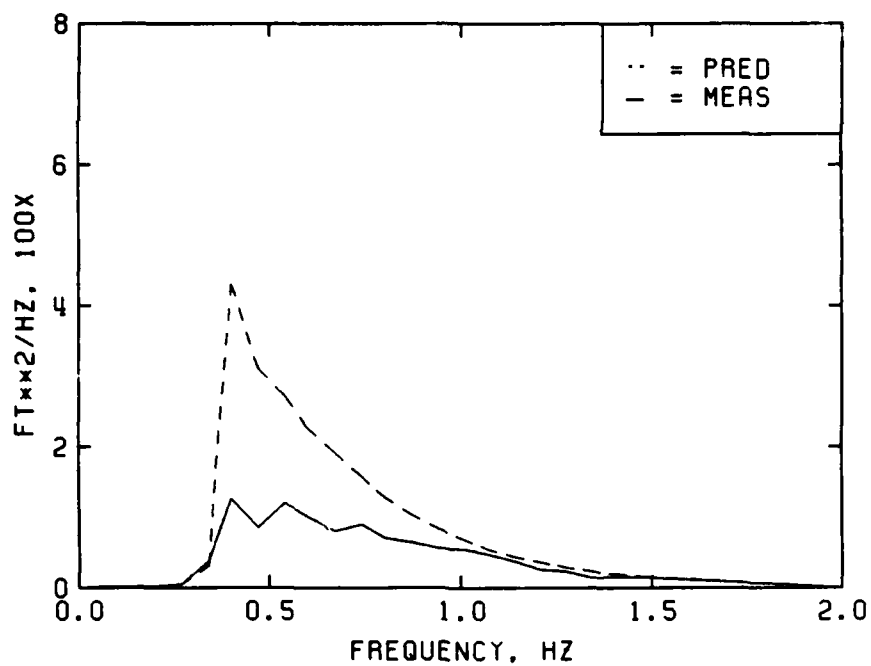
MEASURED VS PREDICTED FREQUENCY SPECTRA
CASE 69U1 -- FP=0.40, HMO=5.95, H=1.11
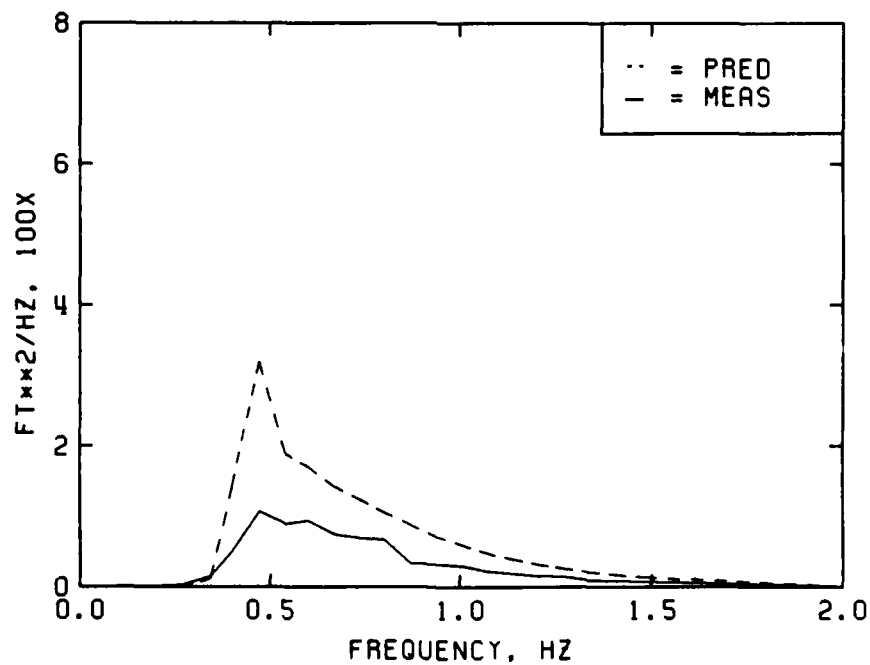
MEASURED VS PREDICTED FREQUENCY SPECTRA
CASE 70U1 -- FP=0.47, HMO=5.07, H=1.11

C3
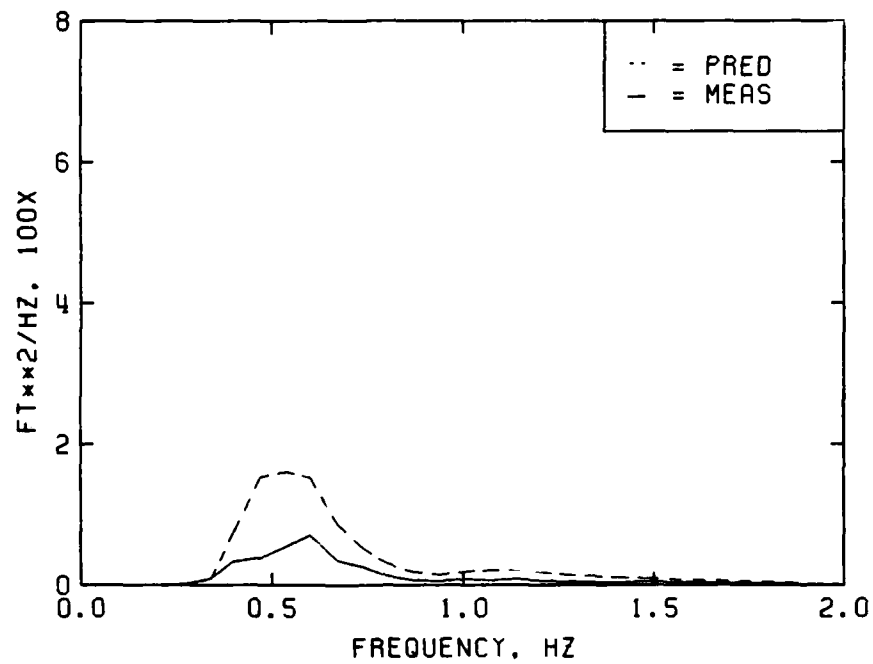
MEASURED VS PREDICTED FREQUENCY SPECTRA
CASE 72U1 -- FP=0.54, HMO=3.85, H=1.11
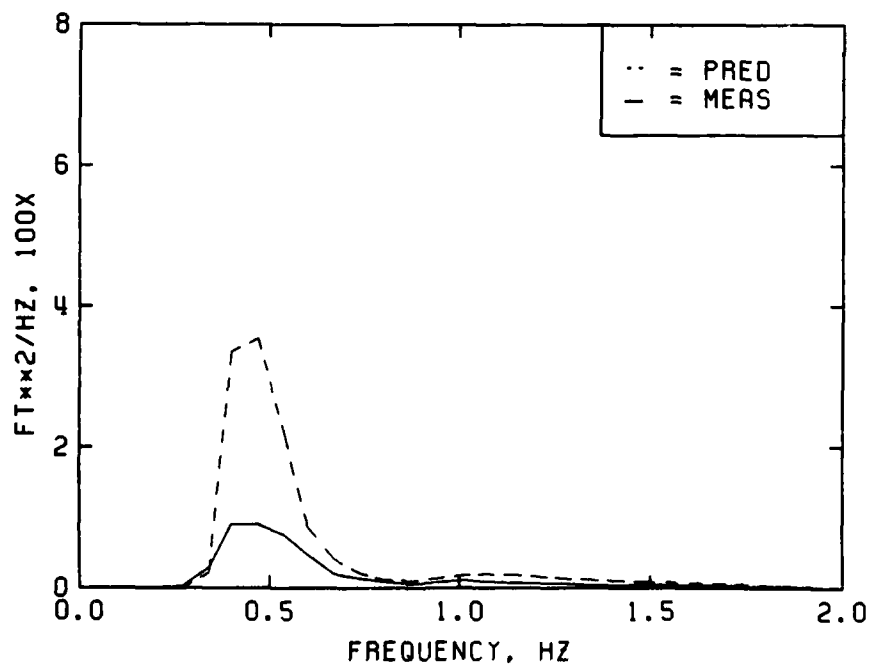
MEASURED VS PREDICTED FREQUENCY SPECTRA
CASE 73U1 -- FP=0.47, HMO=4.46, H=1.11
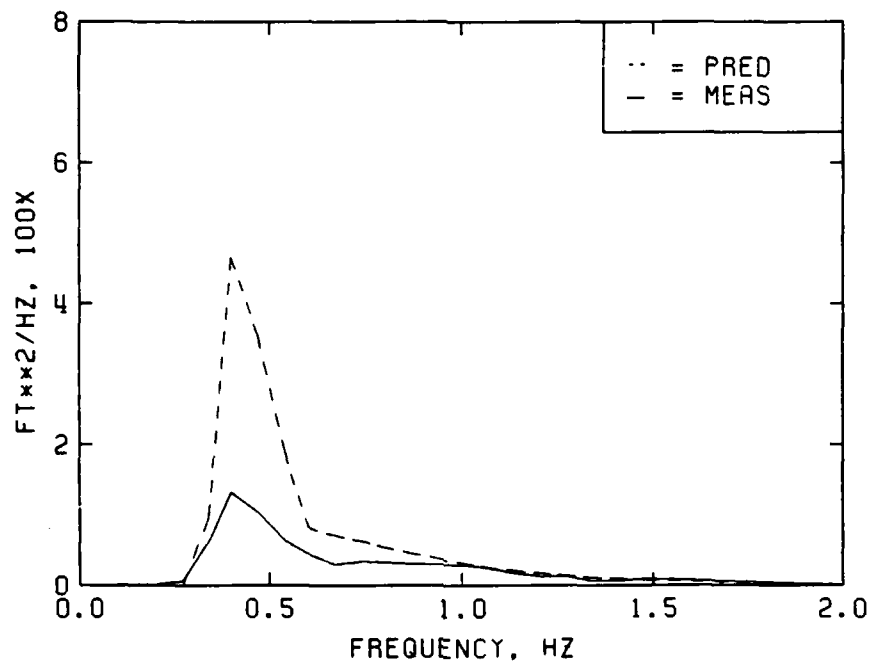
MEASURED VS PREDICTED FREQUENCY SPECTRA
CASE 83U1 -- FP=0.40, HMO=4.99, H=1.11
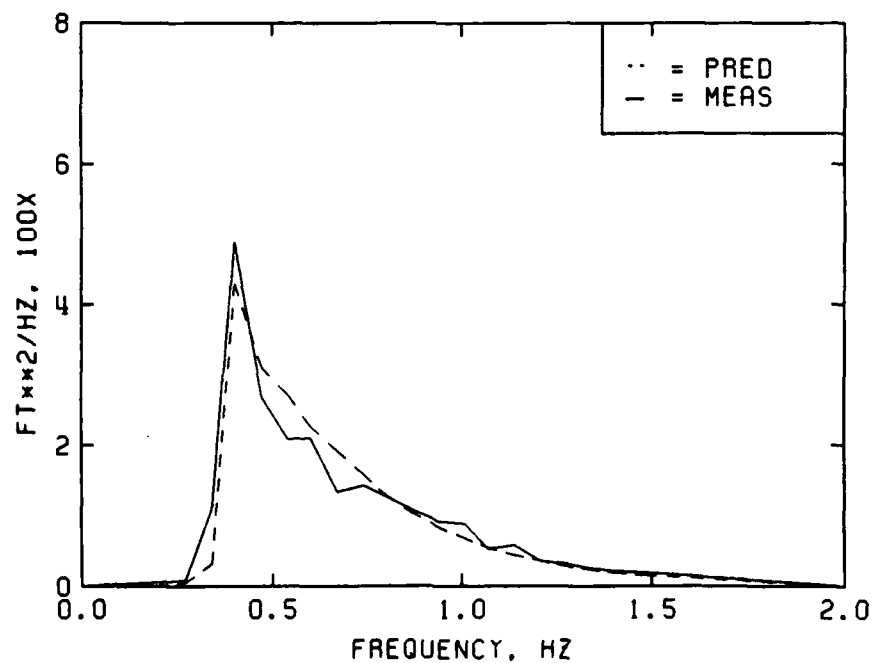
MEASURED VS PREDICTED FREQUENCY SPECTRA
CASE 69U2 -- FP=0.40, HMO=5.95, H=1.29

C5
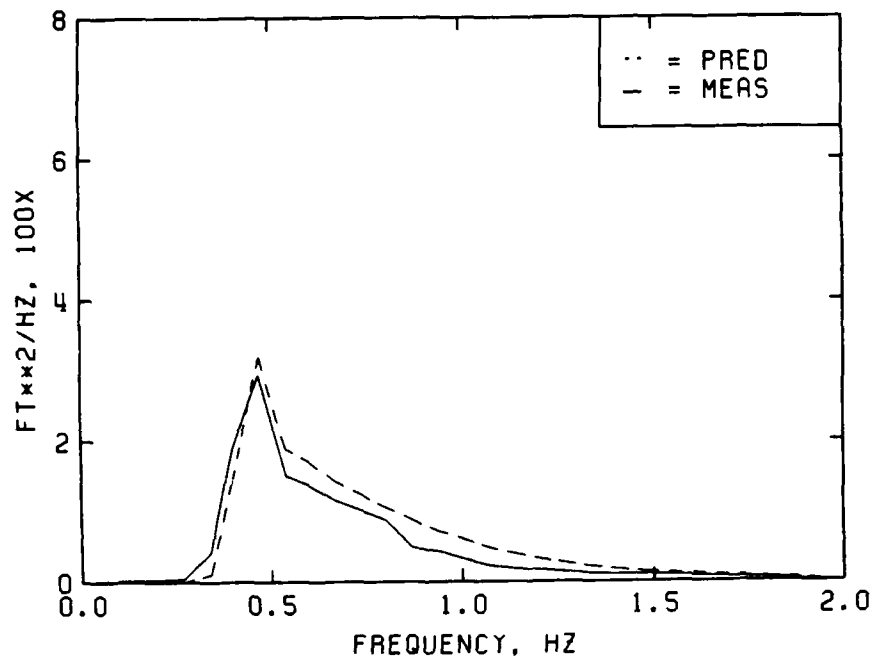
MEASURED VS PREDICTED FREQUENCY SPECTRA
CASE 70U2 -- FP=0.47, HMO=5.07, H=1.29
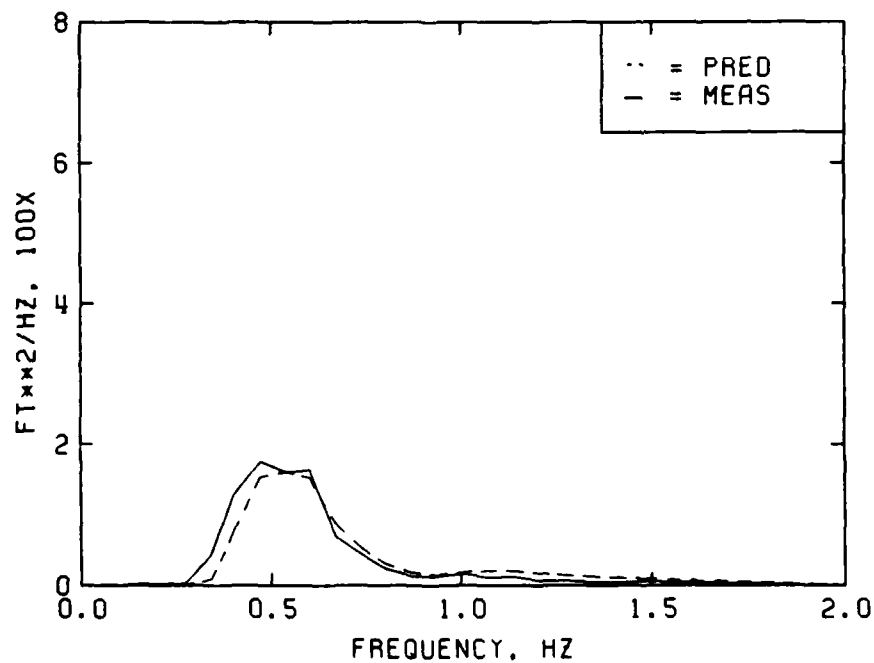
MEASURED VS PREDICTED FREQUENCY SPECTRA
CASE 72U2 -- FP=0.54, HMO=3.85, H=1.29

C6
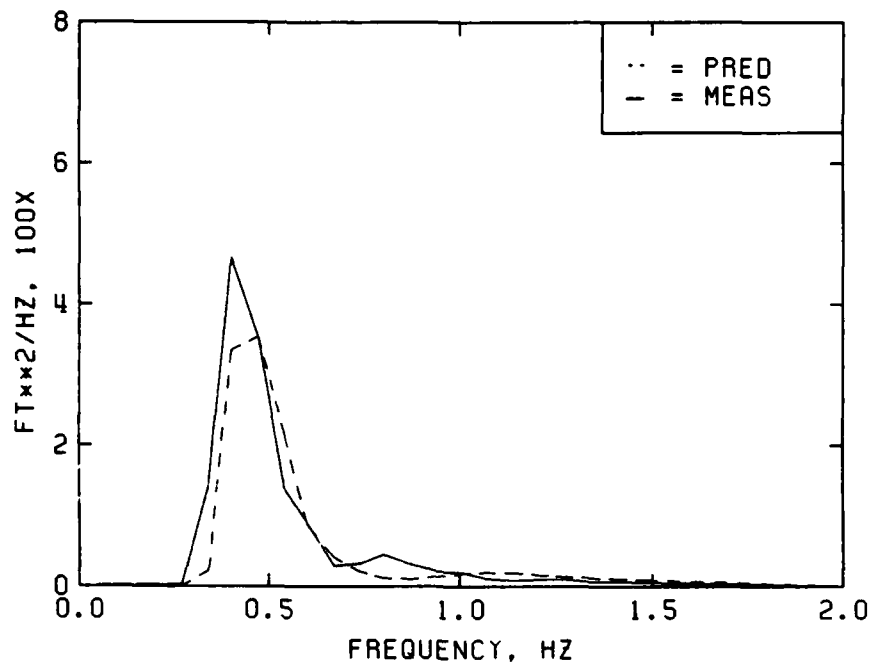
MEASURED VS PREDICTED FREQUENCY SPECTRA
CASE 73U2 -- FP=0.47, HMO=4.46, H=1.29
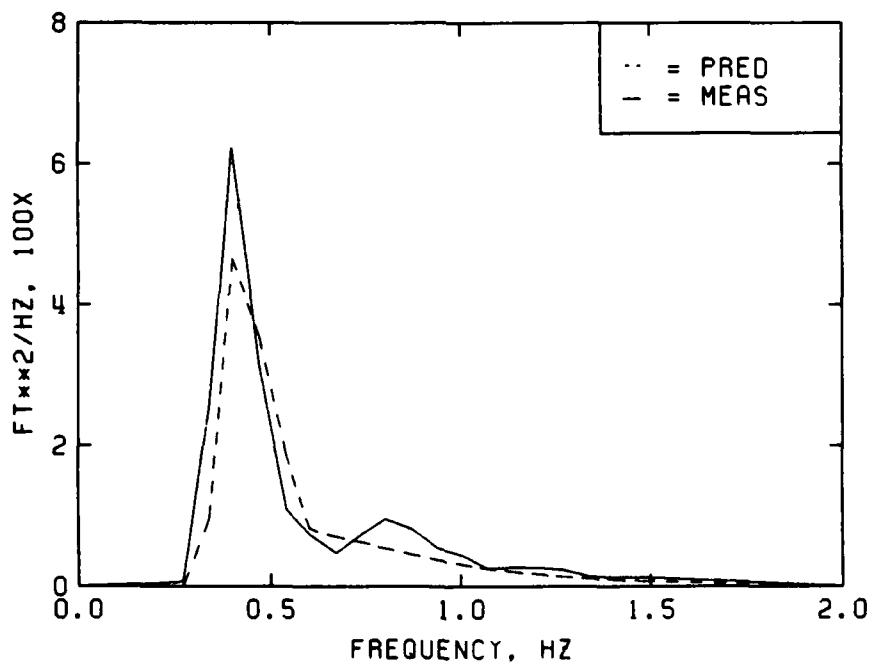
MEASURED VS PREDICTED FREQUENCY SPECTRA
CASE 83U2 -- FP=0.40, HMO=4.99, H=1.29

C7
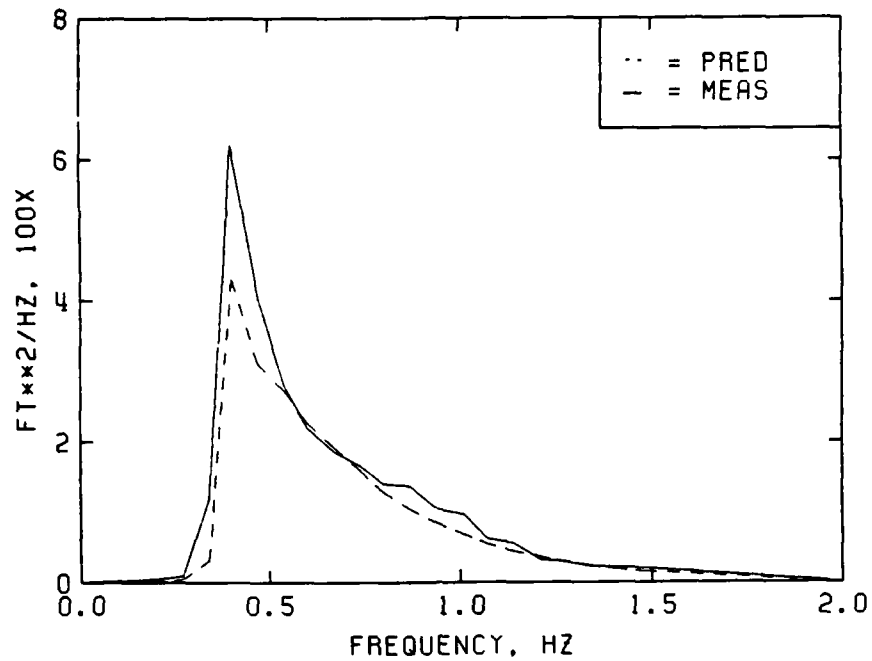
MEASURED VS PREDICTED FREQUENCY SPECTRA
CASE 69U3 -- FP=0.40, HMO=5.95, H=1.51
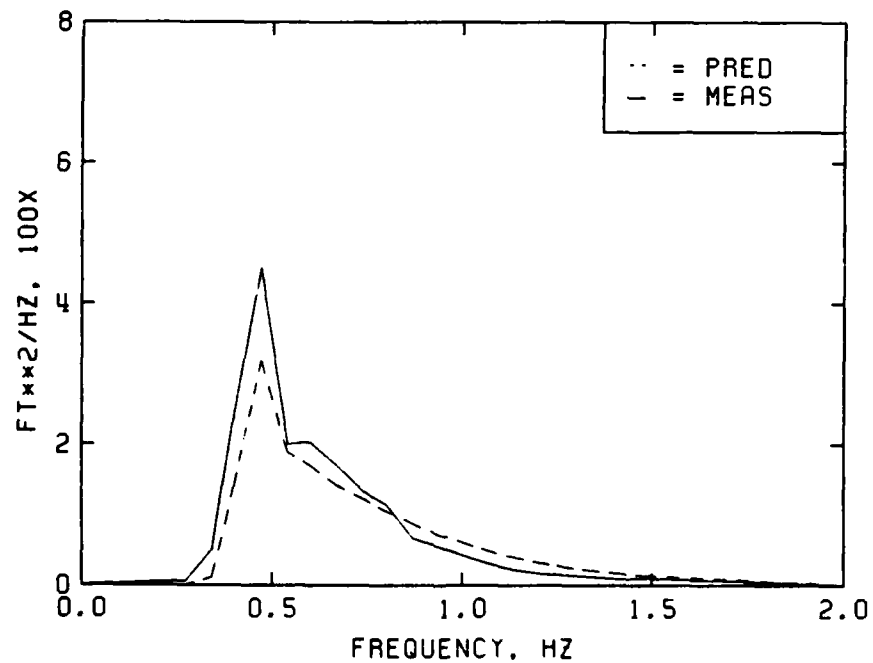
MEASURED VS PREDICTED FREQUENCY SPECTRA
CASE 70U3 -- FP=0.47, HMO=5.07, H=1.51

C8
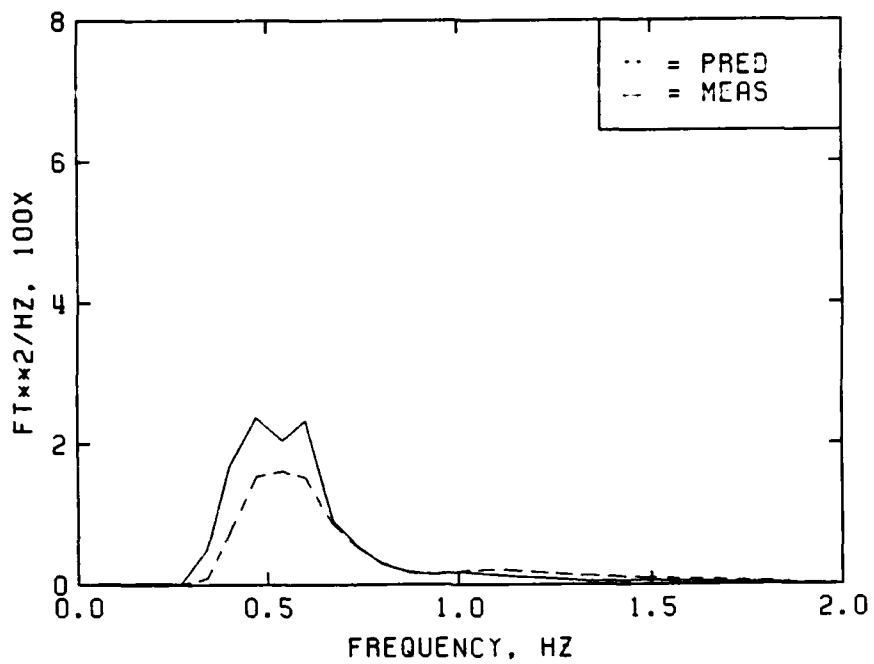
MEASURED VS PREDICTED FREQUENCY SPECTRA
CASE 72U3 -- FP=0.54, HMO=3.85, H=1.51
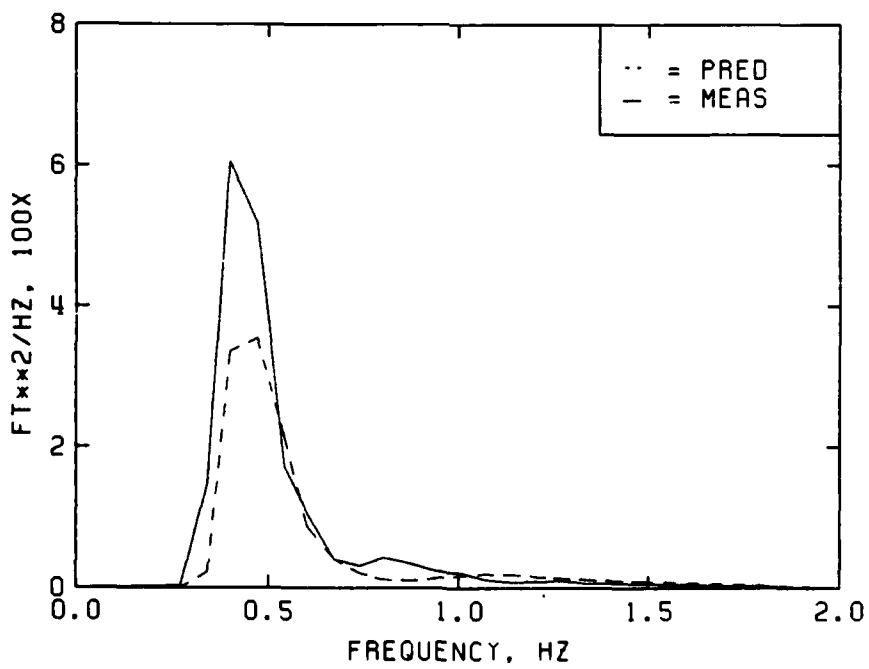
MEASURED VS PREDICTED FREQUENCY SPECTRA
CASE 73U3 -- FP=0.47, HMO=4.46, H=1.51
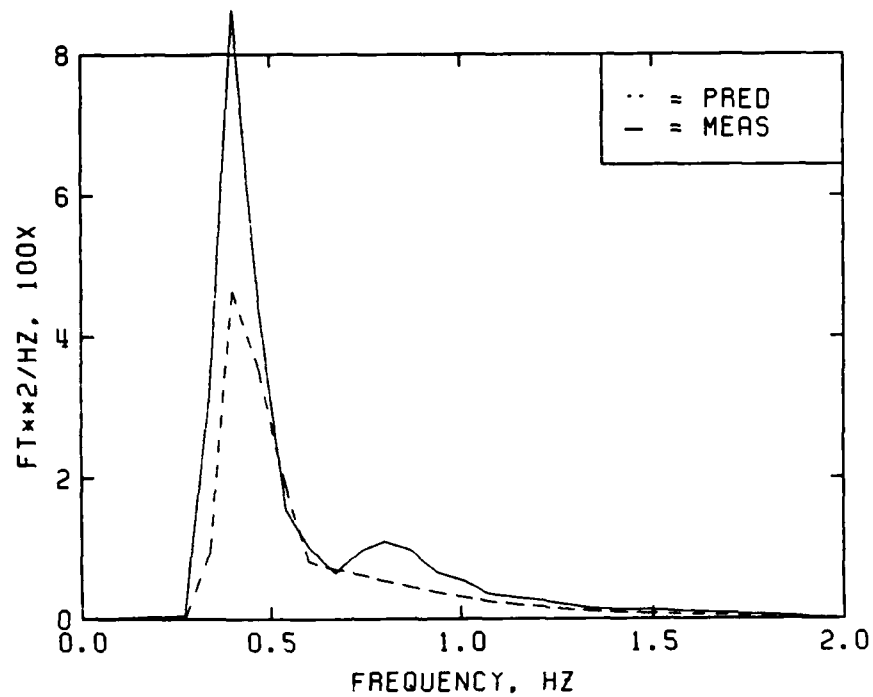
MEASURED VS PREDICTED FREQUENCY SPECTRA
CASE 83U3 -- FP=0.40, HMO=4.99, H=1.51
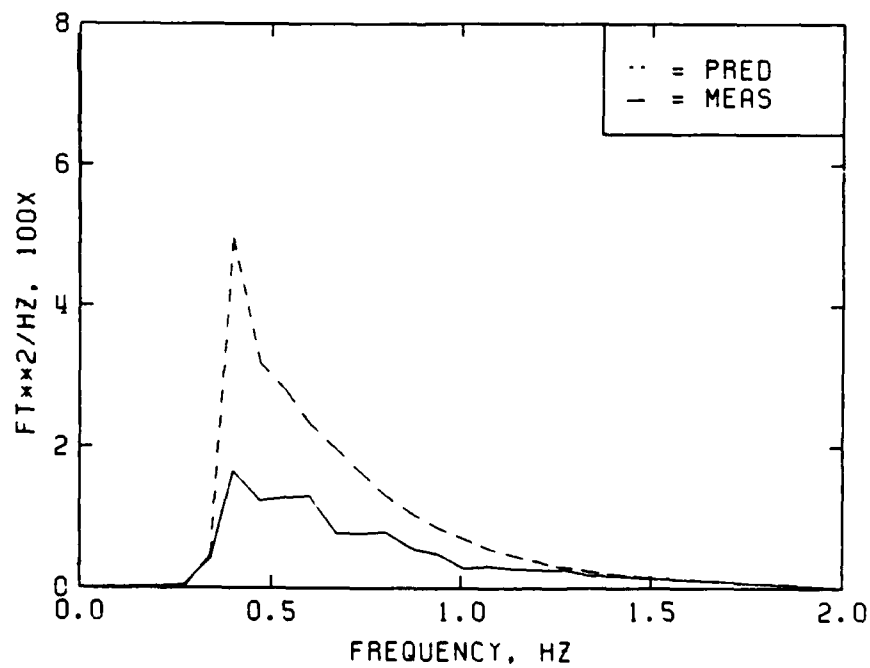
MEASURED VS PREDICTED FREQUENCY SPECTRA
CASE 69D1 -- FP=0.40, HMO=6.12, H=1.11

C10
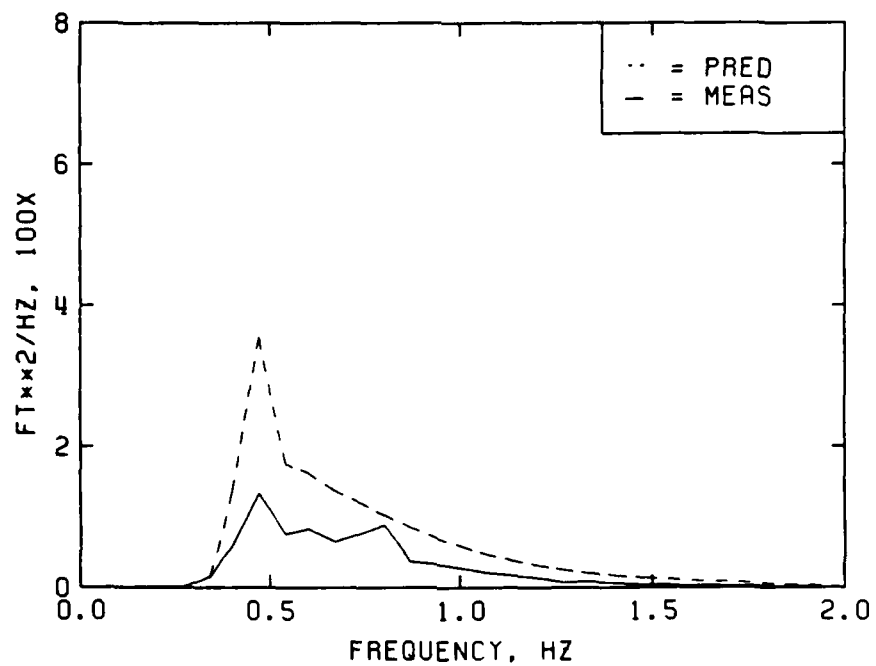
MEASURED VS PREDICTED FREQUENCY SPECTRA
CASE 70D1 -- FP=0.47, HMO=5.07, H=1.11
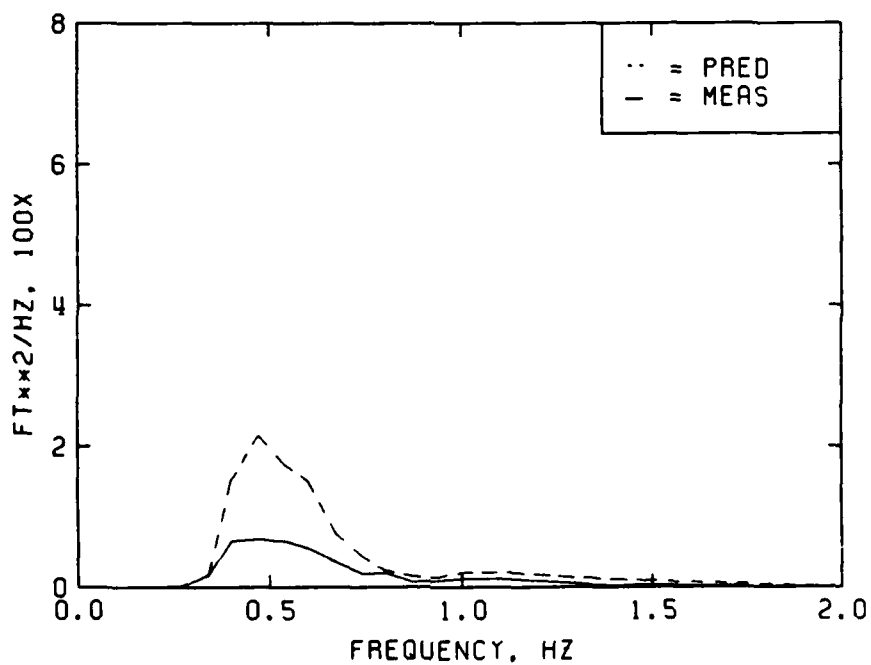
MEASURED VS PREDICTED FREQUENCY SPECTRA
CASE 72D1 -- FP=0.47, HMO=4.11, H=1.11

C11
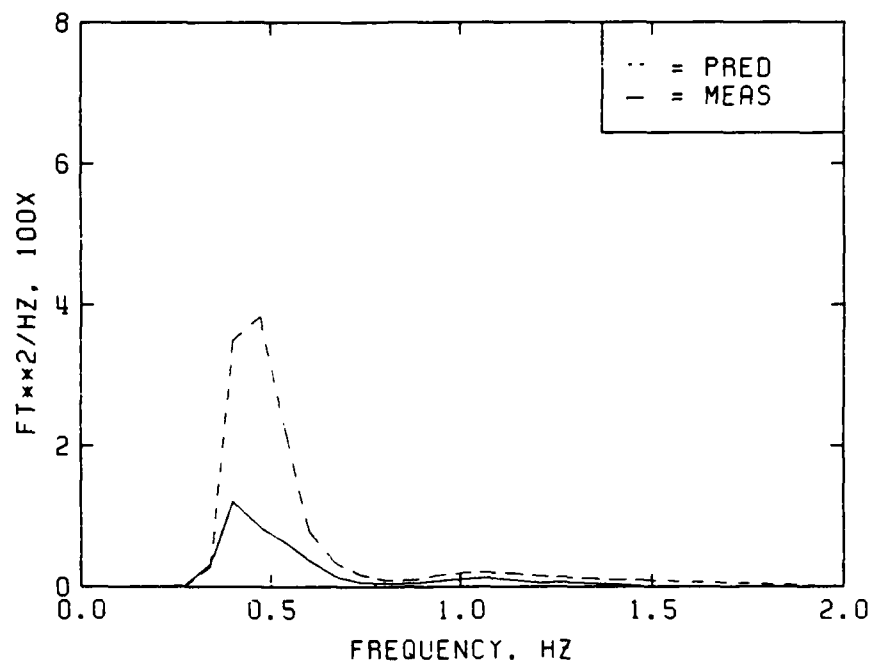
MEASURED VS PREDICTED FREQUENCY SPECTRA
CASE 73D1 -- FP=0.40, HMO=4.55, H=1.11
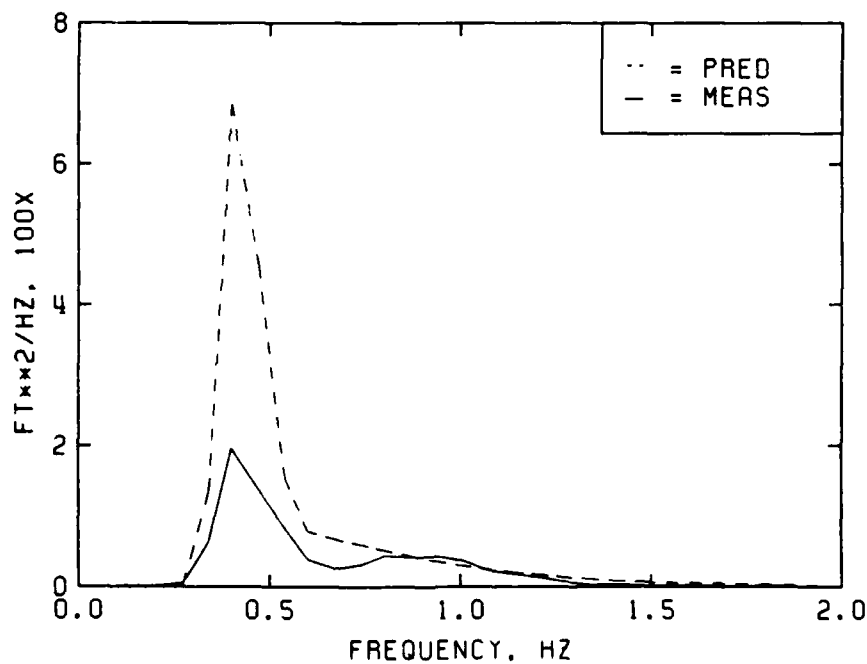
MEASURED VS PREDICTED FREQUENCY SPECTRA
CASE 83D1 -- FP=0.40, HMO=5.42, H=1.11

C12
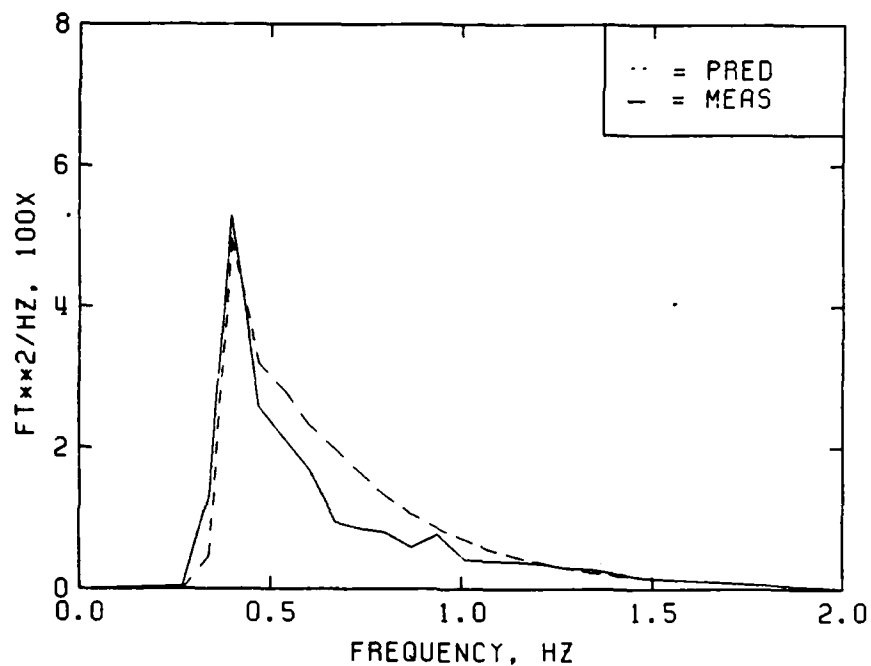
MEASURED VS PREDICTED FREQUENCY SPECTRA
CASE 69D2 -- FP=0.40, HMO=6.12, H=1.29
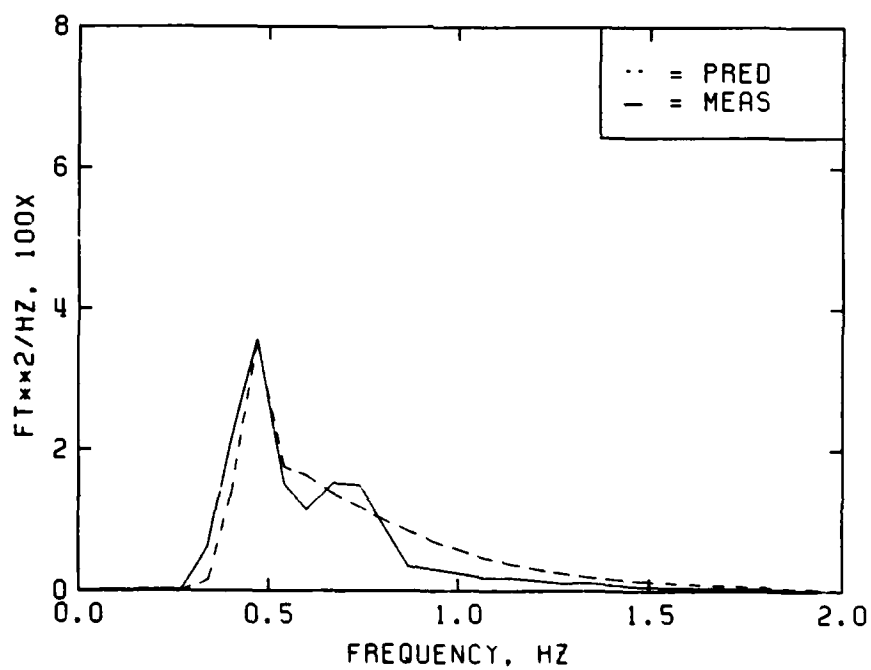
MEASURED VS PREDICTED FREQUENCY SPECTRA
CASE 70D2 -- FP=0.47, HMO=5.07, H=1.29
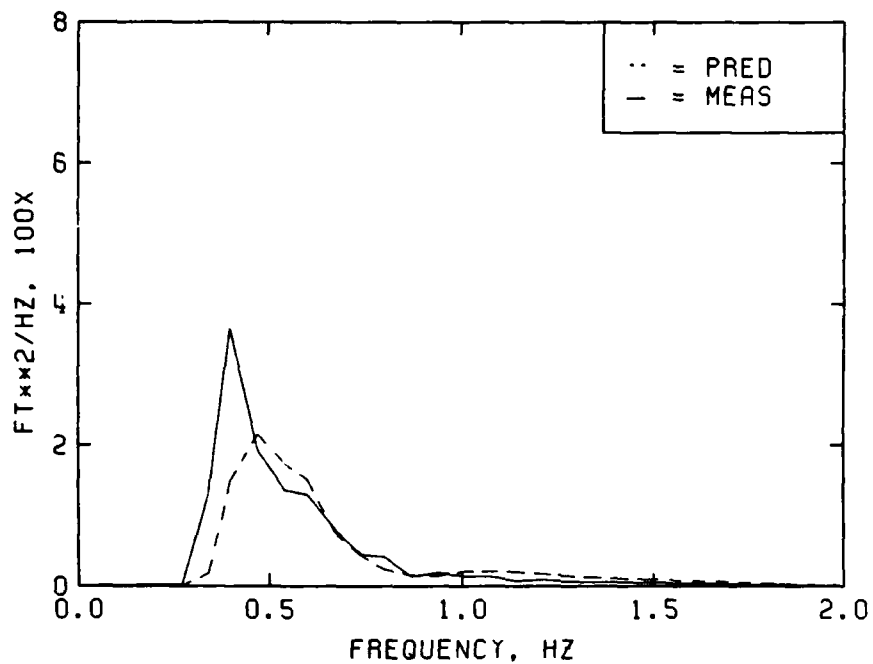
MEASURED VS PREDICTED FREQUENCY SPECTRA
CASE 72D2 -- FP=0.47, HMO=4.11, H=1.29
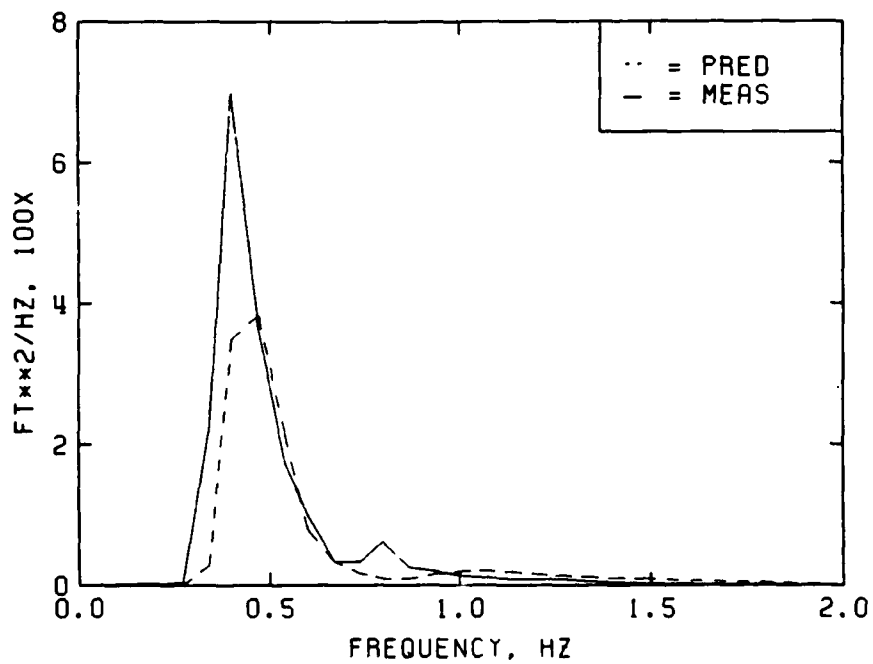
MEASURED VS PREDICTED FREQUENCY SPECTRA
CASE 73D2 -- FP=0.40, HMO=4.55, H=1.29
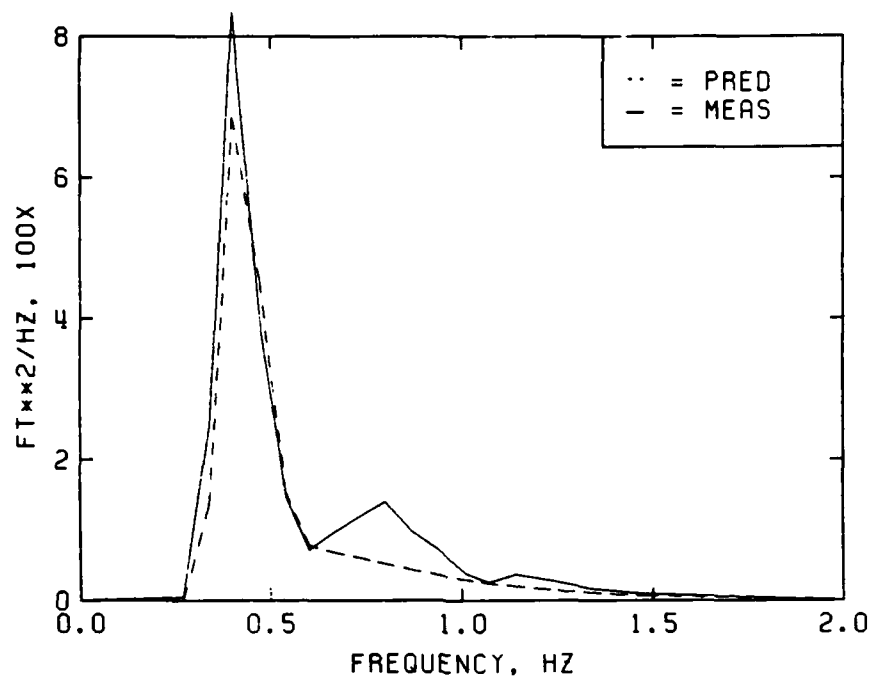
MEASURED VS PREDICTED FREQUENCY SPECTRA
CASE 83D2 -- FP=0.40, HMO=5.42, H=1.29
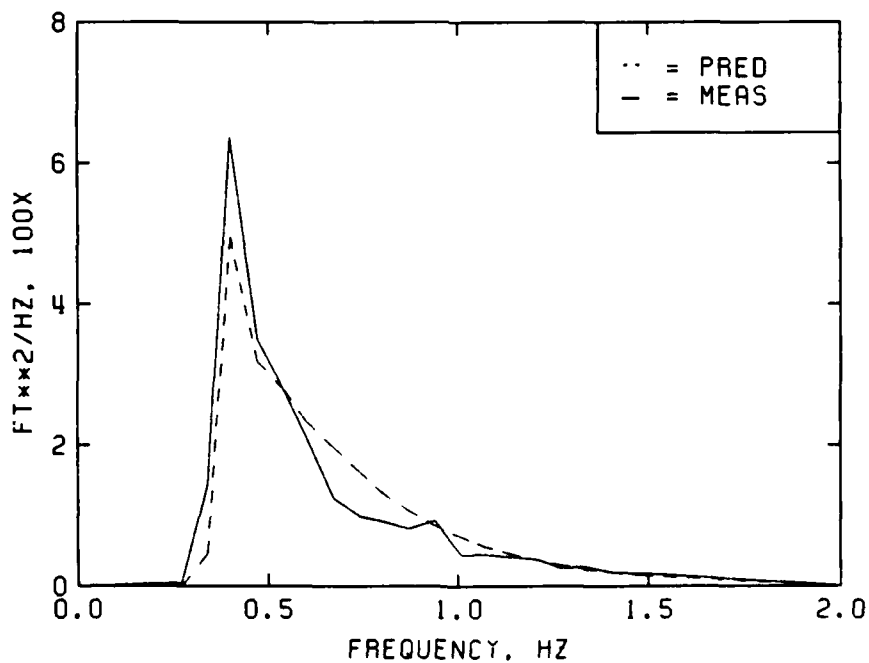
MEASURED VS PREDICTED FREQUENCY SPECTRA
CASE 69D3 -- FP=0.40, HMO=6.12, H=1.51

C15
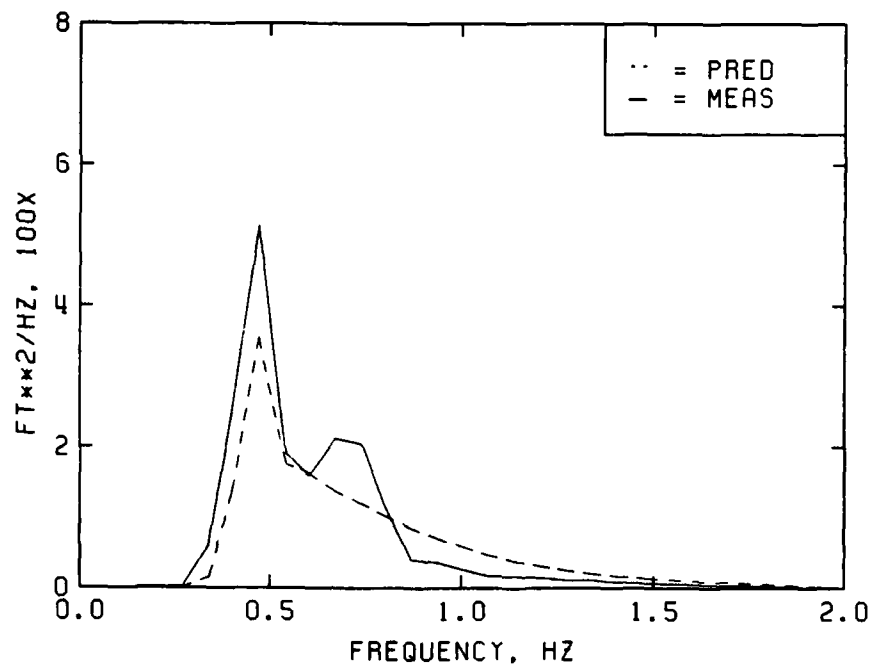
MEASURED VS PREDICTED FREQUENCY SPECTRA
CASE 70D3 -- FP=0.47, HMO=5.07, H=1.51
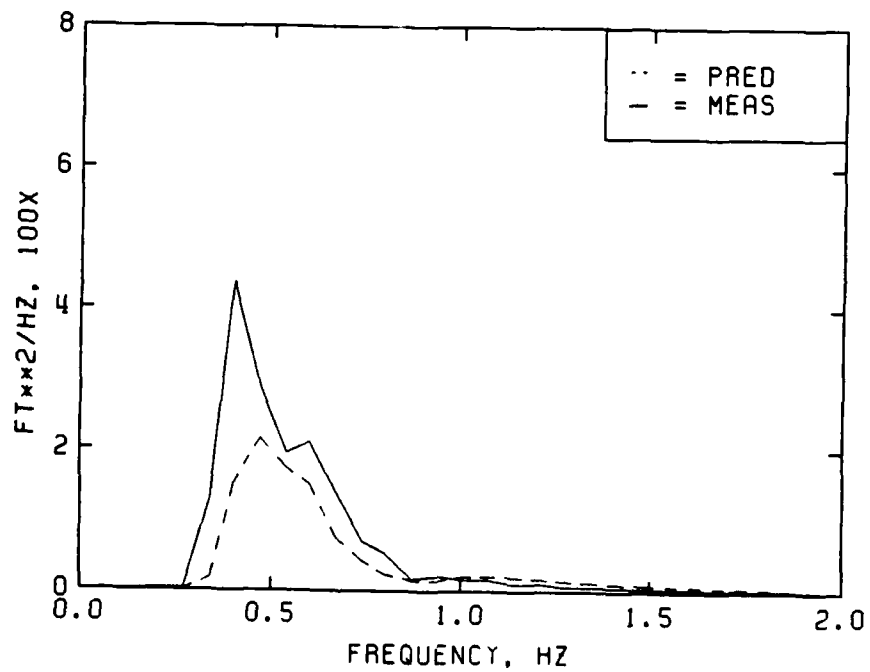
MEASURED VS PREDICTED FREQUENCY SPECTRA
CASE 72D3 -- FP=0.47, HMO=4.11, H=1.51

C16
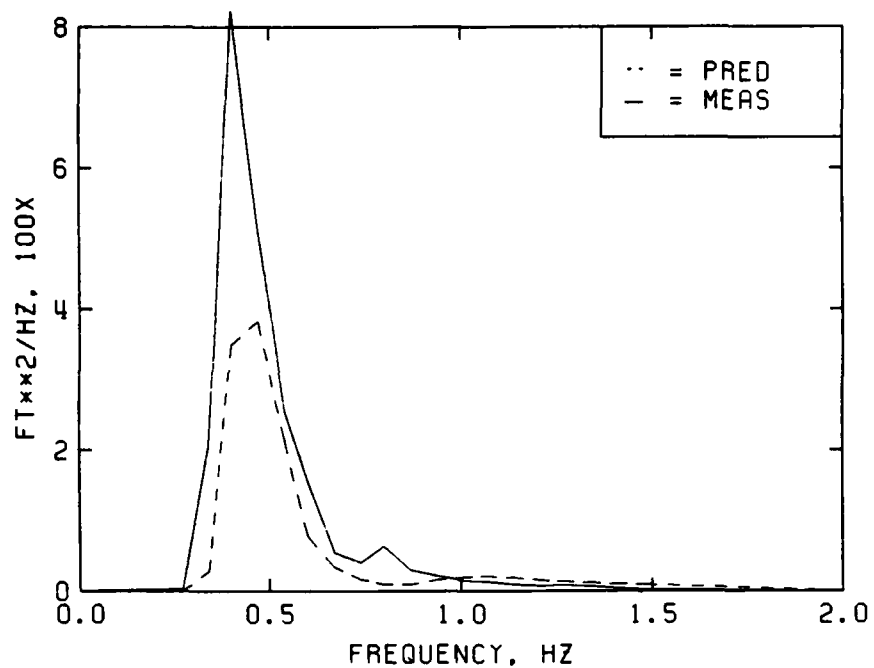
MEASURED VS PREDICTED FREQUENCY SPECTRA
CASE 73D3 -- FP=0.40, HMO=4.55, H=1.51

MEASURED VS PREDICTED FREQUENCY SPECTRA
CASE 83D3 -- FP=0.40, HMO=5.42, H=1.51

C17
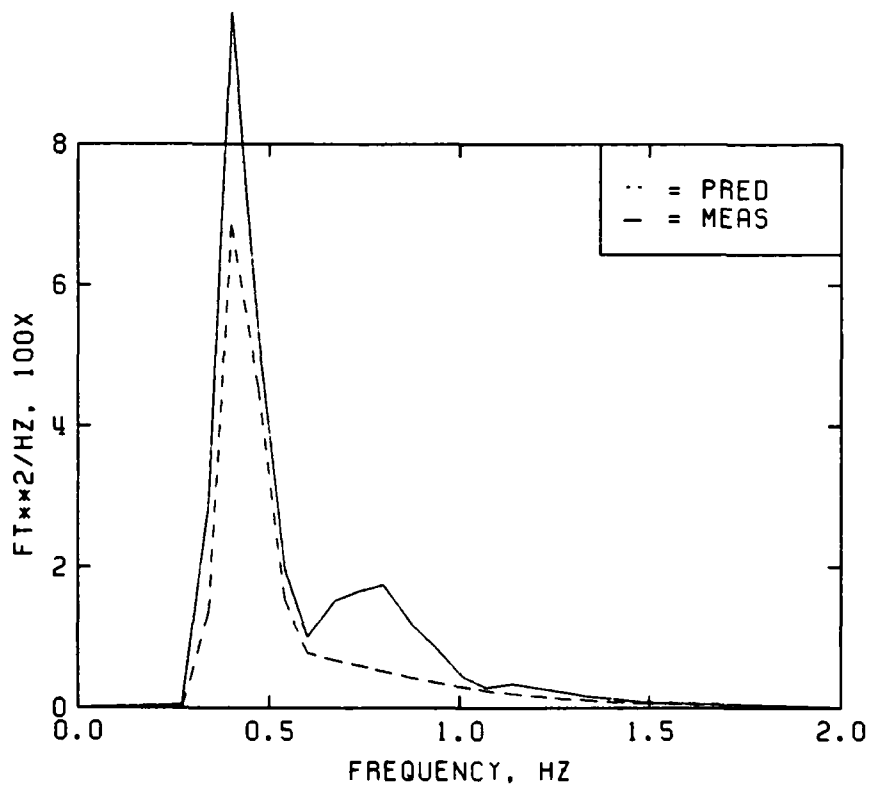
APPENDIX D: MEASURED DIRECTIONAL SPREADING FUNCTIONS
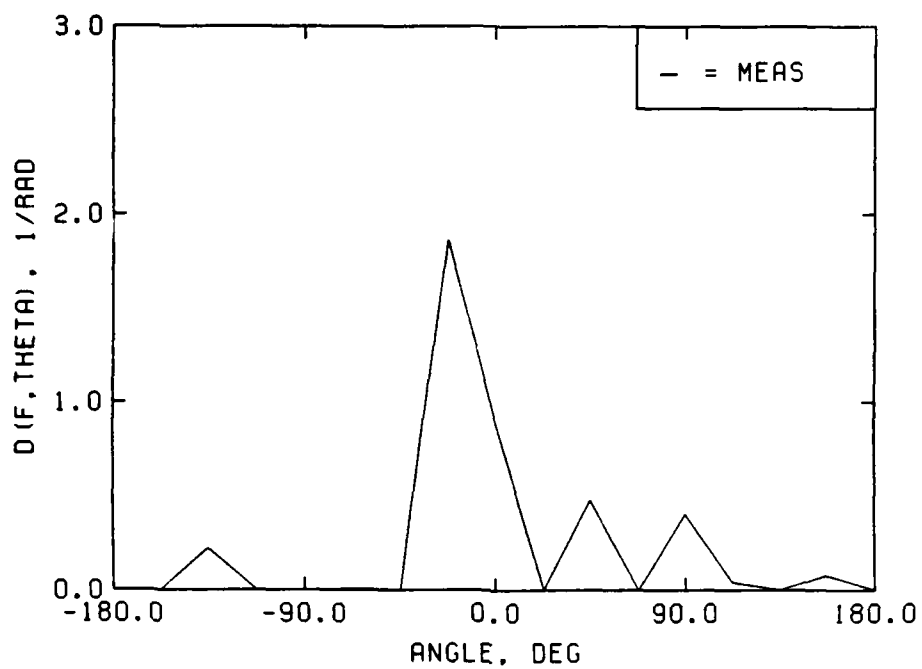
MEASURED DIRECTIONAL SPREADING
CASE 69U1 -- FP=0.40, HMO=5.95, D=-15, H=1.11
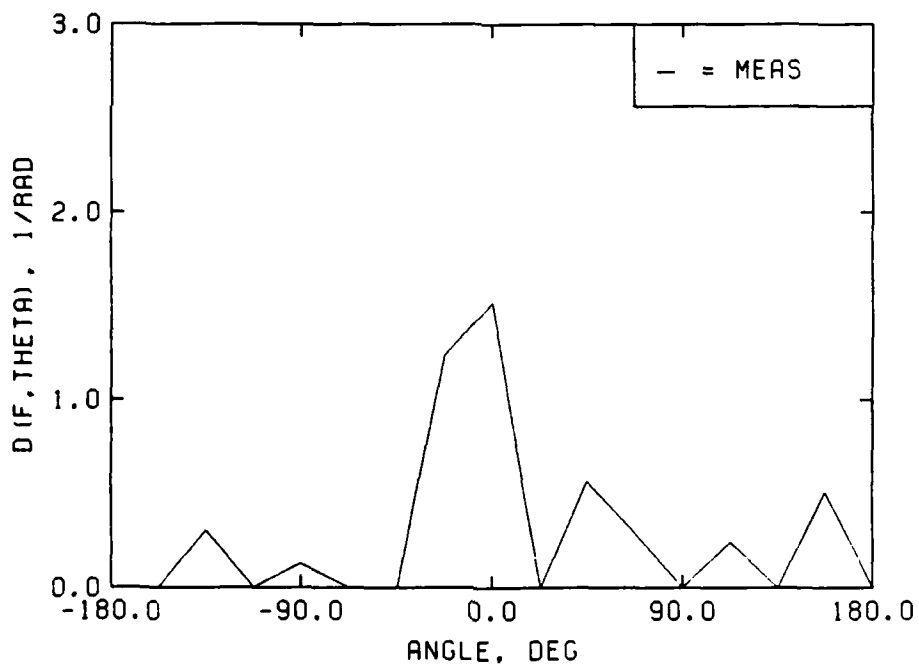
MEASURED DIRECTIONAL SPREADING
CASE 70U1 -- FP=0.47, HMO=5.07, D=-9, H=1.11
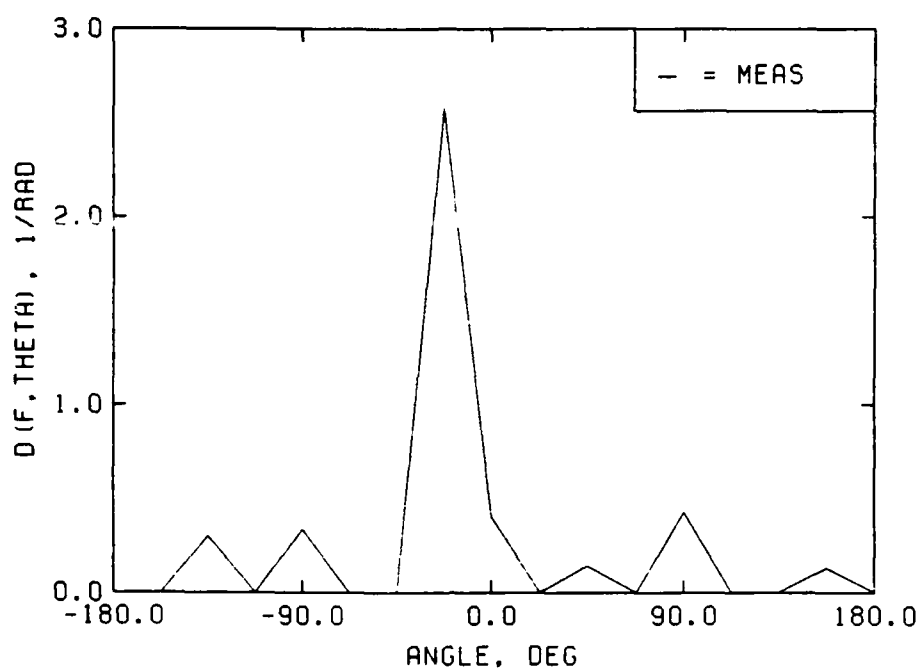
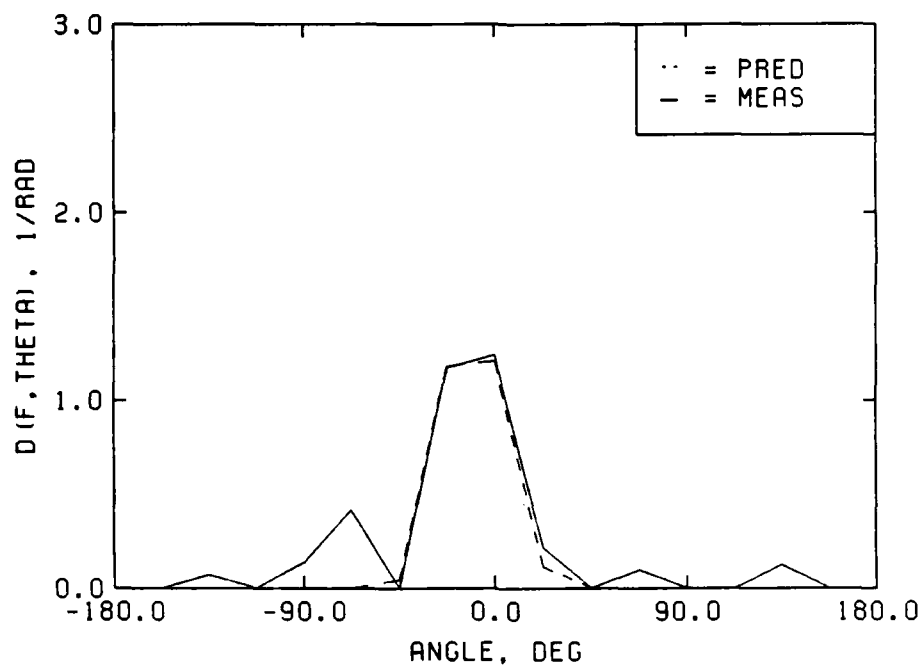MEASURED DIRECTIONAL SPREADING
CASE 72U1 -- FP=0.47, HMO=4.11, D=-19, H=1.11
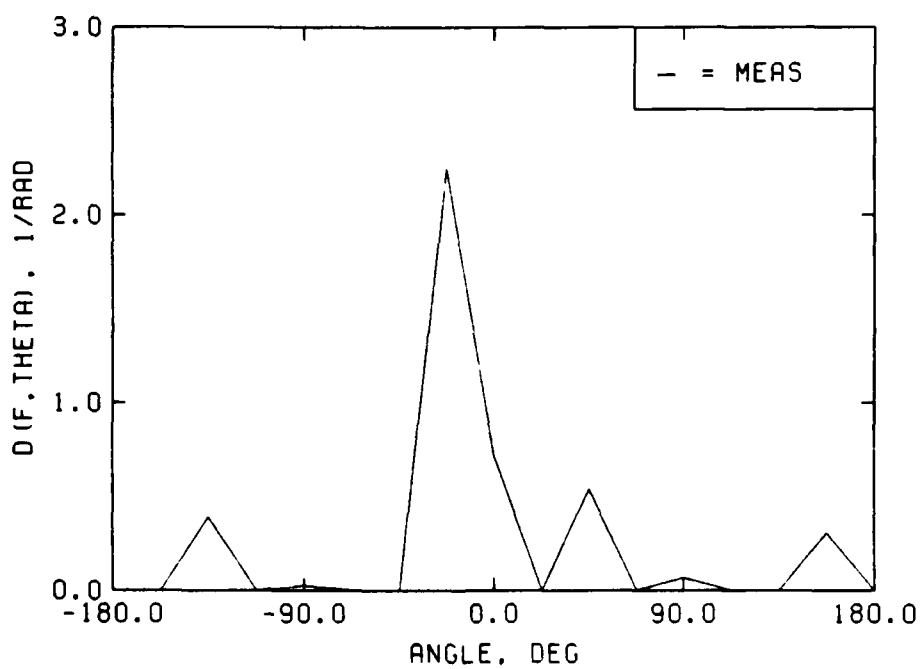
MEASURED DIRECTIONAL SPREADING
CASE 73U1 -- FP=0.47, HMO=4.55, D=-15, H=1.11

D4

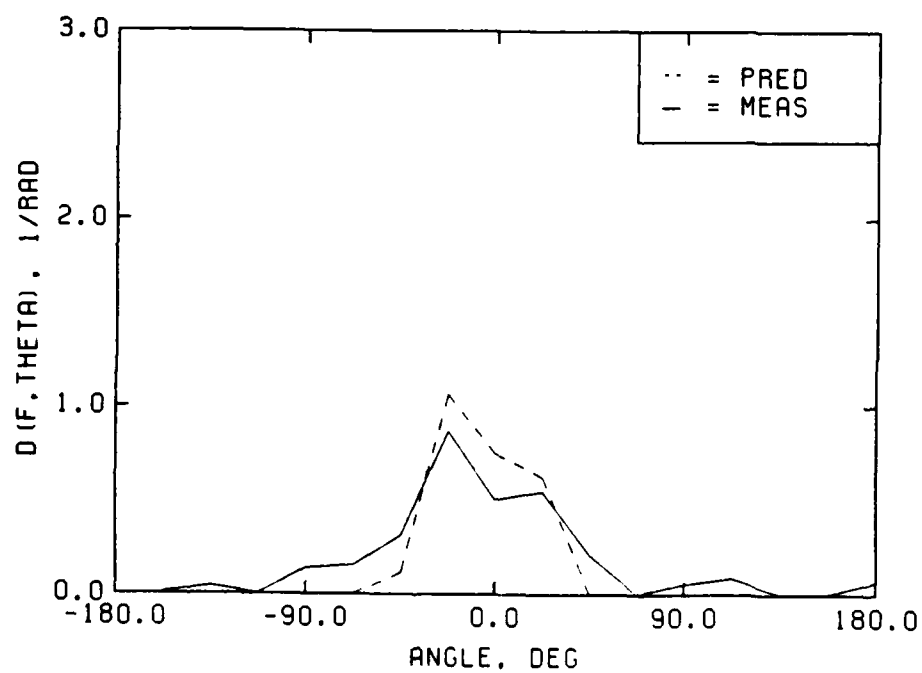MEASURED DIRECTIONAL SPREADING
CASE 83U1 -- FP=0.40, HMO=5.42, D=-14, H=1.11

MEASURED DIRECTIONAL SPREADING
CASE 69U2 -- FP=0.40, HMO=5.95, D=-15, H=1.29

D5
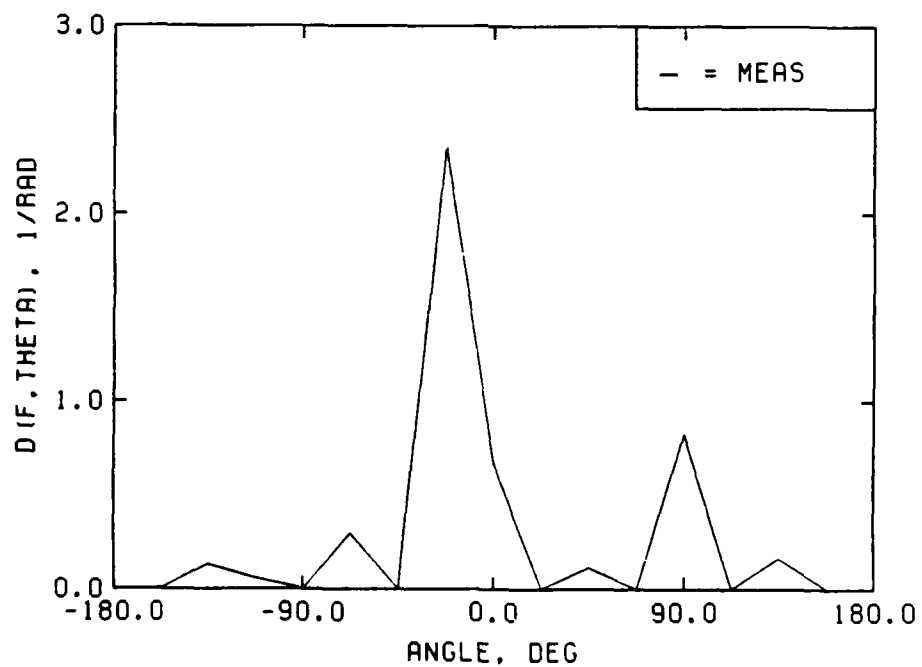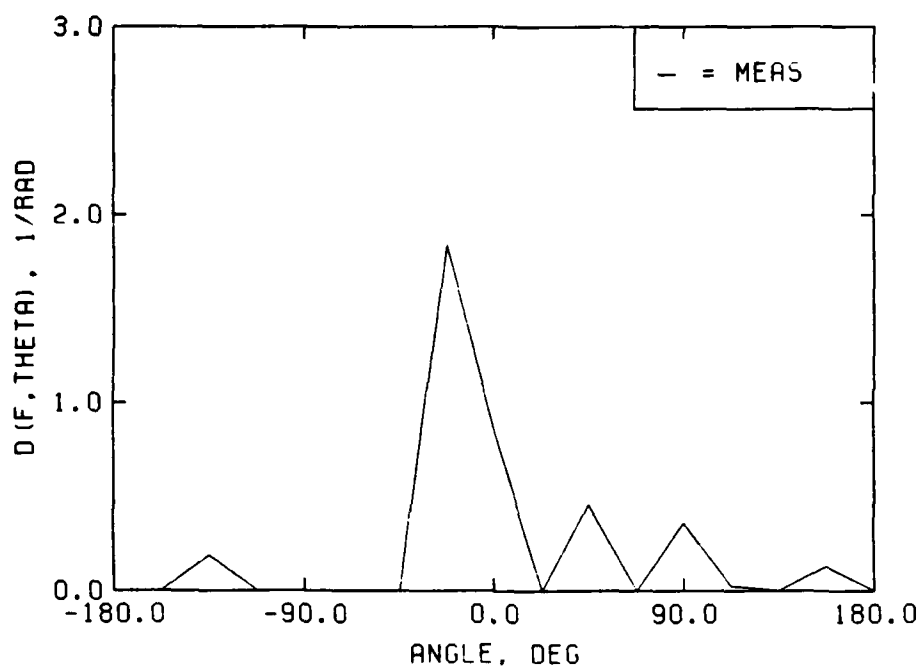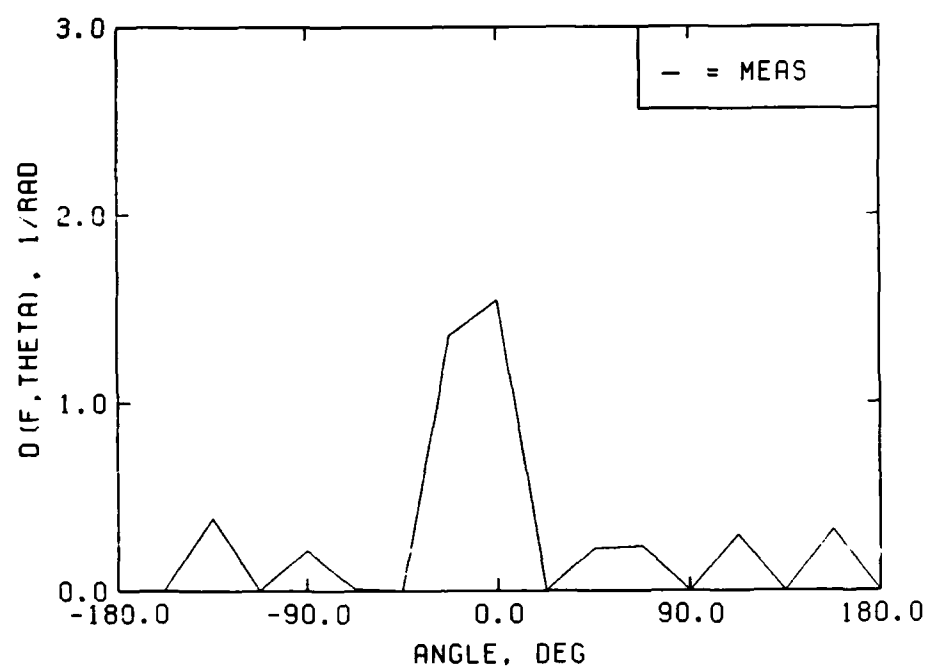
MEASURED DIRECTIONAL SPREADING
CASE 70U2 -- FP=0.47, HMO=5.07, D=-9, H=1.29
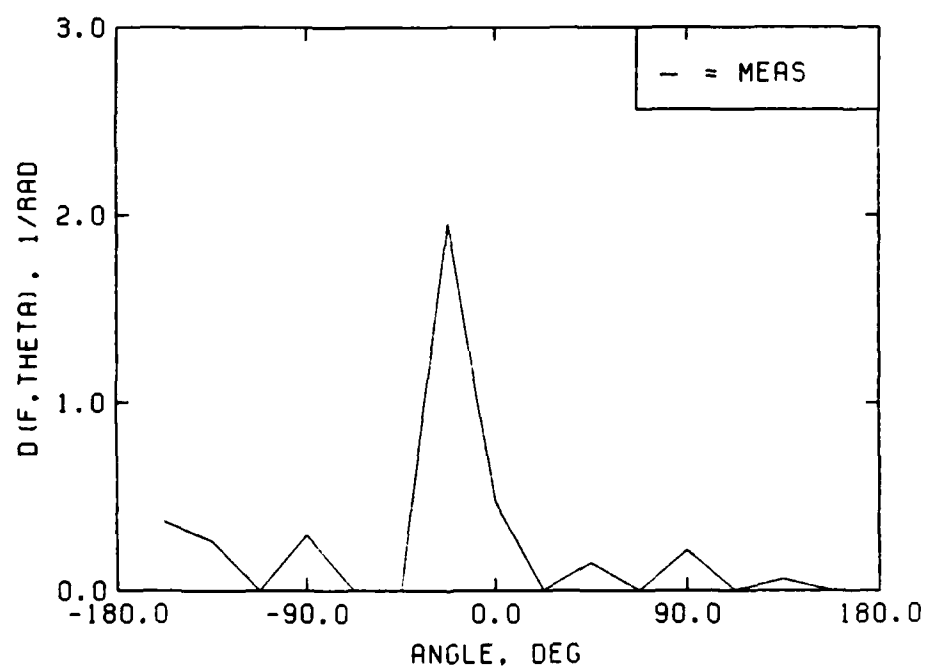
MEASURED DIRECTIONAL SPREADING
CASE 72U2 -- FP=0.47, HMO=4.11, D=-19, H=1.29

D6

MEASURED DIRECTIONAL SPREADING
CASE 73U2 -- FP=0.47, HMO=4.55, D=-15, H=1.29

MEASURED DIRECTIONAL SPREADING
CASE 83U2 -- FP=0.40, HMO=5.42, D=-14, H=1.29

D7
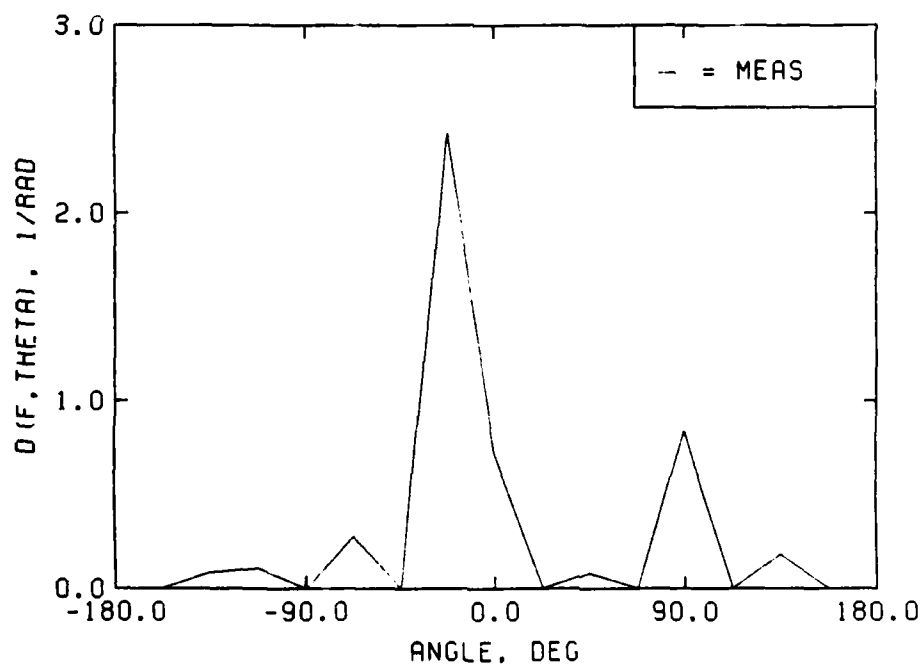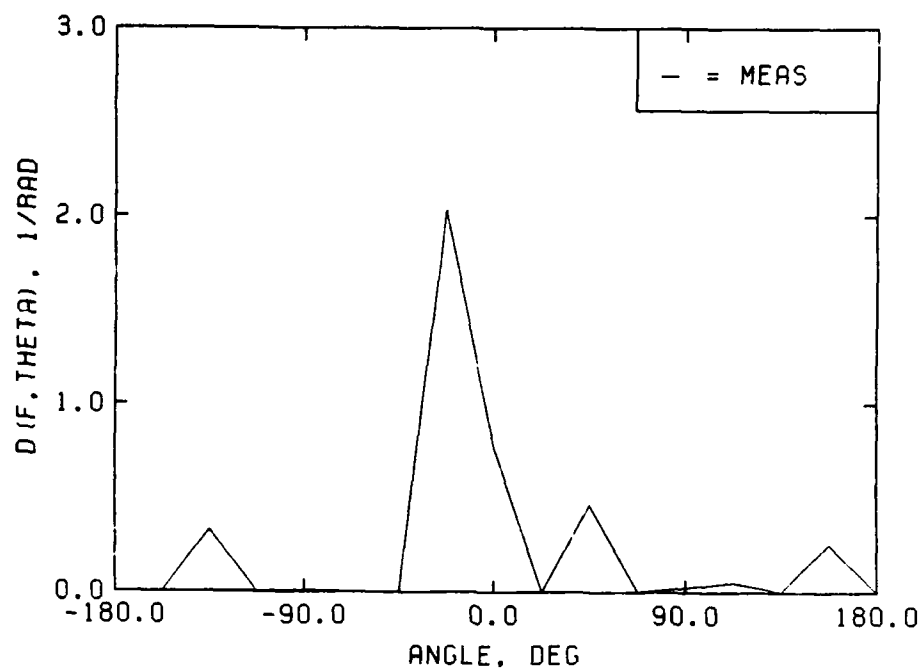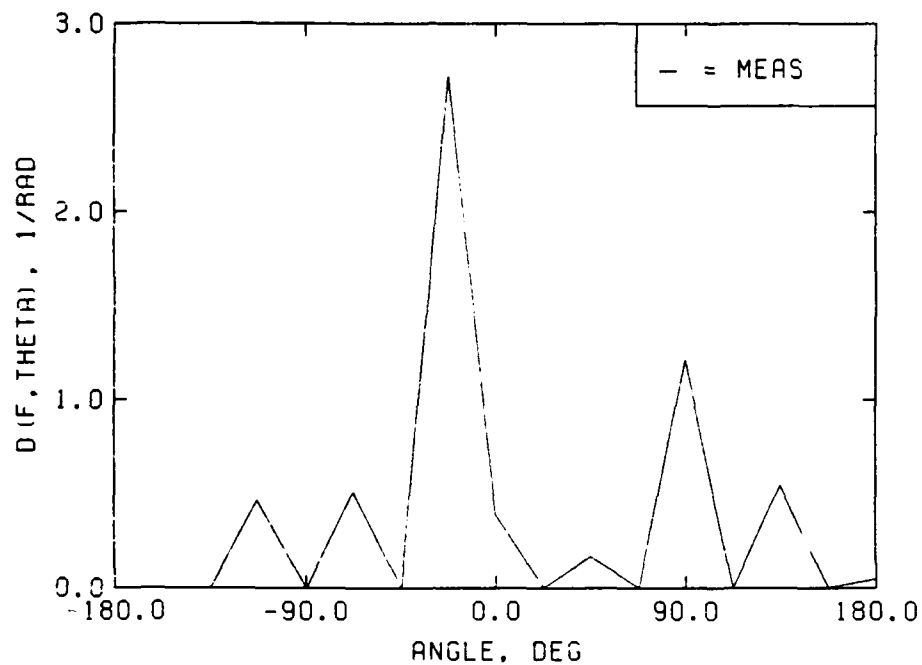
MEASURED DIRECTIONAL SPREADING
CASE 69U3 -- FP=0.40, HMO=5.95, D=-15, H=1.51
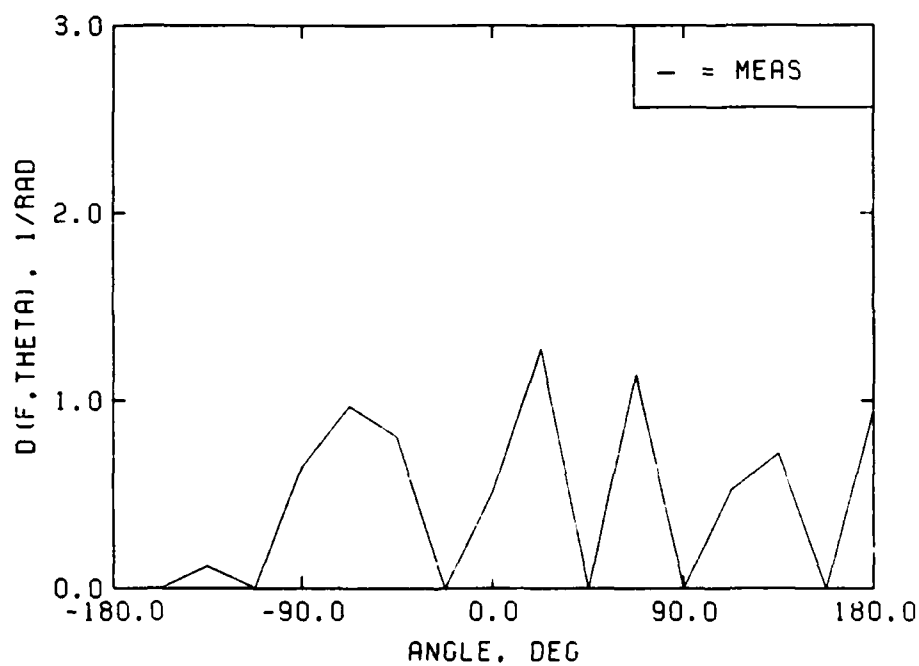
MEASURED DIRECTIONAL SPREADING
CASE 70U3 -- FP=0.47, HMO=5.07, D=-9, H=1.51
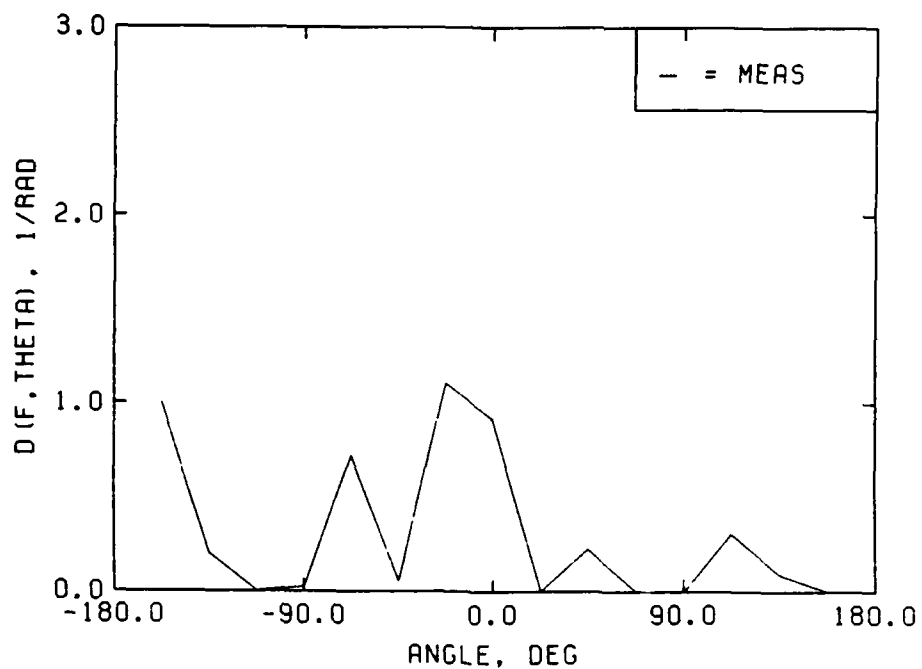
MEASURED DIRECTIONAL SPREADING
CASE 72U3 -- FP=0.47, HMO=4.11, D=-19, H=1.51
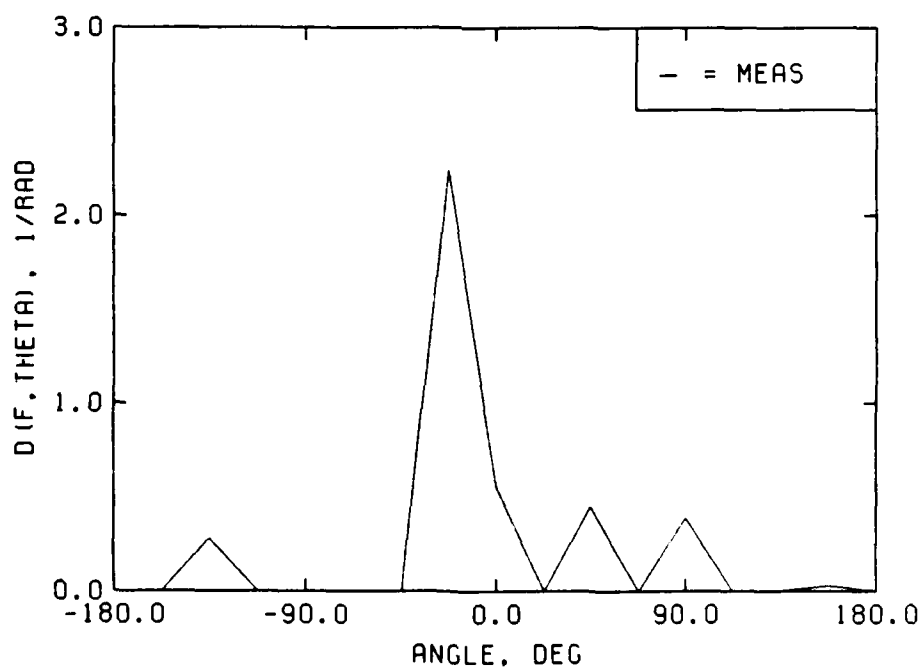
MEASURED DIRECTIONAL SPREADING
CASE 73U3 -- FP=0.47, HMO=4.55, D=-15, H=1.51

D9
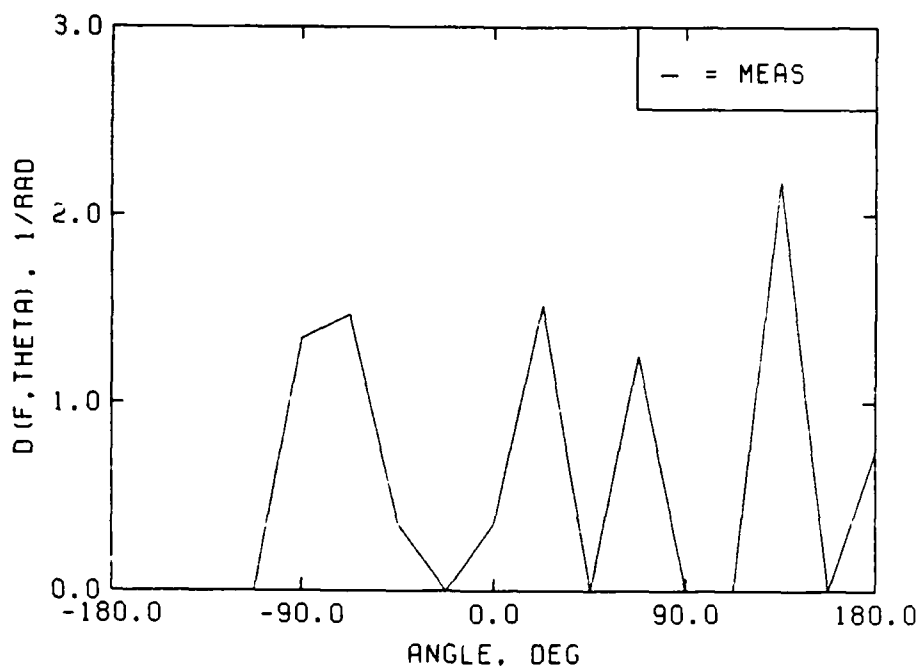
MEASURED VS PREDICTED DIRECTIONAL SPREADING
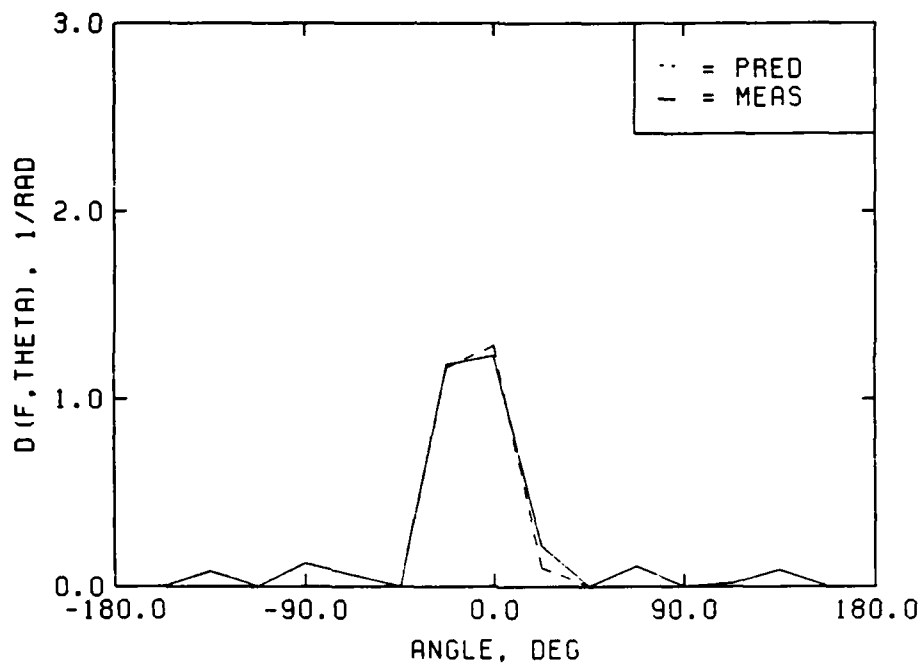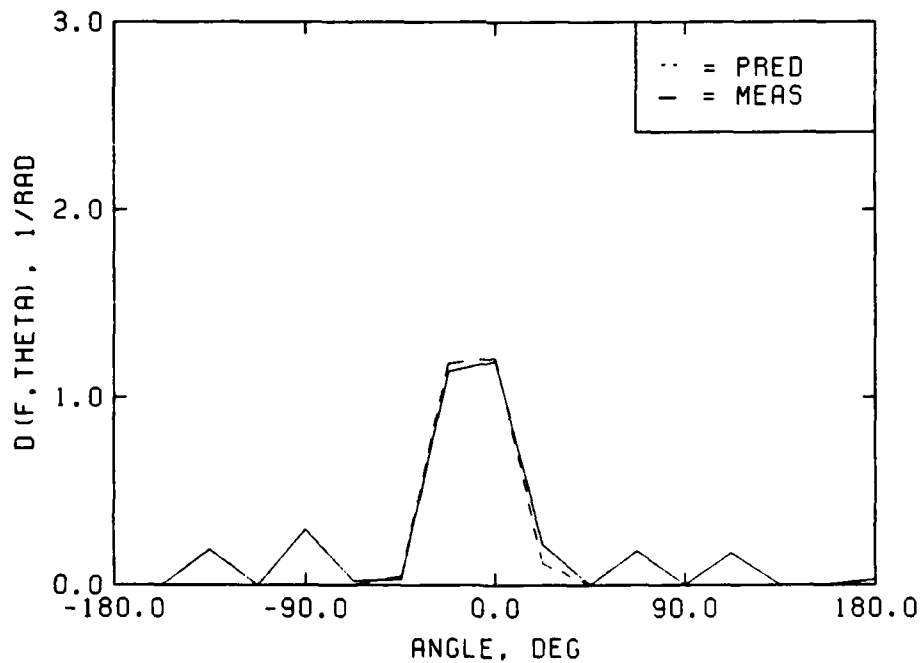CASE 83U3 -- FP=0.40, HMO=5.42, D=-14, H=1.51
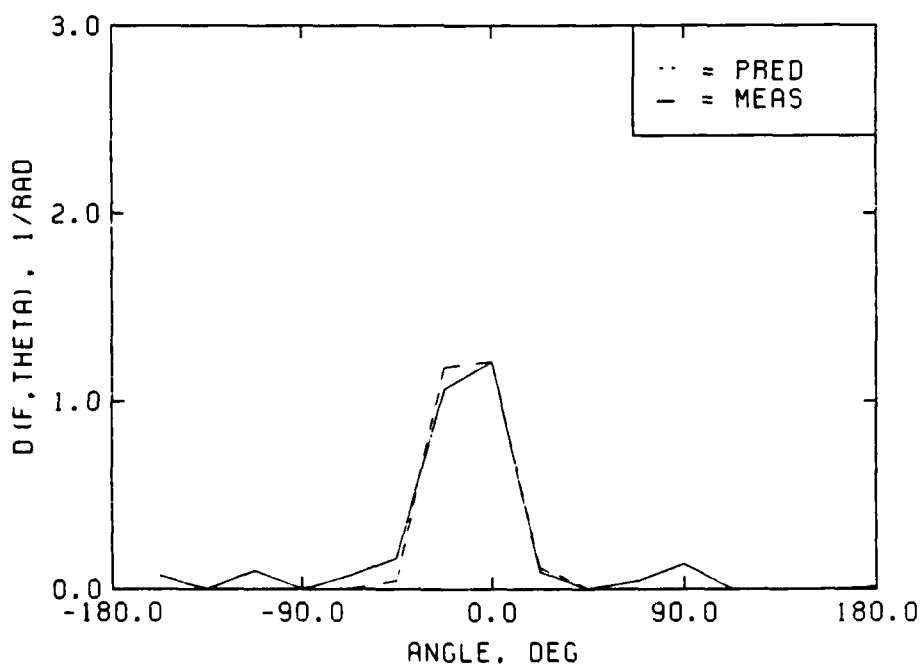
MEASURED VS PREDICTED DIRECTIONAL SPREADING
CASE 69D1 -- FP=0.40, HMO=6.12, D=-10, H=1.11

D10
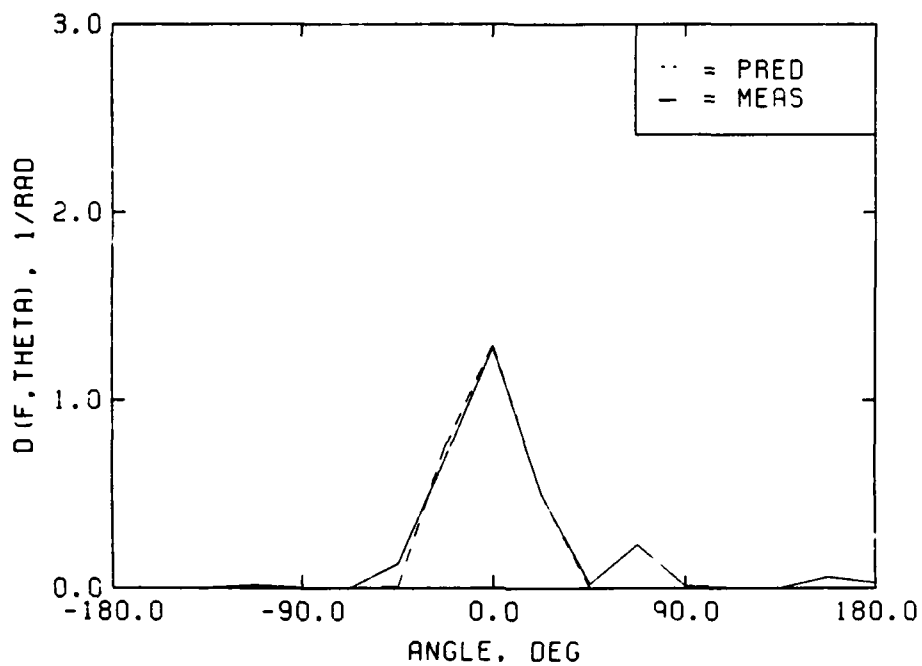
MEASURED VS PREDICTED DIRECTIONAL SPREADING
CASE 70D1 -- FP=0.47, HMO=5.07, D=-2, H=1.11
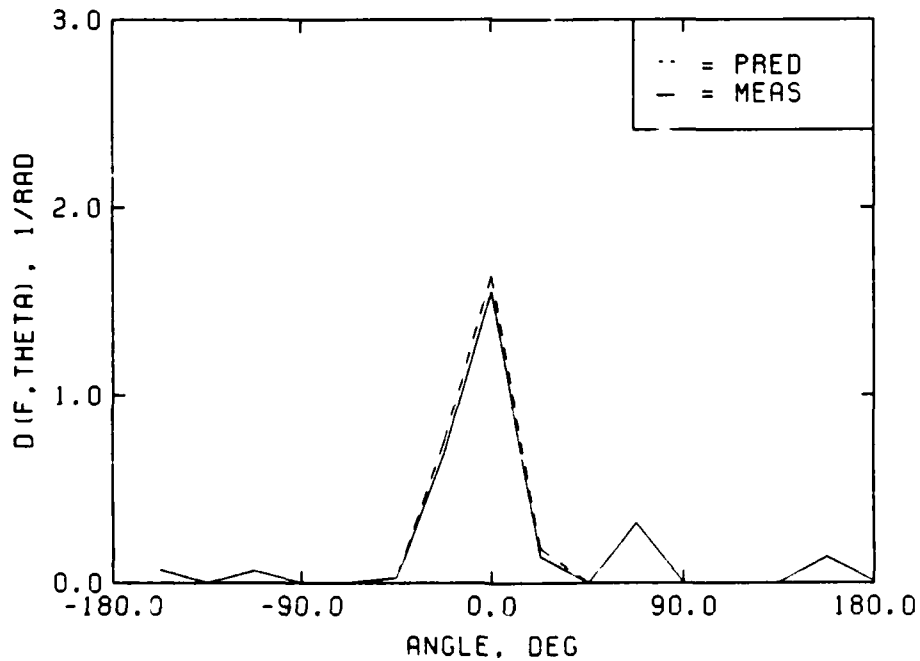
MEASURED VS PREDICTED DIRECTIONAL SPREADING
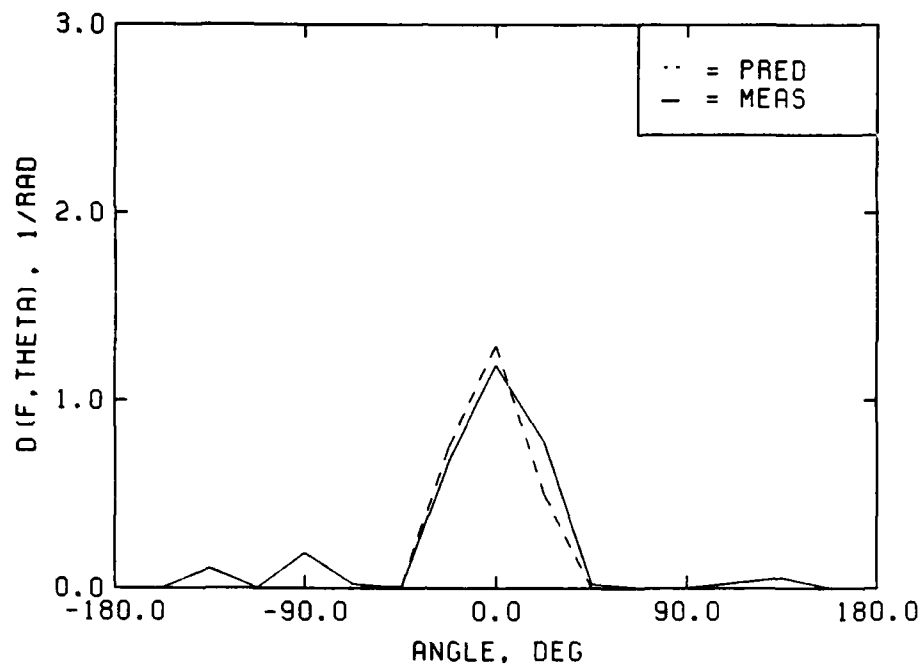CASE 72D1 -- FP=0.47, HMO=4.11, D=-11, H=1.11

D11
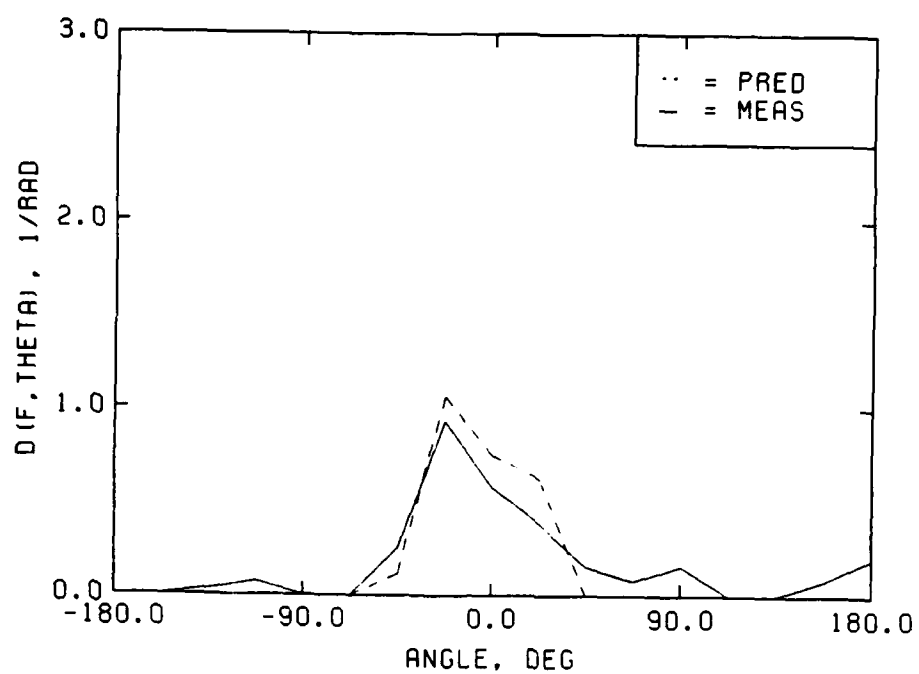
MEASURED VS PREDICTED DIRECTIONAL SPREADING
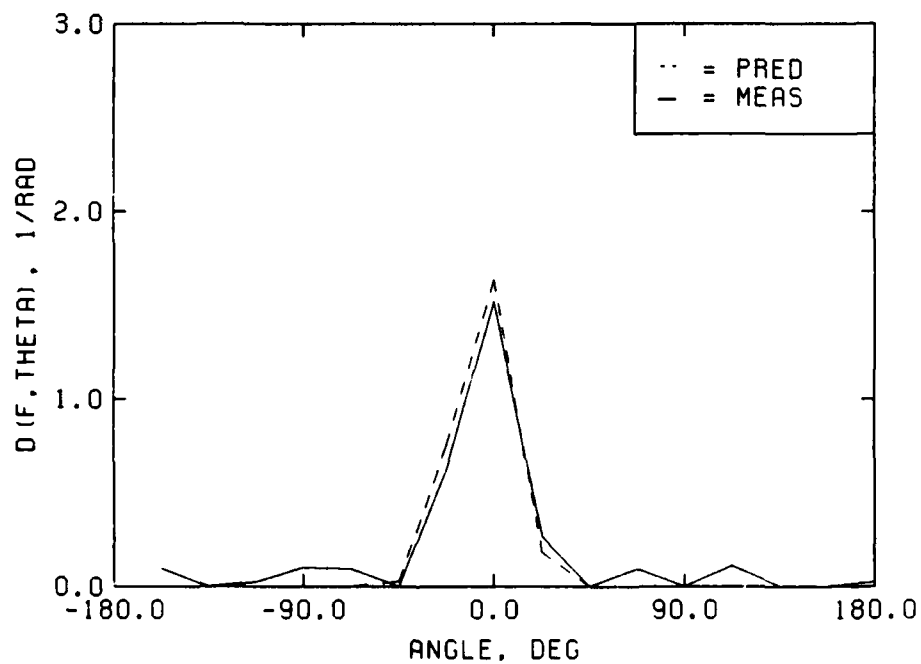CASE 73D1 -- FP=0.47, HMO=4.55, D=-4, H=1.11
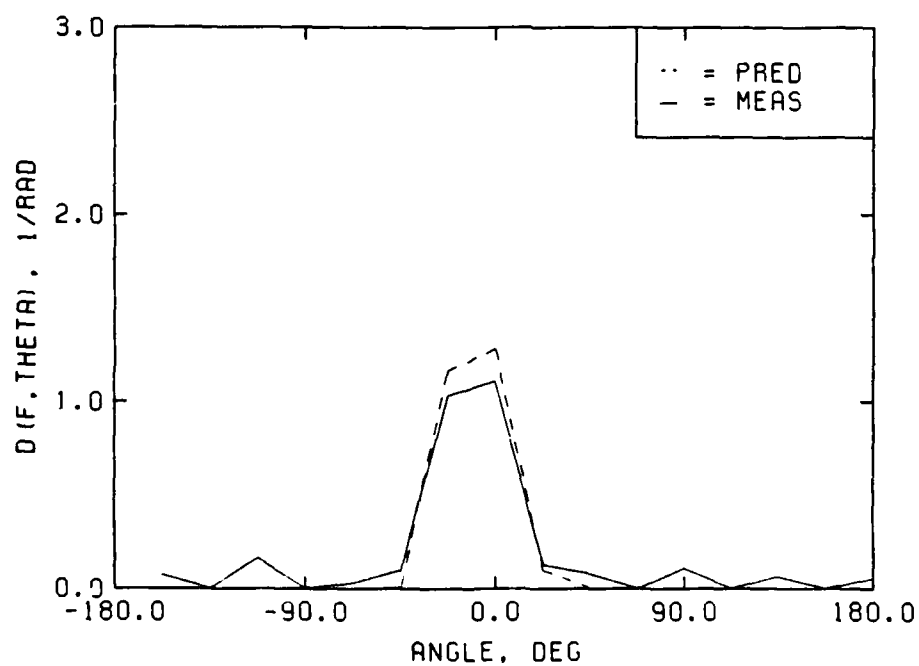
MEASURED VS PREDICTED DIRECTIONAL SPREADING
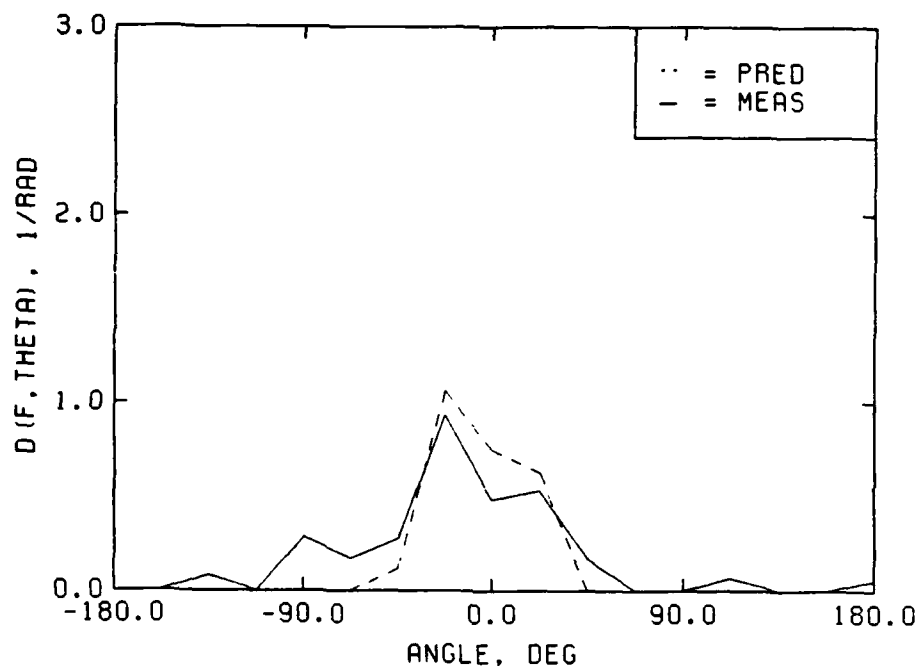CASE 83D1 -- FP=0.40, HMO=5.42, D=-9, H=1.11

D12

MEASURED VS PREDICTED DIRECTIONAL SPREADING
CASE 69D2 -- FP=0.40, HMO=6.12, D=-10, H=1.29

MEASURED VS PREDICTED DIRECTIONAL SPREADING
CASE 70D2 -- FP=0.47, HMO=5.07, D=-2, H=1.29
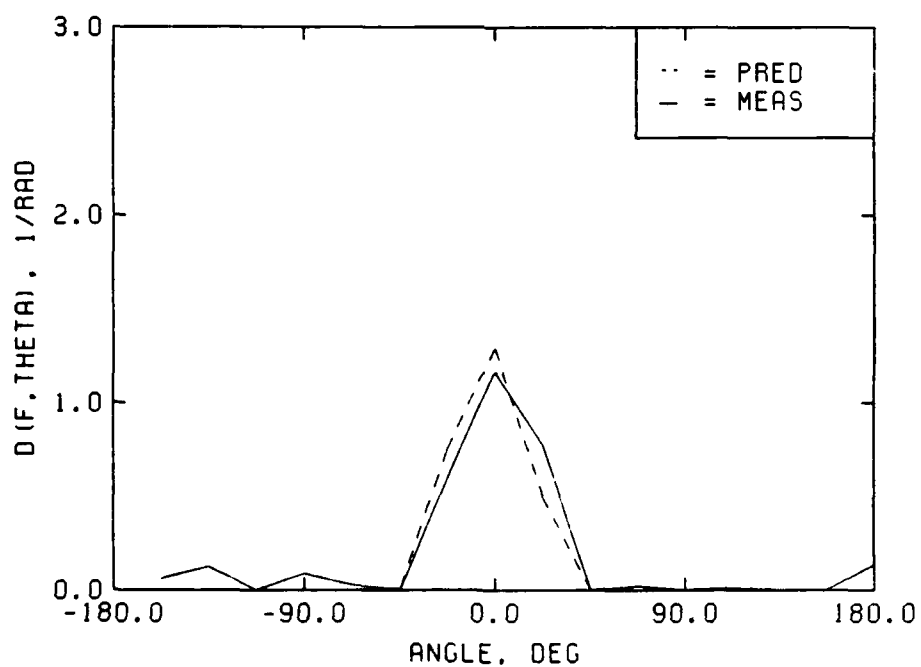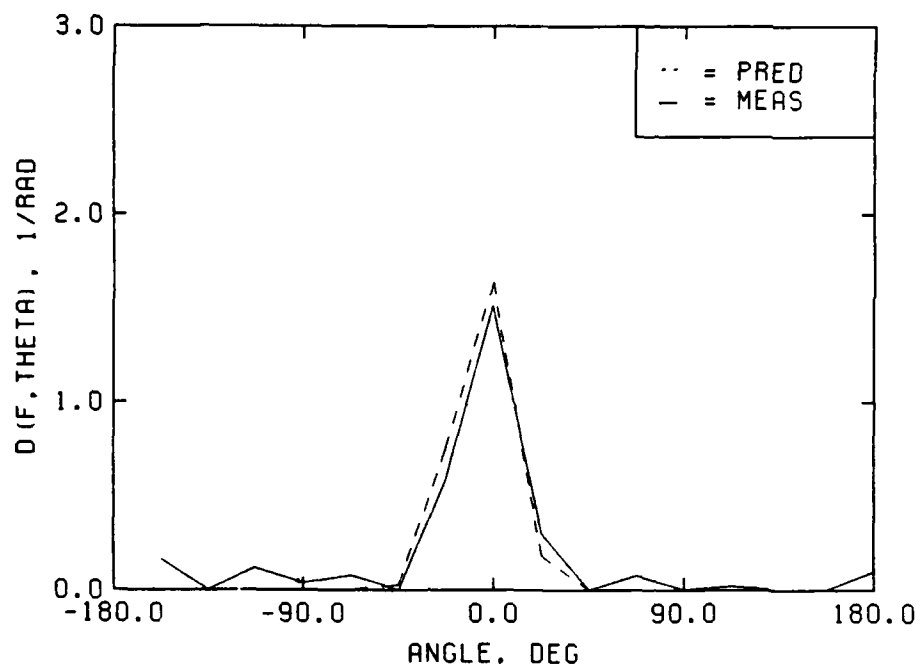
MEASURED VS PREDICTED DIRECTIONAL SPREADING
CASE 72D2 -- FP=0.47, HMO=4.11, D=-11, H=1.29

MEASURED VS PREDICTED DIRECTIONAL SPREADING
CASE 73D2 -- FP=0.47, HMO=4.55, D=-4, H=1.29

MEASURED VS PREDICTED DIRECTIONAL SPREADING
CASE 83D2 -- FP=0.40, HMO=5.42, D=-9, H=1.29

MEASURED VS PREDICTED DIRECTIONAL SPREADING
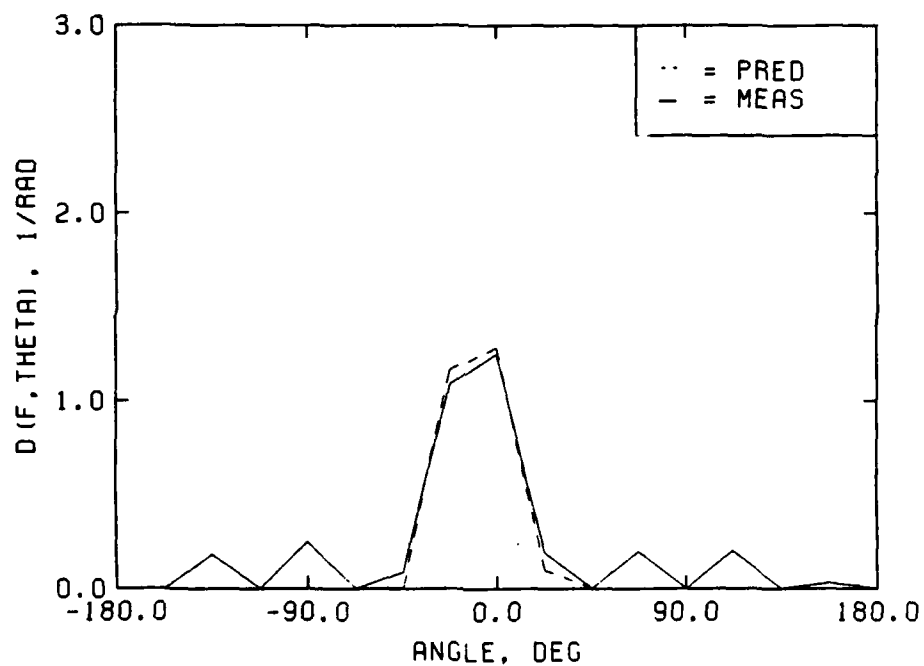CASE 69D3 -- FP=0.40, HMO=6.12, D=-10, H=1.51

D15

MEASURED VS PREDICTED DIRECTIONAL SPREADING
CASE 70D3 -- FP=0.47, HMO=5.07, D=-2, H=1.51

MEASURED VS PREDICTED DIRECTIONAL SPREADING
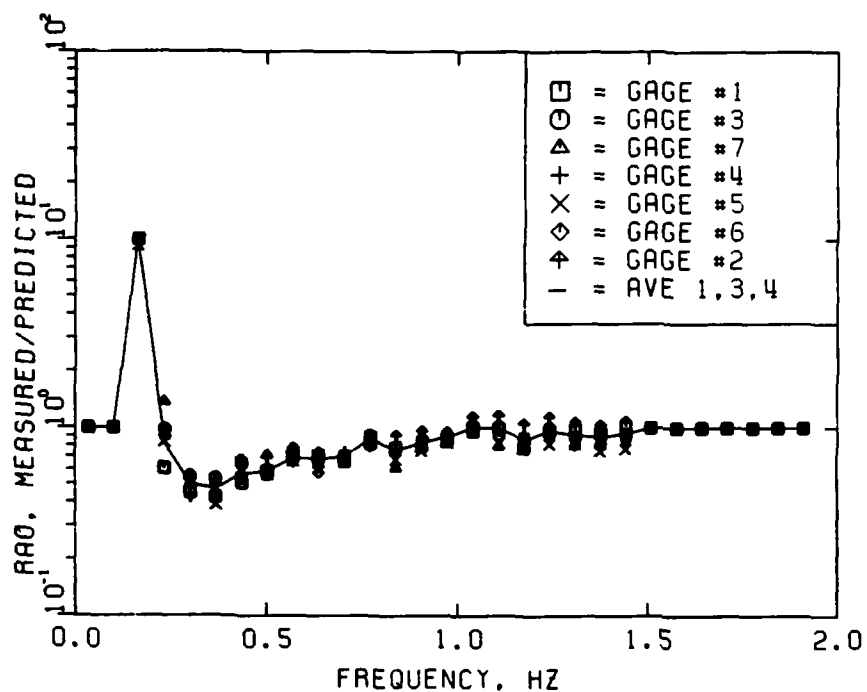CASE 72D3 -- FP=0.47, HMO=4.11, D=-11, H=1.51

D16

MEASURED VS PREDICTED DIRECTIONAL SPREADING
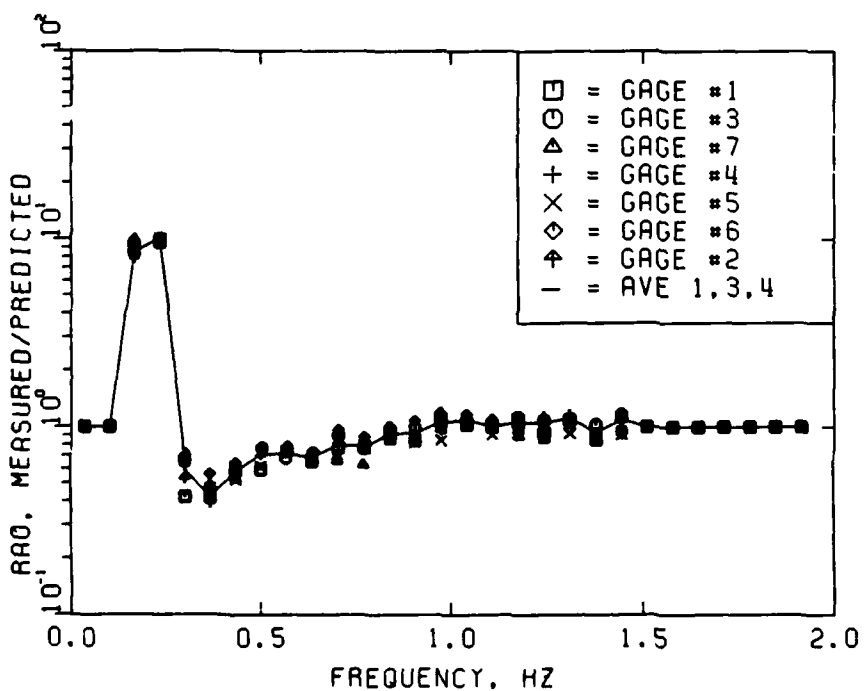CASE 73D3 -- FP=0.47, HMO=4.55, D=-4, H=1.51

MEASURED VS PREDICTED DIRECTIONAL SPREADING
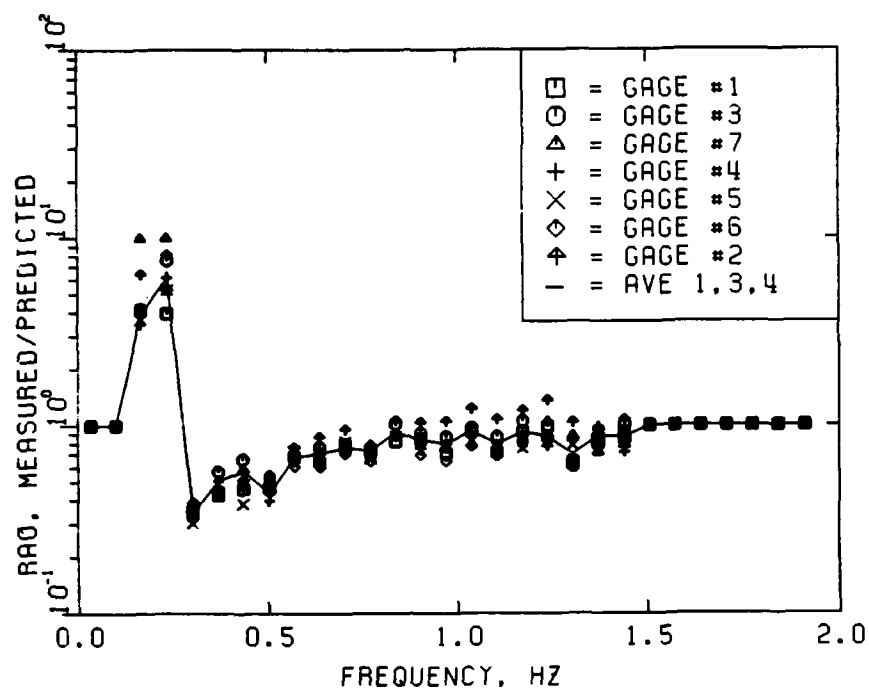CASE 83D3 -- FP=0.40, HMO=5.42, D=-9, H=1.51
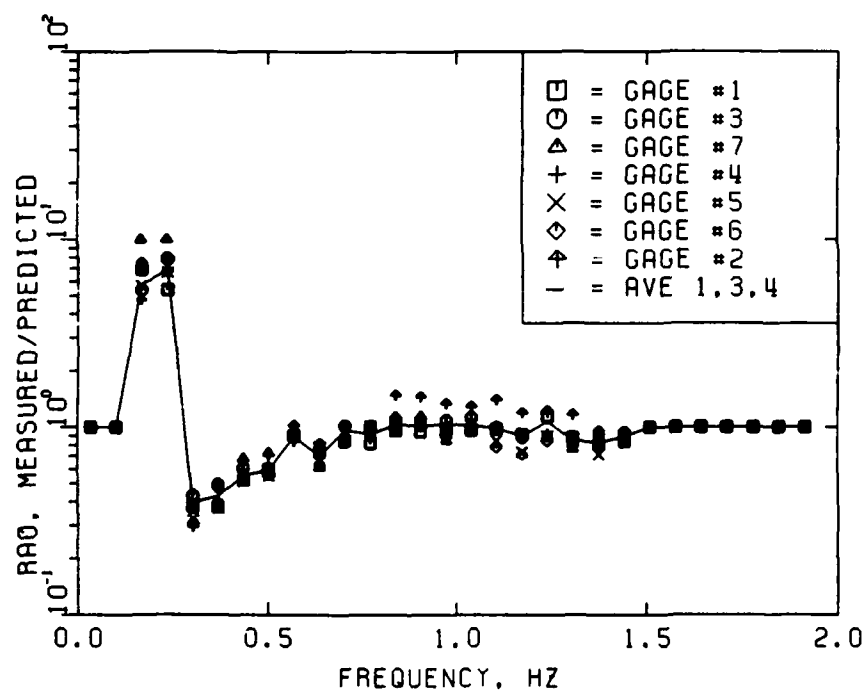
D17

APPENDIX E: RAO TRANSFER FUNCTIONS

RAO FROM MEASURED FREQUENCY SPECTRA
69U1 -- TP=2.49, HMO=5.99, D=-15, H=1.11

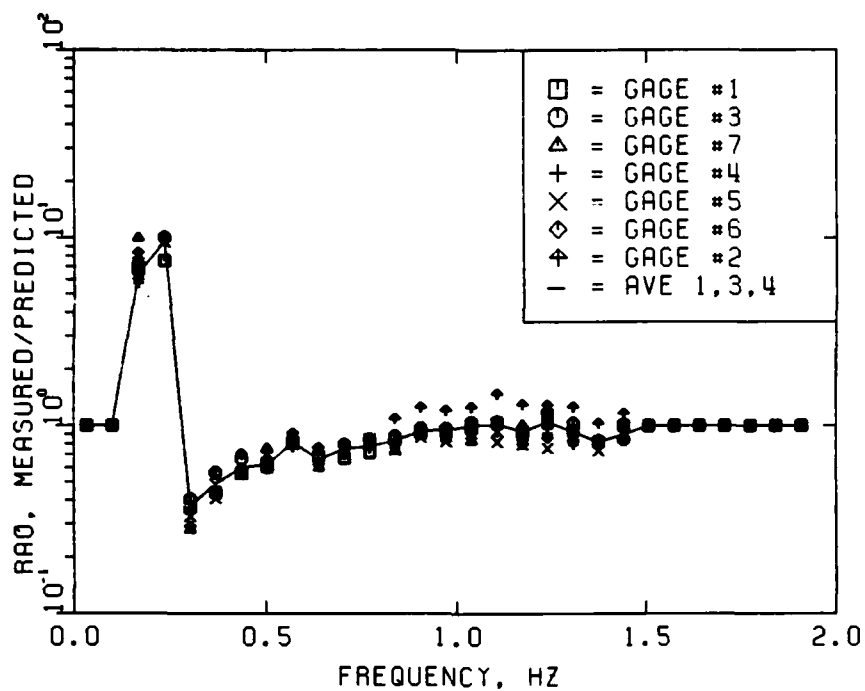RAO FROM MEASURED FREQUENCY SPECTRA
70U1 -- TP=2.13, HMO=5.07, D=-9, H=1.11

E3

RAO FROM MEASURED FREQUENCY SPECTRA
72U1 -- TP=1.86, HMO=3.85, D=-19, H=1.11

RAO FROM MEASURED FREQUENCY SPECTRA
73U1 -- TP=2.13, HMO=4.46, D=-15, H=1.11

E4

RAO FROM MEASURED FREQUENCY SPECTRA
83U1 -- TP=2.49, HMO=4.99, D=-14, H=1.11

RAO FROM MEASURED FREQUENCY SPECTRA
69D1 -- TP=2.49, HMO=6.12, D=-10, H=1.11

RAO FROM MEASURED FREQUENCY SPECTRA
70D1 -- TP=2.13, HMO=5.07, D=-2, H=1.11
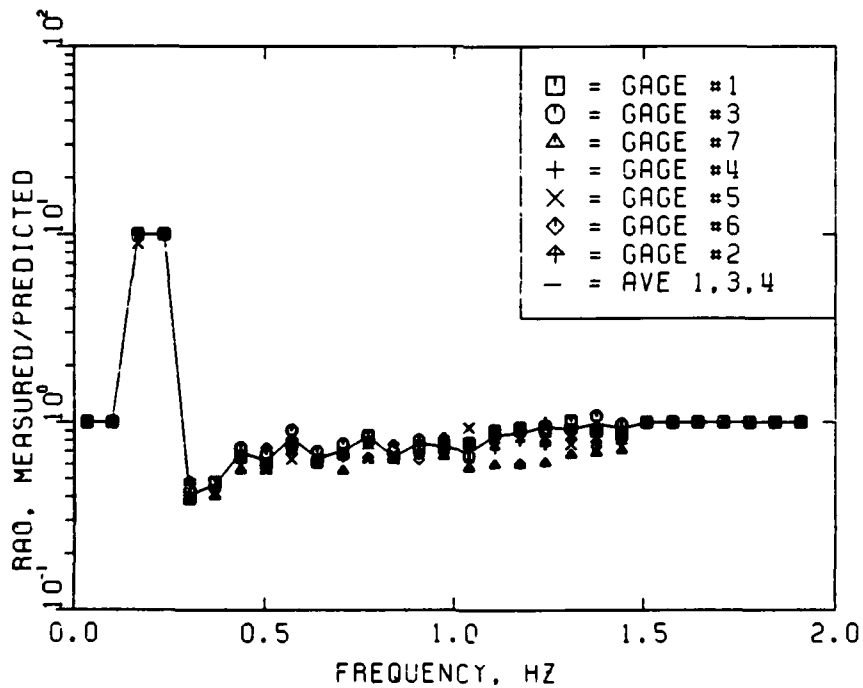

RAO FROM MEASURED FREQUENCY SPECTRA
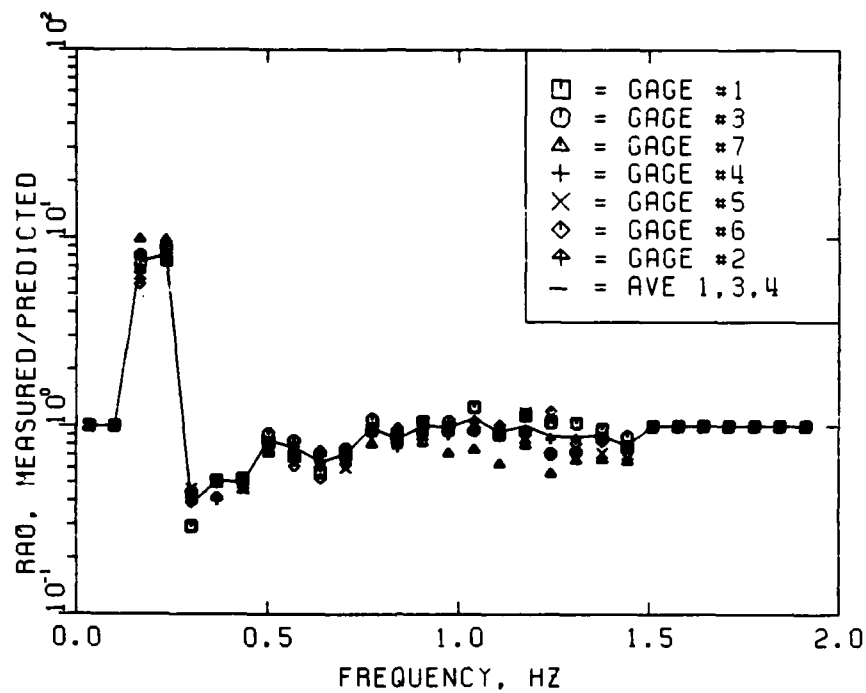72D1 -- TP=2.13, HMO=4.11, D=-11, H=1.11

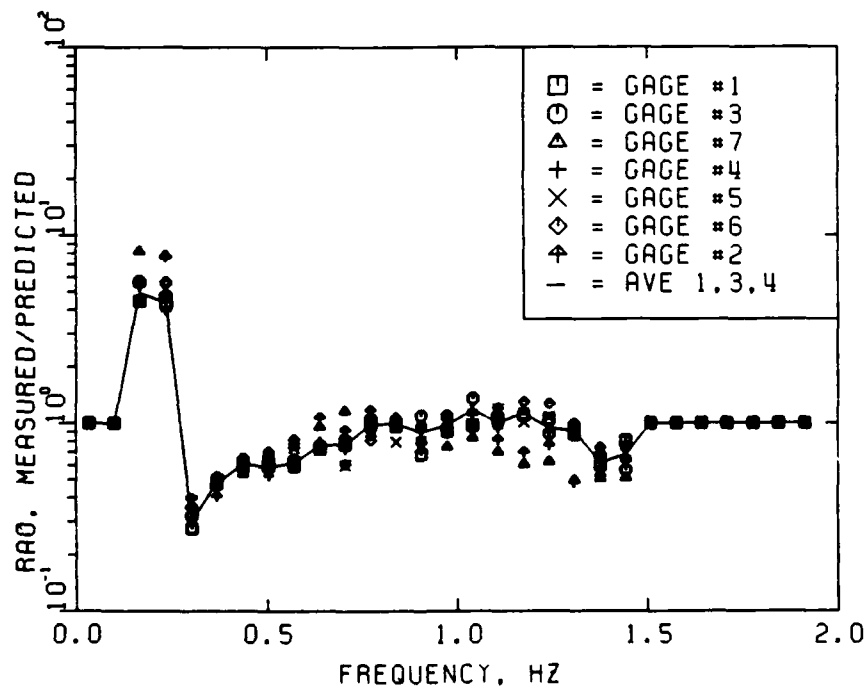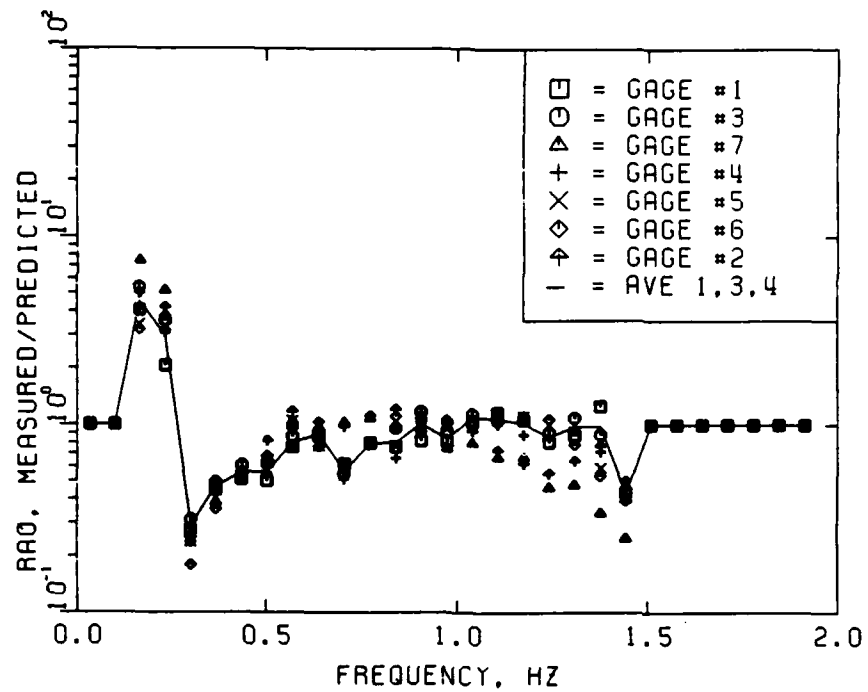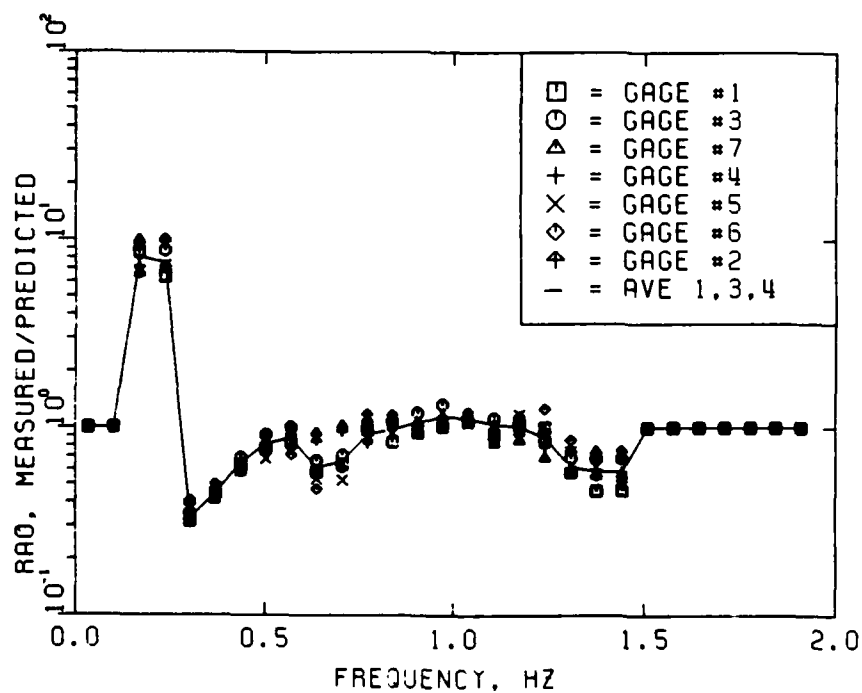RAO FROM MEASURED FREQUENCY SPECTRA
73D1 -- TP=2.13, HMO=4.55, D=-4, H=1.11

RAO FROM MEASURED FREQUENCY SPECTRA
83D1 -- TP=2.49, HMO=5.42, D=-9, S=10, V

E7

APPENDIX F: MEASURED PEAK PERIODS AND H_{mo} HEIGHTS

Measured Tp Peak Periods
Calibration Phase, Series 1 (H=1.11 Ft.)

Storm Year	Target Period	1	2	3	4	5	6	7	Channel Average 1,3,4	Channel Average 1-7
				Channel Number						
Unidirectional Cases										
1969	2.49	2.49	1.94	2.52	2.52	1.50	2.40	2.45	2.51	2.26
1970	2.13	2.30	2.20	2.20	2.20	1.76	2.20	2.26	2.23	2.16
1972	1.86	1.86	1.69	1.69	1.69	1.86	1.86	1.69	1.75	1.76
1973	2.13	2.26	2.26	2.32	2.32	2.32	2.32	2.24	2.30	2.29
1974	2.49	2.45	2.61	2.51	2.56	2.56	2.56	2.51	2.51	2.54
1983	2.49	2.47	2.33	2.56	2.56	2.33	2.33	2.22	2.53	2.40
Directional Cases										
1969	2.49	2.49	1.87	2.49	2.46	2.50	2.50	2.49	2.48	2.40
1970	2.13	2.01	1.90	2.01	1.67	1.26	1.90	2.12	1.90	1.84
1972	2.13	2.17	1.74	2.44	2.44	1.90	1.90	1.66	2.35	2.04
1973	2.13	2.51	2.03	2.48	2.48	2.13	2.11	2.53	2.49	2.32
1974	2.49	2.16	2.46	2.56	2.16	2.49	2.44	2.56	2.29	2.40
1983	2.49	2.47	2.46	2.46	2.46	2.49	2.49	2.54	2.46	2.48

* Note: All measurements in seconds.

F3

Measured Tp Peak Periods
Calibration Phase, Series 2 (H=1.29 Ft.)

Storm Year	Target Period	Channel Number							Channel Average 1,3,4	Channel Average 1-7
		1	2	3	4	5	6	7		

Unidirectional Cases

1969	2.49	2.52	2.40	2.43	2.43	2.46	2.43	2.54	2.46	2.46
1970	2.13	2.25	2.20	2.20	2.20	2.20	2.20	2.25	2.22	2.21
1972	1.86	2.22	2.22	2.22	2.22	1.69	1.69	1.69	2.22	1.99
1973	2.13	2.26	2.26	2.26	2.32	2.26	2.26	2.26	2.28	2.27
1974	2.49	2.52	2.56	2.47	2.47	2.52	2.52	3.36	2.49	2.63
1983	2.49	2.56	2.56	2.47	2.51	2.51	2.51	2.51	2.51	2.52

Directional Cases

1969	2.49	2.49	2.54	2.49	2.49	2.50	2.50	2.52	2.49	2.50
1970	2.13	2.01	2.22	2.01	2.00	2.10	1.90	2.14	2.01	2.05
1972	2.13	2.54	2.54	2.51	2.51	2.59	2.59	2.54	2.52	2.55
1973	2.13	2.53	2.57	2.51	2.51	2.57	2.56	2.53	2.52	2.54
1974	2.49	2.56	2.50	2.56	2.56	2.16	2.16	2.56	2.56	2.44
1983	2.49	2.47	2.56	2.47	2.47	2.49	2.50	2.55	2.47	2.50

* Note: All measurements in seconds.

F4

Measured Tp Peak Periods
Calibration Phase, Series 3 (H=1.51 Ft.)

Storm Year	Target Period	Channel Number 1	2	3	4	5	6	7	Channel Average 1,3,4	Channel Average 1-7
Unidirectional Cases										
1969	2.49	2.52	2.40	2.45	2.43	2.52	2.52	2.41	2.47	2.46
1970	2.13	2.20	2.20	2.20	2.20	2.20	2.20	----	2.20	2.20
1972	1.86	2.22	2.22	1.69	2.22	1.69	1.69	----	2.04	1.96
1973	2.13	2.26	2.32	2.26	2.26	2.32	2.22	2.26	2.26	2.27
1974	2.49	2.56	3.25	2.51	2.51	2.54	2.51	3.11	2.53	2.71
1983	2.49	2.56	2.56	2.51	2.51	2.56	2.51	----	2.53	2.54
Directional Cases										
1969	2.49	2.49	2.60	2.49	2.49	2.50	2.50	2.49	2.49	2.51
1970	2.13	2.01	2.22	2.14	2.14	1.95	1.91	2.07	2.10	2.06
1972	2.13	2.54	2.20	2.51	2.54	2.59	2.59	2.46	2.53	2.49
1973	2.13	2.51	2.57	2.51	2.51	2.50	2.56	2.53	2.51	2.53
1974	2.49	2.56	2.50	2.56	2.57	2.16	2.16	2.32	2.56	2.40
1983	2.49	2.47	2.56	2.47	2.47	2.51	2.52	2.55	2.47	2.51

* Note: All measurements in seconds.

Measured Tp Peak Periods
WIS Calibration Phase

Gage Number

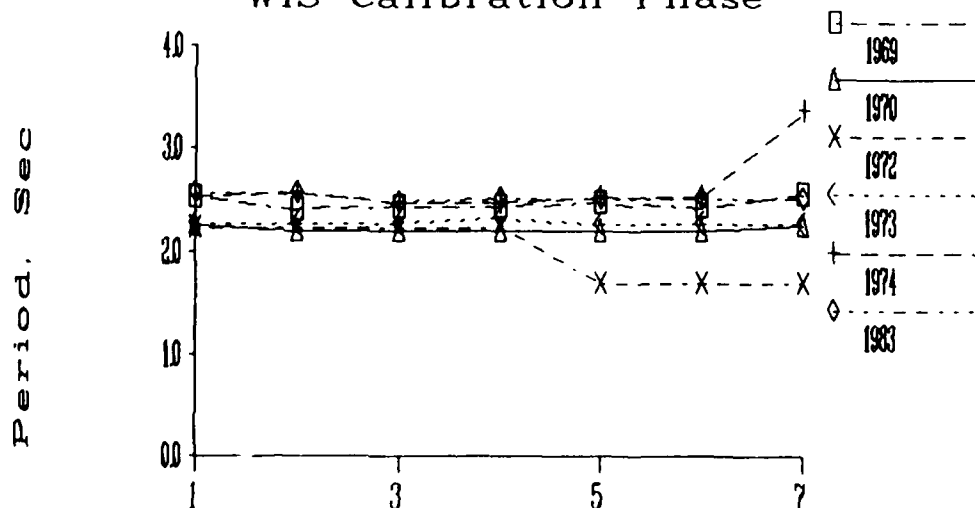Series U1, H=1.11 Ft

Measured Tp Peak Periods
WIS Calibration Phase

Gage Number

Series U2, H=1.29 Ft

Measured Tp Peak Periods

WIS Calibration Phase

Period. Sec

Gage Number

Series U3, H=1.51 Ft

Legend: 1969, 1970, 1972, 1973, 1974, 1983

Measured Tp Peak Periods

WIS Calibration Phase

Period. Sec

Gage Number

Series D1, H=1.11 Ft

Legend: 1969, 1970, 1972, 1973, 1974, 1983

Measured Tp Peak Periods
WIS Calibration Phase

Series D2, H=1.29 Ft

Measured Tp Peak Periods
WIS Calibration Phase

Series D3, H=1.51 Ft
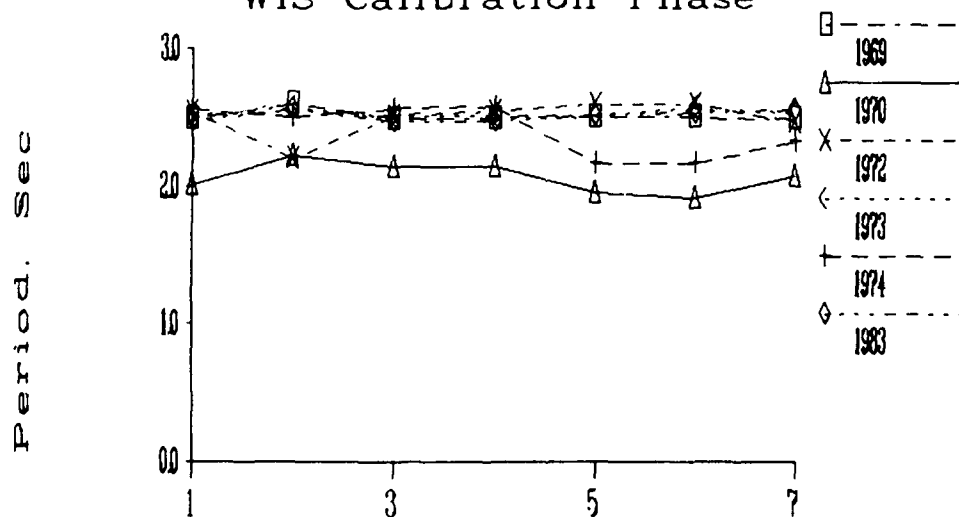
Measured Hmo Wave Heights
Calibration Phase, Series 1 (H=1.11 Ft.)

Storm Year	Target Height	1	2	3	4	5	6	7	Channel Average 1,3,4	Channel Average 1-7
				Channel Number						
Unidirectional Cases										
1969	5.95	3.91	4.37	4.17	3.96	3.78	3.98	4.01	4.01	4.03
1970	5.07	3.71	4.13	3.99	3.80	3.62	3.87	3.62	3.83	3.82
1972	3.85	2.31	2.82	2.56	2.34	2.30	2.20	2.44	2.40	2.42
1973	4.46	2.68	3.17	2.94	2.71	2.63	2.90	2.95	2.78	2.85
1974	5.16	2.99	3.52	3.45	3.06	2.99	2.93	3.20	3.17	3.16
1983	4.99	3.09	3.59	3.41	3.11	2.96	3.32	3.29	3.20	3.25
Directional Cases										
1969	6.12	4.03	3.89	4.31	3.97	3.83	3.89	3.44	4.10	3.91
1970	5.07	3.81	3.63	3.93	3.63	3.64	3.65	3.35	3.79	3.66
1972	4.11	2.64	2.92	2.84	2.61	2.73	2.76	2.71	2.70	2.74
1973	4.55	2.59	3.08	2.92	2.63	2.85	2.78	2.61	2.71	2.78
1974	5.42	3.61	3.66	3.91	3.69	3.61	3.51	3.39	3.74	3.63
1983	5.42	3.38	3.75	3.80	3.37	3.41	3.55	3.58	3.52	3.55

* Note: All measurements in inches.

Measured Hmo Wave Heights
Calibration Phase, Series 2 (H=1.29 Ft.)

Storm Year	Target Height	Channel Number							Channel Average 1,3,4	Channel Average 1-7
		1	2	3	4	5	6	7		
Unidirectional Cases										
1969	5.95	5.70	5.89	5.97	5.71	5.67	5.58	5.31	5.79	5.69
1970	5.07	4.96	5.20	5.05	4.92	5.16	4.99	5.06	4.98	5.05
1972	3.85	3.80	4.31	3.94	3.83	3.85	3.77	4.10	3.86	3.94
1973	4.46	4.74	5.01	5.11	4.87	4.77	4.69	4.74	4.91	4.85
1974	5.16	5.06	5.80	5.22	5.03	5.07	5.02	5.15	5.10	5.19
1983	4.99	5.25	5.41	5.58	5.37	5.27	5.12	4.92	5.40	5.27
Directional Cases										
1969	6.12	5.46	5.86	5.33	5.32	5.17	4.95	4.86	5.37	5.28
1970	5.07	4.86	5.30	5.02	5.10	4.83	4.67	4.78	4.99	4.94
1972	4.11	4.15	4.95	4.64	4.52	4.44	4.30	4.52	4.44	4.50
1973	4.55	5.21	6.15	5.58	5.25	5.31	5.38	4.94	5.35	5.40
1974	5.42	5.59	5.89	5.47	5.39	5.52	5.54	5.25	5.48	5.52
1983	5.42	5.89	6.42	6.14	6.16	5.89	5.85	5.50	6.06	5.98

* Note: All measurements in inches.

Measured Hmo Wave Heights
Calibration Phase, Series 3 (H=1.51 Ft.)

Storm Year	Target Height	Channel Number							Channel Average 1,3,4	Channel Average 1-7
		1	2	3	4	5	6	7		
Unidirectional Cases										
1969	5.95	6.34	6.65	6.66	6.16	6.50	6.43	5.95	6.39	6.38
1970	5.07	5.65	6.15	5.80	5.53	5.95	5.89	----	5.66	5.83
1972	3.85	4.23	5.02	4.57	4.22	4.28	4.36	----	4.34	4.45
1973	4.46	5.37	5.86	5.82	5.41	5.42	5.60	5.47	5.53	5.56
1974	5.16	5.46	6.81	5.80	5.49	5.51	5.84	6.08	5.58	5.86
1983	4.99	5.93	6.30	6.41	5.86	6.19	6.03	----	6.07	6.12
Directional Cases										
1969	6.12	6.06	6.57	5.86	5.80	5.72	5.69	5.54	5.91	5.89
1970	5.07	5.52	6.09	5.68	5.63	5.42	5.20	5.51	5.61	5.58
1972	4.11	4.87	5.60	5.39	5.22	5.13	5.04	5.07	5.16	5.19
1973	4.55	6.04	7.14	6.14	5.80	6.04	6.39	5.74	5.99	6.18
1974	5.42	6.23	6.75	6.24	5.94	6.14	6.20	6.20	6.14	6.24
1983	5.42	6.63	7.30	6.88	6.74	6.76	6.81	6.46	6.75	6.80

* Note: All measurements in inches.

Measured Hmo Heights
WIS Calibration Phase
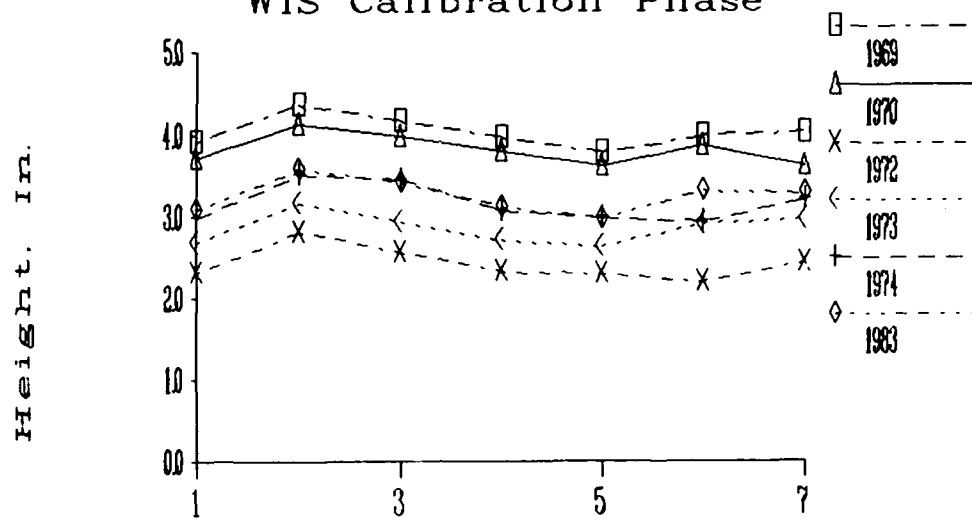
Gage Number
Series U1, H=1.11 Ft

Measured Hmo Heights
WIS Calibration Phase

Gage Number
Series U2, H=1.29 Ft

Measured Hmo Heights
WIS Calibration Phase

Gage Number

Series U3, H=1.51 Ft

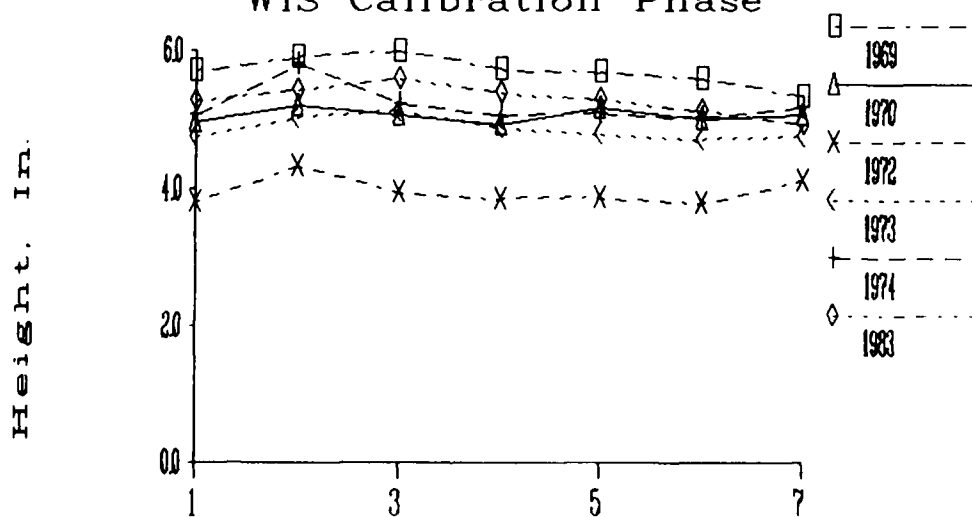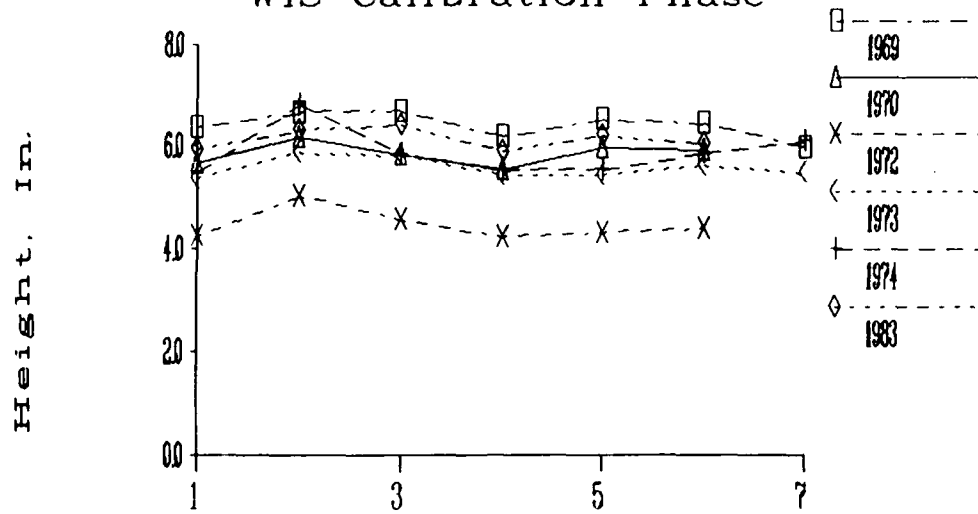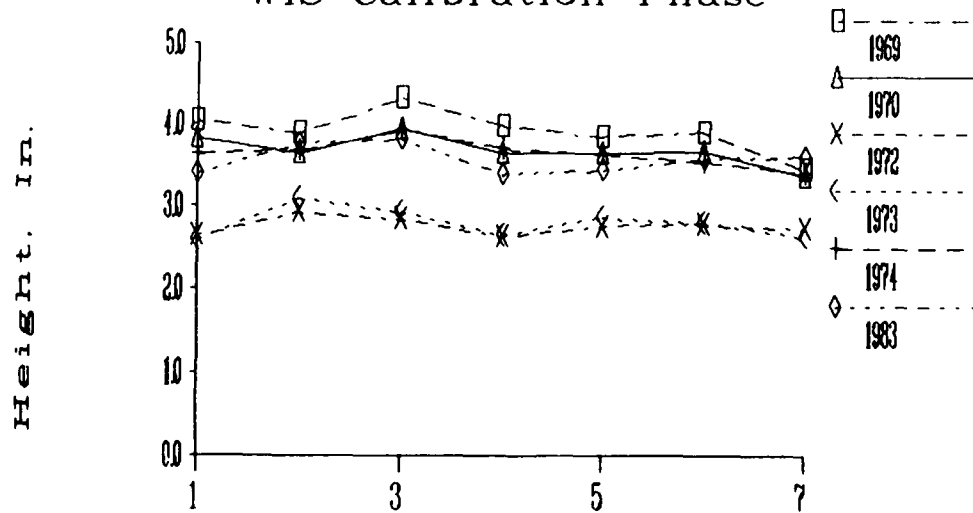# Measured Hmo Heights
WIS Calibration Phase
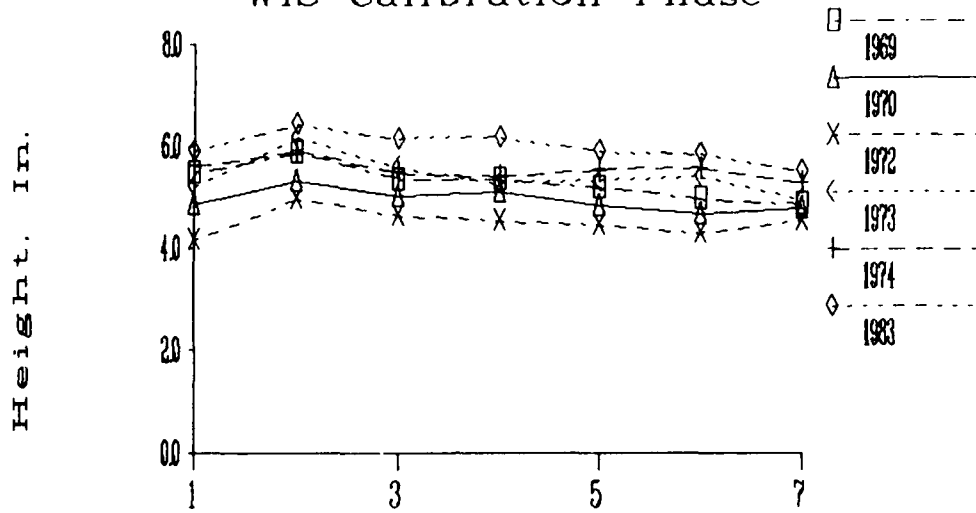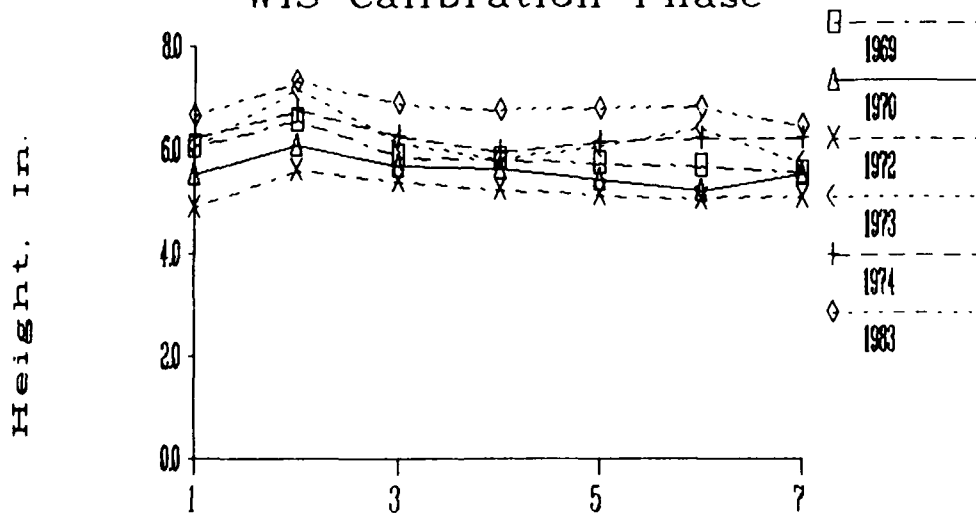

Gage Number

Series D1, H=1.11 Ft

F13

Measured Hmo Heights

WIS Calibration Phase

Gage Number

Series D2, H=1.29 Ft

Measured Hmo Heights

WIS Calibration Phase

Gage Number

Series D3, H=1.51 Ft

APPENDIX G: NOTATION

a_j	Real fourier coefficient of spreading function
$A(f)$	Deterministic spectral amplitude
b	Resolution bandwidth
b_j	Imaginary fourier coefficient of spreading function
B_{ij}	Dummy variable for directional spectra
$C_{ij}(f)$	Co-spectral density estimate
$D(f,\theta)$	Directional spreading function
{DIR}	Vector of directional fourier coefficients, frequency f
f	Frequency
f_M	Lower cutoff frequency
f_p	Spectral peak frequency
f_u	Upper cutoff frequency
$H_3(f,\theta)$	Three-dimensional wave height transfer function
g	Gravitational constant
h	Water depth
H	Wave height
H_b	Maximum prebreaking wave height at wave maker
H_c	Cutoff or threshold wave height
H_m	Mean wave height
H_{mo}	Zero-moment wave height
i	Imaginary unit number
j	Summation index
k	Wave number
kh	Nondimensional water depth
k_m	Wave number at frequency $m\Delta f$
k_y	Y-axis component of wave number
K	Integer exponent for factor 2 in 235 FFT
ℓ	Space domain summation index
L	Linear, shallow-water wavelength Number of harmonics in directional spreading function Integer exponent for factor 3 in 235 FFT
L_p	Wavelength associated with peak frequency f_p
L_y	Y-axis component of wavelength
m	Frequency domain summation index
m_0	Zero moment
M	Equivalent number of bands for Gaussian smoothing Integer exponent for factor 5 in 235 FFT

n	Time domain summation index
N	Total number of data samples Number of harmonics in fourier series Number of wave gages
Q_p	Goda's spectral peakedness parameter
$Q_{ij}(f)$	Quadrature spectral density component
RAO_i	Response amplitude operator function for gage i
s_c	Stroke control signal
$S(f)$	Frequency spectrum
$\bar{S}(f)$	Harmonic mean of autospectral density estimate
$\bar{S}_m$	Gaussian smoothed spectral density at frequency $m\Delta f$
$S(f,\theta)$	Directional wave spectrum
$S_{ii}(f)$	Autospectral density estimate
$S_{ij}(f)$	Cross-spectral density estimate
{SPECTRA}	Vector of measured autospectra and cross spectra, frequency f
t	Time
T	Wave period
T_p	Spectral peak period
T_r	Length of time series
[TRANSFER]	Matrix of directional spectra terms at frequency f
$U(f)$	Real amplitude component of $A(f)$
U_m	Real fourier coefficient of control signal at $m\Delta f$
$V(f)$	Imaginary amplitude component of $A(f)$
V_m	Imaginary fourier coefficient of control signal at $m\Delta f$
w_j	Weighting function for Gaussian smoothing
x	X-axis coordinate Random variable
[X]	Matrix of independent variables in regression analysis
X_{ij}	Distance between gage i & j along x-axis
y	Y-axis coordinate
{Y}	Dependent variables vector in regression analysis
Y_{ij}	Distance between gage i & j along y-axis
α	Spectral parameter
{B}	Regression coefficients vector
τ	Peak enhancement factor
Δf	Basic frequency increment
Δt	Time interval

$\{\epsilon\}$	Prediction errors vector
$\eta(x,y,t)$	Water surface elevation time series
θ	Wave direction, angle of wave propagation
θ_m	Principal or mean wave direction at frequency $m\Delta f$
θ_0	Constant term of θ_m
θ_1	Slope term of θ_m
$\bar{\theta}$	Overall mean wave direction for all frequencies
π	3.14159
σ	Directional spreading standard deviation
σ_a	Left spectral width parameter
σ_b	Right spectral width parameter
σ_m	Mean spreading standard deviation
σ_0	Constant term of σ_m
σ_1	Slope term of σ_m
ϕ	Directional spectra dummy variable
Φ	Independent, random phase